Mechanisms of Transcription Activation by the DNA-binding Transfactor Repressor Activator Protein 1 (Rap1) Uncovered Using an Altered DNA-binding Specificity Variant

By

Amanda N. Meyer

Dissertation

Submitted to the Faculty of the

Graduate School of Vanderbilt University

in partial fulfillment of the requirements

for the degree of

DOCTOR OF PHILOSOPHY

In

Molecular Physiology & Biophysics

August 11, 2017

Nashville, Tennessee

Approved:

P. Anthony Weil, Ph.D.

Roland Stein, Ph.D.

William P. Tansey, Ph.D.

Bryan Venters, Ph.D.

Roger Colbran, Ph.D.

ACKNOWLEDGEMENTS

especially thankful for the members of my PhD thesis committee, Drs. Roger Colbran, Roland Stein, Bill Tansey, and Bryan Venters, all of whom often went out of their way to offer me advice and support during my training.   Dr. Stein encouraged me early on in my efforts to generate an altered DNA-binding specificity Rap1 (Rap1^{AS}) to perform my screen in yeast (which worked!) instead of *E. coli* (which ultimately didn't work). Dr. Colbran provided needed advice on statistical analyses/data presentation and encouragement on using seminars as an opportunity to ask questions and learn from other scientists.   Dr. Tansey suggested important controls that ultimately made my data much more convincing and asked questions that challenged me think more deeply about how my research fits in the field of transcription regulation. Dr. Venters shared his expertise in genomics and ChIP with me; he helped me better understand the many published genomic datasets that have provided important insight into Rap1 function and suggested helpful alternative experimental approaches when I struggled to set up a technique.

I must also thank the members of the Weil lab whose efforts greatly assisted me in my PhD training. Although I have never met her, I am very grateful to Dr. Krassimira Garbett, a former Weil lab member who also worked on Rap1. Her impeccable notebooks and reagent cataloging supplied a strong foundation for my work on Rap1 and provided an example for me to emulate. I would also like to thank Drs. Justin Layer and Iulia Gilchuck who shared their reagents with me and guided me through protocols they had worked out early in my training. I also really appreciate all the help I received from the two Weil lab members I shared the most time in lab with: Drs. Chirie Sumanasekera and Jordan Feigerle. Chirie mentored me when I was just a rotation student. I am grateful to her for sharing technical expertise and for encouraging me to think critically about how each of my

my brother and me. Because of her choice, she was able to support us as we learned and grew, whether that was cooking good nutritious meals, making sure we took our schoolwork seriously, or taking us to sports or band practice. My dad Chris has supported our family over the years through his work as a chemical engineer. He may have known early on that I would somewhat follow in his career footsteps when his reading of Chemistry and Engineering textbooks failed its intended goal of putting baby Amanda to sleep. Both of my parents have set good examples of what it means to be a good person. They have also instilled in me the value of hard work and education. When something didn't come naturally to me, they always encouraged me to keep trying and helped me to build excellent habits that have ultimately helped me overcome struggles through the course of my lifetime. I think it is probably safe to say that I would not be where I am today without the lifetime of support I have received from my parents.

Finally, I am not sure if I would have made it this far without my husband, best friend, and love of my life, Jarrod Johnson. At the time we were married, Jarrod was enrolled in a PhD program in Clinical Pyschology in Lafayette, IN. When we married, he left the program with an MS so we could be together. He has also worked really hard to move his way up in healthcare data industry to support us. He has been so patient with me through my long hours at work and his encouragement has helped me keeping going in the face of my fear of failure. Through his actions, he has helped set me free to pursue my dream of using science to help make a difference in the world. I couldn't ask for a better spouse and I hope I can repay him as we continue our life adventure together.

TABLE OF CONTENTS

LIST OF TABLES

LIST OF FIGURES

CHAPTER I

INTRODUCTION

<u>Overview</u>

All cells across the tree of life carry the instructions for their identity and function

within their DNA. A portion of this DNA consists of genes, which can be turned into a

functional product (RNA or protein) via the processes of transcription (DNA → RNA) and

translation (RNA → protein) outlined by the "central dogma" of molecular biology (Crick,

1970). Specifically, protein-coding genes, whose products carry out many diverse cellular

functions, make up an estimated 88% of the 4.6Mb genome in the model bacterium

Escherichia coli (4,288 genes (Blattner et al., 1997)), 70% of the 12Mb genome in the

baker's yeast *Saccharomyces cerevisiae* (5,885 genes (Goffeau et al., 1996)), and 1.2% of the

3Gb human genome (20,000-25,000 genes (Consortium and others, 2004)). The rest of

each genome either encodes RNA (including ribosomal RNA (rRNA), transfer RNA (tRNA),

small non-coding RNA (ncRNA), or long non-coding RNA (lncRNA)), or is regulatory DNA.

As its name implies, this regulatory DNA plays an important role in regulating the

expression of RNAs and protein. Such regulation of expression, which can occur through

altering RNA synthesis/transcription, RNA degradation, protein synthesis/translation, and

protein degradation, ultimately determines a cell's responses to changes in environmental

signals. The importance of this regulation is underscored by the fact that an "incorrect"

cellular response may result in death for a single-celled organism such as *E. coli* and yeast,

or disease for the human, where the problem is compounded by the presence of multiple cell types that must communicate appropriately to ensure the health of the organism.

My dissertation research is broadly aimed at understanding how the cell achieves an appropriate response to environmental stimuli through regulation of transcription, the first step in gene regulation. Transcription is catalytically accomplished by RNA polymerases that generate RNA based on a DNA template. While prokaryotes possess only one RNA polymerase (Murakami, 2015), yeast and higher eukaryotes from the animal kingdom possess three nuclear RNA polymerases (Vannini and Cramer, 2012). The three eukaryotic nuclear RNA Polymerases are: (1) RNA polymerase I (Pol I), which is responsible for rRNA gene transcription, (2) RNA polymerase II (Pol II), which is responsible for mRNA (the RNA that encodes protein) gene transcription as well as most lncRNA, micro RNA (miRNA), and small nuclear RNA (snRNA), and (3) RNA polymerase III (Pol III), which transcribes small RNA encoding genes, including tRNAs and certain ncRNAs (Vannini and Cramer, 2012). Importantly for my work, much of the process of transcription regulation is similar across all domains of life. Indeed, the transcription process is highly conserved from baker's yeast to higher eukaryotes (Hahn and Young, 2011). This fact justifies the use of yeast, which provides the advantages of a rapid doubling time (90 min) and facile genetics and biochemistry, in the use of my studies that were aimed at uncovering mechanisms of transcription regulation.

My work specifically focuses on Pol II transcription regulation. Each one of the thousands of protein-coding genes in eukaryotes must be transcribed at the right time and in the right amount for healthy cellular function (Shandilya and Roberts, 2012; Weake and Workman, 2010). The challenge for the cell is that many of these genes have unique

expression requirements, with transcript levels among different expressed protein-coding genes varying ~8,000-10,000 fold under normal growth conditions (Djebali et al., 2012; Nagalakshmi et al., 2008). How does Pol II achieve this variability in transcription output? Through analysis of the literature and the studies presented herein on how one transcription activator, Repressor Activator Protein 1 (Rap1), drives transcription of the robustly transcribed Ribosomal Protein (RP) genes, this document explores the answers we have to this question in terms of the contributions made by DNA elements, transcription factors, and the interactions among them.

<p style="text-align: center">DNA Elements Guide Pol II Transcription Regulation</p>

As mentioned above in "Overview," the genome of every organism consists of coding and regulatory DNA, both of which form critical elements in the structures of protein encoding genes (**Figure 1.1**). These DNA elements help direct the three phases of Pol II transcription cycle: initiation, elongation, and termination (Shandilya and Roberts, 2012). Some of these elements affect transcription output through their presence, position, and binding affinity for a DNA-binding transcription factor(s) as observed in prokaryotes (Browning and Busby, 2004; Mitchell et al., 2003; Pribnow, 1975; Ross et al., 1993; Schaller et al., 1975). They can also be divided into two categories: (1) the enhancer/silencer-promoter and (2) the transcription unit (defined below, see also **Figure 1.1**).

The enhancer/silencer-promoter is a set of regulatory DNA elements that are of particular importance to Pol II transcription because they regulate when, where, and to what level each gene gets transcribed (Levo and Segal, 2014). In fact, the ~60 years of research on these DNA sequences that has followed the discovery of regulatory DNA in
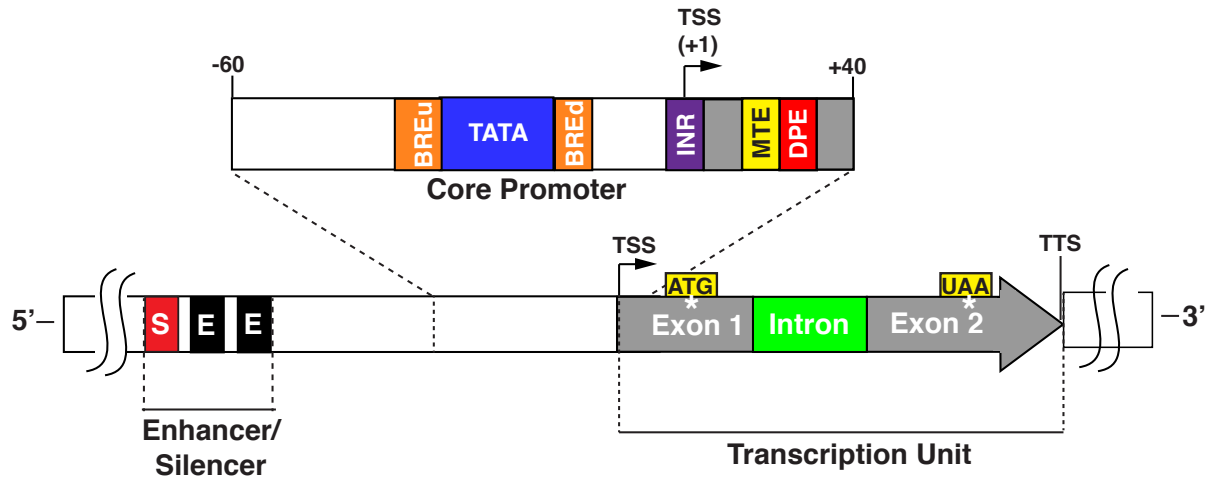
Figure 1.1. Structure of a protein encoding gene. A diagram of a protein-encoding gene is presented. In this model, the DNA elements of the protein encoding gene are divided into enhancer/silencer, core promoter, and transcription unit regions. The enhancer/silencer-promoter consists of enhancer (E, black) elements (functionally equivalent to the *UAS* in yeast) and/or silencer (S, red) elements, (functionally equivalent to the *URS* in yeast), which represent DNA recognition elements for DNA-binding transcription factors, which can be located anywhere from 200bp to several kb away from the transcription unit. The enhancer/silencer-promoter also contains a core promoter, which may contain *BREu* (orange), *TATA* (blue), *BREd* (orange), *INR* (purple), *MTE* (yellow), and/or *DPE* (red), elements, is located immediately 5' to the transcription unit. The transcription unit extends from the transcription start site (TSS, arrow, +1) to the transcription termination site (TTS) and overlaps slightly with the enhancer/silencer-promoter. It contains exons (gray), which encode protein. It may also contain introns (light green), which are non protein-coding sequenced that are spliced out during the production of mature mRNA. The start codon (ATG) and stop codon (UAA), required for translation of the mRNA into protein are marked by the white star (*) and yellow labels. Although not labeled, the sequence between the TSS and the ATG encodes the mRNA 5' untranslated region (UTR) while the sequence between the stop codon and the TSS encodes the 3' UTR.

bacterial systems (Jacob and Monod, 1961) has defined their function, location relative to the transcription unit, and consensus sequences.

Enhancers and silencers influence transcriptional activity largely independent of position and orientation relative to the transcription unit (Li et al., 2016). Enhancers, which act to stimulate transcription, and silencers, which act to repress transcription, consist of 6-12 base pair recognition sites for one or more transcription factors (Levo and Segal, 2014). In metazoans, these DNA elements may be located several kb upstream/downstream of the transcription unit or even within an intron (Li et al., 2016). However, in *S. cerevisiae*, possibly due to its more compact genome, these elements are

located 1,000 base pairs or less upstream of the transcription unit and are termed

Upstream Activating Sequences (*UAS*) and Upstream Repressing Sequences (*URS*) (Hahn

and Young, 2011).

While the consensus sequences for many of the transcription factors that bind DNA

within enhancers and silencers have been defined and annotated (Jolma et al., 2013;

Sandelin, 2004), the rules guiding the configuration of transcription factor binding sites

within an enhancer/silencer remain poorly understood. Some of the data obtained from

analyses of both individual chromosomal enhancers and libraries of synthetic enhancers

supports a "billboard model" of enhancer configuration. In this model, the identity and

number of transcription factor binding sites within an enhancer influences transcription

levels largely independent of binding site arrangement (Liu and Posakony, 2012; Rastegar

et al., 2008; Smith et al., 2013). On the other hand, data obtained from dissection of other

chromosomal enhancers supports an "enhanceosome model," wherein transcriptional

activity depends on a specific order and spacing among transcription factor binding sites

(Liu and Posakony, 2012; Thanos and Maniatis, 1995). Chromosomal enhancers may

follow either model in practice depending on a gene's regulatory demand, with "billboard"

enhancers operating predominantly on genes where a response to each environmental

stimulus independently is appropriate and "enhanceosome" enhancers operating on genes

that require carefully orchestrated integration of multiple signals (Levo and Segal, 2014;

Liu and Posakony, 2012).

All enhancers regardless of configuration must operate in conjunction with a core

promoter. The core promoter, which is generally located 30-120 base pairs 5' of the

transcription unit (Li et al., 1994), is the minimal stretch of DNA required for accurate RNA

Pol II transcription initiation (Kadonaga, 2012). A core promoter may be sub-divided into several separate DNA units that, like the enhancer/silencer elements, form recognition sites for transcription factors and influence transcription activity. The core promoter elements whose position and consensus sequences have been defined to date are: (1) the TATA box (*TATA*) (Nagawa and Fink, 1985), (2) the Initiator (*INR*) (Smale and Baltimore, 1989), (3) the downstream promoter elements (*DPE)* (Burke and Kadonaga, 1997), (4) the Motif-Ten Element (*MTE*) (Lim et al., 2004), and (5) the TFIIB recognition element (*BRE*) motifs BRE upstream (*BREu*) and BRE downstream (*BREd*) (Kadonaga, 2012; Lagrange et al., 1998) (**Figure 1.1**). Gene class-specific promoter elements, such as the polypyrimidine initiator motif (TCT) which is found in place of the Inr in the promoters of metazoan RP genes, have also been defined (Parry et al., 2010). The majority of these elements have been discovered in the fruit fly *Drosophila melanogaster* and human, although no native promoter in either of these organisms contains every element (Kadonaga, 2012). Meanwhile, the *TATA* is the only element that has been defined in yeast, where 20% of promoters are designated "*TATA*-containing" due to the presence of a consensus *TATA* (Basehoar et al., 2004) and 80% are designated "*TATA*-like" due to one or two base pair mismatches from the consensus (Rhee and Pugh, 2012).

Pol II initiation and elongation influenced by the core promoter (Kadonaga, 2012) enables transcription of the transcription unit, a sequence of DNA that extends from the promoter through the transcription start site (TSS) to the transcription termination site (TTS). This stretch of DNA sequence, which ultimately encodes the mRNA, consists of at least one exon, which encodes protein. It may also contain intron(s), which are non-protein-coding sequences that are co-transcriptionally spliced out to allow the exons to be

6

joined together during the production of mature mRNA (Neugebauer and Roth, 1997).

Mature mRNA is ultimately exported out of the nucleus to be used as a template to direct

protein synthesis. The sequence that becomes the part of the mature RNA that extends

from the start codon (AUG) to the stop codon (UAA, UGA, or UAG) contains the open

reading frame (ORF) to be translated into protein. ORF sequences direct translation and

may influence both mRNA and protein stability. Thus the sequences of the

enhancer/silencer-promoter and transcription unit ultimately determine regulation of

gene expression at the levels of transcription, mRNA degradation, translation, and protein

degradation.

Pol II Function and Structure

RNA polymerases synthesize RNA from all transcription units in a cell. As

mentioned in "Overview", while bacteria possess only one RNA polymerase (Murakami,

2015), eukaryotes (excluding plants, which have up to five distinct nuclear DNA-dependent

RNA polymerases (Haag and Pikaard, 2011)) have three nuclear RNA polymerases: Pol I,

Pol II, and Pol III (Roeder and Rutter, 1969), each of which synthesizes a different class of

RNA (Weinmann and Roeder, 1974; Zylber and Penman, 1971). RNA Pol II function and

structure are detailed here due to the emphasis of this dissertation on mRNA gene

transcription. Areas of homology between Pol II and the other Polymerases (Vannini and

Cramer, 2012) are also noted.

RNA Polymerase II in all eukaryotes accomplishes its mRNA synthesis function

through the initiation, elongation, and termination phases of the transcription cycle

(**Figure 1.2**) (Shandilya and Roberts, 2012), processes directed by the DNA elements
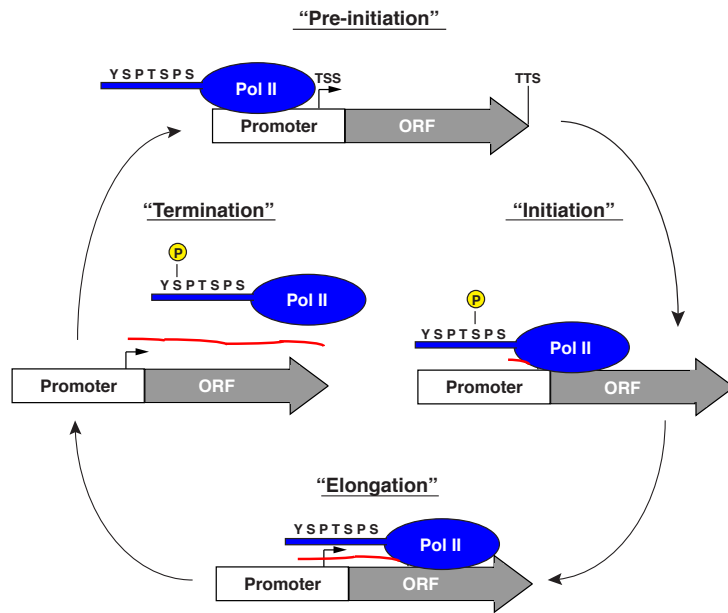
Figure 1.2. The RNA Polymerase II Transcription Cycle. A diagram illustrating the phases of the RNA Polymerse II transcription cycle is shown. In the "Pre-initiation" phase, Pol II (blue, only one of the multiple CTD heptad repeats (N'-YSPTSPS-C') is shown) is bound to promoter DNA. The TSS and TTS sites on the sample protein-coding gene are indicated here for reference. The "Initiation" phase begins when Pol II proceeds into the TSS and begins its entrance into the gene ORF, synthesizing the first few mRNA (red) nucleotides. At this phase, Pol II is located where levels of phosphorylated Pol II CTD heptad repeat Ser5 are highest. Following promoter clearance, Pol II enters the "Elongation" phase of transcription, extending the synthesis of the mRNA. Once it reaches the TTS, Pol II and the synthesized full-length mRNA are released from the ORF in the "Termination" phase of transcription. During this phase, Pol II is located at the 3' end of the gene, where Pol II CTD heptad repeat amino acid Ser2 phosphorylation levels are highest. Once it is released from the template, Pol II is free to begin the cycle of transcription anew.

described above and the general transcription factors (GTFs) required for accurate transcription initiation described in the "Basal Transcription Factors" section. The initiation phase begins when RNA Pol II binds the promoter and synthesizes the first phosphodiester bonds of RNA (Hahn, 2004). However, initiation does not guarantee full-length transcript generation; transcription may be aborted at 5 or fewer nucleotides (Holstege et al., 1997). To synthesize a full-length transcript, Pol II must escape the promoter. After promoter escape, Pol II may pause transcription (Gilmour and Lis, 1986; Muse et al., 2007), providing an opportunity to regulate transcription elongation that is particularly important in metazoans (Adelman and Lis, 2012). Alternatively, Pol II may proceed into the elongation phase of transcription, a process facilitated by Pol II-associated elongation factors such as TFIIS (Rappaport et al., 1987; Reinberg and Roeder, 1987; Sekimizu et al.,

1979), and transcribe the entire transcription unit. Upon completing transcription unit

mRNA synthesis, both Pol II and the mRNA it has recently generated are released from the

template in the termination phase of transcription. Pol II is then free to begin another

round of transcription. It may reinitiate transcription on the same gene, a process

facilitated by transcription factors that remain at the promoter during the transcription

cycle (Yudkovsky et al., 2000) and/or gene looping guided by transcription termination

factors (El Kaderi et al., 2009). Alternatively, Pol II may initiate transcription of a different

gene.

Like all enzymes, Pol II achieves its transcription activity through its structure.

Yeast Pol II, whose structure is largely conserved in higher eukaryotes and is the focus of

this discussion, consists of 12 subunits, designated Rpb1-12 (**Table 1.1**) (Edwards et al.,

1990; Kolodziej et al., 1990; Treich et al., 1992; Vannini and Cramer, 2012). All subunits

except Rpb4 and Rpb9 are essential, although cells lacking Rpb4 and Rpb9 exhibit a slow-

growth phenotype (Woychik and Young, 1989; Woychik et al., 1991, 1993). 10 Pol II

subunits (Rpb1, Rpb2, Rpb3, Rpb5, Rpb6, Rbp8, Rpb9, Rpb10, and Rpb12) form the

enzyme's stable catalytic core, while Rbp4 and Rpb7 dissociate during elongation (Mosley

et al., 2013). However, Rbp4 and

Rpb7 are required for initiation

(Edwards et al., 1990). Rbp9 provides

RNA cleavage activity and helps

relieve Pol II stalling (Awrey et al.,

1997). Five of the catalytic core

subunits (Rpb5, Rpb6, Rpb8, Rpb10,

Table 1.1: Yeast RNA Pol II Structure and Function		
RNA Pol II Subunit	**Subunit Size (kDa)**	**Subunit Function**
Rpb1	192	Active center
Rpb2	139	Active center
Rpb3	35	Catalytic core structure
Rpb4	25	Initiation complex formation
Rpb5	25	Catalytic core structure
Rpb6	18	Catalytic core structure
Rpb7	19	Initiation complex formation
Rpb8	17	Catalytic core structure
Rbp9	14	RNA Cleavage
Rpb10	8	Catalytic core structure
Rpb11	14	Catalytic core structure
Rpb12	8	Catalytic core structure

*Note: Subunit sizes are derived from the Saccharomyces Genome Database
(SGD): http://www.yeastgenome.org/

and Rpb12) are shared with Pol I and Pol III (Vannini and Cramer, 2012).

Some Pol II subunits also possess sequence and structural homology to the bacterial RNA polymerase, which consists of two α subunits, the β and β' subunits, an ω subunit, and a σ subunit (Murakami, 2015). The catalytic core subunits Rpb3 and Rpb11 resemble the two bacterial RNA polymerase α subunits (Zhang and Darst, 1998). Rpb6 serves structural roles and is most similar to ω (Minakhin et al., 2001). Meanwhile, Rpb1 and Rpb2 form the Pol II active center and are similar to the β and β' subunits, respectively (Allison et al., 1985; Cramer et al., 2001; Sweetser et al., 1987). These subunits contain the nucleotide binding pocket and catalyze the formation of phosphodiester bonds needed to build the mRNA chain (Riva et al., 1987). Rpb1 and Rpb2 can also bind the death cap mushroom toxin α–amanitin. This binding event inhibits the translocation of DNA and RNA needed to extend the mRNA chain (Bushnell et al., 2002) and is responsible for the observed sensitivity of Pol II to α–amanitin (Schultz and Hall, 1976).

In addition to its role in catalysis, Rpb1 contributes to transcription via its essential C-terminal domain (CTD) (Allison et al., 1988; Zehring et al., 1988). The Rpb1 CTD consists of 25 repeats in yeast (up to 52 in higher eukaryotes) of the amino acid sequence $Y^1S^2P^3T^4S^5P^6S^7$ (Allison et al., 1985; Corden et al., 1985). These repeats are the target for post-translational modification, particularly phosphorylation. Indeed, Rpb1 phosphorylation was noted in early studies that defined RNA Pol II subunit composition (Kolodziej et al., 1990). The two most well studied CTD post-translational modifications are Ser5 phosphorylation (Ser5-P) and Ser2 phosphorylation (Ser2-P) (Hsin and Manley, 2012). Chromatin immunoprecipitation (ChIP) experiments have found that Ser5-P levels are highest at the 5' end of the transcription unit while Ser2-P levels are highest at the 3'

end of the transcription unit (Komarnitsky et al., 2000) (**Figure 1.2**). Perhaps consistent with this localization, Ser5-P is catalyzed by the Kin28 subunit of the GTF TFIIH (Lu et al., 1992) found at gene promoters (see "Basal Transcription Factors) and removed primarily by Ssu72 (Krishnamurthy et al., 2004), a subunit of the yeast cleavage/polyadenylation factor (CPF) complex. Meanwhile, Ser2-P is catalyzed by the Bur1/Bur2 and Ctk1 kinases (Keogh et al., 2003; Lee and Greenleaf, 1991; Qiu et al., 2009) involved in elongation and removed by Fcp1 (Cho et al., 2001).

The Ser5-P and Ser2-P RNA Pol II CTD modifications create binding sites for factors important for cotranscriptional mRNA processing and completion of the transcription cycle. For example, Ser5-P is recognized by mRNA capping enzymes (Cho et al., 1997) that act on the 5' end of transcription unit while Ser2-P is associated with transcription termination/mRNA polyadenylation factors (Barillà et al., 2001) that act on the 3' end of the transcription unit. In support of this simple "CTD code," a recent mass spectrometry analysis showed that Ser5-P and Ser2-P rarely co-exist on the same repeat, and CTD-interacting factors associate primarily with either Ser5-P or Ser2-P repeats (Suh et al., 2016). Thus, CTD phosphorylation appears to provide a means to permit transcription accessory factors to specifically associate with the phase of the transcription cycle that is most appropriate for their activity.

<u>Basal Transcription Factors</u>

In spite of its complex structure and function, eukaryotic Pol II, in contrast to bacterial RNA polymerase, cannot accurately initiate transcription on its own (Weil et al., 1979). Instead, eukaryotic Pol II requires factors, termed basal transcription factors or

11

Table 1.2: Structure and Function of the Yeast Pol II GTFs

GTF	Function	Subunits	Subunit Size (kDa)
TFIIA	Stabilizes TBP and TFIID-DNA binding.	Toa1	32
		Toa2	13
TFIIB	Binds TBP, Pol II, and promoter DNA to determine TSS	Sua7	38
TFIID	Binds promoter elements, enables binding of TFIIB, and may serve as a target for transfactors	Taf1	121
		Taf2	161
		Taf3	40
		Taf4	42
		Taf5	89
		Taf6	58
		Taf7	67
		Taf8	58
		Taf9	17
		Taf10	23
		Taf11	41
		Taf12	61
		Taf13	19
		Taf14	27
		TBP	27
TFIIE	Binds promoter and helps stabilize transcription initiation activities	Tfa1	55
		Tfa2	37
TFIIF	Binds Pol II and aids in Pol II promoter binding	Tfg1	82
		Tfg2	47
		Taf14	27
TFIIH	Provides kinase and helicase functions required for transcription initiation activities	Ssl2	95
		Rad3	90
		Tfb1	73
		Tfb2	59
		Ssl1	52
		Tfb3	38
		Ccl1	45
		Tfb4	37
		Kin28	35
		Tfb5	8

*Note: Subunit sizes are derived from the Saccharomyces Genome Database (SGD): http://www.yeastgenome.org/

general transcription factors (GTFs), to initiate transcription. Like Pol II, each of the six GTFs (transcription factor for RNA Polymerase II A (TFIIA), TFIIB, TFIID, TFIIE, TFIIF, and TFIIH (**Table 1.2**) are obligate components of transcription machinery (Thomas and Chiang, 2006). These six GTFs, which were named according to their fractionation from crude cell extracts (Matsui et al., 1980; Sayre et al., 1992), and Pol II form the pre-initiation complex (PIC). Each of the GTFs interacts with the promoter elements described in "DNA Elements Guide Pol II Transcription Regulation," plays a critical role in Pol II promoter binding and PIC formation (**Figure 1.3**), and adds ways to regulate gene expression (Roeder, 2005). Yeast GTFs will be the focus of this discussion. As was the case for Pol II, the structure and function of these transcription factors are largely conserved, and important differences are noted.

TFIIA: The 45kDa TFIIA complex is composed of two subunits: Toa1 (32kDa) and Toa2 (13kDa) (Ranish and Hahn, 1991), each encoded by a single copy essential gene (Ranish et al., 1992). Although it does not bind DNA on its own, TFIIA aids in PIC formation by enhancing the binding of the TATA Binding Protein (TBP) to promoter DNA via direct
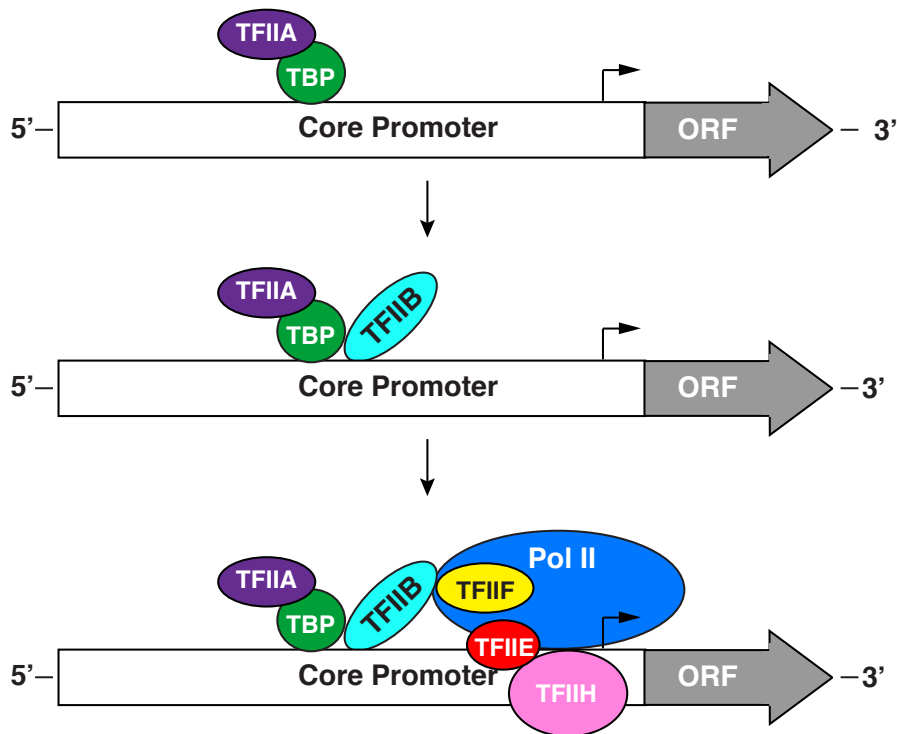
Figure 1.3. Model for PIC Assembly. A model for PIC complex assembly. PIC nucleation begins with the promoter binding of TBP (green), which can be stabilized by TFIIA (purple). TBP and TFIIA promoter binding is stable, while TFIIB (light blue) promoter binding is dynamic. TFIIB direct interaction with TBP (green) stabilizes TBP-DNA binding. TFIIB binding to the core promoter enables the association of the remaining GTFs, including Pol II (medium blue), TFIIF (yellow), TFIIE (red), and TFIIH (pink). This fully assembled PIC enables Pol II initiation of transcription. Importantly, the first step of TBP-binding can be stimulated by interaction between the Taf subunits of the TBP-containing complex TFIID (not shown) and transcription factors called transcription activator proteins (not shown) described in "Transfactors Confer Gene-Specific Transcription Regulation." TFIID Tafs may also be required for promoter-binding in the absence of a consensus *TATA*.

TFIIA-TBP interaction (Yokomori et al., 1994). This TFIIA-TBP interaction can

competitively displace interactions between TBP and a part of the subunit of the TBP-

containing complex TFIID (TBP-associated factor 1 (Taf1) N-terminal domain (TAND) (Bai

et al., 1997; Kotani et al., 1998)) that prevents TBP binding to DNA (Kokubo et al., 1998;

Ozer et al., 1998), explaining the requirement of TFIIA for TFIID promoter binding under

certain conditions (Emami et al., 1997; Lieberman and Berk, 1994; Sanders et al., 2002a).

Additionally, TFIIA interacts directly with transcription activators such as VP16 and Zta to

coactivate transcription, usually by stimulating TFIID DNA-binding (Kobayashi et al., 1995; Lieberman, 1994; Lieberman et al., 1997; Ozer et al., 1996).

TFIIB: The 38kDa GTF TFIIB is encoded by a single-copy essential gene: *SUA7* (Pinto et al., 1992). Like TFIIA, TFIIB can directly bind TBP and stabilize TBP DNA-binding (Imbalzano et al., 1994). TFIIB also interacts directly with Pol II and TFIIF (Buratowski and Zhou, 1993; Ha et al., 1993). Through these interactions, TFIIB plays an important role in PIC formation. In the step-wise model of PIC formation, TFIIB recognizes the complex formed between TBP, TFIIA, and DNA (Buratowski et al., 1989; Maldonado et al., 1990) (**Figure 1.3**). TFIIB may then in turn enable Pol II and the rest of the GTFs to enter the PIC (Buratowski et al., 1989; Killeen et al., 1992). TFIIB interaction with Pol II also guides transcription initiation and TSS selection (Pardee et al., 1998). Finally, TFIIB can interact with the activation domains (ADs) of transcription activators and thus may serve as a coactivator in some gene contexts (Chiang et al., 1996).

TFIID: TFIID (MW ~1MDa) consists of at least 19 polypeptides depending on the species, including TBP and various Taf subunits, some of which are present in two or more copies within the complex (Sanders et al., 2002a; Tansey and Herr, 1997; Tora, 2002). In *S. cerevisiae,* the model organism used for this dissertation research, TFIID possesses 14 distinct Tafs (Taf1 → 14) (Sanders et al., 2002a). The genes encoding each of the TFIID subunits are essential except for *TAF14* (Klebanow et al., 1996, 1997; Moqtaderi et al., 1996; Poon et al., 1995; Ray et al., 1991; Reese et al., 1994; Sanders and Weil, 2000). Additionally, Taf14, which is also a component of other transcription-related complexes including TFIIF (Henry et al., 1994; Sanders et al., 2002b), is not present in the TFIID complexes of other organisms (Tora, 2002).

While in yeast, TFIID exists as one holo-TFIID complex (Sanders and Weil, 2000) which will be described in more detail in a later section of this Chapter, in metazoan systems the situation is much more complicated. One factor complicating the definition of what constitutes the TFIID complex in metazoans is the existence of alternate versions of both Tafs and TBP in differentiated tissue (D'Alessio et al., 2009). The earliest of the alternative Tafs to be identified was Taf4b, which was originally identified in B cells (Dikstein et al., 1996) and is required for cell-type specific gene activation in ovaries and testes (Geles et al., 2006). Since then, other tissue-specific versions of Tafs and TBP have been identified, including *cannonball/can* (Taf5 paralog), *no hitter/nht* (Taf4 paralog), *meiosis I arrest/mia* (Taf6 paralog), *spermatocyte arrest/sa* (Taf8 paralog), and *ryan express/rye* (Taf12 paralog) (Hiller, 2004) and TBP-Related Factor 1 (TRF1) in *Drosophila* (Crowley et al., 1993). Tissue differentiation in metazoans may also result in the replacement of canonical TFIID with a TFIID sub-complex such as the Taf3/TRF complex which was found to replace TFIID in differentiated myotubes (Deato and Tjian, 2007). These TFIID sub-complexes and alternative TFIID subunits likely provide interaction surfaces for other transcription factors that are required for tissue-specific gene activation but are not available in the canonical holo-TFIID complex. Consistent with this idea, holo-TFIID is unable to substitute for Taf3/TRF3 to activate muscle-specific gene transcription *in vitro* (Deato et al., 2008) and some mammalian activators are reportedly unable to function in yeast which lack alternative Tafs/TFIID (Attardi and Tjian, 1993; Ponticelli et al., 1995).

No matter its exact composition, one of the primary functions of TFIID is promoter recognition (Albright and Tjian, 2000). In this role, TFIID is akin to the σ subunits (σ^{70} and

alternative σ variants (Burgess et al., 1969; Fox et al., 1976; Haldenwang et al., 1981)) of bacterial RNA Polymerase, which are required for consensus and alternative promoter DNA recognition in prokaryotes (Sugiura et al., 1970).   As its name implies, TBP binds the *TATA* DNA elements of core promoters (Hahn et al., 1989). PIC formation absolutely requires TBP promoter association because the other GTFs cannot bind promoter DNA in the absence of TBP (Buratowski et al., 1989). TBP is capable of binding consensus *TATA*-containing DNA independently of the other TFIID subunits, a property that has been used to achieve *in vitro* transcription using purified components (He et al., 2016; Myers et al., 1997). However, the Taf subunits likely play an important role in TFIID binding to most of the promoters it occupies, which contain non-consensus *TATA* elements (Huisinga and Pugh, 2004). Some of the Taf subunits have indeed been shown to directly interact with either core promoter DNA elements or promoter-proximal nucleosomes. Specifically, at least in metazoans, Taf2 binds the promoter *INR* element (Chalkley and Verrijzer, 1999; Verrijzer et al., 1994, 1995) while Taf6 and Taf9 interact with the *DPE* promoter DNA element (Burke and Kadonaga, 1997). Additionally, Taf3 in metazoans and Taf14 in yeast may contribute to TFIID promoter occupancy through interactions with modified promoter-proximal nucleosomes mediated via their plant homeobox domain (PHD) and Yaf9, ENL, AF9, Taf14, Sas5 (YEATs) domains respectively (Andrews et al., 2016; Feigerle and Weil, 2016; Lauberth et al., 2013; Shanle et al., 2015; Vermeulen et al., 2007). These Taf-DNA and Taf-chromatin interactions likely facilitate TFIID promoter binding particularly on gene promoters that lack a consensus *TATA* box.

Like TFIIA and TFIIB, TFIID can function as a coactivator (Chen et al., 1994; Gill et al., 1994; Pugh and Tjian, 1990; Thut et al., 1995). This coactivator function requires the

TFIID Taf subunits since TBP alone does not respond to transcription activators (Dynlacht et al., 1991; Pugh and Tjian, 1990; Tanese et al., 1991). As such, there has been and continues to be much interest in the field of transcription in defining activator-Taf interactions and their biochemical consequences. Indeed, TFIID has been viewed as an ideal coactivator target in transcription regulation (Albright and Tjian, 2000). The many Taf subunits of TFIID offer a multitude of interaction surfaces for transcription activator binding, and activator-Taf interactions likely aid TBP promoter association (which, as described above, is rate-limiting in PIC formation (Buratowski et al., 1989)) with the genes that depend on TFIID. Due to the importance of TFIID for this dissertation, these ideas, along with other details regarding TFIID structure and coactivator function, will be further described in the "TFIID Structure and Coactivator Function" section appearing later in this Chapter.

TFIIE: TFIIE is a heterotetrameric complex (~184 kDa) (Inostroza et al., 1991) consisting of two copies each of the subunits Tfa1 and Tfa2 encoded by single copy essential genes (Feaver et al., 1994). TFIIE interaction with the promoter causes a conformational change in promoter DNA required for transcription initiation (Buratowski et al., 1991; Holstege et al., 1996). TFIIE also interacts directly with Pol II and the GTF TFIIH (Maxon et al., 1994). TFIIE interaction with TFIIH stimulates TFIIH kinase and helicase activities required for transcription initiation (Lu et al., 1992; Ohkuma and Roeder, 1994).

TFIIF: The 156 kDa yeast GTF TFIIF is made up of three subunits. Two of those subunits (Tfg1 and Tfg2) (Henry et al., 1992) are unique to TFIIF and one (Taf14) is shared with TFIID (Henry et al., 1994). *TFG1* and *TFG2* are essential (Henry et al., 1994).

Meanwhile, *TAF14* is neither essential (though *taf14Δ* cells grow very slowly) (Henry et al., 1994) nor present in metazoan TFIIF (Flores et al., 1989). TFIIF associates tightly with Pol II in the context of the PIC (Rani et al., 2004). This TFIIF-Pol II interaction enables Pol II incorporation into the PIC and TSS selection (Flores et al., 1991; Ghazy et al., 2004). The TFIIF-Pol II interaction also stimulates both the initiation and elongation phases of transcription (Conaway et al., 2000; Ghazy et al., 2004).

TFIIH: TFIIH is a 532 kDa complex consisting of 10 subunits in budding yeast: Ssl2, Rad3, Tfb1, Tfb2, Ssl1, Tfb3, Ccl1, Tfb4, Kin28, and Tfb5 (Murakami et al., 2012; Ranish et al., 2004; Svejstrup et al., 1994). All subunits are encoded by essential genes with the exception of *TFB5* (Feaver et al., 1997; Gileadi et al., 1992; Gulyas and Donahue, 1992; Higgins et al., 1983; Naumovski and Friedberg, 1983; Park et al., 1992; Simon et al., 1986; Valay et al., 1993; Yoon et al., 1992). TFIIH functions as both a helicase and a kinase (Guzder et al., 1994; Lu et al., 1992); TFIIH helicase and kinase activities are both stimulated by the TFIIH-TFIIE interaction described above. These enzymatic activities, which in bacteria are contained within the RNA polymerase itself (Risher and Blumenthal, 1980; Wigneshweraraj et al., 2003), are required for transcription initiation. The TFIIH subunit Ssl2 provides the helicase activity that unwinds template DNA, allowing Pol II to locate the TSS (Guzder et al., 1994). Meanwhile, the Kin28 subunit provides the kinase activity and is responsible for the important Rpb1 CTD heptad repeat Ser 5 phosphorylation (Hengartner et al., 1998; Lu et al., 1992) described above.

The Role of Chromatin in Eukaryotic Transcription Regulation

The process of transcription in eukaryotic cells occurs on DNA that has been packaged into chromatin (Struhl, 1999). This chromatin compaction both allows the roughly 2m of DNA possessed by eukaryotic cells to fit inside a nucleus only microns in diameter and, as importantly, impacts transcription regulation (Venkatesh and Workman, 2015; Zaret and Carroll, 2011). Chromatin compaction is achieved through multiple levels of chromatin structure, the most basic and well understood of which is the nucleosome (Woodcock and Ghosh, 2010). A canonical nucleosome structure consists of 147bp of DNA wrapped 1.5 times around a histone octamer formed by two copies of each of the histone proteins H2A, H2B, H3, and H4 (Kornberg, 1974; Luger et al., 1997). Perhaps not surprisingly, the packaging of DNA into these nucleosome structures is largely inhibitory to transcription (Han and Grunstein, 1988; Lorch et al., 1987). This is due to the fact that most DNA binding proteins cannot recognize their cognate cis elements when packaged into a nucleosome (Archer et al., 1991; Morse, 2003; Simpson, 1990). Eukaryotic cells modulate this inhibitory effect in two ways: (1) altering nucleosome positioning and (2) nucleosome post-translational modification (summarized in **Figure 1.4A,B**).

The role of nucleosome positioning in transcription regulation is particularly evident in the case of genes whose activation requires nucleosome remodeling (see **Figure 1.4A**). These genes are conditionally silenced by the blocking of the binding sites for key transcription regulators with nucleosomes. For example, in budding yeast, the *PHO5* gene is repressed under phosphate rich conditions in part by nucleosome occlusion of both the promoter *TATA* element and a binding site for the Pho4 transcription activator (*UAS$_{PHO4}$*)(Almer and Hörz, 1986; Almer et al. , 1986; Bergman and Kramer, 1983; Bergman

et al., 1986; Venter et al., 1994). *PHO5* expression becomes activated when these nucleosomes are removed. In wild-type cells, the nucleosomes occluding *TATA* and *UAS_{PHO4}* DNA are removed by ATP-dependent chromatin remodeling factors, a class of enzymes that use the energy of ATP hydrolysis to remodel nucleosomes and includes the RSC, Swi/Snf, and INO80 complexes (Lorch and Kornberg, 2015), that are brought to *PHO5* under phosphate starvation conditions (Barbaric et al., 2007). Alternatively, *PHO5* activation may be achieved in the absence of phosphate starvation conditions by the genetic disruption of the histone chaperones responsible for maintaining the nucleosome occlusion of the *PHO5* promoter *TATA* and enhancer (i.e. *UAS_{PHO4}*) (Adkins and Tyler, 2006).

Figure 1.4. Nucleosome Positioning and Post Translational Modification Contribute to Transcription Regulation.
A, Model for how nucleosome positioning contributes to transcription. A nucleosome positioned over the promoter and TSS may block PIC formation. However, the action of ATP-dependent chromatin remodeling factors can reposition nucleosomes to create a nucleosome free promoter that can be bound by the GTFs (TFIID in light green, other GTFs same colors as in **Figure 1.3**) and Pol II (medium blue). *B*, Model for how nucleosome post-translational modification contributes to transcription. The +1 nucleosome (located just downstream of the promoter) is the target for nucleosome post-translational modifications. Histone code "writers" such as methyltransferases and acetyltransferases may add post-translational marks to the +1 nucleosome guided in part by the presence of H2A.Z in this nucleosome rather than H2A. These modified nucleosomes may serve as binding sites for GTFs (such as TFIID via the PHD domain of its Taf3 subunit or the YEATS domain of Taf14), which may enhance binding of the GTFs and therefore, Pol II, to the promoter.

Meanwhile, transcription of constitutively active genes seems to be aided by the placement of their promoters within nucleosome free regions (NFRs) (Choder et al., 1984; Jakobovits et al., 1980; Saragosti et al., 1980; Yuan et al., 2005). The mechanisms for establishing this NFR remain unclear, although three contributing components have been proposed (Venters and Pugh, 2009): (1) poly dA-dT tracts, which intrinsically disfavor nucleosome formation (Kunkel and Martinson, 1981; Prunell, 1982), (2) transcription factors that bind nucleosomal consensus sequences and open chromatin (Cirillo et al., 1998, 2002; Perlmann and Wrange, 1988; Yu and Morse, 1999; Zaret and Carroll, 2011), and (3) ATP-dependent chromatin remodelers. In a recent study, NFRs very similar to those observed *in vivo* were reconstituted *in vitro* using purified yeast genomic DNA, histones, the yeast transcription factors Abf1 and Reb1 that can affect chromatin structure (Ganapathi et al., 2011), and chromatin remodelers (Krietenstein et al., 2016). The difference between the nucleosome positioning observed *in vivo* and in the reconstituted system may be due to other factors that likely contribute to NFR maintenance and may refine NFR positioning such as PIC promoter occupancy, the act of Pol II transcription, and the activity of factors associated with the Pol II CTD.

The post-translational modification of the histone tails that protrude out of nucleosomes provides another avenue through which nucleosomes may affect transcription (**Figure 1.4B**). Nucleosome post-translational modification (PTM) may contribute to transcription in one of two ways: (1) by altering nucleosome structure or (2) by creating a binding site for a transcription factor (Bannister and Kouzarides, 2011). Many different histone PTMs (which include ubiquitylation, methylation, and acylation (commonly acetylation)), the protein factors that deposit/"write", remove/"erase", or

recognize/"read" them, and their impact on transcription have been studied. The +1

nucleosome (the nucleosome immediately downstream of the NFR) appears to be a "hub"

for post-translational modification, which may be guided at least in part by the H2A.Z

which replaces H2A at this nucleosome (Raisner et al., 2005). For example, deposition of

the H2BK123ub mark at the +1 nucleosome catalyzed by Rad6/Bre (Dover et al., 2002;

Hwang et al., 2003; Sun and Allis, 2002; Wood et al., 2003) is associated with transcription

activation, perhaps because its reported enhancement of nucleosome stability

(Chandrasekharan et al., 2009) improves the ability of proteins that contribute to activated

transcription to associate with this nucleosome. One of these proteins is the

Set1/COMPASS complex, which requires H2BK123ub to deposit the H3K4me3 mark

(Krogan et al., 2002; Miller et al., 2001) that is associated with actively transcribed gene

promoters (Pokholok et al., 2005; Roguev et al., 2001; Santos-Rosa et al., 2002; Strahl et al.,

1999) and is recognized by the Taf3 PHD (Lauberth et al., 2013; Vermeulen et al., 2007).

H4 acetylation at the 5' end of genes (Pokholok et al., 2005) catalyzed by the

acetyltransferase NuA4 is also associated with gene activation (Allard et al., 1999).

Meanwhile, H3K36me3 deposited by the Set2 methylase in gene bodies (Kizer et al., 2005;

Krogan et al., 2003; Strahl et al., 2002) helps repress spurious intragenic transcription by

creating a binding site for factors that help maintain nucleosome occupancy in the wake of

Pol II transcription (Carrozza et al., 2005; Keogh et al., 2005). Taken together, the studies

of these and other histone PTMs supports a model wherein "activating" and "repressing"

PTMs act together to influence appropriate access of transcription factors to the DNA

underlying nucleosomes.

Transfactors Confer Gene-Specific Transcription Regulation

Although the basal transcription machinery and chromatin clearly play important roles in transcription regulation, it is members of a class of proteins termed transfactors that confer gene specificity to transcriptional control by selectively responding to discrete cell-external and/or cell-internal molecular cues (Struhl, 1995). Transfactors, whose importance is underscored by the designation of some members of this class of proteins in metazoans as "master regulators" of development and differentiation (Chan and Kyba, 2013; Davis et al., 1987; Tapscott et al., 1988), achieve their effect on transcription regulation through the use of (minimally) two modular functionally distinct domains (Ptashne, 1988). One of these domains is a DNA-Binding Domain (DBD), the minimal protein domain required to bind the specific consensus sequence of a transfactor (Keegan et al., 1986), generally with extremely high affinity ($K_d = 10^{-11}\text{-}10^{-12}$ M) (Letovsky and Dynan, 1989; Sawadogo, 1988; Vignais et al., 1990; Wu et al., 1987).

Since transfactor-DNA binding largely determines which gene(s) that transfactor will regulate, many transfactor DBD structure characterization studies have been performed with the long-term goals of understanding how endogenous transfactors work and providing guidelines for the design of synthetic transcription factors (Todeschini et al., 2014). The characterization of >1500 protein-DNA complex structures have greatly improved our understanding of how DNA recognition is achieved. In general, these studies have revealed two modes of protein-DNA recognition: (1) base-readout, where a DBD directly recognizes DNA bases and (2) shape readout, where a DBD recognizes a sequence-dependent DNA shape (Rohs et al., 2010). Most transfactor DBDs possess one of three structural motifs, each of which uses both modes of protein-DNA recognition: (1) zinc-

finger, (2) helix-turn-helix/homeodomain, or (3) basic leucine zipper (bZIP) (Hahn and Young, 2011). Out of these, zinc-finger transfactors are the most abundant in yeast and human (Hahn and Young, 2011; Vaquerizas et al., 2009). Zinc finger DNA-binding has been described well enough to produce zinc-finger-DNA interaction codes that have been frequently utilized to generate zinc finger DBDs with altered DNA-binding specificity (Gupta et al., 2012; Nguyen et al., 2007; Sera and Uranga, 2002; Zhu et al., 2013). In contrast, there are only a few altered DNA-binding specificity variants that use the other structural motifs, including the leucine zipper DBD of yeast Gcn4 (Kim et al., 1993) and the helix-turn-helix DBD of λ phage Cro (Nilsson and Widersten, 2004).

DBD structure analyses have been complemented by *in vitro* selection and genomic DNA-binding approaches aimed at defining the sequences each transfactor can and does bind *in vivo* where, as described above, chromatin may occlude potential binding sites (Todeschini et al., 2014). As mentioned in the "DNA Elements Guide Pol II Transcription Regulation" section, these studies have defined the consensus sequences for many enhancer/silencer-binding transfactors (Jolma et al., 2013; Sandelin, 2004). However, some limitations in our understanding of what constitutes a binding site for a particular transfactor remain. For example, a recent study showed that the sequences recognized by the *Drosophila* Hox proteins is altered upon binding the Hox cofactor Extradentical (Exd), providing evidence that transfactor-cofactor interactions likely influence transfactor DNA recognition *in vivo* (Slattery et al., 2011). Recognition site flanking sequences, which can impact DNA recognition through influencing DNA shape readout (Gordân et al., 2013) and DNA-bendability (Leonard et al., 1997), represent another, perhaps underappreciated factor in protein-DNA recognition and transfactor activity.

In addition to a DBD, transfactors usually possess (at least one) activation domain (AD) and/or a silencing domain (SD) depending on whether a transfactor is a transcription activator, a transcription repressor, or both. ADs, whose structure and function will be detailed here due to the emphasis of my thesis project on transcription activation, are domains that generally activate transcription when fused to a DBD module. This DBD module can be either the transfactor's native DBD or, more frequently, a heterologous DBD such as that of the yeast Gal4 or bacterial LexA DBDs (Ma and Ptashne, 1987; Seipel et al., 1992). Essentially, ADs transmit the signal for activation to the rest of the transcription machinery (Ptashne, 1988), a process usually accomplished via direct interaction(s) between the domain and a transcription coregulator.

The ADs of several transfactors have been identified over the last ~30 years of study. ADs are typically 30-100 amino acids (aa's) in length; they can be classified into one of three groups based on the kinds of aa's that make up 20-25% of the domain: (1) acidic, (2) proline-rich, and (3) glutamine-rich (Mitchell and Tjian, 1989; Titz, 2006). Site-directed mutagenesis has been performed on members of all three AD groups in order to identify important AD aa's. These factors include the herpes virus activators VP16 and ZTA (aka ZEBRA), the mammalian activators Sp1, p53, and glucocorticoid receptor (GR), and the yeast activators Gcn4 and Gal4. These studies have generally revealed that, while the overall properties conferred by the dominant aa type do contribute somewhat to AD function, these ADs depend primarily on small clusters of 2-3 hydrophobic aa's, usually the aromatics Tryptophan (W), Tyrosine (Y), and Phenylalanine (F) (Almlöf et al., 1997; Cress and Triezenberg, 1991; Deng et al., 2001; Drysdale et al., 1995; Gill et al., 1994; Leuther et al., 1993; Lin et al., 1994; Regier et al., 1993).

Biophysical characterization of these ADs has demonstrated that these domains are unstructured in solution; however, upon interaction with a coregulator target, ADs appear to adopt an α–helical conformation around the important hydrophobic residues (Brzovic et al., 2011; Jonker et al., 2005; Krois et al., 2016; Radhakrishnan et al., 1997; Uesugi et al., 1997). Although among ADs, transcriptional activation correlates with the strength of AD-coregulator target binding (Chang et al., 1995; Warfield et al., 2014), direct AD-coregulator interaction is a low-affinity interaction, with the K_ds of 10^{-5}-10^{-7} M (Brzovic et al., 2011; Jonker et al., 2005; Krois et al., 2016). It has been hypothesized that this property of AD-coregulator binding may be important *in vivo* to permit transcription activators to dissociate from the transcription complex once transcription initiation has occured. It may also allow ADs to dissociate and bind a different coregulator target (Berlow et al., 2015; Jonker et al., 2005). Indeed, some ADs, such as viral activator VP16, bind multiple coregulators *in vitro*, although it is not clear which, if any, of these interactions are physiologically relevant (Jonker et al., 2005; Stringer et al., 1990; Vojnic et al., 2011). Meanwhile, ADs that have been so characterized (the yeast activators Gal4 and Gcn4) contact only a few coregulators *in vivo*, and not all of these interactions are required for transcription (Bhaumik and Green, 2003; Bhaumik et al., 2004; Fishburn et al., 2005; Reeves and Hahn, 2005).

Given that coregulator target binding is theoretically mediated primarily by just a few of the hydrophobic aa's in each AD, it is surprising that ADs display any specificity in coregulator binding/activity. Indeed, how so few aa's achieve any target binding specificity is a major unanswered question in the field of transcription (Hahn and Young, 2011). A recent study conducted by the Hahn lab attempted to address this question using synthetic

derivatives of a Gcn4 AD (Warfield et al., 2014). Consistent with previous analysis of the

VP16 AD (Cress and Triezenberg, 1991), these workers found that replacing the key Gcn4

AD hydrophobic aa's with different hydrophobic aa's negatively impacted AD activity,

reinforcing the notion that the particular identities of these aa's are critical determinants of

AD function (Warfield et al., 2014). These workers also found that adding extra

hydrophobic aa's to the Gcn4 AD increased AD activity and AD-coregulator binding without

fundamentally altering the structure formed between the AD and its coregulator target

(Warfield et al., 2014). While admittedly, these results leave open the question of how an

AD achieves coregulator target specificity, they do serve as a powerful reminder of the

importance of the key AD aa's in determining AD activity.

<u>Transcription Activation Mechanisms</u>

Identifying AD-coregulator interactions and understanding their mechanistic

outcomes is an active area of research (Green, 2005; Hahn and Young, 2011; Weake and

Workman, 2010). The biochemical processes that coregulators use to relay the signal from

the transfactor AD to the rest of the transcription machinery following the critical first step

of AD-coregulator interaction are not well understood. The identity of the particular

coregulator target may determine in part which processes are utilized. Indeed,

transcription coregulators are a diverse class of proteins that can be classified as either

coactivators or corepressors depending on whether the signal they relay from the

transfactor to the rest of the transcription machinery triggers activation or repression.

Some characterized coregulators like TFIIA and TFIID are obligate, critical components of

the transcription machinery (Chen et al., 1994; Kobayashi et al., 1995; Lieberman, 1994;

Lieberman et al., 1997; Ozer et al., 1996; Tanese et al., 1991), whereas others such as SAGA,

Mediator, Swi/Snf, p300, Rpd3, and OCA-B target chromatin and/or other coregulators

(Brownell et al., 1996; Kadosh and Struhl, 1998; McKenna et al., 2015; Meyer et al., 2010;

Ren et al., 2011; Tomar et al., 2008; Wallberg et al., 2002). Based on studies of both

prokaryotic (Browning and Busby, 2004) and eukaryotic transcription (Ptashne and Gann,

1990), two models of transcription activation have been proposed to explain how AD-

coregulator interaction affects PIC activity: (1) "recruitment"/cooperative binding and (2)

conformational change (**Figure 1.5**).
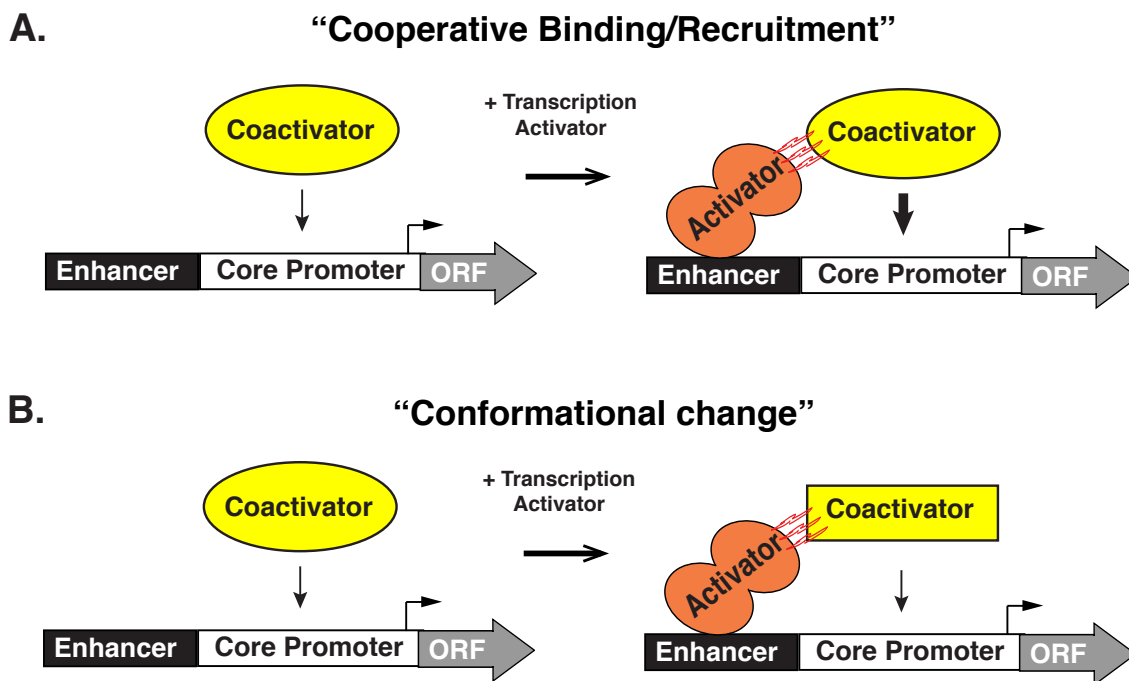
Figure 1.5. Mechanisms of Transcription Activation. *A*, The "Cooperative binding/Recruitment" model of transcription activation. In this model of activation, a coactivator displays at best weak binding to a gene promoter. However, direct interaction between an enhancer DNA-binding transcription activator and the coactivator greatly enhancers coactivator association with the target gene. "Recruitment" of this coactivator may then either indirectly enhance transcription by creating a more favorable chromatin environment or directly enhancing transcription by completing a rate-limiting step in PIC formation *B*, The "Conformational change" model of transcription activation. In this model, a coactivator may associate with a target gene independently. However, the key step in this model is a coactivator conformational change driven by direct interaction between the activator and coactivator. This conformational change may occur either off DNA (as shown here) or on DNA.

The "recruitment"/cooperative binding model (**Figure 1.5A**) was the first proposed

and is the best-studied activation mechanism (Hahn and Young, 2011; Klein and Struhl,

1994a; Ptashne and Gann, 1997; Pugh and Tjian, 1990). In this model, PIC

formation/function is enhanced as a result of cooperative binding of a transcription

activator and a coactivator to target gene DNA. Because this cooperative binding occurs

due to a direct binding interaction between a DNA-bound transcription activator AD and

the coactivator, the activator is said to "recruit" the coactivator to the target gene. Early

support for this model was provided by a series of *in vivo* studies that achieved dramatic

enhancement of transcription in yeast using artificial proteins generated by fusing a DBD to

subunits of three multi-subunit coactivator complexes considered important because

essentially all protein-coding genes depend on at least one of them: TFIID, SAGA, and

Mediator (Andrau et al., 2006; Basehoar et al., 2004; Chatterjee and Struhl, 1995; Holstege

et al., 1998; Huisinga and Pugh, 2004; Keaveney and Struhl, 1998; Klages and Strubin,

1995; Xiao et al., 1995). Since then, studies of native activation have provided evidence

that enhanced coactivator binding to a target gene can stimulate PIC formation/function

either indirectly by creating a favorable chromatin environment or by directly contributing

to PIC formation.

The transcription activation of the yeast *PHO5* gene described previously serves as

an example of a transcription activation mechanism wherein coactivator recruitment

indirectly stimulates PIC formation/function. Under phosphate starvation conditions, the

PHO5 transcription activator protein Pho4 enters the nucleus of the cell and binds its

recognition sequence (*UAS_{PHO4}*) located upstream of the *PHO5* ORF (Barbaric et al., 1998;

O'Neill et al., 1996). Once there, Pho4 does not need to interact with the general

transcription machinery to activate *PHO5*. Instead, its interaction with chromatin-

modifying factors results in the eviction of *PHO5* promoter nucleosomes such that the PIC

is able to form on the *PHO5* promoter and initiate transcription (Barbaric et al., 2007;

Gregory et al., 1999; Svaren et al., 1994) (*cf* **Figure 1.4A**). Indeed, as stated above, simply

remodeling *PHO5* promoter nucleosomes results in *PHO5* activation in the absence of the

Pho4 transcription activator (Adkins and Tyler, 2006).

Meanwhile, given that TBP, which is a subunit of both TFIID (Sanders et al., 2002a)

and SAGA (Grant et al., 1997), nucleates PIC formation (Buratowski et al., 1989) and the

proposed requirement of Mediator for transcription initiation *in vivo* (Koleske and Young,

1994), it is thought that activator recruitment of these coactivators stimulates

transcription primarily by directly increasing PIC formation/function. Early support for

this model came from work performed by the Tjian lab using the *Drosophila* model system

demonstrating that TBP-Taf complex recruitment to the promoter required transcription

activator ADs and specific Taf subunits (Sauer et al., 1995a, 1995b). Although not direct

tests of cooperative binding, other *in vivo* evidence consistent with the direct recruitment

model comes from ChIP studies showing that the yeast activators Gal4 and Gcn4 as well as

their respective coactivator targets SAGA and Mediator are required for coactivator

occupancy and target gene transcription (Bhaumik and Green, 2001; Bhaumik et al., 2004;

Herbig et al., 2010; Jedidi et al., 2010; Larschan and Winston, 2001). Finally, perhaps the

best evidence for native activator-dependent coactivator recruitment directly enhancing

PIC activity comes from a recently published study of transcription regulation by human

TFIID and HEB, a transcription activator that regulates cell-fate determination (Chen et al.,

2013). This study identified regions of both HEB and the TFIID subunit Taf4 required for

HEB-TFIID interaction and transcription of HEB-dependent genes. Most importantly, this

study also demonstrated via gel shift, immobilized template assay, and DNase footprinting

that HEB-Taf4 interaction was required for cooperative binding of TFIID to enhancer-

promoter DNA (Chen et al., 2013).

In addition to coactivator "recruitment," direct activator-coactivator interaction has

been proposed to stimulate transcription via triggering a conformational change (**Figure

1.5B**). Evidence for this model of transcription activation comes from electron microscopy

(EM) structural analyses of complexes formed between Mediator and several mammalian

activator proteins, including VP16, SREBP, p53, thyroid receptor (TR), and vitamin D

receptor (VDR) (Meyer et al., 2010; Taatjes et al., 2002, 2004). The structure of Mediator in

these activator-Mediator complexes is different from the structure of Mediator alone;

interestingly, Mediator structure varies even among the different activator-Mediator

complexes (Taatjes et al., 2002, 2004). Activator-Mediator binding has also been shown via

mass spec to enable Mediator interaction with other coactivators (Ebmeier and Taatjes,

2010). How these Mediator conformational changes and changed Mediator-cofactor

interactions affect PIC activity (or even if they occur in functional transcription complexes)

is currently unclear. A recent EM structural analysis of p53 and Mediator showed that the

p53 domain required for activation triggered the formation of a pocket within Mediator.

Since this pocket was located in the region of Mediator that binds Pol II, these investigators

proposed that pocket formation enabled the enhanced Pol II promoter escape observed in

the presence of p53 (Meyer et al., 2010). However, the affect of p53 on Mediator-Pol II

binding was not tested biochemically. More information regarding how Mediator achieves

conformational changes is needed in order to generate Mediator mutants defective in

conformational change that can be used to test the transcriptional consequences of Mediator conformational change in both *in vitro* and *in vivo* assays.

<div align="center">TFIID Structure and Coactivator Function</div>

While the cooperative binding and conformational change models may generally describe much of Pol II transcription activation, neither model has been rigorously tested using iterative genetic, biochemical, and structural approaches. Further, much of the data supporting both models was obtained using deletion variants of the transcription activators and coactivators in question. Such mutants provide imprecise tools for dissecting the mechanistic consequences of activator-coactivator binding. More rigorous testing should be performed using coactivator, and most importantly, transcription activator AD point mutant variants. Such rigorous testing is particularly warranted for the TFIID coactivator whose function is required for 90% of protein-coding yeast genes (Huisinga and Pugh, 2004) and whose multiple subunits make contacts critical for both transcription activation and for structural integrity of the TFIID complex.

As stated in "Basal Transcription Factors," the TFIID structure formed by its many subunits may make it ideally suited to serve the coactivator function. The yeast TFIID used for my project is a 1.2MDa complex consisting of TBP and 14 Taf subunits (Taf1 → 14) (Sanders and Weil, 2000; Sanders et al., 2002a) (**Figure 1.6A**). The genes encoding all TFIID subunits except for *TAF14* are essential (Klebanow et al., 1996, 1997; Moqtaderi et al., 1996; Poon et al., 1995; Ray et al., 1991; Reese et al., 1994; Sanders and Weil, 2000). Tafs 4, 5, 6, 9, 10, and 12 are present in two copies within TFIID and Taf14 is present at potentially more than two copies (Sanders et al., 2002a) (**Figure 1.6B**).
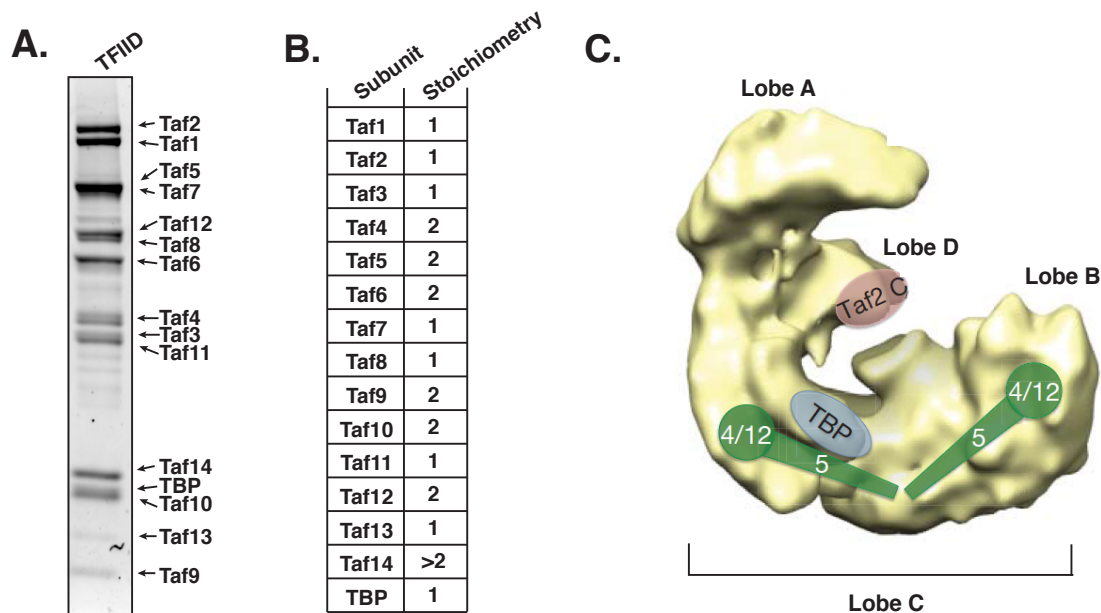
Figure 1.6. Yeast TFIID Structure and Subunit Composition. *A*, TFIID subunit (Taf1 → Taf14 and TBP) composition as revealed by SDS-PAGE and Sypro-Ruby staining of TFIID. This TFIID was purified by Dr. Jordan T. Feigerle. *B*, TFIID subunit stoichiometry (mole subunit/mole TFIID) as determined by quantification of each subunit on a stained SDS-PAGE gel. *C*, The structure of the TFIID complex obtained at a resolution of 23 Angstroms using cryo-EM (image adapted from Papai et al., 2010). The four lobes (A, B, C, and D) are indicated. Additionally, the localization of a few of the Taf subunits/Taf domains, including Tafs 4, 5, and 12, which are important for the work presented in this dissertation, is indicated.

Cryo-Electron microscopy (Cryo-EM) analyses of yeast TFIID structure have revealed that TFIID exists as an asymmetric structure resembling a catcher's mitt (Papai et al., 2009, 2011). This mitt shape has been divided into 4 lobes: A, B, C, and D (**Figure 1.6C**). Using immunolabeling and difference mapping, the locations of all TFIID subunits except Taf14 have been roughly mapped within the context of the TFIID structure. With few exceptions, localization of all TFIID subunits is consistent with their known biochemically-defined stoichiometry and subunit interactions (Birck et al., 1998; Gangloff et al., 2001; Hisatake et al., 1995; Sanders et al., 2002a; Selleck et al., 2001; Werten et al., 2002). EM structural analyses of human TFIID show that it too forms a similar four-lobed structure (Bieniossek et al., 2013a; Louder et al., 2016). Indeed, biochemical, structural, and

33

bioinformatics analyses of TFIID and its subunits have repeatedly demonstrated that TFIID

structure and function are highly conserved in all eukaryotes (Bai et al., 1997; Bieniossek et

al., 2013b; Birck et al., 1998; Durso et al., 2001; Gangloff et al., 2001; Hisatake et al., 1995;

Klebanow et al., 1997; Louder et al., 2016; Malkowska et al., 2013; Matangkasombut et al.,

2000; Papai et al., 2009; Scheer et al., 2012; Trowitzsch et al., 2015; Werten et al., 2002)

(**Figure 1.7**).

      While TBP and some of the Taf subunits may be important for promoter DNA-

binding, TFIID coactivator function occurs through direct interaction between Tafs and

activator proteins.

Early studies performed in metazoan systems by the Tjian lab have shown that TBP alone

does not respond to transcription activators; instead TFIID Tafs are required for activated

transcription (Dynlacht et al., 1991; Pugh and Tjian, 1990; Tanese et al., 1991). Several

lines of evidence suggest that Tafs are required for activated transcription because of their

direct interaction with activators. The metazoan activators Sp1, p53, NTF-1, and c-Jun all

interact directly with Tafs (Chen et al., 1994; Liu et al., 2009; Thut et al., 1995). Meanwhile,

transcription levels are eliminated/reduced in the absence of the direct Taf target of these

activators within TFIID sub-complexes formed *in vitro* and/or by an activator AD mutation

that reduces activator binding to its Taf target (Chen et al., 1994; Gill et al., 1994; Thut et al.,

1995).

      Based on the results of these direct activator-Taf interaction studies, the

requirement of TBP promoter association for PIC formation (Buratowski et al., 1989), and

the observed correlation between TBP occupancy and transcription (Kuras and Struhl,

1999), it has been hypothesized that activator-mediated "recruitment" of TBP via TFIID

Subunit Structure		TFIID Specific?	Conserved Functional Characteristics
hTaf1	Kin/TAND HAT Doublebromo Kin 1827	Yes	TBP Interaction/ Negative Regulation, Scaffold for TFIID Assembly
scTaf1	Kin/TAND 1066		
hTaf2	Amino Peptidase IDR 1199	Yes	?
scTaf2	Amino Peptidase IDR 1407		
hTaf3	HF D PHD 929	Yes	Dimerizes with Tafs 8 and 10 Via the HFD
scTaf3	HF D 353		
hTaf4	HF D 1085	Yes	Dimerizes with Taf12 Via the HFD
scTaf4	HF D 388		
hTaf5	WD40 800	No	WD40 Repeats Interact With Taf6/9 Heterodimers
scTaf5	WD40 798		
hTaf6	HFD HEAT Repeats 677	No	Dimerizes with Taf9 Via the HFD
scTaf6	HFD HEAT Repeat		
hTaf7	349	Yes	Interacts with Taf1 C-Terminus
scTaf7	590		
hTaf8	HFD 310	Yes	Dimerizes with Taf3 Via the HFD
scTaf8	HFD 510		
hTaf9	HFD 264	No	Dimerizes with Taf6 Via the HFD
scTaf9	HFD 157		
hTaf10	HFD 218	No	Dimerizes with Taf3 Via the HFD
scTaf10	HFD 206		
hTaf11	HFD 211	Yes	Dimerizes with Taf13 Via the HFD
scTaf11	HFD 346		
hTaf12	HFD 162	No	Dimerizes with Taf4 Via the HFD
scTaf12	HFD 540		
hTaf13	HFD 124	Yes	Dimerizes with Taf11 Via the HFD
scTaf13	HFD 167		
hTBP	CORE 339	No	Binds the TATA Promoter Element
scTBP	CORE 240		

Figure 1.7. Structure and Function Conservation of TFIID Subunits. Schematics of the primary sequence information derived from UniProt of the conserved TFIID subunits (Taf1 → Taf13) and TBP from human (h) and *Saccharomyces cerevisiae* (sc) are shown, along with notes on conserved function and whether or not the subunit is exclusive to TFIID. Conserved sequences are highlighted in red, while non-conserved sequences are indicated by white boxes or empty regions. Functional domains are indicated. Kin = Kinase, TAND = Taf1 N-terminal Domain, HAT = Histone Acetyl Transferase, IDR = Intrinsically Disordered Region, WD40 = WD40 Repeats, HFD = histone fold domain, CORE = highly conserved (90%) TBP C-terminal sequence.

Taf-activator interaction represents a likely mechanism of transcription regulation. Consistent with this idea, as described in "Transcription Activation Mechanisms," the Tjian lab showed that *Drosophila* activator-TFIID Taf interaction enhanced TFIID promoter binding (Sauer et al., 1995a, 1995b). The mammalian ETO-Taf4 also described in "Transcription activation mechanisms" (Chen et al., 2013) and an acetylated p53-Taf1 interaction study (Li et al., 2007) have also demonstrated that TFIID coactivator function operates via the direct recruitment/cooperative binding mechanism.

TFIID may indeed coactivate transcription via recruitment in the cases described above. However, observations made by other studies raise the possibility that cooperative binding/"recruitment" is not the exclusive mechanism by which TFIID coactivates gene transcription. First, one yeast study performed using chimeric reporter genes demonstrated that it was the promoter, not the enhancer binding site for a transcription activator, that determined whether a gene was TFIID-dependent or SAGA-dependent (Cheng et al., 2002), suggesting that these coactivators may bind promoter DNA independently of their recruitment by activators. Second, although EM analyses of the metazoan p53-TFIID, c-Jun-TFIID, and Sp1-TFIID complexes showed no dramatic TFIID conformational changes (Liu et al., 2009), another study revealed via DNase I footprinting that a TFIIA-TFIID-DNA isomerization step mediated by the Epstein-Barr virus transcription activator ZEBRA was required for PIC assembly and transcription activation (Chi and Carey, 1996). This isomerization step may represent a conformational change missed in the TFIID EM analyses either due to the use of different activator proteins or the absence of TFIIA and/or DNA. Finally, the Nogales lab has found that human TFIID binds promoter DNA in a rearranged conformation (Cianfrocco et al., 2013; Louder et al., 2016),

and conversion to this rearranged conformation is enhanced in the presence of the p53

activator (Coleman et al., 2017). Taken together, these observations support continued

investigation of TFID coactivator function to determine whether it operates via

recruitment, conformational change, or both mechanisms of transcription activation.

Although essentially all of the discoveries regarding TFIID coactivator function to

date have been derived from metazoan systems, yeast provides an excellent model system

for continued investigations of TFIID coactivator function. As stated above, the discoveries

in metazoans systems were made using deletion mutant variants. While important findings

can and have been uncovered using such variants, studies performed using such deletion

variants do suffer from some amount of imprecision, particularly when an AD-coactivator

interaction involves multiple ADs and/or coactivator targets. In yeast, it has historically

been much faster and easier to generate mutants, particularly the point mutant variants

required for rigorous activation mechanism testing. Importantly, it is also relatively easy in

yeast to perform iterative and complementary genetic, biochemical, and biophysical

experiments to carefully characterize such point mutant variants. Additionally, in contrast

to metazoan cells whose TFIID subunit composition may vary (Fong et al., 2012), the

composition of yeast TFIID appears to be largely invariant (Sanders and Weil, 2000). The

reliability of yeast TFIID existing in a defined subunit composition and stoichiometry

greatly facilitates the design of experiments to carefully test TFIID coactivator function.

Meanwhile, the evolutionary conservation of TFIID in all eukaryotes suggests that

discoveries made in yeast are likely generalizable to metazoans. The Weil lab began

pursuing investigations of TFIID coactivator function in yeast prior to my joining the lab for

precisely these reasons.

Transcription Regulation of the TFIID-Dependent Ribosomal Protein (RP) Genes

As a first step to investigate TFIID coactivator function in budding yeast, our lab sought a gene or set of genes for which TFIID served as a coactivator. The RP gene regulon emerged as a candidate set of genes likely to meet this criterion. Multiple studies have demonstrated that this gene regulon, which consists of the 138 genes that encode the protein components of the ribosome (Warner, 1999), depends on TFIID (Garbett et al., 2007; Holstege et al., 1998; Irvin and Pugh, 2006; Kuras et al., 2000; Layer and Weil, 2013; Layer et al., 2010; Li et al., 2000, 2002; Mencía et al., 2002; Ohtsuki et al., 2010; Papai et al., 2010; Shen and Green, 1997; Shen et al., 2003; Singh et al., 2004; Tsukihashi et al., 2001). Additionally, TFIID occupancy can be conferred on a reporter containing a TFIID-independent promoter by fusing this reporter gene to two binding sites for the transcription factor Repressor Activator Protein 1 (Rap1) derived from an RP gene (Garbett et al., 2007; Li et al., 2000; Mencía et al., 2002). This occupancy is likely achieved through direct interaction between TFIID and Rap1 (Garbett et al., 2007; Layer and Weil, 2013; Layer et al., 2010; Papai et al., 2010). Rap1 binding sites are required for transcription of 93% of the RP genes (Knight et al., 2014; Lieb et al., 2001; Rudra and Warner, 2004), and thus, part of the observed RP gene dependence upon TFIID is likely to be due to a coactivator function triggered through direct interaction with Rap1.

In addition to their observed TFIID dependence, the yeast RP genes also possess several characteristics that make them an interesting case study for transcription activation. Since the RP genes represent the protein component of the translation machinery, a basic requirement for cell life and growth, the cell dedicates prodigious resources to their transcription regulation. Indeed, RP gene transcription has been

estimated to account for up to 50% of all Pol II initiation events in the yeast cell during log phase growth, making this gene class one of the most robustly transcribed gene classes in the cell (Warner, 1999). These genes are coordinately regulated to ensure generation of a functional ribosome (Lempiäinen and Shore, 2009) and transcription is tightly coupled to growth and nutrient signals to ensure that the correct amount of ribosomes for a given condition is produced (Marion et al., 2004; Rudra and Warner, 2004; Rudra et al., 2005; Schwalder et al., 2004; Wade et al., 2004a).

Although little is known regarding RP gene transcription in metazoans aside from their similar transcription output requirements (Rudra and Warner, 2004) and apparent TFIID-dependence (ENCODE Project Consortium, 2012), many of the factors that guide RP gene regulation in yeast have been identified and described. One of these factors is Rap1, which, as described above occupies the enhancer element of 129 out of 138 of the RP genes (Knight et al., 2014; Lieb et al., 2001; Rudra and Warner, 2004). 54 of these genes have one Rap1 binding site while the other 75 have two Rap1 binding sites (Knight et al., 2014). Rap1 binding to RP genes is a prerequisite for binding of the other RP gene transcription factors (Hall et al., 2006; Knight et al., 2014; Zhao et al., 2006), a role achieved perhaps through its possible nucleosome remodeling activity (Ganapathi et al., 2011). The 8 RP genes that aren't occupied by Rap1 depend on the transcription factor Abf1 instead for this activity. (Ganapathi et al., 2011; Knight et al., 2014). The DNA binding factor Hmo1 binds the enhancer of many of the RP genes, and where it binds, is required for the DNA-binding of another RP gene transcription factor Fhl1 (Hall et al., 2006; Knight et al., 2014). Fhl1 also occupies RP genes that don't bind Hmo1, suggesting that there must also be Hmo1-independent mechanisms of Fhl1 DNA-binding (Knight et al., 2014; Reja et al., 2015).
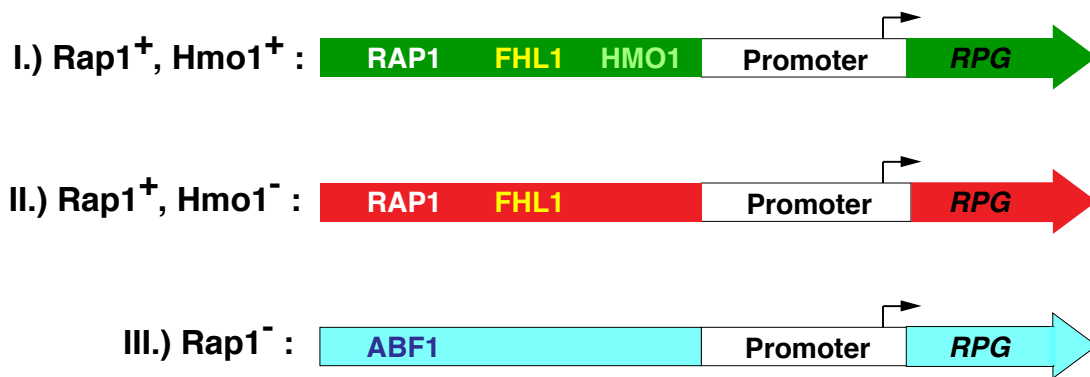
Figure 1.8. Three Types of RPGs. Schematics of the three types of RP genes as defined by recent genomic analyses. RP genes are divided into one of these three categories based on the occupancy of the DNA-binding factors Rap1, Fhl1, and Abf1. Category I contains 69 members, Category II contains 60 members, and Category III contains 9 members. Although only one Rap1 binding site is indicated here, several Category I and Category II RP genes contain two Rap1 binding sites.

Unlike Rap1 and Hmo1, Fhl1, and the transcription factor it recruits via its forkhead-associated domain to RP genes, Ifh1 (Wade et al., 2004a), exclusively participate in RP gene transcription and are therefore thought to modulate some of the unique characteristics of RP gene regulation. Indeed, the results of several studies show that Ifh1 plays the important roles of linking RP gene transcription to stress, nutrient signaling, Pol I transcription of rRNA, and Pol III transcription of 5S rRNA (Albert et al., 2016; Rudra et al., 2005; Schwalder et al., 2004; Wade et al., 2004a). Other important RP gene transcription regulators include the transcription factor Sfp1, which aids in the RP gene transcriptional response to stress and nutrient signals (Marion et al., 2004), and the histone acetyltransferase NuA4 (Allard et al., 1999; Reid et al., 2000; Uprety et al., 2016).

Based on which of these factors are bound to its *UAS*, each of the RP genes has been recently classified into one of three types: Category I (Rap1^{+}, Hmo1^{+}), Category II (Rap1^{+}, Hmo1^{-}), and Category III (Rap1^{-}, dependends on Abf1) (**Figure 1.8**) (Knight et al., 2014; Reja et al., 2015). Recent genomic analyses of RP gene *UAS*-promoter architectures

identified an interesting feature of all three types of RP genes; the *UAS*-promoter is unusually MNase sensitive (Knight et al., 2014; Reja et al., 2015). A later study detected MNase sensitivity at other promoters and correlated MNase sensitivity with robust transcription levels, such as those observed from the RP gene regulon (Kubik et al., 2015). Using genomic analyses, synthetic chimeric genes, and Rap1 anchor away, this study showed that promoter DNA and the transcription factor Rap1 contribute to the formation of an unusually MNase sensitive region upstream of RP gene ORFs (Kubik et al., 2015). This MNase sensitive region was proposed to represent a "fragile nucleosome" whose occupancy on RP gene promoters is unusually weak (Knight et al., 2014; Kubik et al., 2015). These authors hypothesize that generation of fragile nucleosomes by chromatin remodeling plays a key role in mediating high-level RP gene transcription. By contrast, another study speculated that RP genes instead possess an unusually long NFR, where the MNase sensitive region represents the binding of Fhl1, Ifh1, Sfp1, and Hmo1 instead of a nucleosome (Reja et al., 2015). Either mechanism points to the critical importance of Rap1 in RP gene transcription as proposed by earlier studies demonstrating that Rap1 is the only activator absolutely required for transcription of the RP genes (Garbett et al., 2007; Mencía et al., 2002; Schwalder et al., 2004; Wade et al., 2004a). Thus, Rap1 is the key to unlocking the molecular mechanism of RP gene transcription activation. To determine whether it is interaction with the TFIID coactivator, chromatin remodeling, and/or enhanced binding of the other RP gene transcription factors that are the main drivers of high-level RP gene transcription, the Rap1 AD must be mapped and its direct coactivator targets must be identified.

<u>Repressor Activator Protein 1 (Rap1) Structure and Interaction with TFIID</u>

The Rap1 transfactor was originally identified over 30 years ago as a budding yeast RP gene enhancer-binding protein (Huet et al., 1985). Budding yeast Rap1 is encoded by an essential gene (Shore and Nasmyth, 1987). As the name "Repressor Activator Protein 1" implies, Rap1 performs both key repression and activation functions in the cell. In addition to its role in RP gene transcription activation described above, Rap1 plays critical roles in the transcription activation of the SAGA-dependent glycolytic enzyme (GE)-encoding genes (Basehoar et al., 2004; Chambers et al., 1989, 1995), telomere stabilization, meiotic DNA recombination and mating type locus silencing (Morse, 2000; Shore, 1994). Consistent with these diverse activities, genome-wide microarray and ChIP studies have documented the presence of Rap1 on RP genes, GE genes, telomeres, and even some genes required for Pol I and Pol III transcription (Lickwar et al., 2012a; Lieb et al., 2001; Rhee and Pugh, 2011). Many structure-function studies have been performed on Rap1 since its discovery in order to shed light on how Rap1 contributes to these diverse cellular activities. These analyses divide the 827 aa Rap1 protein into three major domains: a central DBD (aa's 361-599 (Henry et al., 1990)), an N-terminus (aa's 1-360), and a C-terminus (aa's 600-827) (**Figure 1.9A**).

Of these three major domains, the DBD is probably the best understood in terms of DNA binding site, structure, and activity. Rap1 recognizes its DNA binding site via its DBD with an affinity comparable to those observed for other transcription factors (K_d = 1.3×10^{-11} M) (Vignais et al., 1990). This DBD is the only essential domain of Rap1, although yeast expressing just the Rap1 DBD are extremely slow growing (Garbett et al., 2007; Graham et al., 1999). Several studies of the DNA sequence element recognized by the Rap1 DBD

(*UAS_Rap1*) have been conducted. These studies have defined a 13-base pair *UAS_Rap1* consensus sequence 5'-$(A/G)_1(C/A)_2A_3(C/T)_4C_5C_6(A/G)_7(C/A)_8N_9C_{10}A_{11}(C/T)_{12}(C/T)_{13}$-3' (Lascaris et al., 1999; Lieb et al., 2001; Vignais et al., 1990) and determined the contribution of each consensus sequence nucleotide to Rap1-*UAS_Rap1* DNA-binding (Vignais et al., 1990) and Rap1-dependent reporter gene activity (Nieuwint et al., 1989). Biologically important functional differences in the sequences of *UAS_Rap1* sites involved in transcription activation, transcription repression, and telomere functions have also been identified (Idrissi et al., 1998, 2001; Kasahara et al., 2007a; Lickwar et al., 2012b; Vignais et al., 1987).

Multiple co-crystal structures of the Rap1 DBD (Henry et al., 1990) in complex with DNA have been solved, shedding light on how Rap1 achieves *UAS_Rap1* recognition. These structures revealed that the Rap1 DBD is composed of two very similar homeodomain motifs and an unstructured tail that make multiple specific protein-DNA contacts
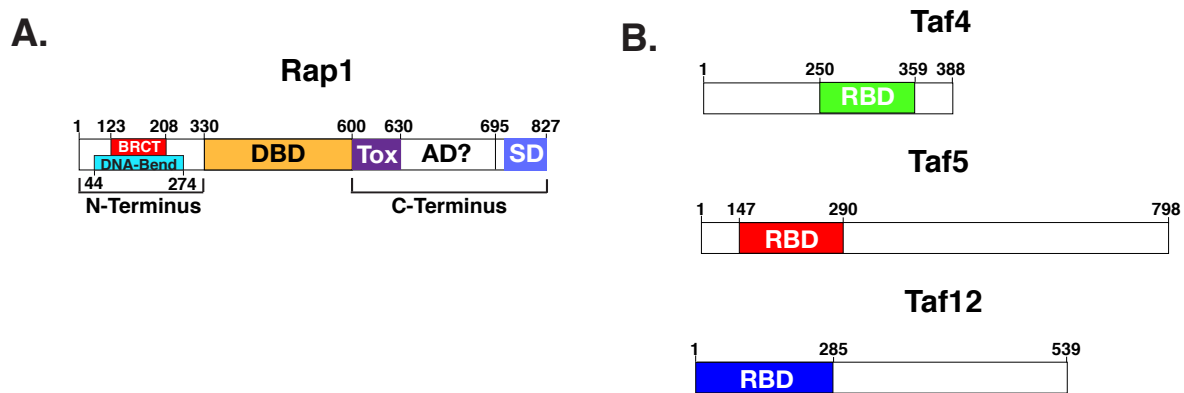
Figure 1.9 Map of Known Rap1 Functional Domains and TFIID Taf4, 5, and 12 subunit Rap1 Binding Domains (RBDs). *A*, Rap1 is divided into three major domains: an N-terminus, a central DBD, and a C-terminus (aa locations indicated). The non-essential N-terminus is further subdivided into overlapping BRCT and DNA-Bending (DNA-Bend) domains. The C-terminus is subdivided into Tox, SD, and a possible AD (labeled AD?). *B*, Localization of the RBDs in the TFIID subunits shown to interact directly with Rap1 (Tafs 5, 12, and 4) to activate RP gene transcription. With the exception of Taf12, these RBDs are located in aa that are essential and conserved.

throughout the Rap1-DNA complex (König et al., 1996; Matot et al., 2012; Taylor et al., 2000). These contacts do not appear to vary radically among the complexes formed between Rap1 and variant UAS_{Rap1} sites (Taylor et al., 2000). Rap1 must also be able to form most of these contacts with UAS_{Rap1} sites when they are occluded by a nucleosome since Rap1 is capable of efficiently binding nucleosomal UAS_{Rap1} sites *in vitro* and *in vivo* (Koerber et al., 2009; Rossetti et al., 2001). The ability of Rap1 to bind nucleosomal UAS_{Rap1} sites may be key to Rap1-driven transcription activation, at least for the *HIS4* gene where the Rap1 DBD alone is sufficient to open chromatin and activate transcription (Ganapathi et al., 2011; Yu and Morse, 1999; Yu et al., 2001).

Unlike the Rap1 DBD, the Rap1 N-terminus appears completely dispensable since deletion of the Rap1 N-terminus has no obvious effect on cell growth (Graham et al., 1999). Although its lack of impact on growth suggests that the Rap1 N-terminus does not contribute critically to Rap1 essential cellular activities, a few studies have proposed functions for the Rap1 N-terminus. An early study implicated aa's 44-274 in Rap1 DNA-bending activity (Müller et al., 1994). Meanwhile, sequence alignments have identified a Breast Cancer 1 C-terminal (BRCT) domain within aa's 121-208 of the Rap1 N-terminus (Callebaut and Mornon, 1997; Zhang et al., 2011), and a Gal4 DBD-Rap1 BRCT domain fusion protein weakly activates transcription and remodels chromatin (Miyake et al., 2000). Although this transcription activation effect could be artificial, the results of other analyses are consistent with a role for the Rap1 N-terminus in the activation of some Rap1-dependent genes. The Rap1 N-terminus facilitates binding of the glycolytic transcription activator glycolysis regulatory protein 1 (Gcr1) to DNA (López et al., 1998), and Rap1 N-terminal deletion results in synthetic lethality when combined with *GCR1* deletion (Mizuno

et al., 2004). Thus, the Rap1 N-terminus may contribute to glycolytic gene transcription activation, perhaps via its BRCT domain.

Like the N-terminus, the Rap1 C-terminus is not essential, although cells that lack the Rap1 C-terminus display a very slow growth phenotype (Garbett et al., 2007; Graham et al., 1999). Studies of the Rap1 C-terminus have divided it into three partially overlapping regions: (1) a Tox domain (aa's 596-630) whose deletion abolishes Rap1 over-expression toxicity (Freeman et al., 1995), (2) a silencing domain (SD) located in the very C-terminus (Chen et al., 2011; Feeser and Wolberger, 2008; Graham et al., 1999; Kyrion et al., 1992; Moretti et al., 1994a), and (3) a potential activation domain (aa's 630-695) (Hardy et al., 1992a). Although SD deletion has little reported impact on cell viability (Chen et al., 2011; Feeser and Wolberger, 2008; Graham et al., 1999; Kyrion et al., 1992; Moretti et al., 1994a), it is important for multiple telomere functions as well as *HML/HMR* mating type silencing (Feeser and Wolberger, 2008; Kyrion et al., 1992). The SD achieves these functions through direct binding of the silent information regulator (Sir) and Rap1 interacting factor (Rif) proteins, which serve to modulate telomere length and repress gene transcription (Chen et al., 2011; Feeser and Wolberger, 2008; Hardy et al., 1992b, 1992a; Kyrion et al., 1992; Moretti et al., 1994a). Meanwhile, the potential Rap1 AD was mapped using Gal4 DBD-Rap1 fusion proteins (Hardy et al., 1992a). Deletion of these potential AD aa within the context of the intact Rap1 protein does induce slow growth; however, mRNA transcript analysis actually revealed an increase in transcript levels of the RP genes tested over wild-type (Graham et al., 1999). Additionally, several studies performed after the original Gal4 DBD-Rap1 fusion AD mapping reported that Rap1-heterolgous DBD fusions fail to robustly drive reporter gene transcription *in vivo* (Klein and Struhl, 1994b; Mencía et al., 2002; Zhao

et al., 2006). These data, especially in light of studies demonstrating the sufficiency of the

Rap1 DBD in *HIS4* activation (Ganapathi et al., 2011; Yu and Morse, 1999; Yu et al., 2001),

left open the questions of whether or not Rap1 possessed an AD, and if so, what Rap1 aa's

constituted such an AD.

      Because of the ambiguity regarding the existence of a Rap1 AD, the Weil lab began

investigating the possibility of RP gene activation driven by direct Rap1-TFIID interaction

encouraged by the multiple demonstrations of the absolute dependence of RP gene

transcription on Rap1 (Schwalder et al., 2004; Wade et al., 2004a), the observation that

Rap1 binding sites were necessary and sufficient for TFIID promoter occupancy (Mencía et

al., 2002), and the opportunity to dissect TFIID coactivator function in yeast. These efforts

were rewarded; direct Rap1-TFIID interaction ($K_{d,app}$ = ~300nM) was detected via pull-

down assay. Further pull-down assays performed using Rap1 truncation mutants revealed

that this Rap1-TFIID interaction depended upon both the Rap1 DBD and the Rap1 C-

terminus. Meanwhile, far western analyses revealed that Rap1-TFIID interaction occurred

via TFIID Taf subunits 4, 5, and 12 (Garbett et al., 2007). The mapped Rap1 Binding

Domain (RBD) of Taf12 was not essential, however, mutation of the Tafs 4 and 5 RBDs

(**Figure 1.9B)** where shown to drastically reduce Rap1-Taf4/12 and Rap1-Taf5 binding, RP

gene transcript levels, and yeast cell growth rate (Garbett et al., 2007; Layer et al., 2010).

Interestingly, the K_ds measured for the Rap1-Taf5 and Rap1-Taf4/12 interaction were ~ 1

x 10^{-9} M (Layer et al., 2010), indicating an unusually tight binding compared to other

activator-coactivator binding interactions whose K_ds have been measured at 1 x 10^{-5}-10^{-7} M

(Brzovic et al., 2011; Jonker et al., 2005; Krois et al., 2016). Finally, deletion of the Rap1 C-

terminus (aa's 600-827) also resulted in decreased RP gene and Rap1-dependent reporter

gene transcript levels (Garbett et al., 2007). Taken together, these data support the hypothesis that direct, specific, high-affinity Rap1-TFIID interaction drives RP gene transcription.

<div align="center">Rap1, TFIID, and TFIIA RP Gene Activation Mechanism</div>

Having demonstrated the dependence of RP gene transcription on direct Rap1-TFIID interaction (Garbett et al., 2007; Layer et al., 2010), our lab sought to address the mechanistic consequences of Rap1-TFIID interaction. The goal of these studies was to determine how TFIID served as a coactivator on the RP genes. Cooperative binding was tested first since the strongest prior studies of TFIID coactivator function suggested that TFIID coactivates target genes via the cooperative binding (i.e. "recruitment") model of transcription activation (Li et al., 2007; Liu et al., 2009; Sauer et al., 1995a, 1995b). However, repeated DNase I footprinting and gel shift DNA binding analyses performed using Rap1, TFIID, and TFIIA (which is required for TFIID-promoter binding) failed to demonstrate any cooperative binding (Krassi A. Garbett, unpublished observation).

To try to gain more insight into TFIID coactivator function on RP genes, EM analyses were performed on binary, ternary, and quaternary complexes formed using Rap1, TFIID, TFIIA, and DNA in collaboration with the lab of Dr. Patrick Schultz at the IGBMC in Strasbourg, France. Analyses of Rap1-TFIID and Rap1-TFIID-DNA complexes revealed two Rap1 densities, each of which interacted with a face of TFIID lobe B (Papai et al., 2010) (**Figure 1.10A**). This co-localization of Rap1 with a TFIID lobe that contains one copy of Tafs 4, 5, and 12 (Leurent et al., 2002, 2004; Papai et al., 2010) is consistent with the results of the Rap1-Taf interaction studies described above (Garbett et al., 2007; Layer et al.,

2010). The Rap1 density located on the DNA-proximal face of TFIID lobe B accommodates

the crystal structure of the Rap1 DBD (König et al., 1996; Matot et al., 2012; Taylor et al.,

2000). This localization is consistent with Rap1 DNA-binding and Rap1 DBD-TFIID

interaction (Garbett et al., 2007). Importantly, this Rap1 DBD localization does not place

the Rap1 DBD in proximity with TBP, which has been mapped to lobes A and C of TFIID

(Leurent et al., 2004) and whose interaction with the Rap1 DBD may repress transcription

(Bendjennat and Weil, 2008). The second Rap1 density located on the opposite face of

TFIID lobe B could be the Rap1 C-terminus or the DBD of a second Rap1 molecule.

Consistent with the analyses of other activator-TFIID complexes that had been performed

prior to the Rap1-TFIID study (Liu et al., 2009), no TFIID conformational rearrangements
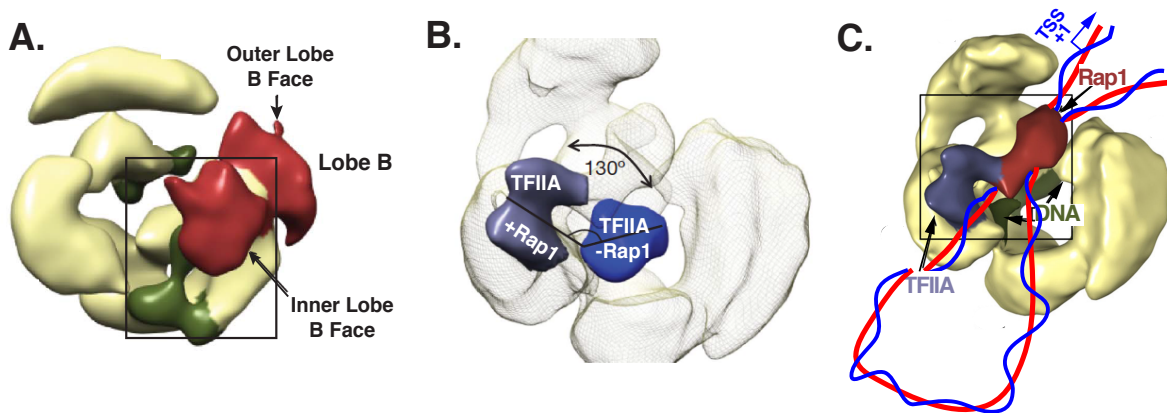
Figure 1.10. Model of Rap1-TFIID, TFIIA-TFIID, and Rap1-TFIID-TFIIA EM Used to Propose the "Lock to Load" Model of RP Gene Transcription Activation. *A*, Localization of Rap1 within the Rap1-TFIID structure. TFIID is shown in yellow while densities corresponding to DNA are shown in green. Rap1 (red densities) is localized to both faces (outer and inner) of TFIID lobe B, which contains one copy of Tafs 4, 5, and 12 (*cf* Figure **1.6A**) shown to interact directly with Rap1 in biochemical analyses. The inner Rap1 density fits the Rap1 DBD crystal structure and is thought to represent the Rap1 DBD. The outer Rap1 density may be the Rap1 C-terminus. *B*, Localization of TFIIA in the TFIIA-TFIID-DNA complex compared with the Rap1-TFIIA-TFIID-DNA complex (i.e. –Rap1 (blue) and + Rap1 (purple), indicating the TFIIA conformational change observed when Rap1 is added to the complex. *C*, Final "Lock to Load" complex thought to represent the critical step in RP gene transcription activation proposed based on results of EM analyses of TFIID-containing complexes. TFIID is shown in yellow, Rap1 is shown in red, conformation changed TFIIA is shown in purple, DNA densities observed in EM are shown in green, and the hypothesized enhancer-promoter DNA loop is indicated by the red and blue lines. Note: all images used in this figure have been adapted from Papai et al., 2010.

48

were detected in either the Rap1-TFIID or the Rap1-TFIID-DNA complexes.

Meanwhile, analyses of TFIID-TFIIA-DNA complexes revealed a globular TFIIA density located near lobe C of TFIID (Papai et al., 2010), placing TFIIA in proximity to TBP consistent with known TFIIA-TBP interaction (Geiger et al., 1996; Tan et al., 1996). Excitingly, comparison of this TFIID-TFIIA-DNA structure with the Rap1-TFIID-TFIIA-DNA structure revealed a 130° rotation of TFIIA around its TFIID interaction site (**Figure 1.10B**), indicative of a TFIIA conformational change (Papai et al., 2010). This conformational change places TFIIA in proximity to directly interact with the density corresponding to the Rap1 DBD. However, a direct Rap1-TFIIA interaction has yet to be detected. Thus, although TFIIA changes conformation and performs a coactivator role in some contexts (Kobayashi et al., 1995; Ozer et al., 1996), the direct Rap1-TFIID interaction supports the notion that TFIID serves a coactivator function in this case by forming the structural scaffold upon which TFIIA rearrangement occurs.

The Weil lab has hypothesized that the TFIIA conformational change observed within the Rap1-TFIID-TFIIA-DNA complex represents a key step in RP gene activation. The lab has termed this model the "Lock to Load" model (**Figure 1.10C**) of transcription activation because the TFIIA conformational change "locks" enhancer-promoter DNA into a loop, which in turn could enhance subsequent PIC formation or loading. This enhanced PIC formation may be required for the high levels of transcription of RP genes. Importantly, by proposing a TFIID-dependent conformational change model of transcription activation, "Lock to Load" challenges the dogma that TFIID coactivates transcription strictly via cooperative binding. Consistent with this model, the lab has shown that RP gene transcription depends on direct specific high-affinity TFIID-Rap1 (Layer et al., 2010) and

TFIID-TFIIA (Layer and Weil, 2013) interactions. Also consistent with this model, a class

of TFIIA mutants that can stimulate DNA-binding but fail to activate transcription and form

DNA loops have been identified (Papai et al., 2010), suggesting that loop formation is

indeed an important step in transcription activation. Importantly however, if indeed "Lock

to Load" represents a critical step in RP gene activation, formation of the rearranged Rap1-

TFIID-TFIIA-DNA complex should depend on direct interactions between the Rap1 AD and

the various components of TFIID and/or TFIIA.

Specific Aims

As stated multiple times throughout this Chapter, the Rap1 AD had never been

unambiguously mapped, preventing any identification of the Rap1 AD coactivator target(s)

prior to my thesis research. I believed that carefully defining the Rap1 AD would

contribute importantly to our understanding of transcription activation for two key

reasons. First, Rap1 is the key RP gene transcription activator, and mapping the Rap1 AD

represents an important unrealized step in dissecting the molecular mechanisms required

for transcription activation of this important highly transcribed class of genes. Second,

Rap1 AD mapping would set up future rigorous testing of the lab's novel "Lock to Load"

model of transcription activation described above in "Rap1, TFIID, and TFIIA RP Gene

Activation Mechanism." Ideally, my efforts to define the key Rap1 AD amino acids would

result in the generation of separation-of-function mutants that could be used to determine

the consequences of Rap1 AD interaction with the multiple possible coactivator targets

within the "Lock to Load complex (specifically TFIID Tafs 4, 5, and 12 and TFIIA).

To address my goal of mapping the Rap1 AD, I proposed the following <u>specific aims</u>:

Aim 1: Generate an altered DNA-Binding specificity Rap1 variant (Rap1^{AS}) to provide a tool to unambiguously dissect Rap1 structure-function relationships.

Aim 2: Map and characterize the Rap1 AD and investigate its interaction with TFIID and/or TFIIA.

The results of my studies performed to accomplish these Aims are described in Chapters II-III. Future directions to follow up on the findings of these studies are discussed in Chapter IV.

CHAPTER II

GENERATION OF AN ALTERED DNA-BINDING SPECIFITY VARIANT OF RAP1

Considerations in Dissecting Rap1 Structure-Function Relationships

As stated in Chapter I, prior to my thesis work, the published studies performed

using traditional approaches left open the questions of which Rap1 domain(s) and by what

molecular mechanism(s) Rap1 turns on target gene transcription. Several observations

supported the notion that Rap1 is indeed a *bona fide* transcription activator and thus must

possess an AD whose interaction with a coactivator(s) contributes importantly to RP gene

transcription. Both UAS_{Rap1} mutation and acute Rap1 nuclear depletion reduce mRNA

levels by 50-90% depending on the gene in question (Chambers et al., 1989; Knight et al.,

2014; Mencía et al., 2002; Scott and Baker, 1993), demonstrating that Rap1 DNA-binding is

required for ongoing transcription of these genes. Rap1 binds the purified coregulators

Swi/Snf and TFIID (Garbett et al., 2007; Tomar et al., 2008). Importantly for our work, RP

gene transcription absolutely requires Rap1 (Garbett et al., 2007; Schwalder et al., 2004;

Wade et al., 2004a) and depends significantly upon Rap1-TFIID interaction (Layer et al.,

2010). Collectively, these data motivated me to identify, characterize, and ultimately

generate mutant variants of an AD within Rap1 to dissect the molecular mechanism(s) by

which it turns on transcription and as importantly test our "Lock to Load" model of RP gene

transcription activation (Papai et al., 2010).

As an alternative approach to identify an AD within budding yeast Rap1, I devised a

strategy to generate an altered DNA-binding specificity variant of the protein termed

Rap1[AS]. My goal was to identify a form of Rap1 that exhibited true Altered Specificity (AS) of DNA binding. A true altered DNA-binding specificity Rap1[AS] would not efficiently bind at 'WT' UAS_{Rap1} elements, but could bind and drive the expression of an integrated selectable reporter gene from a distinct, mutated form of the UAS_{Rap1} enhancer. Because of this true altered DNA-binding specificity, Rap1[AS] would obviate the complications that arise as a result of the myriad Rap1 activities required for the proper expression of hundreds of essential Rap1-dependent genes as well as regulation of telomere function described in Chapter I.

Rap1[AS] would allow for the straightforward molecular genetic dissection of Rap1 structure-function relationships by scoring function/expression of the Rap1[AS]-dependent reporter gene in cells containing engineered deletion or point-mutated variant forms of Rap1[AS]. Breakthroughs in the understanding of transcription mechanisms have been made through the generation and utilization of altered DNA-binding specificity mutants of other essential transcription factors, in both prokaryotes and eukaryotes. Examples include AS variants of bacteriophage l cro protein (Nilsson and Widersten, 2004), *E. coli* Trp repressor (Pfau et al., 1994) and sigma factor σ^{70} (Gregory et al., 2005); yeast TBP (Strubin and Struhl, 1992) and transcription factor Gcn4 (Kim et al., 1993), mammalian estrogen receptor (ER) (Mader, S et al., 1989; Voss et al., 2011), and *Drosophila* transcription factor Engrailed (Chu et al., 2012). These altered DNA-binding variant proteins proved key in unlocking the molecular mechanisms by which these disparate DNA-binding proteins operate.

In this Chapter, I describe my approach to Rap1[AS] generation, some of which was originally published in the *Journal of Biological Chemistry* (*JBC*) (Johnson and Weil, 2017) ©

the American Society for Biochemistry and Molecular Biology. This approach consists of the structure-guided site-directed mutagenesis of UAS_{Rap1} DNA and the gene encoding the Rap1 protein itself, coupled with a sensitive yeast screening strategy. Using my approach, I was able to identify a true altered DNA-binding specificity variant of Rap1, termed Rap1[AS]. This Rap1[AS] variant possessed all the characteristics desired for use as a tool for Rap1 AD mapping and will likely also prove valuable to investigators who study Rap1 function in transcription repression, telomere length regulation, chromatin opening, and meiotic recombination (Morse, 2000; Rudra and Warner, 2004; Shore, 1994).

Methods

General Cloning Approach

All cloning experiments used to generate *E. coli* expression plasmids, yeast expression plasmids, and yeast genomic integration constructs were performed using restriction enzyme based methods. The details for the generation of individual vectors are provided below or in Chapter III according to their appearance in this dissertation. Cassette swap was performed where possible due to the presence of desired DNA sequence with compatible restriction endonuclease recognition sequences to transfer a portion of an already-existing vector into another. Generally, where cassette swap was not possible, a DNA sequence of interest was generated via PCR using primers containing the desired restriction enzyme sites and either the *Pyrococcus furiosis* (*Pfu*) polymerase (Dabrowski and Kur, 1998; Lu and Erickson, 1997) or Q5 high-fidelity DNA polymerases (New England Biolabs (NEB)) according to standard protocols. To prepare inserts for cloning, PCR

generated fragments (or, in the case of a cassette swap, vector DNAs) were subjected to restriction enzyme digest. The vector to receive the insert was digested with the same restriction enzyme(s) and treated with Antarctic Phosphatase (NEB) according to the manufacturer's instructions to reduce self-ligation. Both vector and insert DNAs were agarose gel purified and gel extracted using a Qiagen Gel Extraction Kit and either Qiagen or Denville Scientific gel extraction columns according to the manufacturers' instructions. For general (i.e. not library) cloning reactions, ligations of vector and insert DNA were performed in 10μL reaction volumes using 20-50ng vector DNA, a 2-3 fold molar excess of insert DNA, 1X T4 DNA ligase buffer (NEB), and T4 DNA ligase (NEB) for 30min to overnight at room temperature prior to transformation into *E. coli* (see below) and selection on antibiotic-containing plates. Isolated clones were analyzes via restriction enzyme digest and sequencing to confirm the presence of the desired construct.

E. coli and Yeast Cell Culture and Basic Manipulations

      E. coli manipulations- The following *E. coli* strains were used for various experiments in this dissertation: DH5α (genotype: *fhuA2 lacΔU169 phoA gInV44* Φ80*lac*ZDM15 *gyr*A96 *rec*A1 *rel*A1 *end*A1 *thi*-1 *hsd*R17, Vanderbilt Molecular Biology Core), Rosetta II DE3 (genotype: F⁻ *ompT hsd*S$_B$(r_B^- m_B^-) *gal dcm* (DE3) pRARE2 (Cam^R), Novagen), USO omega selection (genotype: SB3930 *lac*-, *ΔhisB463*, *ΔpyrF, ΔrpoZ*:zeo [F' *proAB lacIZΔM15* Tn*10* (Tet)], (Noyes et al., 2008)), and ElectroMAX DH10B cells (genotype: F⁻*mcr*A D (*mrr*-hsdRMS-*mcr*BC) Φ80*lac*ZDM15 Δ*lac*X74 *rec*A1 *end*A1 *ara*D139 Δ(*ara*, *leu*)7697 *gal*U *gal*K λ-*rps*L *nup*G, Life Technologies).

All plasmid propagation and cloning (except for that performed to generate libraries) was done using chemically competent DH5α cells (Vanderbilt Molecular Biology Core). Standard chemical transformation reactions were performed to generate clones using these cells. In brief, 5μL of ligation reaction was mixed with 50μL of cells in 15mL polypropylene round-bottom tubes (Fisher Scientific) and incubated on ice for 30min. Cells were heat shocked for 30s at 42°C and recovered in 950μL Super Optimal broth with Catabolite repression (SOC) medium (2% w/v tryptone, 0.5% w/v yeast extract, 10mM NaCl, 2.5mM KCl, 10mM $MgCl_2$, 10mM $MgSO_4$, and 20mM dextrose) for 1hr at 30°C with shaking at 250rpm. For simple plasmid propagation, a shorter 1min transformation protocol (Golub, 1988), which uses just 10μL of cells, at least 10ng of intact plasmid DNA, and 100μL of SOC, and eliminates the ice and recovery incubation steps, was utilized. Plasmid selections were performed overnight on 30-50% of each standard chemical transformation reaction or 100% of each 1min transformation using Luria Bertani (LB) plates (1% w/v tryptone, 0.5% w/v yeast extract, 0.5% NaCl)(Sezonov et al., 2007) supplemented with a final concentration of 100μg/mL Ampicillin (Amp) or 50μg/mL Kanamycin (Kan) depending on which antibiotic resistance marker (Amp^R or Kan^R) was present on the plasmid to be maintained. Plasmids were amplified via growth of colonies selected on antibiotic plates in 5mL LB + antibiotic for 12-16hrs at 37°C with shaking at 250rpm and isolated using a Qiagen Mini-Prep kit and a Qiagen Mini-Prep column (or multiple columns when >10μg of vector DNA was required) according to the manufacturer's instructions.

Rosetta II DE3 cells (Novagen) were used for recombinant protein expression. Competent Rosetta II DE3 cells were generated via the Inoue method (Inoue et al., 1990).

The transformation efficiency of these Rosetta II DE3 cells was generally much lower than that of *E. coli* stains such as DH5α that are typically used for cloning (1 x 10^3 transformants/μg DNA compared to the transformation efficiency of 1 x 10^8 transformants/μg typically obtained in chemically competent DH5α prepared using the Inoue method. To compensate for this, a greater amount (200-500ng) of protein expression vector DNA (individual constructs described below) was added to 30-50μL of Rosetta II DE3 cells in standard chemical transformation reactions performed largely otherwise as described above for DH5α cells. Following the 1hr recovery in SOC, 50-80% of each transformation was plated on LB + 34μg/mL Chloramphenicol (Cam) and 10μg/mL Kan. When expressing proteins, individual colonies formed on these selection plates were grown for 3-5 hrs in 5mL LB + 34μg/mL Cam and 10μg/mL Kan and then overnight in 20mL LB + 34μg/mL Cam and 10μg/mL Kan at 37 °C with shaking at 250rpm. The optical density at 600nm (OD_{600}) of each overnight culture was measured using a NanoDrop 2000c spectrophotometr (Thermo Scientific); this measurement was used to guide the inoculation of fresh LB + 34μg/mL Cam and 10μg/mL Kan to an OD_{600} of 0.03. These fresh cultures were grown at 37℃ with shaking at 250rpm to an OD_{600} of 0.5-1, at which point 1M stock Isopropyl-β-D-1-thiogalactopyranoside (IPTG) was added to each culture to a final concentration of 1mM to begin induction. Protein inductions were allowed to proceed for 4hrs at 37°C with shaking at 250rpm at which point cells were harvested via centrifugation for 10min at 4,000rpm in a J6-HC (Beckman Coulter). For small-scale inductions (5-50mL cultures), supernatants were discarded and pellets were stored at -80℃. For large-scale inductions (0.5-1L cultures), supernatants were discarded and pellets were resuspended in

sterile water. Resuspended pellets were transferred to 50mL conical tubes and re-pelleted

by centrifugation prior to the final supernatant removal and pellet storage at -80°C.

USO omega selection cells (Noyes et al., 2008) were used for all bacterial omega

one-hybrid experiments. These cells contain genes encoding resistance to Tetracycline

(Tet) and Zeocin (Zeo) (see genotype above); USO omega cells used for omega one-hybrid

screening additionally contained a Kan^R plasmid. Electrocompetent USO omega selection

cells were prepared in-house using a published protocol (Dower et al., 1988). This protocol

results in the production of electrocompetent cells with high transformation efficiencies (1

x 10^9- 1 x 10^{10} transformants/μg DNA) regardless of strain background. Additionally, in

contrast to chemical transformation efficiency decreases outside of a 1pg – 1 x 10^3 pg DNA

input range (Hanahan, 1983), the transformation efficiency of electrocompetent cells is

maintained over a wider range of DNA input (1pg – 1 x 10^6 pg) (Dower et al., 1988),

reducing the number of transformation reactions needed to generate a large number of

transformants.

To prepare electrocompetent USO omega selection cells, cells were grown overnight

in 2X Yeast Extract Tryptone (YT) Broth (1.6% w/v tryptone, 1% w/v yeast extract, 0.5%

NaCl) with appropriate antibiotic selection (final concentrations of 10μg/mL Tet, 50μg/mL

Zeo, and 10μg/mL Kan (where a Kan^R plasmid was present) at 37°C with shaking at

250rpm. The next day, overnight cultures were used to inoculate fresh 2X YT containing

the same antibiotic selection as the overnight growth to a starting OD_{600} of 0.0625. These

fresh cultures were grown at 37°C with shaking at 250rpm until they reached an OD_{600} of

0.5-0.6, at which point cultures were immediately immersed in an ice water bath where

they were incubated for 30min. After the incubation, cells were transferred to centrifuge

bottles (pre-chilled in an ice water bath) and cells were pelleted via centrifugation for 10min at 4°C in a J6-HC centrifuge (Beckman Coulter). Supernatant was removed and pellets from 250mL culture were resuspended in 100mL sterile H_2O pre-chilled at 4°C. The centrifugation and 100mL sterile 4°C H_2O pellet resuspension steps were repeated. Cells were once again pelleted via centrifugation, supernatants were removed, and pellets were resuspended in 20mL sterile 10% glycerol pre-chilled at 4°C. Cells resuspended in 20mL sterile 10% glycerol were pelleted again by centrifugation, supernatant was removed, and pellets were resuspended in 5mL sterile 10% glycerol. Each pellet resuspended in 5mL sterile 10% glycerol was then distributed in 4 X 1.25mL aliquots in 1.5mL Eppendorf tubes. Cells were re-pelleted by spinning for 1min at 13,000rpm, 4°C in an Eppendorf Centrifuge 5417C, resuspended in a final volume of 80μL sterile 10% glycerol, immediately frozen on dry ice, and stored at -80°C until use. Electroporation reactions were performed on 40μL cells incubated for 1min on ice with 100-200ng of DNA resuspended in 1mM Tris-Cl (pH 8.5) (to keep ions in the reaction to a minimum) in a 0.1cm Gene Pulser Cuvette (BioRad) using a Gene Pulser (BioRad) set at 25μF and 2.5kV and a Pulse Controller (BioRad) set at 200 ohms. Immediately following pulse delivery, cells were resuspended in 1mL SOC. Cells were recovered and plasmid selections were performed as described for the standard chemical transformation above. Using this method, electrocompetent cells with a transformation efficiency of ~1 x 10^9 transformants/μg intact DNA were routinely generated.

Electrocompetent USO selection cells and ElectroMAX DH10B cells (Life Technologies) were used to generate plasmid DNA libraries for screening because of their extremely high transformation efficiency (1 x 10^9-1 x 10^{10} transformants/μg intact

plasmid).   The protocol for omega one hybrid system library generation (Meng and Wolfe, 2006) was used to create all Rap1 variant libraries. In this protocol, multiple electroporation reactions, each containing 150-300ng worth of library ligation DNA, were performed as described for the USO selection cells above. Each electroporation reaction was resuspended in 1mL SOC. Prior to recovery, all electroporation reactions performed using library DNA were combined and added to a greater volume of SOC, resulting in a 5-fold dilution of the library culture. After recovering this diluted culture for 1hr at 37°C with shaking at 250rpm, a small aliqot (20μL) was titrated onto multiple selective media plates to estimate the library size. To select for and begin propagation of library variant plasmids, LB containing the appropriate selective antibiotic was added directly to the recovered SOC culture to increase its volume 2.5X. This culture was grown for 3hrs at 37°C with shaking at 250rpm. Following this expansion, another 20μL of culture was titrated on selective media to confirm library expansion and half of the culture (estimated to contain at least one complete copy of the library) was pelleted and frozen as glycerol stock for possible later library propagation. The remaining culture (also estimated to contain at least one complete copy of the library) was allowed to continue to expand until it reached an OD_{600} of 0.6-2 (much less than an OD_{600} of 5, at which point *E. coli* cell density reaches saturation and antibiotic selection for the plasmid cannot be guaranteed). Cell cultures were pelleted and frozen at -20°C overnight. Library DNA was isolated from these pellets using multiple Qiagen mini-prep columns (10mL cell culture pellet representing 20 OD_{600} units/column) and a Qiagen Mini-Prep kit.

   Yeast manipulations- Several yeast strains were generated as described below to perform the experiments presented in this dissertation. All yeast manipulations were

performed the same irrespective of strain background. All growth steps were performed at 30°C and, for liquid cultures, with shaking at 250rpm. Where no selectable markers for a yeast strain were available, yeast were grown on either solid or liquid Yeast Extract Peptone Dextrose (YPD, 1% w/v yeast extract, 2% w/v peptone, 2 % w/v dextrose). Selection for yeast bearing a drug resistance cassette such as *HPHMX4*, which encodes resistance for Hygromycin B (Corning), or *KANMX4*, which encodes resistance for G418 Sulfate (Corning) were performed on YPD + 200μg/mL Hygromycin B and YPD + 200μg/mL G418 Sulfate, respectively. Selection for yeast bearing genes encoding auxotrophic markers such as Tryptophan (Trp), Histidine (His), Leucine (Leu), Adenine (Ade), and Uracil (Ura) were performed using Synthetic Complete (SC) medium (0.67% w/v yeast nitrogen base without aa's, 2% w/v dextrose, and 0.2% w/v aa dropout mix) (Murthy et al., 1975) lacking the amino acid produced by the auxotrophic marker gene.

Yeast transformations performed to introduce plasmid DNA or genomic integration cassettes following the high-efficiency yeast transformation protocol (Gietz and Schiestl, 2007). In this protocol, yeast cultures inoculated with a single colony were grown overnight at 30°C with shaking at 250rpm to saturation in appropriate selective media. The next day, overnight yeast cultures were used to start fresh cultures again using appropriate selective media (5mL/transformation reaction) at an OD_{600} of 0.125. Cultures were grown for 5hrs at 30°C with shaking at 250rpm at which point they reached an OD_{600} of 0.5-1. Cultures were pelleted by centrifugation for 5min at 4,000rpm in a J6-HC centrifuge (Beckman Coulter). Supernatants were removed and cell pellets were resuspended in sterile H_2O (1mL/transformation reaction) and transferred in 1mL aliquots to 1.5mL Eppendorf tubes. Cells were re-pelleted via centrifugation for 30s at 13,000rpm in an

Eppendorf Centrifuge 5417C, supernatants were aspirated, and pellets were resuspended

in a 360μL transformation mix consisting of 240μL 50% PEG 3500, 36μL 1M LiAc, 50μL

1mg/mL salmon-sperm DNA, at least 100ng of DNA, and sterile water added to the final

360μL volume. Cells resuspended in a transformation reaction were heat shocked for

40min at 42˚C. Following heat shock, cells were pelleted by spinning for 30s at 13,000rpm.

Transformation reaction mix was removed via aspiration, cell pellets were resuspended in

1mL sterile H_2O, and 10-100% of a reaction (depending on whether the DNA being

introduced was a plasmid or integration construct) was plated on appropriate selective

media. Selective plates were grown for 36-38hrs at 30˚C. As a negative control, a no DNA

transformation reaction was performed to confirm that only cells that had taken up the

DNA of interest survived the selection.

Rap1 Bacterial Omega One-Hybrid Vectors

The bacterial omega one-hybrid system depends on the function of two vectors: (1)

an Amp[R] plasmid that drives the expression of a bacterial RNA Polymerase ω subunit-

transcription factor DBD fusion under the control of a mutant *lac* promoter used to drive a

low level expression of fusion proteins whose expression at higher levels might otherwise

be toxic to the cell (pB1H2, Addgene, (Noyes et al., 2008)), and (2) a Kan[R] plasmid that

contains *HIS3* and *URA3* reporters driven by a weak *lac* promoter and transcription factor

binding site (pH3U3, Addgene, (Noyes et al., 2008)). A pB1H2 *RAP1* DBD plasmid was

generated by cloning a *Pfu* polymerase PCR generated KpnI to XbaI fragment containing the

DNA sequences encoding the Rap1 DBD (*RAP1* nts 1081-1788, encoding aa's 361-596

(Henry et al., 1990)) in frame with the pB1H2 ω subunit sequence. Meanwhile, pH3U3

UAS_{Rap1} variants were generated by cloning EcoRI to NcoI variants of the *UAS_{Rap1}* sequence

(5'-AATTCATAT<u>ACACCCATACATT</u>GACGC- 3'; *UAS_{Rap1}* sequences underlined) generated by

annealing synthetic oligonucleotides (IDT) into the pH3U3 multiple cloning site (MCS)

located upstream of the promoter and reporter gene sequences.

Yeast Strains

All of the yeast strains used in this chapter are listed in **Table 2.1**. These strains

were derived from a *rap1Δ* null strain created in the BY4741 background (Brachmann et

al., 1998), often via the utilization of the pRS series of yeast expression vectors (Brachmann

et al., 1998). Because budding yeast *RAP1* is a single copy essential gene (Shore and

Nasmyth, 1987), these strains carry *RAP1* covering plasmids. The plasmid covering *rap1Δ*

in these strains was either a previously generated pRS415 *MYC₅-RAP1* plasmid (Garbett et

al., 2007) or a pRS416 *FLAG₃– RAP1* vector created by inserting a *FLAG₃* tag flanked by

EcoRI restriction sites generated by annealing synthetic oligonucleotides obtained from

IDT at the EcoRI site located between the *RAP1* promoter and *RAP1*. Both constructs

express *RAP1* under the control of the native *RAP1* promoter (*RAP1* nt position -433 to + 1

(Graham et al., 1999) and

terminator (*RAP1* nt position

+2485 to +2533).

TAF1 was genomically

tagged in these strains with

an *HA₃* epitope to facilitate its

possible study via ChIP assay.

Table 2.1: Yeast Strains Used In This Chapter

Name	Strain	Genotype	Reference
BY4741	BY4741	*MAT**a** his3Δ1 leu2Δ0 met15Δ0 ura3Δ0*	Brachman et. al., 1998
rap1Δ	BY4741 rap1Δ	*MAT**a** his3Δ1 leu2Δ0 met15Δ0 ura3Δ0 rap1Δ::HPHMX4* (pRS416 *UAS_{ADH}-RAP1*)	Layer et. al., 2010
3T4A-HIS3 #1	YAM23	*MAT**a** his3Δ1 leu2Δ0 met15Δ0 ura3Δ0 rap1Δ::HPHMX4* (pRS415 *UAS_{Rap1}-MYC₅-RAP1*) *trp1Δ::KANMX4 HA₃-TAF1 UAS_{Rap1(3T4A)}-TATA-HIS3::TRP1::DED1*	(Johnson and Weil, 2017)
WT-HIS3	YAM30	*MAT**a** his3Δ1 leu2Δ0 met15Δ0 ura3Δ0 rap1Δ::HPHMX4* (pRS416 *UAS_{Rap1} FLAG₃-RAP1*) *trp1Δ::KANMX4 HA₃-TAF1 UAS_{Rap1(WT)}-TATA-HIS3::TRP1::DED1*	(Johnson and Weil, 2017)
3T4A-HIS3 #2	YAM31	*MAT**a** his3Δ1 leu2Δ0 met15Δ0 ura3Δ0 rap1Δ::HPHMX4* (pRS416 *UAS_{Rap1} FLAG₃-RAP1*) *trp1Δ::KANMX4 HA₃-TAF1 UAS_{Rap1(3T4A)}-TATA-HIS3::TRP1::DED1*	(Johnson and Weil, 2017)
ΔUAS-HIS3	YAM32	*MAT**a** his3Δ1 leu2Δ0 met15Δ0 ura3Δ0 rap1Δ::HPHMX4* (pRS416 *UAS_{Rap1} FLAG₃-RAP1*) *trp1Δ::KANMX4 HA₃-TAF1 UAS_{Rap1(Δ)}-TATA-HIS3::TRP1::DED1*	(Johnson and Weil, 2017)
3G5G-HIS3	YAM33	*MAT**a** his3Δ1 leu2Δ0 met15Δ0 ura3Δ0 rap1Δ::HPHMX4* (pRS416 *UAS_{Rap1} FLAG₃-RAP1*) *trp1Δ::KANMX4 HA₃-TAF1 UAS_{Rap1(3G5G)}-TATA-HIS3::TRP1::DED1*	(Johnson and Weil, 2017)

To generate the *HA3-TAF1* tagging construct, PCR was performed using Q5 polymerase on a previously existing pRS313 *HA3-TAF1* plasmid (Bai et al., 1997) to generate an XmaI to NotI fragment containing the *TAF1* promoter (nt position -900 to +1 (Bai et al., 1997)), *HA3* epitope, and *TAF1* nts +2-+1648. This fragment was cloned using the general approach outlined above into the pRS306 integration vector. The resulting pRS306 *HA3-TAF1* plasmid was linearized via digestion with MscI (NEB) which cuts once within the *TAF1* ORF and integrated into the yeast genome via transformation, ends-in recombination (Hastings et al., 1993), and selection for the *URA3* marker provided by the pRS306 vector. The *URA3* marker was recycled via counter-selection on SC media containing uracil and 0.1% 5-Fluoroorotic Acid (5-FOA), a compound that selects against cells that express the Orotidine-5'-phosphate decarboxylase enzyme encoded by the *URA3* gene (Boeke et al., 1987; Längle-Rouault and Jacobs, 1995). Cells that maintained *HA3-TAF1* following counter-selection to remove *URA3* were identified via immunoblotting (see "Immunoblotting" below) using anti-HA 3F10 (Roche catalog no. 11867423001) and anti-β-actin (Abcam catalog no. ab8224) loading control antibodies.

To enable selection for *HIS3* reporter integration independent of *HIS3* expression in the BY4741 background (Brachmann et al., 1998), the *TRP1* gene (which provides the selectable marker on *HIS3* reporter integration constructs) was replaced with the *KANMX4* drug-resistance cassette. This replacement was performed using a pFA6a-based plasmid (Wach et al., 1994) generated by my colleague Dr. Chirie Sumanasekara termed pFA6a *KANMX trp1Δ* by the addition of ~1kb of *TRP1* upstream and downstream sequences on either side of the *KANMX4* cassette. This plasmid was digested with the SacII and SalI-HF enzymes used to clone the *TRP1* homology arms, transformed into yeast, integrated via

ends-out recombination (Hastings et al., 1993), and selected on YPD + 200μg/mL G418

Sulfate. Transformants possessing *KANMX4* replacement of the *TRP1* gene were identified

by screening on SC-Trp and confirmed by PCR.

The various *UAS~Rap1~-HIS3* reporter genes were derived from a similar reporter

characterized in previous studies (Garbett et al., 2007; Mencía et al., 2002). This reporter

contains two copies of the Rap1 binding site (*UAS~Rap1~*) derived from the *RPS8A* gene, a

promoter (*TATA*), the *HIS3* reporter gene, a *TRP1* selectable marker, and ~1.5kb flanking

arms with homology to the *HIS3* locus, including the *DED1* gene located 3' of *HIS3*. To

generate reporter variants with mutant *UAS~Rap1~* binding sites, the 48bp NcoI to SacII DNA

fragment encompassing the two *UAS~Rap1~* binding sites in the WT *UAS~Rap1~-HIS3* reporter

generated in previous studies (Garbett et al., 2007; Mencía et al., 2002) was replaced with a

48bp NcoI to SacII DNA fragment containing 3T4A or 3G5G *UAS~Rap1~* binding sites generated

by annealing double-stranded synthetic oligonucleotides obtained from IDT. The ΔUAS

reporter was generated by replacing the NcoI to EcoRI fragment encompassing the *UAS~Rap1~*

and *TATA* sequences with an NcoI to EcoRI fragment containing just the *TATA* sequence

generated by PCR using *UAS~Rap1~-HIS3* as a template. All reporters were digested with SpeI

and SalI, transformed into yeast, and integrated into the *HIS3::DED1* locus via ends-out

recombination (Hastings et al., 1993). Transformants were selected on SC-Trp and correct

integration of the reporter was confirmed via PCR.

Test Rap1 Yeast Expression Vectors

The test *RAP1* yeast expression vectors are the same as the pRS415 *MYC~5~ RAP1*

expression vector described in "Yeast Strains" above except those generated for a purpose

other than testing omega one-hybrid screen hits in yeast contain the SV40 nuclear

localization signal (*NLS*; PKKKRKV (Kalderon et al., 1984)) inserted by replacing the EcoRI

to XhoI fragment of pRS415 *MYC$_5$ RAP1*, which contains the *RAP1* ORF, with an EcoRI to

XhoI fragment containing *NLS RAP1* generated via PCR. Mutant *RAP1* test expression

vectors used in this chapter were created in one of two ways: (1) replacing the BlpI to BglII

fragment of *RAP1* in pRS415-*MYC$_5$-NLS-RAP1* with a BlpI to BglII fragment of a pBluescript

RAP1 variant whose DBD-encoding sequences had been replaced with those of a *RAP1* DBD

isolated in an omega one-hybrid screen (see "Bacterial Omega One-hybrid Rap1[AS] Screen"

below for details) or (2) replacing the BlpI to SphI fragment of *RAP1* in plasmid pRS415-

MYC$_5$-NLS-RAP1 with the BlpI to SphI fragment of a mutant *RAP1* generated via targeted

randomization Rap1 library construction (see below).

Rap1 Expression and Purification for Gel Shift DNA-Binding Assays

      To prepare Rap1 for DNA binding assays, Rap1 ORF sequences were excised from

pRS416-Rap1 yeast expression plasmids generated in this study (see "Targeted

Randomization Mutagenesis of Rap1 DBD and Construction of Rap1 Variant Expression

Library") or a previous study (Garbett et al., 2007) with EcoRI and XhoI and ligated into

similarly digested pET28a expression vector, in-frame with the vector encoded N-terminal

His$_6$ tag. Plasmids were transformed and propagated at 37°C in the *E. coli* Rosetta II (DE3)

expression strain (Novagen) in LB media (Sezonov et al., 2007) supplemented with a final

concentration of 10μg/mL Kan and 34μg/mL Cam. His$_6$-Rap1 expression was induced for

4hr following addition of IPTG to 1mM. Cell pellets from 500 ml of culture were

resuspended in 20ml of Lysis/Wash buffer (25mM HEPES NaOH (pH 7.6), 10% v/v

glycerol, 300mM NaCl, 0.01% v/v NP-40, 1mM Benzamidine, 0.2 mM PMSF). Cells were lysed by treatment with lysozyme (final concentration of 1mg/mL) and sonication. After centrifugation, each cleared lysate was incubated with 2.5 ml Ni-NTA agarose (Qiagen) pre-equilibrated with an equal volume of Lysis/Wash Buffer. Proteins were bound for 3 hours at 4°C, washed 3X with Lysis/Wash buffer, transferred to a disposable column (Bio-Rad), and bound proteins eluted using Lysis/Wash buffer containing 200mM Imidazole.

Rap1 Gel Shift DNA-Binding Assays

10ng (~100fmol) of purified His_6-Rap1 WT/variant proteins were incubated with 0.6ng (~50fmol, ~35,000dpm) of 19bp ^{32}P-labeled duplex DNA containing a Rap1 binding site (either WT: 5'-ATAT<u>ACACCCATACATT</u>GA-3' or the 3T4A mutant 5'-ATAT<u>AC**TA**CCATACATT</u>GA- 3'; UAS_{Rap1} sequences underlined; mutated residues bolded) in the presence or absence of variable amounts of unlabeled WT or 3T4A UAS_{Rap1} DNA (see Figure legends) for 20min at room temperature in Binding buffer (20mM HEPES KOH (pH 7.6), 10% v/v glycerol, 100mM KCl, 0.1mM EDTA, 1mM DTT, 25 µg/mL BSA, 2.5 µg/ml Poly(dG-dC) (double-stranded, alternating copolymer, Sigma) in a final volume of 20µl. Reactions were loaded on 0.5X TBE-buffered (44.5mM Tris, 44.5mM Boric acid, 1mM EDTA (pH 8.0)) 6% polyacrylamide gels and electrophoresed for 45 min at 200 V at room temperature, and the gels vacuum dried. ^{32}P-DNA signals were detected via K-screen imaging using a Pharos FX imager (Bio-Rad). The intensity of the bands representing Rap1-^{32}P-DNA complexes were quantified using Quantity One software (Bio-Rad).

<u>Rap1 DBD Error-Prone (EP)-PCR Mutagenesis and Library Construction</u>

Random mutagenesis of the *RAP1* DBD was accomplished via EP-PCR performed

according to the protocol utilized to mutagenize the Taf4 and Taf5 RBDs in order to

generate temperature sensitive (Ts[+]) Taf4 and Taf5 variants (Cadwell and Joyce, 1992,

1994; Layer et al., 2010). Random PCR mutagenesis was performed in 100 μL reactions

using the same primers used to clone the Rap1 DBD in frame with the pB1H2 ω subunit

sequence at a final concentration of 0.3μM and 5 units *Thermus aquaticus* (*Taq*) DNA

Polymerase (the thermostable DNA Polymerase with the highest error rate) in mutagenic

PCR buffer (7mM $MgCl_2$, 10mM Tris-HCl (pH 8.3), 50mM KCl, 0.5mM $MnCl_2$, 0.2mM dGTP,

0.2mM dATP, 1mM dCTP, 1mM dTTP). The increased $MgCl_2$ concentration, increased *Taq*

units, addition of $MnCl_2$, and uneven dNTP concentrations provided by the mutagenic PCR

buffer over the standard Taq PCR buffer (1.5mM $MgCl_2$, 50mM KCl, 10mM Tris-HCl (pH

8.3), 0.2mM dGTP, 0.2mM dATP, 0.2mM dCTP, 0.2mM dTTP, 2.5 units *Taq*) increase the

error rate of *Taq* from 10^{-3}/nucleotide to 7 X 10^{-3}/nucleotide (Cadwell and Joyce, 1994).

Multiple rounds of PCR were performed using 20, 25, and 30 cycles in order to vary the

number of mutations introduced into the *RAP1* DBD, with mutant *RAP1* DBDs generated

using 20 PCR cycles generally possessing fewer mutations than those generated using 30

PCR cycles.

Mutagenic PCR products were digested with KpnI and XbaI restriction enzymes and

ligated into similarly digested pB1H2, a plasmid that drives expression of ω-transcription

factor DBD fusion proteins using a mutant *lac* promoter (see above; "Rap1 Bacterial Omega

One-Hybrid Vectors"). Ligation products were purified using a Qiagen PCR purification kit

and Qiagen PCR purification columns to remove the salt in the ligation buffer and

electroporated into USO selection cells. Multiple electroporation reactions were used to create a library of ~1 x 10^6 that was expanded according to the procedure described above in "*E. coli* and Yeast Cell Culture and Basic Manipulations." Sanger sequencing of library expression plasmid isolated from ten individual clones was used to confirm the random introduction of mutations into the sequences encoding the Rap1 DBD.

Targeted Randomization Mutagenesis of the Rap1 DBD and Library Construction

Codon randomization of N401, S402, R404, H405, R408, and V409 of the *RAP1* DBD was achieved by overlap extension PCR (Heckman and Pease, 2007) using the mutagenic oligonucleotide (see also **Figure 2.3**): 5'CATTATGTGCCTAACCACACGGGT**NNSNNS**ATT **NNSNNS**CGATTT**NNSNNS**TATCTTTCCAAAAGACTAGAGTACG3', its reverse complement, and two flanking/outside primers containing either KpnI and StuI restriction sites (for the omega one-hybrid screening library) or BlpI and StuI restriction sites (for the yeast screening library). Mutagenic PCR products were digested with SphI-HF and either KpnI or BlpI restriction enzymes and ligated into similarly digested pB1H2-*RAP1* or pRS416-*RAP1*, respectively. The pB1H2-*RAP1* plasmid drives expression of an ω-*RAP1* DBD fusion protein using a mutant *lac* promoter (see above; "Rap1 Bacterial Omega One-Hybrid Vectors") while pRS416-*RAP1* drives *RAP1* expression using the native *RAP1* enhancer-promoter (see above; "Yeast strains"). Ligation products were purified using a Qiagen PCR purification kit and Qiagen PCR purification columns to remove the salt in the ligation buffer and electroporated into ElectroMAX DH10B cells (Life Technologies, see genotype above in "*E. coli* and Yeast Cell Culture and Basic Manipulations"). Multiple electroporation reactions were used to create a library of ~1 x 10^8 independent bacterial clones, a number that

exceeds the 8.6×10^7 variations theoretically generated by the codon randomization of six amino acids, using the protocol described above in "*E. coli* and Yeast Cell Culture and Basic Manipulations." Sanger sequencing of library expression plasmid isolated from ten individual clones was used to confirm that the mutagenesis targeted the expected amino acids.

<u>Bacterial Omega One-hybrid Rap1^{AS} Screen</u>

To screen for a mutant *RAP1* variant that could drive expression of a reporter gene containing a mutant Rap1 binding site (i.e. *UAS$_{RAP1}$* 5G or *UAS$_{RAP1}$* 3T4A) in the omega one-hybrid system, plasmid libraries generated by either EP-PCR or targeted randomization were introduced into USO selection cells containing a Kan^R pH3U3 *UAS$_{Rap1}$* reporter plasmid via electroporation using the settings outlined above in "*E. coli* and Yeast Cell Culture and Basic Manipulations." After recovering electroporated cells for 1hr 10min in SOC at 37°C with shaking at 250rpm, a small aliquot (20μL) of cells was titrated onto a 2 X YT + 100μg/mL Amp and 25μg/mL Kan to estimate the number of cells carrying both the Kan^R pH3U3 *UAS$_{Rap1}$* reporter plasmid and an Amp^R pB1H2-*RAP1* expression plasmid. The remaining cells were pelleted by centrifugation for 10min at 4,000rpm in a J6-HC centrifuge (Beckman Coulter) and resuspended in 1mL/electroporation reaction NM (1X M9 Salts (42mM Na_2HPO_4, 22mM KH_2PO_4, 8.6mM NaCl, 19mM NH_4Cl), 4mg/mL glucose, 200mM adenine-HCl, 1X amino acid mixture (0.013% w/v Phe, 0.005% w/v Lys, 0.011% w/v Arg, 0.001% w/v Gly, 0.003% w/v Val, 0.004% w/v Ala, 0.002% w/v Trp, 0.003% w/v Thr, 0.036% w/v Ser, 0.02% w/v Pro, 0.004% w/v Asn, 0.005% w/v Asp, 0.081% w/v K-Glu, 0.13% w/v Gln, 0.003% w/v Tyr, 0.003% w/v Ile, 0.003% w/v Leu), 1mM $MgSO_4$,

10mg/mL thiamine, 10mM $ZnSO_4$, 100mM $CaCl_2$, 10µM IPTG) + 0.1% w/v His, 0.0025%w/v

Ura, 100µg/mL Amp, and 25µg/mL Kan. Growth of these cells was allowed to proceed for

1hr at 30℃ with shaking at 250rpm. After this growth step, cells were washed 3 X with

sterile H_2O using repeated centrifugation, supernatants were aspirated, and pellet were

resuspended in sterile H_2O. A small aliquot (20µL) of cells was titrated onto NM + 0.1%

w/v His, 0.0025% w/v Ura, 100µg/mL Amp, and 25µg/mL Kan to estimate the number of

cells in the screen while the remaining cells were screened on selective media (NM-His +

0.25, 0.5, 1, 2.5 5, 10, 25, 50, or 100mM 3-Amino-1, 2, 4-Triazole (3-AT) (Sigma)) and

incubated for 3-7 days at 30℃.

Over the course of the 3-7 day incubation, colony formation on selective plates

containing cells transformed with pB1H2-*RAP1* variants was monitored and compared to

colony formation on selective plates representing "background" pH3U3 *UAS_{Rap1}* reporter

expression (USO cells containing a pH3U3 *UAS_{Rap1}* reporter plasmid and ω-*RAP1* DBD WT

expression plasmid) prepared in parallel. Plasmids were recovered from colonies that

appeared on selective media earlier than "background" using a Qiagen Mini-Prep kit. The

purified plasmid preparations were treated with the restriction endonuclease XhoI (NEB),

which cuts the pH3U3 *UAS_{Rap1}* reporter plasmid but NOT the pB1H2-*RAP1* expression

plasmid. The digest was used to transform *E. coli* to Amp[R] and the resulting plasmids

isolated to generate putative Rap1[AS]-encoding pB1H2-*RAP1* mutant plasmids. The pB1H2-

RAP1 plasmids recovered in this step were retransformed into USO selection cells

containing the cognate pH3U3 *UAS_{Rap1}* reporter plasmid and retested for growth on 1, 2.5,

5, 10, and 25mM 3-AT to confirm that 3-AT resistant growth was conferred by the mutant,

pB1H2-*RAP1* plasmid. *RAP1* sequences from pB1H2-*RAP1* plasmids passing this filter were

transferred into yeast expression vectors for analysis in yeast. To accomplish this transfer, an AfeI to BsrGI fragment containing sequences encoding a mutant Rap1 DBD was generated via PCR using pB1H2-*RAP1* plasmids isolated from the omega one-hybrid screen as a template. These PCR products were cloned into an Afe1/BsRGI restriction enzyme digested pBluescript II KS$^+$ plasmid containing a full-length *RAP1* with Afe1 and BsRG1 restriction sites introduced via silent mutations on either side of the sequences encoding the DBD in overlap extension PCR (Heckman and Pease, 2007). The BlpI to BglII fragment encompassing the Rap1 DBD-encoding sequences of the Bluescript II KS$^+$ *RAP1* variants were transferred into a similarly digested yeast pRS415 *UAS$_{Rap1}$ MYC$_5$ RAP1* expression vector. These pRS415 *UAS$_{Rap1}$ MYC$_5$ RAP1* expression vectors were transformed into yeast containing a *UAS$_{Rap1}$-HIS3* reporter variant whose mutant *UAS$_{Rap1}$* sites matched the pH3U3 *UAS$_{Rap1}$* site used to isolate the *RAP1* expression plasmid in the omega one-hybrid screen and tested for 3-AT resistant growth in yeast.

Yeast Rap1^{AS} Screen

To screen for a mutant *RAP1* variant that could drive expression of a reporter gene containing a mutant Rap1 binding site (i.e. *UAS$_{RAP1}$* 3T4A) in yeast, the Rap1 yeast expression vector library generated via targeted randomization of Rap1 DBD codons was introduced into yeast strain 3T4A-HIS3 #1 (see **Table 2.1** above). A small aliquot (10µL) of transformation reaction was plated onto Sc-Ura to estimate the number of *URA3*-marked mutant *RAP1* expression vectors that had been introduced into yeast via the transformation while the rest was plated onto selective media for screening (SC media containing 5mM 3-AT) (Sigma). Plates were incubated for 4 days at 30˚C. Colonies were

then replica plated to SC media plates containing 5mM 3-AT and 0.1% 5-FOA to determine whether growth of the colony on 5mM 3-AT required Rap1 produced from the *URA3*-marked pRS416 *RAP1* library plasmid. *RAP1* expression plasmids were recovered from colonies that grew on 5mM 3-AT and failed to grow on 5mM 3-AT + 0.1% 5-FOA using a yeast mini-prep protocol developed in the Weil lab (Singh and Weil, 2002). These purified plasmid preparations were treated with the restriction endonuclease BsRGI (NEB) that cuts the pRS415-*MYC$_5$-RAP1* covering plasmid, but not the pRS416-*RAP1* library plasmid. The digest was used to transform *E. coli* to Amp[R] and the resulting plasmids isolated to generate putative Rap1[AS]-encoding pRS416-*RAP1* mutant plasmids. The recovered pRS416-*RAP1* plasmids were retransformed into yeast strain 3T4A-HIS3 #1 and retested for growth on 5mM 3-AT to confirm that 3-AT resistant growth was conferred by the mutant, pRS416-*RAP1* plasmid.

Yeast Cell Growth Assays

For plate assays, yeast strains were grown overnight to saturation, serially diluted 1:4 in sterile water in 96-well plates, and spotted using a pinning tool (Sigma) onto non-selective media plates (SC+His), and selective media plates (SC-His+3-AT), and grown overnight at 30°C for 2-4 days. Plate images were acquired using a ChemiDoc MP imager (Bio-Rad) and processed using ImageLab software (Bio-Rad); images were saved at a resolution of 300 DPI.

To generate growth curves, the OD$_{600}$ of yeast cultures grown to saturation overnight was measured using a NanoDrop 2000c Spectrophotometer (Thermo Scientific)

to determine how to dilute each culture to a starting OD_{600} of 0.5. The OD_{600} of these

diluted cultures was recorded every hour over the course of 12hr.

<u>Immunoblotting</u>

Total protein was extracted from yeast cell pellets containing ~1 x 10^7 cells (1 OD_{600}

unit) via mild alkali treatment and heating in standard electrophoresis buffer. In brief, cell

pellets were resuspended in 0.1M NaOH (Kushnirov, 2000) and incubated for 10min at

room temperature. Cells were re-pelleted, the 0.1M NaOH was removed, and pellets were

incubated for 10 min at 75°C in SDS-PAGE sample buffer (1X LDS Sample Buffer (Life

Technologies) with DTT added to 62.5mM). Proteins were fractionated on denaturing 4-

12% Bis-Tris polyacrylamide gels (Life Technologies); gels were equilibrated in transfer

buffer (30mM Bicine, 25mM Bis-Tris, 1mM EDTA, 60μM chlorobutanol), and then

electrotransferred to PVDF membranes pre-equilibrated in transfer buffer (GE, Immobilon-

P. 0.45μM). Loading and transfer efficiency was monitored after transfer by staining with

0.5% w/v Ponceau S in 1% v/v acetic acid. After imaging, stain was removed using

multiple changes of H_2O. Blots were blocked with 5% w/v non-fat milk in 1 X Tris-buffered

saline (TBS) (100mM Tris-Cl (pH 7.5), 150mM NaCl). Myc_5-Rap1 was detected using an

anti-Myc antibody conjugated to HRP (Roche #11667203001) at a 1:2,000 dilution.

Endogenous actin was used as an additional loading control. Actin was detected using a

1:5,000 dilution of anti-ß actin antibody (Abcam #ab8224) followed by incubation with a

1:2,500 dilution of HRP-conjugated horse anti-mouse IgG antibody (Cell Signaling #7076S).

Both anti-Myc and anti-ß-actin antibody incubations were performed in 1 % w/v non-fat

milk blocking in 1X TBS. HRP-generated immune complexes were detected by exposing

blots to enhanced chemiluminescence reagent (GE) followed by exposure to X-ray film. X-ray films were scanned at 600 dpi and saved as TIFF images.

Steady State RNA Analysis

Total RNA was extracted and purified from equal numbers of yeast

Table 2.2: qRT-PCR Primers Used In This Chapter

Gene	Primer Name	Primer sequence (5'-> 3')
HIS3	HIS3_F2	ATGACAGAGCAGAAAGCCC
	HIS3_R2	GCACTCAACGATTAGCGAC
ACT1	ACT1_F2	TGGTCGGTATGGGTCAAAAA
	ACT1_R2	AAGGACAAAACGGCTTGGAT

cells using the hot phenol method (Köhrer and Domdey, 1991). RNA concentration was

measured by monitoring absorbance at 260 and 280 nm using a NanoDrop 2000c

Spectrophotometer. RNA integrity was assessed by agarose gel electrophoresis, ethidium

bromide staining and scanning using a Pharos FX imager (Bio-Rad). The intensity of the

bands representing large (26S) and small (18S) yeast rRNAs were quantified using

Quantity One software (Bio-Rad). Reverse transcription was performed using 2.5 μg of

RNA from each strain using Superscript III (Life Technologies) per manufacturer

instructions. Priming for cDNA synthesis was achieved using oligo(dT)$_{16}$ (Life

Technologies). Quantitative real-time PCR (qRT-PCR) reactions were performed using

equal amounts of RNAs (-/+ RT (Reverse Transcription) controls) and cDNAs using IQ

RealTime Sybr Green PCR Supermix (Bio-Rad), an iCycler (Bio-Rad), and the gene-specific

primers used in this chapter are listed in **Table 2.2**. Relative transcript levels for each gene

of interest were determined by comparing Cycle threshold (C_t) values generated from

cDNA-containing reactions to standard curves obtained in parallel by measuring serial 1:10

dilutions of yeast genomic DNA and normalizing to the reference gene *ACT1*. Scatter plots

generated using Prism 7 (GraphPad) and representing data obtained from both biological

(individual points) and technical replicates of each sample are expressed relative to the

normalized amount of a target gene of interest in the indicated positive control sample.

Results

Generation of Rap1[AS]

I approached Rap1[AS] generation in two steps. In the first step, I systematically

mutagenized specific subsequences of the *UAS*_{*Rap1*} element in order to identify variants that

significantly decreased binding of Rap1[WT] to *UAS*_{*Rap1*} DNA. The goal of these experiments

was to identify a specific 'inactivated' *UAS*_{*Rap1*}. In the second step, I mutagenized *RAP1*

sequences encoding the Rap1 DBD and performed a genetic screen in cells that contained a

reporter gene driven by the 'inactivated' *UAS*_{*Rap1*} variants identified in step one. Using a

growth selection, I selected for cells that expressed the mutant *UAS*_{*Rap1*} reporter and thus

likely contained a mutant *RAP1* variant that could bind and drive gene expression from the

mutant *UAS*_{*Rap1*}.

Because others have proposed that *UAS*_{*Rap1*} 3' sequences (bp 7-14) determine

whether Rap1 exerts activator or repressor activity when bound to a particular genomic

locus (Idrissi et al., 1998; Lickwar et al., 2012a; Rhee and Pugh, 2011), I focused my *UAS*_{*Rap1*}

mutagenesis efforts on the 5' half of the *UAS*_{*Rap1*}. All possible single point mutant variants

of *UAS*_{*Rap1*} bps 1-6 were tested for the ability to bind purified Rap1[WT] via gel shift

competition DNA binding analyses. The assays used Rap1[WT] protein, ^{32}P-labeled duplex

WT *UAS*_{*Rap1*} probe, and increasing concentrations of unlabeled WT and mutated duplex

competitor DNAs. Consistent with prior mutational analyses of *UAS*_{*Rap1*} (Vignais et al.,

76

1990), these analyses identified a few UAS_{Rap1} sites where mutations significantly

decreased Rap1[WT]-DNA binding (**Table 2.3** and data not shown). The best of these

mutants, 5G UAS_{Rap1} and 6G UAS_{Rap1} were chosen to serve as the inactivated UAS_{Rap1}

sequences in my first screens for selection of Rap1[AS] variants.

Rap1 Mutagenesis Via Error-Prone PCR and Bacterial Omega One Hybrid Screening
Strategy

      Having identified potential Rap1[AS] binding sites, I proceeded to the second step of

my Rap1[AS] generation strategy: mutagenesis of the *RAP1* sequences encoding the DBD and

screening to identify a Rap1[AS]. To generate mutant *RAP1* variants, I performed error-prone

(EP)-PCR (Cadwell and Joyce, 1992) designed to introduce mutations randomly into the

Rap1 DBD. Although co-crystal structures of the Rap1 DBD (Henry et al., 1990) in complex

with DNA existed (König et al., 1996; Matot et al., 2012; Taylor et al., 2000), this unbiased

approach was chosen to allow for the possibility realized in enzyme engineering studies that aa may affect protein activity even if structural data does not directly implicate them (Daugherty et al., 2000; Zaccolo and Gherardi, 1999). A screen based on the omega bacterial one-hybrid selection system (**Figure 2.1A-D**), which had been used successfully to

Table 2.3: Single mutant UAS_{Rap1} Gel Shift Competition Analysis

UAS_{Rap1} variant	UAS_{Rap1} variant sequence (mutant nts are bolded and red)	% No competitor ^{32}P-Rap1[WT]-DNA Complex present at 100X cold UAS_{Rap1} variant
WT	ACACCCATACATT	3
1T	**T**CACCCATACATT	7
1C	**C**CACCCATACATT	3
1G	**G**CACCCATACATT	0.5
2A	A**A**ACCCATACATT	1
2T	A**T**ACCCATACATT	2
2G	A**G**ACCCATACATT	4
3T	AC**T**CCCATACATT	13
3C	AC**C**CCCATACATT	4
3G	AC**G**CCCATACATT	2
4A	ACA**A**CCATACATT	8
4T	ACA**T**CCATACATT	5
4G	ACA**G**CCATACATT	5
5A	ACAC**A**CATACATT	70
5T	ACAC**T**CATACATT	30
5G	ACAC**G**CATACATT	92
6A	ACACC**A**ATACATT	20
6T	ACACC**T**ATACATT	10
6G	ACACC**G**ATACATT	100

A. ω + *UAS*$_{RAP1WT}$

E. coli RNA Polymerase

β β'
ω α$_2$
σ

UAS$_{RAP1WT}$ | Weak Promoter | *HIS*

His⁻

B. ω−Rap1^{WT} + *UAS*$_{RAP1WT}$

ω-Rap1 Fusion Protein

β β'
ω α$_2$
σ

Rap1 DBD

UAS$_{RAP1WT}$ | Weak Promoter | *HIS*

His⁺

C. ω−Rap1^{WT} + *UAS*$_{RAP1MUT}$

β β'
ω σ α$_2$

Rap1 DBD

UAS$_{RAP1MUT}$ | Weak Promoter | *HIS*

His⁻

D. ω−Rap1^{AS} + *UAS*$_{RAP1MUT}$

β β'
ω α$_2$
σ

Rap1^{AS}

Rap1 DBD**

UAS$_{RAP1MUT}$ | Weak Promoter | *HIS*

His⁺

Growth Phenotype
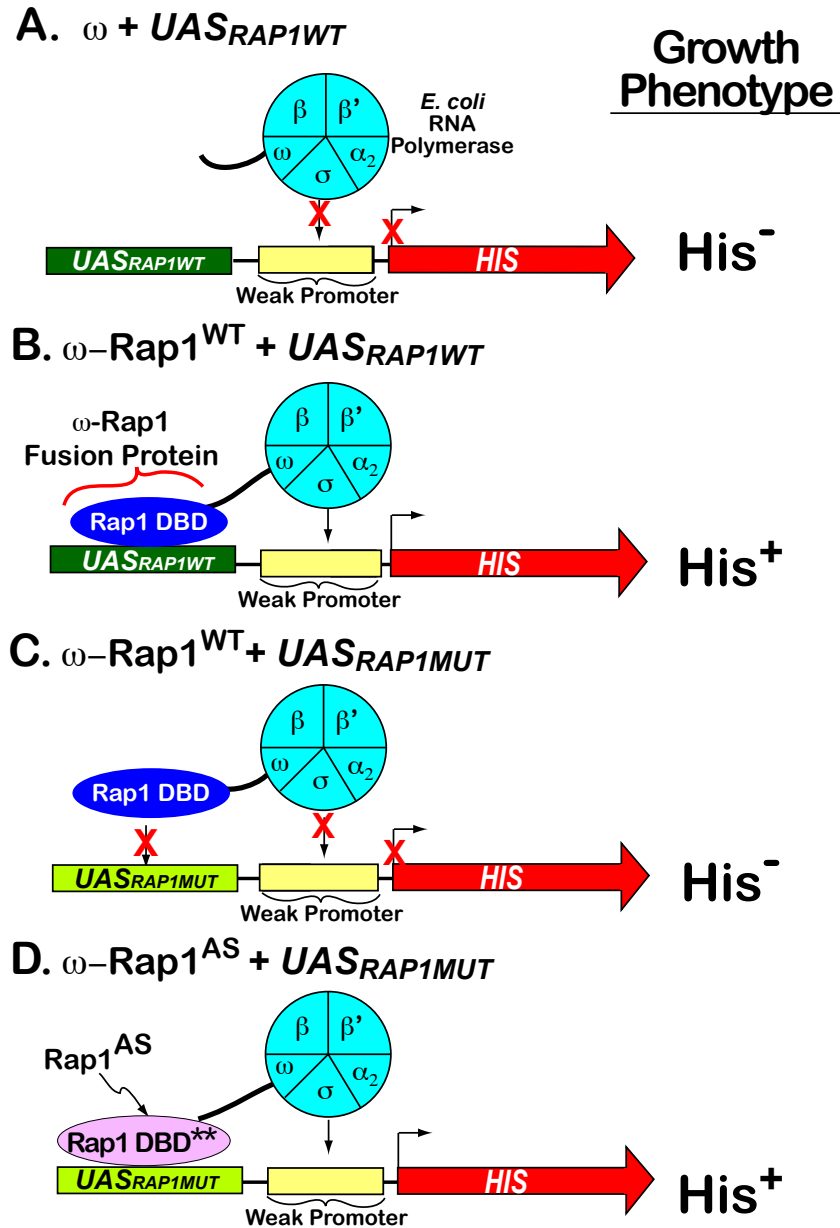
Figure 2.1. Bacterial Omega One Hybrid Rap1^{AS} Screen. The bacterial omega one hybrid screen depends on an interaction between two components: (1) a *HIS* reporter gene driven by a weak promoter and a *UAS* site (such as *UAS*$_{Rap1}$ shown here) and (2) an ω−transcription factor DBD fusion protein. *A*, Because the promoter upstream of the *HIS* gene is weak, the bacterial RNA Polymerase cannot drive *HIS3* expression on its own, resulting in a His⁻ growth phenotype. *B*, In contrast, fusion of the ω subunit of the polymerase to a DBD that can recognize the *UAS* (in this case Rap1 DBD^{WT}, which binds *UAS*$_{Rap1WT}$) enables *HIS3* expression and a His⁺ growth phenotyp. *C*, A version of the *HIS* reporter containing a *UAS*$_{Rap1MUT}$ that the Rap1 DBD cannot bind is not expressed and cells are His⁻. *D*, The only way *UAS*$_{Rap1MUT}$-*HIS3* cells will be His⁺ is if they contain a fusion protein consisting of ω and a Rap1 mutant DBD (Rap1 DBD**) that can bind *UAS*$_{Rap1MUT}$ because it possesses altered DNA-binding specificity (Rap1^{AS}).

78

define the DNA recognition sequences of several transcription factor DBDs (Meng and Wolfe, 2006; Meng et al., 2005), was designed to identify a Rap1[AS] variant capable of functionally interacting with the 5G or 6G *UAS_{Rap1}* sites. Activity in the omega one-hybrid system depends on a functional interaction between two components: (1) A fusion protein consisting of the bacterial RNA Polymerase non-essential subunit ω (Gentry and Burgess, 1989) and a transcription factor DBD fusion protein expressed from an Amp[R] plasmid and (2) a low-copy number *HIS3* reporter Kan[R] plasmid (pH3U3) driven by a weak promoter and a *UAS*. *HIS3* expression levels are very low in the presence of the bacterial RNA Polymerase alone because the weak promoter upstream of *HIS3* provides a poor recognition site for the RNA Polymerase (**Figure 2.1A**). However, *HIS3* expression can be greatly enhanced by the incorporation into the polymerase complex of the ω subunit fused to a DBD that can recognize the *UAS* upstream of the *HIS3* reporter (Dove and Hochschild, 1998; Noyes et al., 2008)(**Figure 2.1B**).

Versions of the pH3U3 *HIS3* reporter (Noyes et al., 2008) containing the 5G and 6G *UAS_{Rap1}* sites were created. *HIS3* reporter gene expression can be selected for by the addition of 3-Amino-Triazole (3-AT) to the growth media. Aminotriazole is a competitive inhibitor of the *HIS3* gene product, the enzyme imidazole glycerol-phosphate dehydratase (Brennan and Struhl, 1980), hence simple growth tests can be used to select for increasing levels of *HIS3* gene expression by varying the concentration of 3-AT in the growth media. Because Rap1[WT] does not bind 5G or 6G *UAS_{Rap1}* efficiently (*cf.* **Table 2.3**), *E. coli* containing an ω-Rap1DBD that is not functionally different than ω-Rap1DBD[WT] should have no means to drive 5G or 6G *UAS_{Rap1}-HIS3* expression above background (**Figure 2.1C**), and thus support growth on media containing 3-AT. By contrast, a cell expressing an ω-Rap1DBD[AS]

variant that can bind and drive efficient pH3U3 $UAS_{Rap1(5G)}$-*HIS3* and/or pH3U3 $UAS_{Rap1(6G)}$-

HIS3 expression (**Figure 2.1D**) will confer resistance to 3-AT (3-AT[R]), and thus grow in the

presence of the inhibitor.

<u>Omega One-hybrid Rap1[AS] Screen</u>

The omega one-hybrid Rap1[AS] screen was performed using selection strain USO

(relevant genotype Δ*hisB* Δ*rpoZ,* see "*E. coli* and Yeast Cell Culture and Basic Manipulations"

above. The EP-PCR generated library of ω-Rap1DBD variants was introduced into USO

selection cells that contained either the pH3U3 $UAS_{Rap1(5G)}$ reporter or pH3U3 $UAS_{Rap1(6G)}$

reporter plasmids (both possess Kan[R]) via electroporation. An estimated 2.4 x 10^{8}

transformants (~100X the number of variants present in my error-prone PCR generated

RAP1 library) were plated on NM-His media + 0.25, 0.5, 1, 2.5, or 5 mM 3-Amino-1, 2, 4-

Triazole and incubated for 3 days at 30°C.   Although 30-40 *E. coli* colonies appeared on

each of the two selection plates used for each pH3U3 UAS_{Rap1} reporter variant, not one of

the ω-Rap1DBD variant expression plasmids isolated from these colonies could confer 3-

AT[R] once reintroduced into USO cells containing the pH3U3 UAS_{Rap1} reporter variant used

for the selection. Thus, the omega one hybrid screen of my EP-PCR generated *RAP1*

variants failed to identify any "true positive" hits that could drive expression of either a 5G

UAS_{Rap1} or 6G UAS_{Rap1} reporter (data not shown).

The negative result from this first Rap1[AS] generation attempt motivated me to

reevaluate my strategy. As part of the reevaluation process, I analyzed the structure of the

Rap1 DBD bound to various target DNAs. These Rap1-DNA structures show that the Rap1

DBD binds its recognition motif primarily via two homeodomains and an unstructured tail
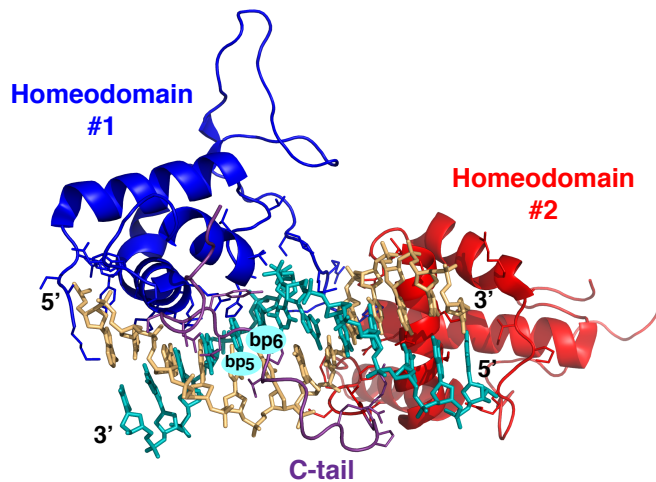
Figure 2.2. The Rap1 DBD-DNA Cocrystal Structure. The Rap1 DBD-DNA cocrystal structure reveals that Rap1 binds its DNA recognition site (top strand, tan hues and bottom strand, teal hues) via two homeodomains (homeodmain #1 (blue) and homeodomain #2 (red)) and an unstructured C-tail (purple). bp$_5$ and bp$_6$ (light blue circles, labeled) of the *UAS$_{Rap1}$* site are located proximal to both portions of homeodomain #1 and the C-tail.

as described in "Chapter I".

Additionally, these structures show that the *UAS$_{Rap1}$* bp 5 and 6 mutated in my 5G and 6G *UAS$_{Rap1}$* sites are located between the two homeodomains and are contacted by both the unstructured DBD tail and a portion of one of the homeodomains (**Figure 2.2**) (König et al., 1996; Matot et al., 2012; Taylor et al., 2000). These facts challenged the generation of a Rap1[AS] that could recognize either the 5G or 6G *UAS$_{Rap1}$*. The error-prone PCR approach used to mutagenize the Rap1 DBD was unlikely to produce variants with the needed changes in both the homeodomain portion and the unstructured tail outside of mutagenizing the DBD beyond recognition. Meanwhile, design of a targeted mutagenesis strategy was difficult because the regions of the DBD involved constituted an unusual recognition module. To improve my chances of generating a Rap1[AS], I would need to generate a potential Rap1[AS] binding site whose mutant *UAS$_{Rap1}$* bps were contacted by a portion of the DBD that used a well-studied recognition motif to bind DNA.

Identification of Potential Rap1[AS] Binding Sites Guided by the Rap1 DBD-DNA Structure

Although the portion of the Rap1 DBD contacting *UAS$_{Rap1}$* bps 5 and 6 uses an unusual mode of DNA recognition, the Rap1 homeodomains themselves do indeed

constitute highly recognizable DNA-binding motifs. Indeed, multiple studies have shown

that within a homeodomain, the third, or recognition helix of the three helix bundle

mediates sequence-specific DNA recognition (Fraenkel et al., 1998; Wolberger et al., 1991).

The apposition of the homeodomain recognition helix #1, which contacts the upstream half

of the Rap1 binding sequence and is the focus of my Rap1 DNA mutagenesis efforts is

shown in **Figure 2.3A**. This recognition helix specifically contacts DNA bp_2, bp_3 and bp_4

(**Figure 2.3A** (bp labeled: **bp_2**, **bp_3** and **bp_4,** homeodomain is dark blue).

Since no single mutant variants of UAS_{Rap1} bp2, bp3 and bp4 significantly reduced

Rap1^{WT}-DNA binding, double mutant UAS_{Rap1} were generated and tested via gel shift

competition DNA-binding analyses. Several of these double base pair mutant UAS_{Rap1}

binding sites caused a significant decrease in Rap1^{WT}-DNA binding. The 3T4A UAS_{Rap1}

mutant reduced Rap1^{WT} binding by over 20-fold relative to the WT UAS_{Rap1} (compare loss

of Rap1-DNA complex in the presence of WT and 3T4A competitor DNAs at 2-, 5-, 10- and

25-fold mole excesses; **Figure 2.3B**). This reduction in affinity (competition strength) was

the largest of the double mutants tested (data not shown). Consequently, the 3T4A UAS_{Rap1}

was selected to serve as the 'inactivated' UAS_{Rap1} sequence in further screens for selection

of Rap1^{AS} variants.

<u>Rap1 DBD-DNA Structure Guided Mutagenesis and Rap1^{AS} Yeast Screening Strategy</u>

As a second mutagenesis approach to generating a Rap1^{AS} variant capable of binding

the 3T4A UAS_{Rap1} site, I utilized a targeted randomization mutagenesis approach recently

employed to create altered DNA-binding specificity variants of the *Drosophila* engrailed

homeodomain (Chu et al., 2012). The six aa's of the Rap1 DBD homeodomain-1 DNA
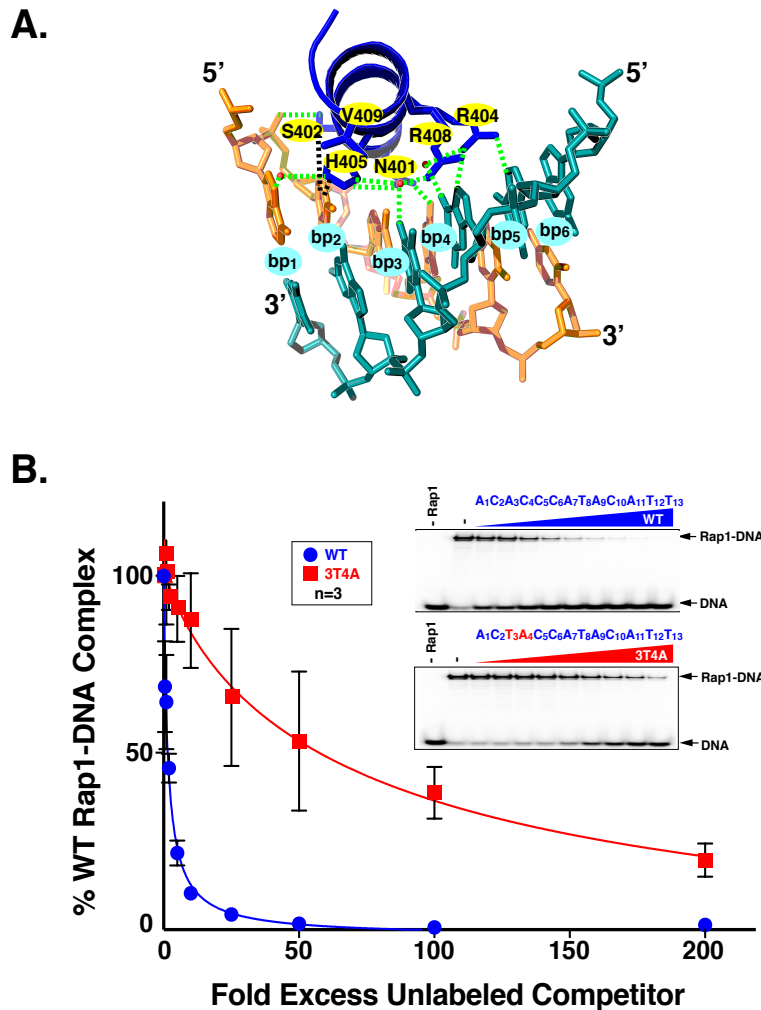
Figure 2.3. Mutation of WT *UAS_Rap1* Nucleotides 3A and 4T to 3T and 4A Significantly Decreases Binding of WT Rap1 to 3T4A *UAS_Rap1* DNA. *A.* The Rap1 DBD homeodomain-1 recognition helix (dark blue; top) is shown in complex with its DNA recognition site labeled **bp_1**, **bp_2**, **bp_3**, **bp_4**, **bp_5**, **bp_6**. Top strand, tan hues (5'**A_1C_2A_3C_4C_5C_6** 3'), bottom strand teal hues. Hydrogen bonds between protein and DNA are indicated by dashed green lines; H-bonds mediated by H_2O molecules are indicated by green dashed lines and red balls; hydrophobic interactions are indicated by black dashed lines. The DNA base pairs mutated to create the 3T4A mutant binding site are **bp_3** and **bp_4**. Rap1 DBD recognition helix amino acid residues targeted for codon randomization mutagenesis are indicated by yellow ovals at amino acid positions: **N_401**, **S_402**, **H_405**, **R_408** and **V_409**. Image generated using the PyMol v 1.5.04 for the MacOS from PDB file 1IGN (Matot et al., 2012). *B.* Gel shift competition DNA binding analyses with WT *UAS_Rap1* or 3T4A *UAS_Rap1* DNAs. Gel shift binding reactions were performed by incubating 100 fmole purified recombinant Rap1[WT] with 50 fmole (700 cpm/fmole) duplex ^{32}P-labeled WT *UAS_Rap1* DNA (5'A_1C_2A_3C_4C_5C_6A_7T_8A_9C_10A_11T_12T_13-3') alone (No Rap1, **-Rap1**), or with Rap1 and either no competitor (**-**), or the indicated fold molar-excess of either cold WT *UAS_Rap1* (top gel scan image) or cold 3T4A *UAS_Rap1* (bottom gel scan image); 0.5X, 1X, 2X, 5X, 10X, 25X, 50X, 100X or 200X left to right (WT: blue circles; 3T4A: red squares) in a final volume of 20 µl. Reactions were fractionated on non-denaturing polyacrylamide gels, vacuum dried, and imaged using a Bio-Rad FX imager. The amount of bound complex from each reaction was quantified using Bio-Rad Quantity One software. Data was analyzed using Microsoft Excel and is expressed as % Rap1[WT]-^{32}P-DNA Complex when no competitor is present (i.e. + Rap1 and **-** competitor). A representative image for each competition was chosen from among three independent replicates. Data for replicates was analyzed via Graph Pad Prism 7 software and the plot shown was generated using an [Inhibitor] vs. response non-linear fit. Error bars represent SDs.

recognition helix that face DNA (**Figure 2.3A**) were chosen as targets for codon-directed

randomization mutagenesis (An et al., 2005) (**Figure 2.4A**; Rap1 aa's **Asn401**, **Ser402**,

Arg404, **His405**, **Arg408** and **Val409**). Screening this library in the omega one-hybrid

system identified DBD variants that could drive 3T4A UAS_{Rap1} reporter expression in

bacteria. However, none of these variants were able to drive 3T4A UAS_{Rap1} reporter

expression in the context of the full-length Rap1 protein in yeast (data not shown).

As a result of the failure of Rap1 DBD variants isolated in *E. coli* to function as expected in yeast, I devised a direct yeast screening strategy that could rapidly test millions of full-length Rap1 mutant variants for the ability to functionally interact with 3T4A UAS_{Rap1} in vivo. As in the omega one-hybrid screen, the functional interaction chosen for this yeast screen utilized a *HIS3* reporter gene, whose expression can be selected for using 3-AT. In the reporter used for Rap1[AS] screening in yeast, the two WT UAS_{Rap1} DNA binding sites present in a previously characterized UAS_{Rap1}-*HIS3* reporter (Garbett et al., 2007; Mencía et al., 2002) were replaced with two copies of the 3T4A variant UAS_{Rap1} (see
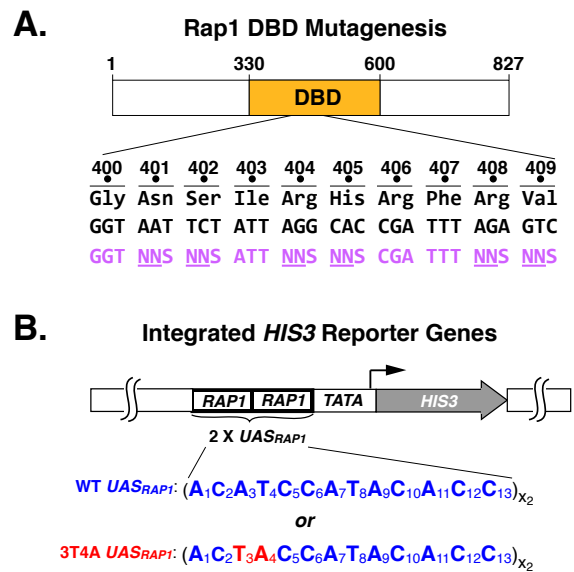
Figure 2.4. Rap1 DBD Mutagenesis Strategy. *A.* Schematic of Rap1 showing the location of the DBD within the 827 aa-long protein. Amino acid sequence of DBD region aa 400 to aa 409 (black, 3 letter code) is shown along with the corresponding nt codon sequence (black) and a portion of one of the primers used for codon randomization (purple) indicating the targeted codons (**NNS**, N= any nt, S = G or C). *B.* Schematic of integrated UAS_{Rap1}-driven *TATA-HIS3* reporter genes used in the selection of the altered DNA-binding specificity variant of Rap1. Two versions of the reporter are shown, **WT** (top) where *HIS3* is driven by tandem copies of the **WT** UAS_{Rap1} enhancer sequence: $A_1C_2A_3T_4C_5C_6A_7T_8A_9C_{10}A_{11}C_{12}C_{13}$; or **3T4A** variant UAS_{Rap1} enhancer: $A_1C_2T_3A_4C_5C_6A_7T_8A_9C_{10}A_{11}C_{12}C_{13}$; mutated nts in red.

Figures 2.3B, 2.4B). Because Rap1^{WT} does not bind 3T4A UAS_{Rap1} efficiently (*cf.* **Figure**

2.3B), yeast expressing only Rap1^{WT} have no means to drive 3T4A UAS_{Rap1}-*HIS3* expression,

and hence fail to grow on media containing 3-AT. By contrast, a cell expressing a Rap1^{AS}

variant that can bind and drive efficient 3T4A UAS_{Rap1}-*HIS3* expression will confer

resistance to 3-AT (3-AT^R), and thus grow in the presence of the inhibitor.

Rap1^{AS} Yeast Screen

 I performed the Rap1^{AS} yeast screen using the haploid yeast strain YAM23 (relevant

genotype: *his3Δ*, *ura3Δ*, *rap1Δ*, *3T4A UAS::TATA::HIS3* + pRS415-*MYC$_5$-RAP1,* **Table 2.1**)

that was transformed to Ura$^+$ with mutagenized Rap1 DBD library plasmids carried on the

URA3-marked plasmid pRS416. An estimated 1 x 10^6 independent Ura$^+$ colonies (~1% of

the total library) were plated onto SC -His + 5mM 3-AT selective media plates. After four

days of incubation at 30°C, 158 His$^+$, 3-AT^R colonies were isolated. The growth phenotype

of these colonies was re-tested by patching onto SC-His + 3-AT plates; 136 colonies out of

the original 158 isolated indeed possessed 3-AT^R. To determine whether the His$^+$, 3-AT^R

phenotype displayed by these colonies was plasmid borne, Rap1 mutant expression

plasmids were isolated from the thirty colonies that had appeared the soonest on the 3-AT-

containing selection plates (ranked in order of appearance with colony #**1** appearing 1st

and colony #**30** appearing 30th). Plasmids were recovered from these 30 strains and used

to transform the original selection yeast strain, YAM23. The resulting transformants were

retested for growth on SC-His + 5mM 3-AT selective media plates. Fourteen of the thirty

recovered Rap1 mutant expression plasmids conferred 3-AT^R, and thus represented

putative altered DNA-binding specificity variants of Rap1.

Analysis of Putative Altered DNA-binding Specificity Rap1[AS] Variants

   The fourteen Rap1 mutants identified in the screen were characterized to allow

selection of one variant for use as a Rap1[AS] in Rap1 AD mapping studies. The complete

ORFs of the fourteen plasmid borne *rap1[AS]* genes were sequenced. All mutations identified

were within the targeted Rap1 aa's (**Figure 2.5A**, **top**). Only two of the mutants (#**10** and

11) possessed identical sequences, indicating that the screen was likely not saturated.

Sequence analyses were performed to identify any patterns present in the types of aa

changes within the Rap1 variants identified in the screen (**MEME Motif**; **Figure 2.5A**,

lower). Rap1 aa N401 was frequently found mutated to a G or a P while residue H405 was
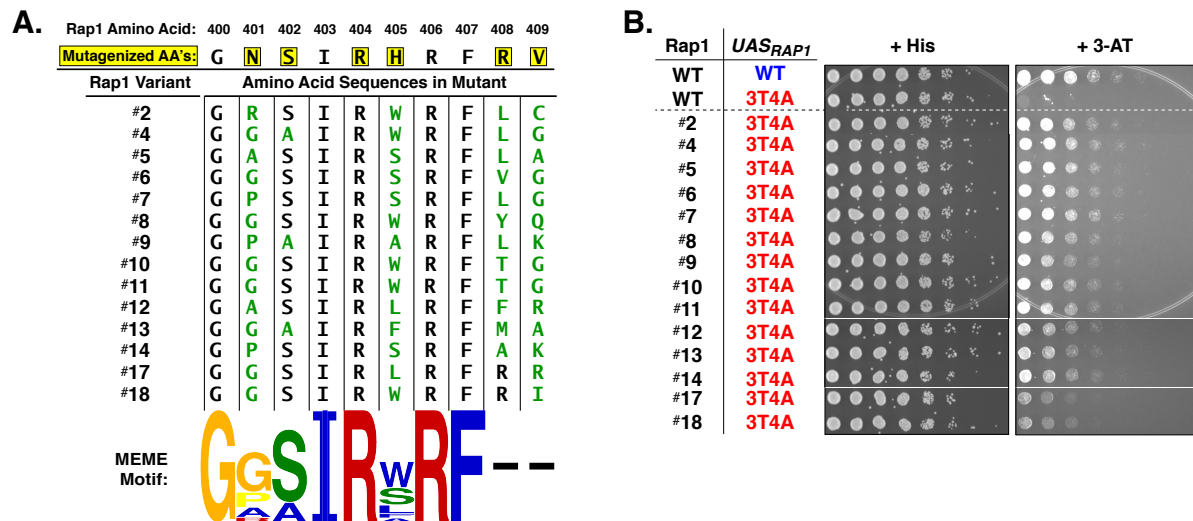
Figure 2.5. The Rap1 Mutagenesis Screen Identifies Rap1 Variants that Functionally Interact with 3T4A UAS_Rap1. *A.* Amino acid sequence of mutagenized Rap1 DBD amino acids 400 to 409 (yellow highlighting) and fourteen variant forms (#**2** to #**18**) of Rap1 identified in the Rap1[AS] screen. Amino acid changes in these variants are indicated (**green**). Lower, a motif of putative Rap1[AS] hit homeodomain-1 recognition helix sequences generated using MEME. The size of each letter is proportional to its frequency of appearance among the Rap1 variant sequences #**2** to #**18**. *B.* Yeast growth test to assess the ability of various forms of Rap1 (WT) or Variant (#**2** to #**18**) to confer resistance to 5mM 3-AT via expression of either the WT *UAS_Rap1-HIS3* reporter variant (blue) or the 3T4A *UAS_Rap1-HIS3* (red) variant, and either a second copy of Rap1[WT] or the indicated Rap1[AS] screen hit. Yeast were serially diluted 1:4 (left to right) and spotted using a pinning tool onto non-selective media (**+ His**) and media that selected from expression of the *UAS_Rap1-HIS3* reporter (**+ 3-AT**). Plates were photographed after growth at 30°C for two days. Images are representative of three independent biological replicates.

frequently mutated to W or S. There were no clear aa substitution patterns for R408 and

R409. In spite of being targeted for mutagenesis, S402 and R404 were mutated only rarely

(S402) or not at all (R404). This data suggests either a failure to efficiently mutagenize

Rap1 aa residue 404, or a strong/absolute requirement of R404 for Rap1 DNA-binding.

As predicted from the competition DNA binding data of **Figure 2.3B**, Rap1^{WT} cannot

utilize the 3T4A *UAS$_{Rap1}$* site to drive *HIS3* expression (compare top two rows of growth

tests, **Figure 2.5B**). By contrast, all of the putative Rap1^{AS} variants have the ability to

promote efficient expression of the 3T4A *UAS$_{Rap1}$-HIS3* reporter gene to confer 3-AT^{R}

growth (mutants **#2** through **#18**; **Figure 2.5B**). Interestingly, those mutant variants

recovered from colonies that appeared the earliest during the screen grow slightly faster

than those recovered from colonies that had appeared later (i.e. variant **#2** to **#14** earlier

than variant **#17** and **#18**; **Figure 2.5B**). Overall, the 3-AT^{R} growth properties of variants

#2 to **#14** are comparable to yeast containing Rap1^{WT} and the WT *UAS$_{Rap1}$-HIS3* reporter,

while variants **#17** and **#18** grow somewhat slower.

To allow unambiguous Rap1 AD mapping, a true altered DNA-binding specificity

mutant that fails to bind WT *UAS$_{Rap1}$* (and thereby interfere with Rap1^{WT} essential function)

was desired. In order to find such a Rap1 mutant whose improved 3T4A *UAS$_{Rap1}$* binding is

accompanied by a reduced WT *UAS$_{Rap1}$* binding, six of the fourteen preliminarily

characterized Rap1 screen hits (see below) were selected for purification and gel shift

DNA-binding competition assays. Because there was no way to predict a priori, which if

any of the Rap1 screen hits possessed true altered DNA-binding specificity, six screen hits

were chosen to cover the sequence variation present in the collection of Rap1 mutants

whose plasmid borne expression supported AT^{R}. Variant **#10** was chosen because its

sequences were highly similar to the logo that was generated by motif analysis. Rap1

variants #**2**, **5**, **13**, **17**, and **18** were selected because of deviations from the sequence logo,

in either the presence of additional mutations (i.e. #**5**), the absence of a mutation that was

present in other variants (#**17** and **18**), or an uncommon mutation (i.e. #**2**) such as a basic

R residue at position 401 instead of an uncharged G, P, or A. All six of these Rap1 mutant

variants bound [32]P-3T4A *UAS_Rap1* in a gel shift assay (**Figure 2.6A**, and data not shown).

Out of the six, Rap1 mutants #**5**, **17**, and **18** displayed expanded DNA-binding specificity,

and bound both WT and 3T4A *UAS_Rap1* sites with similar affinity. By contrast, Rap1 variants

#**2**, **10**, and **13**, whose sequences contrasted with those of the expanded specificity variants

in the possession of a bulky hydrophobic aa (i.e. W or F) at aa 405 and a mutation at aa 408
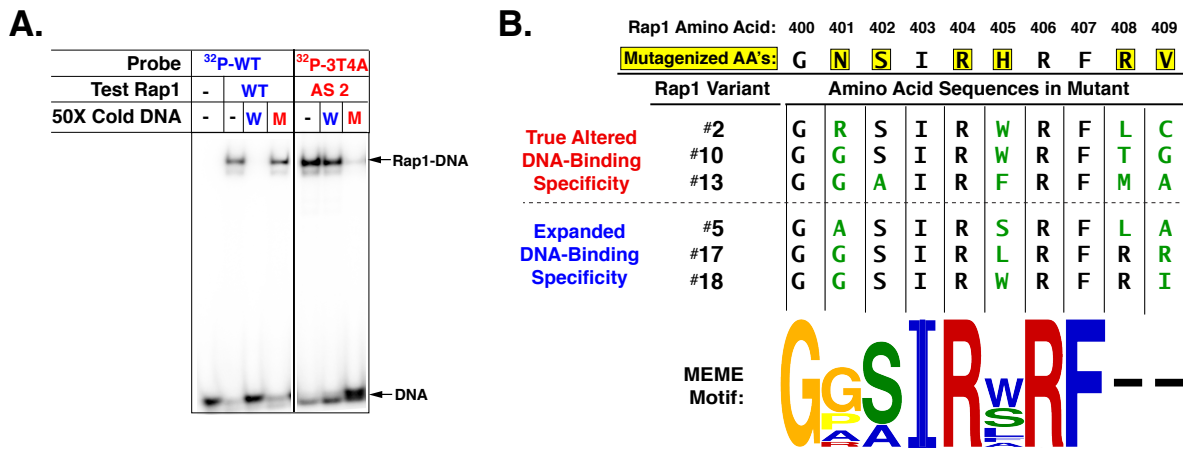
Figure 2.6. Identification of Rap1 Mutagenesis Screen Hits with True Altered DNA-binding Specificity. *A.* Gel shift competition analysis performed to compare the binding affinity of WT and Rap1[AS] screen hit variant #**2** for binding to either WT *UAS_Rap1* or 3T4A *UAS_Rap1* DNAs. Assays were performed (as in **Figure 2.3B**) by incubating purified Rap1[WT] or Rap1 variant #**2** with its cognate binding site, **[32]P-WT** *UAS_Rap1* (**blue**); or **[32]P-3T4A** *UAS_Rap1* (**red**). Binding reactions also included either no competitor (**-**), or 50 fold mole-excess of either cold WT *UAS_Rap1* (**W**, **blue**) or cold 3T4A *UAS_Rap1* (**M**, **red**) as shown. A representative image from two independent replicates is presented. *B.* Amino acid sequence of mutagenized Rap1 DBD amino acids 400 to 409 (yellow highlighting) in the three identified true altered DNA-binding specificity Rap1 variants (red, #**2**, #**10**, and #**13**) and the identified expanded DNA-binding specificity variants (#**5, #17**, and #**18**). Amino acids changes in these variants are indicated (**green**). Lower, the motif of putative Rap1[AS] hit homeodomain-1 recognition helix sequences generated using MEME. The size of each letter is proportional to its frequency of appearance among the Rap1 variant sequences #**2** to #**18** (*cf* **Figure 2.5A**).

(**Figure 2.6B**), showed reduced affinity for the WT UAS_{Rap1} site (**Figure 2.6A** and data not shown). In particular, mutant #**2** displayed the largest reduction in WT UAS_{Rap1} affinity (**Figure 2.6A**, and data not shown).

Consistent with its significantly reduced affinity for WT UAS_{Rap1}, Rap1 mutant #**2** also failed to complement the null *rap1* allele (*rap1Δ*) in a plasmid shuffle assay (**Figure 2.7A**), indicating that it could not efficiently bind the WT UAS_{Rap1} of (at least one) essential Rap1-dependent genes in vivo. As a final *in vitro* test of the DNA-binding specificity of Rap1 mutant #**2**, a gel shift competition analysis was performed using duplex WT and all single and double UAS_{Rap1} variants of bps 3 and 4. Amazingly, this preliminary analysis showed that only cold competitors that contained a 3T and/or a 4A mutation reduced Rap1[AS] [32]P-3T4A UAS_{Rap1} DNA binding (**Figure 2.7B**). Based upon all these data Rap1, variant #**2** showed true altered DNA-binding specificity *in vitro* and *in vivo*, and henceforth is referred to as Rap1[AS] (or AS).

Molecular Genetic Characterization of Rap1[AS]

Rap1[AS] was subjected to further characterization to ensure that it would serve as an appropriate reagent for attempted AD identification and mapping studies. The AS form of Rap1 was tested to document that: (1) Rap1[AS]-driven reporter expression actually requires an enhancer, and is specific to the 3T4A UAS_{Rap1} site; (2) Rap1[AS] efficiently drives *HIS3* reporter expression as scored at the mRNA[HIS3] level; (3) Rap1[AS] is stably expressed at levels similar to Rap1[WT]; and (4) when co-expressed with Rap1[WT], Rap1[AS] does not compete with the WT protein and cause a dominant, slow growth phenotype.

Figure 2.7. Rap1 AS #2 Displays Altered DNA-binding Specificity *in vivo* and Specificity For *UAS_{Rap1}* Variants Containing a 3T and/or 4A Mutation *in vitro*. *A.* Plasmid shuffle analysis of altered DNA-binding specificity Rap1 variant **#2** performed to test its ability to complement the *rap1* null allele. Yeast carrying a chromosomal null *RAP1* allele (*rap1Δ*) and a *URA3*-marked *RAP1* covering plasmid were transformed with a test variant of *RAP1*, labeled **rap1***: (*i*) a second plasmid-borne copy of *RAP1* (labeled **WT**, **blue**); (*ii*) empty plasmid vector (labeled **-**, **black**); or (*iii*) the same plasmid vector expressing Rap1 variant **#2** (labeled **AS#2**, **red**). Yeast were serially diluted 1:4 (left to right) and growth was scored on media lacking 5-FOA ("**Unshuffled**"; relevant genotype: ***RAP1, rap1Δ, rap1****) or containing 5-FOA ("**Shuffled**" relevant genotype: **-**, ***rap1Δ, rap1****). Plates were incubated at 30°C for two days and then photographed; a representative image from three independent replicates is shown. *B.* Gel shift competition analysis performed to compare the binding of Rap1[WT] and Rap1[AS] screen hit variant **#2** to various *UAS_{Rap1}* DNA variants. Assays were performed (as in **Figure 2.3B**) by incubating purified Rap1[WT] or Rap1 variant **#2** with its cognate binding site, **32P-WT** *UAS_{Rap1}* (**blue**); or **32P-3T4A** *UAS_{Rap1}* (**red**). Binding reactions also included either no competitor (**-**), or 100 fold mole-excess of the indicated cold *UAS_{Rap1}* competitor DNAs. Data shown is representative of 1 biological replicate.

A.
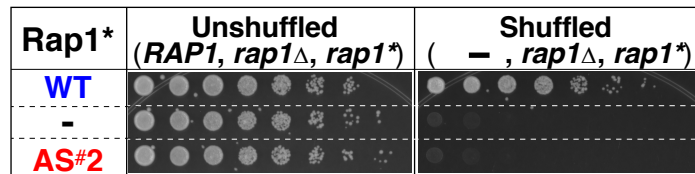
B.
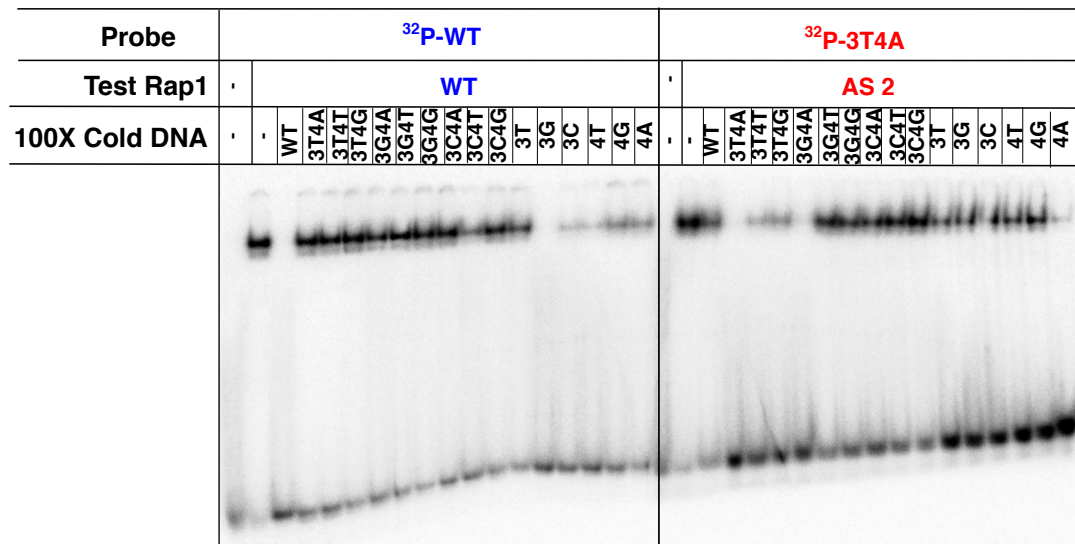
To demonstrate that Rap1[AS] drives reporter gene expression efficiently and specifically from 3T4A *UAS_{Rap1}* as expected from the analyses described in "Analysis of Putative Altered DNA-binding Specificity Rap1[AS] Variants", two new *HIS3* reporter variants were constructed. The first, termed *ΔUAS_{Rap1}*, completely lacks *UAS_{Rap1}* sites upstream of

HIS3. This construct tests the hypothesis that Rap1[AS] might bypass the requirement for an enhancer, while simultaneously defining background expression of the *UAS$_{Rap1}$-TATA-HIS3* reporter. The second construct substituted a 3G5G *UAS$_{Rap1}$* enhancer in place of either the WT or 3T4A enhancer. This variant enhancer tested the functional DNA-binding specificity of Rap1[AS], which was selected to bind the 3T4A site. Previous work has shown that both mutations (i.e. *UAS$_{Rap1}$* deletion, or 3G5G substitution) dramatically reduce Rap1-driven transcription *in vivo* (Garbett et al., 2007; Mencía et al., 2002). *HIS3* expression was scored in appropriate yeast strains by AT[R] growth and qRT-PCR-measured mRNA[HIS3] assays. As shown in both growth (**Figure 2.8A**) and mRNA[HIS3] analyses (**Figure 2.8B**), Rap1[WT] and Rap1[AS] were only able to robustly drive expression of the reporter containing their cognate DNA recognition site (WT *UAS$_{Rap1}$* and 3T4A *UAS$_{Rap1}$*, respectively). It is important to note that as detailed in the "Steady State RNA" section, *HIS3* mRNA levels are scored by qRT-PCR using total RNA extracted from cells grown in SC + Histidine to prevent any selection for reporter gene expression that occurs when 3-AT is added to growth media. Interestingly, Rap1[AS] drives expression of the 3T4A *UAS$_{Rap1}$-HIS3* reporter gene mRNA[HIS3] to a level greater than that observed with the WT *UAS$_{Rap1}$-HIS3* reporter (**Figure 2.8B**). Deletion of the enhancer abolished expression of the *HIS3* reporter regardless of the Rap1 form present (WT or AS; **Figures 2.8A, B**). Immunoblot analysis of yeast whole cell extracts show that Rap1[AS] was stably expressed at levels comparable to Rap1[WT] (**Figure 2.8C**; note that all constructs contain an N-terminal Myc$_5$ tag and a nuclear localization sequence (NLS); see "Test Rap1 Yeast Expression Vectors"). Further, growth curves with pseudodiploid cells (**Figure 2.8D**; Rap1 **WT/WT**; Rap1 **WT/AS**) demonstrate that Rap1[AS] does not induce a dominant, slow growth phenotype. Based on this data, I concluded that

Rap1[AS] possessed all of the characteristics desired for use as a tool to search for an AD within Rap1.

A.

Rap1	*UAS$_{Rap1}$*	+ His	+ 3-AT
WT	**WT**		
WT	**3G5G**		
WT	**ΔUAS**		
WT	**3T4A**		
AS	**3G5G**		
AS	**ΔUAS**		
AS	**3T4A**		

Integrated *HIS3* Reporter Genes

[RAP1] [RAP1] TATA → HIS3

2 X *UAS$_{RAP1}$*

WT *UAS$_{RAP1}$*: ($A_1C_2A_3T_4C_5C_6A_7T_8A_9C_{10}A_{11}C_{12}C_{13}$)$_{x2}$

Δ*UAS$_{RAP1}$*: (————————Δ————————)$_{x2}$

3G5G *UAS$_{RAP1}$*: ($A_1C_2G_3A_4G_5C_6A_7T_8A_9C_{10}A_{11}C_{12}C_{13}$)$_{x2}$

3T4A *UAS$_{RAP1}$*: ($A_1C_2T_3A_4C_5C_6A_7T_8A_9C_{10}A_{11}C_{12}C_{13}$)$_{x2}$

B. % WT (*HIS3 / ACT1*)

WT + WT UAS, WT + ΔUAS, WT + 3G4G UAS, WT + 3T4A UAS, AS + ΔUAS, AS + 3G4G UAS, AS + 3T4A UAS

C.

MW, WT, no tag, AS

185 / 115 — Test Rap1 (Myc) IB
50 / 30 — Actin IB
30 / 25 — Ponceau S

D. OD$_{600}$ vs Hours

WT / WT, WT / AS

Figure 2.8. Functional characterization of Rap1[AS]. *A.* Rap1[AS] specifically drives the mutant 3T4A *UAS$_{Rap1}$-HIS3* reporter. Upper: Test of the ability of WT and AS forms of Rap1 to bind different enhancers to confer amino-triazole resistant growth using the assay detailed in **Figure 2.5B**. Yeast strains carrying the indicated *UAS$_{Rap1}$-HIS3* reporter variant (**WT**, **3G5G**, **ΔUAS** or **3T4A**, as shown) and either a second copy of Rap1[WT] (**blue**) or Rap1[AS] (**red**) were grown on non-selective (**+ His**) or *HIS3*-reporter gene selection (**+ 3-AT**) media. Images shown are representative of three independent replicates. Lower: detailed structures of the *UAS$_{Rap1}$-HIS3* reporters used in these growth tests. *B.* qRT-PCR analyses of the steady state levels of *HIS3* reporter mRNA, relative to *ACT1* in the yeast strains tested in **panel A**. Data were obtained by testing three biological replicates (each indicated by a white circle) analyzed in duplicate and plotted as a percentage of the *HIS3* mRNA levels present in WT Rap1 + WT *UAS$_{Rap1}$* yeast. Mean ± SD is depicted. * = $p < 0.001$, ** = $p < 0.001$. *C.* Steady state protein expression levels of Rap1[WT] and Rap1[AS]. Myc$_5$-tagged Rap1 forms (top, **WT**, **AS**; **Test Rap1 (Myc) IB**) were scored using immunoblotting with anti-Myc IgG. A strain carrying a plasmid expressing only untagged Rap1 was used as a specificity control for the Myc antibody (labeled **no tag**). Prior to incubation with antibodies, blots were stained with Ponceau S to monitor total protein loading (bottom; **Ponceau S**). Equal protein loading was also monitored via immunoblotting with anti-Actin IgG (middle, **Actin IB**). Images are representative of three independent replicates. *D.* Growth curves of yeast expressing WT or AS forms of Rap1 from a plasmid carrying either a second copy of Rap1[WT] or Rap1[AS] (labeled **WT/WT** or **WT/AS**). Overnight-grown yeast starter cultures were diluted to a starting OD$_{600}$ of 0.5, and the optical density of the cultures were monitored over the course of 12 hours. Data shown represents the average of three biological replicates. Error bars represent SDs.

Prior work performed using conventional approaches produced ambiguous data regarding whether Rap1 actually contains a functional AD. As a consequence, I decided to use an alternative approach to identify an AD within budding yeast Rap1. Despite the challenges involved, I undertook the generation of an altered DNA-binding specificity variant of Rap1, termed Rap1^{AS}. Assuming successful Rap1^{AS} generation, my plan was to use Rap1^{AS} as a novel tool to facilitate the identification and high-resolution characterization of an AD within Rap1.

With the exception of proteins that bind DNA via zinc finger motifs, true altered DNA-binding specificity variants are fairly difficult to generate. This is underscored by the fact that few such proteins have been described in the literature. That said, successful generation of altered DNA-binding specificity variant proteins has yielded significant insights into deciphering the determinants of protein-DNA recognition while simultaneously providing novel tools to probe and dissect the activity of DNA-binding proteins. Recognition of a mutant enhancer or *UAS* site requires that a DBD gain the ability to bind the mutant DNA sequence via alteration in the ability of a protein to bind novel DNA sequences and/or shapes. True altered DNA-binding specificity variants (rather than expanded DNA-binding specificity variants) display significantly reduced WT DNA sequence binding in addition to gaining mutant DNA recognition. The AS Rap1 variant identified in this Chapter, termed Rap1^{AS}, exhibits exactly these properties, and hence was deemed ideal for initiating efforts to discover and pinpoint the AD of Rap1 absent the many

complications imposed by the multiple essential cellular functions of the protein (see

Chaper I).

The steps I took to generate Rap1[AS] taught me useful lessons in protein engineering.

In my efforts to obtain Rap1[AS], I found that the "rational" approach to Rap1[AS] design

succeeded where the unbiased mutagenesis approach did not. In personal

communications, scientists from labs whose focus is on protein engineering indicated that,

at least as a first step in generating novel activity, success depends on a rational design

approach. Indeed, most contemporary protein engineering groups generate proteins with

novel function using structure-, and especially in recent years, computationally-guided

design (Chu et al., 2012; Jiang et al., 2008; Kries et al., 2013; Thyme et al., 2014). Only once

a protein possesses a desired activity, can unbiased mutagenesis approaches be used to

further improve that activity, especially if a large number of mutant variants can be

screened (Daugherty et al., 2000; Obexer et al., 2017; Zaccolo and Gherardi, 1999).

Meanwhile, analysis of the aa sequences of the Rap1 AS mutants recovered in my

screen provides some insights into the DNA recognition determinants of WT and mutant

UAS[Rap1] DNA base pairs 3 and 4. The fact that consistent aa sequence patterns were found

among the mutations present at Rap1 aa's 401 and 405 (see **Figure 2.6B**) in all of the Rap1

variants suggests that these aa changes are required to enable Rap1 binding to 3T4A

UAS[Rap1]. Further, the comparison of the sequences of altered DNA-binding specificity Rap1

variants #**2**, #**10** and #**13**, with the sequences of expanded DNA-binding Rap1 variants #**5**,

#**17**, and #**18** suggests that the true altered DNA-binding specificity variants contained

both a mutation at aa 408 and a bulky hydrophobic aa (i.e. W or F) at Rap1 aa 405 (*cf.*

Figure 2.6B). These mutations may decrease Rap1 mutant binding to WT *UAS[Rap1]* by

breaking a favorable water-mediated contact between Rap1 R408 and WT UAS_{Rap1} base-pair 3 (König et al., 1996) or by using a bulky hydrophobic aa at Rap1 position 405 to actively exclude binding to the WT UAS_{Rap1} element (see **Figure 2.3A**).

In addition to providing new knowledge to advance protein-engineering efforts, my work on the generation of Rap1[AS] resulted in the development of a tool to unambiguously dissect Rap1 structure-function relationships. Thus, I set out to see if I could use Rap1[AS] to obtain a high-resolution map of a putative Rap1 AD. The results of these efforts (see Chapter III) show that Rap1[AS] can indeed be used to greatly advance our studies of Rap1 biology.

CHAPTER III

RAP1 ACTIVATION DOMAIN (AD) MAPPING AND IDENTIFICATION OF TFIID TAF5 AS AN

AD COACTIVATOR TARGET

Important Outcomes of Rap1 AD mapping using Rap1[AS]

As stated in Chapters I and II, the Rap1 AD had never been unambiguously mapped

prior to my thesis research. Thanks to the Rap1[AS] generated in Chapter II, I was well

positioned to conclusively answer the question of which domain(s) constitute the Rap1 AD.

My goal was to identify both the region and the key individual aa's within that region

required for AD activity. In addition to characterizing the AD of an important transcription

activator that binds with unusually high affinity to the Taf4, 5, and 12 subunits of the TFIID

coactivator (Layer et al., 2010), my AD mapping would generate a series of point mutant

variants that would provide precise tools for dissecting Rap1-dependent mechanisms of

transcription activation. I also wanted to initiate the identification of coactivator targets of

the Rap1 AD by testing the hypothesis that the Rap1 AD interacts with TFIIA and/or TFIID

Tafs 4, 5, 12 as predicted by our "Lock to Load" model and our prior studies of RP gene

transcription activation (Garbett et al., 2007; Layer and Weil, 2013; Layer et al., 2010; Papai

et al., 2010). Ideally, the Rap1 AD point mutant variants I generated during my AD

mapping would contain separation-of-function variants that could be used in future studies

to tease apart the mechanistic consequences of possible Rap1 AD interaction with these

multiple coactivator targets.

In this Chapter, I describe a structure-function dissection analysis using Rap1^{AS} performed to achieve my Rap1 AD mapping goal, some of which was originally published in my *JBC* manuscript (Johnson and Weil, 2017) © the American Society for Biochemistry and Molecular Biology. In this approach, I subjected the gene encoding Rap1^{AS} to systematic deletion and point mutagenesis to identify a 41-aa long AD within the C-terminal portion of the protein that is responsible for driving high-level reporter gene expression. This AD has the features of acidic activation domains described in other eukaryotes as it contains seven evolutionarily conserved hydrophobic residues within the acidic aa-rich element that contribute critically to the activation potential of Rap1^{AS}. Importantly, mutation of all seven of these conserved aa's to alanine within the context of WT Rap1 (Rap1^{WT}) induces a dramatic slow growth phenotype while simultaneously reducing transcription of RP- and GE-encoding genes, demonstrating that the AD mapped using Rap1^{AS} is physiologically relevant. My protein-protein interaction experiments performed using Rap1^{WT} and a Rap1 AD mutant variant show that mutation of key Rap1 AD residues significantly reduces the binding of the AD mutant variant of Rap1 to Taf5, one of the known TFIID coactivator subunit targets of Rap1 (Garbett et al., 2007; Layer et al., 2010). Thus, in addition to providing a strong case for the use of Rap1^{AS} as a tool to study Rap1 biology, this work definitively establishes the fact that Rap1 contains an AD that is required for Rap1-dependent chromosomal gene transcription and provides multiple, distinct, variant forms of Rap1 that will prove invaluable for further dissection of the molecular mechanisms of Rap1-dependent transcription activation.

Methods

General Cloning and Yeast and *E. coli* Manipulations

The general cloning approach and yeast and *E. coli* manipulations used in this

Chapter were performed according to the approaches described in Chapter II.

Test Rap1 Yeast Expression Vectors

Yeast expression vectors encoding Rap1^{WT} and Rap1^{AS} are the same as described in

Chapter II. Truncation and point mutations were introduced into the gene encoding Rap1^{AS}

(*RAP1^{AS}*) were *RAP1* generated via splicing by overlap extension PCR (Heckman and Pease,

2007) using and primers with BlpI and XhoI ends or (for deletion of the Rap1 N-terminus)

primers with XbaI and XhoI ends and pRS415-*MYC$_5$-NLS-RAP1^{AS}* as a template. These

mutant *RAP1^{AS}* variant PCR products were used to replace the BlpI to XhoI or (for deletion

of the Rap1 N-terminus) XbaI to SphI fragments of *RAP1* in plasmid pRS415-*MYC$_5$-NLS-*

RAP1^{AS} or (for expression of the Rap1 DBD only) plasmid pRS415-*MYC$_5$-NLS-RAP1$^{AS\Delta C}$*,

resulting in the production of mutant Rap1 test expression vectors. Versions of these

mutant Rap1 test expression vectors encoding the Rap1^{WT} (rather than the Rap1^{AS}) DBD

were generated either via the spicing by overlap extension PCR approach described above

using pRS415-*MYC$_{X5}$-NLS-RAP1^{AS}* as a template or by replacing the XbaI to SphI fragment of

pRS415-*MYC$_{X5}$-NLS-RAP1^{AS}* that encompasses the *RAP1* promoter and *RAP1* sequences

encoding the N-terminus and DBD with the XbaI to SphI fragment of pRS415-*MYC$_5$-NLS-*

RAP1. Expression vectors for testing in the silencing strain (see "Yeast Strains" below)

were generated by cloning the XbaI to XhoI fragment of a pRS415-*MYC$_5$-NLS-RAP1* variant

(where the XbaI site was blunted using DNA Polymerase I, Large (Klenow) fragment (NEB) according the manufacturer's instructions) into pRS412 digested with SmaI and XhoI.

Yeast Strains

All of the yeast strains used in this Chapter are listed in **Table 3.1**. All except yeast strains carrying the glycolytic reporter (named YAM42, YAM43, YAM44, and YAM45), silencing reporter (YAM46), and strain background the silencing reporter strain was made in are the same as those used in Chapter II.

The various $UAS_{Rap1-Gcr1}$-*HIS3* glycolytic reporter genes were derived from the UAS_{Rap1}-*HIS3* reporter described in Chapter II. The difference between the $UAS_{Rap1-Gcr1}$-*HIS3* reporters and the UAS_{Rap1}-*HIS3* reporter is that $UAS_{Rap1-Gcr1}$-*HIS3* contains one Rap1 binding site (UAS_{Rap1}) site and one Gcr1 binding site (UAS_{Gcr1}) instead of two UAS_{Rap1} sites. $UAS_{Rap1-Gcr1}$-*HIS3* reporters were generated by replacing the 48bp NcoI to SacII DNA fragment encompassing the two UAS_{Rap1} binding sites in the WT UAS_{Rap1}-*HIS3* reporter generated in previous studies (Garbett et al., 2007; Mencía et al., 2002) with a 39bp NcoI to SacII DNA fragment containing UAS_{Rap1} and UAS_{Gcr1} binding

Table 3.1: Yeast Strains Used In This Chapter

Name	Strain	Genotype	Reference
BY4741	BY4741	*MAT**a** his3Δ1 leu2Δ0 met15Δ0 ura3Δ0*	Brachman et. al., 1998
rap1Δ	BY4741 rap1Δ	*MAT**a** his3Δ1 leu2Δ0 met15Δ0 ura3Δ0 rap1Δ::HPHMX4* (pRS416 UAS_{ADH}-*RAP1*)	Layer et. al., 2010
WT-HIS3	YAM30	*MAT**a** his3Δ1 leu2Δ0 met15Δ0 ura3Δ0 rap1Δ::HPHMX4* (pRS416 UAS_{Rap1} *FLAG₃-RAP1*) *trp1Δ::KANMX4 HA₃-TAF1 $UAS_{Rap1(WT)}$-TATA-HIS3::TRP1::DED1*	(Johnson and Weil, 2017)
3T4A-HIS3 #2	YAM31	*MAT**a** his3Δ1 leu2Δ0 met15Δ0 ura3Δ0 rap1Δ::HPHMX4* (pRS416 UAS_{Rap1} *FLAG₃-RAP1*) *trp1Δ::KANMX4 HA₃-TAF1 $UAS_{Rap1(3T4A)}$-TATA-HIS3::TRP1::DED1*	(Johnson and Weil, 2017)
UASRap1 WT-Gcr1WT	YAM42	*MAT**a** his3Δ1 leu2Δ0 met15Δ0 ura3Δ0 rap1Δ::HPHMX4* (pRS416 UAS_{Rap1} *FLAG₃-RAP1*) *trp1Δ::KANMX4 HA₃-TAF1 $UAS_{Rap1WT-Gcr1WT}$-TATA-HIS3::TRP1::DED1*	This dissertation
UASRap1 WT-Gcr1mut	YAM43	*MAT**a** his3Δ1 leu2Δ0 met15Δ0 ura3Δ0 rap1Δ::HPHMX4* (pRS416 UAS_{Rap1} *FLAG₃-RAP1*) *trp1Δ::KANMX4 HA₃-TAF1 $UAS_{Rap1WT-Gcr1mut}$-TATA-HIS3::TRP1::DED1*	This dissertation
UASRap1 AS-Gcr1mut	YAM44	*MAT**a** his3Δ1 leu2Δ0 met15Δ0 ura3Δ0 rap1Δ::HPHMX4* (pRS416 UAS_{Rap1} *FLAG₃-RAP1*) *trp1Δ::KANMX4 HA₃-TAF1 $UAS_{Rap13T4A-Gcr1mut}$-TATA-HIS3::TRP1::DED1*	This dissertation
UASRap1 AS-Gcr1WT	YAM45	*MAT**a** his3Δ1 leu2Δ0 met15Δ0 ura3Δ0 rap1Δ::HPHMX4* (pRS416 UAS_{Rap1} *FLAG₃-RAP1*) *trp1Δ::KANMX4 HA₃-TAF1 $UAS_{Rap13T4A-Gcr1WT}$-TATA-HIS3::TRP1::DED1*	This dissertation
W3031-B	W3031-B	*MATα HMR**a** ade2-1 trp1-1 can1-100 leu2-3,112 his3-11,15*	(Thomas and Rothstein, 1989)
YLS34	YLS34	*MATα hmrΔA::TRP1 ade2-1 trp1-1 can1-100 leu2-3,112 his3-11,15 rap1::LEU2 pD145 (YCP50, RAP1, URA3, sup-4-o)*	(Sussel and Shore, 1991)
hmrΔA TRP1, WT-HIS3	YAM46	*MATα hmrΔA::TRP1 ade2-1 trp1-1 can1-100 leu2-3,112 his3-11,15 rap1::LEU2 pD145 (YCP50, RAP1, URA3, sup-4-o) $UAS_{Rap1(WT)}$-TATA-HIS3*	This dissertation

sites derived from the *PGK1* gene generated by annealing double-stranded synthetic oligonucleotides obtained from IDT. These reporter variants were integrated into the yeast genome and integration was confirmed as described for the *UAS$_{Rap1}$-HIS3* reporters above.

The silencing strain used for the experiments in this Chapter was derived from the previously described YLS34 strain (Sussel and Shore, 1991), which was derived from W303-1B (Thomas and Rothstein, 1989) by David Shore's lab at the University of Geneva. To generate a strain that would allow the testing of both Rap1 silencing and activation via a growth assay, the WT *UAS$_{Rap1}$-HIS3* reporter genes used in Chapter II was integrated into the YLS34 genome. For this integration, WT *UAS$_{Rap1}$-HIS3* was digested with SpeI and KpnI. Because the KpnI restriction site is located between the *HIS3* and the *TRP1* genes, this digest results in a WT *UAS$_{Rap1}$-HIS3* that does not contain *TRP1*, which serves as the reporter gene for Rap1 silencing activity in YLS34 (Sussel and Shore, 1991). Restriction enzyme digested *UAS$_{Rap1}$-HIS3* was transformed into yeast and integrated into the *HIS3* locus via ends-out recombination (Hastings et al., 1993). Transformants were selected on SC-His. After confirming that transformants were Trp$^-$ as expected since *TRP1* was not present in the WT *UAS$_{Rap1}$-HIS3* integration construct and silent in YLS34 in the presence of Rap1^{WT}, correct integration of the reporter was confirmed via PCR.

Yeast Cell Growth, Immunoblotting, and Steady State RNA Analysis

Yeast cell growth, immunoblotting, and steady-state RNA anlaysis were performed using the same methods outlined in Chapter II. The only exception to this is that Ponceau S staining was not performed as a protein-loading control in addition to probing for Actin in immunoblots that do not appear in my *JBC* manuscript (Johnson and Weil, 2017).

Nascent RNA Labeling and Purification

Nascent RNA levels in yeast strains of interest were assessed using efficient and reversible RNA labeling and purification (Duffy et al., 2015). 200 ml of each yeast culture (500 OD_{600} units) grown in YPD to a cell density of ~ 1.5×10^7 cells/mL (2.5 OD_{600}/ml) were pulse labeled for 2.5 minutes with 5 mM 4-thiouracil (s4U) (Sigma), harvested via vacuum filtration, and immediately immersed in a 1:1 mixture of phenol: RNA Buffer A (50 mM NaAc (pH 5.5), 10 mM EDTA (pH 8), 0.5% SDS) pre-warmed to 65°C. ~4.8×10^8 cells (80 OD_{600} units) of 6-min thiouracil labeled *Schizosaccharomyces pombe* cells were added into each sample prior to RNA extraction for use as a spike-in control. Total RNA from the resulting *S. cerevisiae/S.pombe* mixtures was extracted using the hot phenol method (Köhrer and Domdey, 1991). RNA concentration and integrity were assessed as in Chapter II. To prepare nascent thiolated RNA for separation from total RNA, 400μg of each RNA in 1 ml of Biotinylation Buffer (10 mM Tris-HCL (pH 7.5), 1 mM EDTA) was heat denatured at 65°C for 10 min and then chilled for 2 min on ice. RNA was biotinylated for 30 min at room temperature in the dark on a tiltboard following addition of 20 μl of 1mg/ml (2-((Biotinoyl) amino)-ethyl methanethiosulfonate (MTSEA) (Biotium) dissolved in dimethylformamide (DMF). Unincorporated biotin was removed by two chloroform extractions (once with 1ml, then with 0.75ml), the second of which was performed using a Heavy Phase Lock Gel (5 Prime Inc.). RNA was precipitated using an equal volume (0.75ml) of isopropanol. Isopropanol precipitated RNA was dissolved in 100μl of 0.1% diethylpyrocarbonate (DEPC)-treated H_2O (Fisher). RNA was again heat denatured at 65°C for 10 min and then chilled on ice for 5 min. Biotinylated nascent RNAs were purified using 200μl of a colloidal suspension of μMACs streptavidin beads/sample (μMACs streptavidin kit, Miltenyi Biotec).

Samples were placed in a light-tight container on a tiltboard at room temperature for 15 min. Each RNA/bead mixture was added to a separate µMACs streptavidin kit column that had been placed in the µMACs Separator and washed 2 X with 0.2 ml Nucleic Acid Wash Buffer (µMACs streptavidin kit, Miltenyi Biotec). The flow-through was collected and re-applied to the column. Columns were washed 2X with 0.5 ml of the biotinylated RNA Wash Buffer (100 mM Tris-HCL (pH 7.5), 10 mM EDTA, 1 M NaCl, 0.1% Tween 20) and biotinylated RNA was eluted with two 200ml washes of 0.1M DTT. Biotinylated RNA was ethanol precipitated following addition of 40µg molecular biology grade glycogen (Roche), 0.1X volume of 3M NaOAc (pH 5.5), and 3X volumes of 100% ethanol. Precipitated RNAs were dissolved 10mM Tris Cl pH 7.5 0.1mM EDTA. cDNA synthesis was performed as described in Chapter II; qRT-PCR was performed and relative transcript levels determined as described in Chapter II, except that *S. pombe* β-*TUBULIN* present in the samples due to the *S. pombe* cell spike-in was used as a reference gene (Bonnet et al., 2014) (see **Table 3.2** for the sequences of the primers used in these analyses).

Table 3.2: qRT-PCR Primers Used In This Chapter

Gene	Primer Name	Primer sequence (5'-> 3')
HIS3	HIS3_F2	ATGACAGAGCAGAAAGCCC
	HIS3_R2	GCACTCAACGATTAGCGAC
ACT1	ACT1_F2	TGGTCGGTATGGGTCAAAAA
	ACT1_R2	AAGGACAAAACGGCTTGGAT
ENO1	ENO1_F	CGTCAACGATGTCATTGCTC
	ENO1_R	CCAAAGAAACACCCAAGATAGC
PYK1	PYK1_F	CCAACCTCCACCACCGAAAC
	PYK1_R	GGGCTTCAACATCATCAGTCCA
RPS3	RPS3_F	TACGGTGTCGTCAGATACG
	RPS3_R	GACCAGAGTGAATCAAGAAACC
RPL26B	RPL26B_F	TTTCACCGCCCCATCCTCCC
	RPL26B_R	GGAACGGAAGCACCGTTGAC
RPL3	RPL3_F	TGGACAGACCAGGTTCTAAG
	RPL3_R	AAATGTTCAGCCCAGACGG
TUBULIN	Tubulin_F	CCGCTGGTGGAAAGTATGTT
	Tubulin_R	GCCAATTCAGCACCTTCAGT

Rap1 Purification for GST Pull-Down Assay

To generate Rap1 for GST pull-down assays, Rap1 ORFs encoded on the pRS415 expression plasmid were subjected to PCR to generate Rap1 coding sequences with EcoRI and XhoI ends that could be cloned in frame with the His_6-GST tag in the pBG101

expression vector. His$_6$-GST-Rap1 variants were expressed and subjected to Ni-NTA

purification as described for His$_6$-Rap1 in Chapter II scaled up for 2L of *E. coli* culture. Ni-

NTA purified His$_6$-GST-Rap1 variants were diluted to reduce the concentration of NaCl in

the Lysis/Wash buffer to 150mM and permit binding to 2.5mL Sepharose SP Fast Flow

(Pharmacia) pre-equilibrated in a disposable column (Bio-Rad) with 4 column volumes of

Buffer B150 (25 mM HEPES NaOH (pH 7.6), 10% v/v glycerol, 150 mM NaCl, 0.01% v/v

NP-40, 1 mM Benzamidine, 0.2 mM PMSF). After binding, Sepaharose SP was washed with

4 more column volumes of B150. Bound proteins were eluted using 3 column volumes of

Buffer B1000 (25 mM HEPES NaOH (pH 7.6), 10% v/v glycerol, 1 M NaCl, 0.01% v/v NP-40,

1 mM Benzamidine, 0.2 mM PMSF).

Taf5 Expression and Purification for GST Pull-down Assay

His$_6$-Taf5 aa 1-337 (containing the RBD) was expressed from a previously generated

pET33B expression vector (Layer et al., 2010) and Ni-NTA purified as described for His$_6$-

Rap1 in Chapter II scaled up for 2L of *E. coli* culture.

GST Pull-down Assays

GST pull-down assays were conducted as 200 μL reactions in pull-down buffer

(20mM HEPES NaOH (pH 7.5), 150mM NaAc, 0.05% Triton X-100, 10% glycerol, 1mM DTT,

25 ng/μL BSA) using 5μL of glutathione sepharose 4 Fast Flow beads (GE Healthcare),

12pmol of His$_6$-GST or 6 pmol of His$_6$-GST-Rap1 variant, and either 0 pmol or 100 pmol of

His$_6$-Taf5. Binding reactions were incubated for 1hr at room temperature on the tiltboard.

Following incubation, the glutathione sepharose beads were pelleted by centrifugation for

30s at 1,000rpm and washed once with pull-down buffer. Beads were pelleted again and

bead-bound material was eluted with 1 X NuPAGE sample buffer (1X LDS Sample Buffer

(Life Technologies) with DTT added to 62.5 mM). Bead-bound material was fractionated

on 4-12% NuPAGE gels (Life Technologies), stained with Sypro Ruby (Life Technologies),

and imaged with a Pharos Fx Imager (Bio-Rad). Binding data were quantified using

Quantity One software (Bio-Rad) and plotted using Prism 7 (GraphPad).

<p style="text-align: center;">Results</p>

Identification of a Potential Activation Domain Within aa's 600-671

The analyses of Rap1 described in Chapter I led to the hypothesis that an AD was

located within a C-terminal portion of the protein distinct from the sequences implicated in

silencing of telomere-proximal genes whose deletion has little affect on cell viability (Chen

et al., 2011; Feeser and Wolberger, 2008; Kyrion et al., 1992; Moretti et al., 1994b). To

directly and systematically test the hypothesis that these C-terminal sequences (aa's 600-

671, labeled AD? in **Figure 3.1A**) specifically and solely conferred AD function for the RP

genes, a series of Rap1^{AS} deletion variants were generated. The Rap1 deletion variant

series used for these first AD-mapping experiments consisted of constructs termed ΔN (aa's

1-338), ΔC (aa's 600-827), ΔNΔC (aa's 1-338, 600-827), ΔAD? (aa's 600-671), and ΔSD (aa's

672-827) wherein the *RAP1^{AS}* ORF sequences encoding the indicated aa sequences were

deleted (**Figure 3.1A**).

Yeast carrying an integrated 3T4A *UAS$_{Rap1}$-HIS3* reporter were used to score the

ability of intact Rap1^{WT}, Rap1^{AS}, and the noted Rap1^{AS} deletion variants to promote 3-AT^{R}

<p style="text-align: center;">104</p>
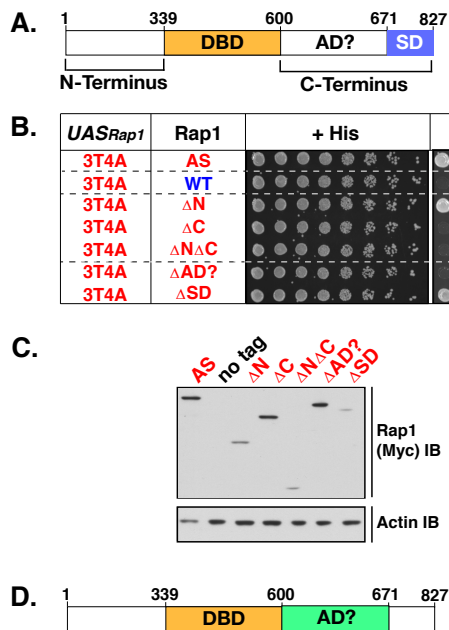
Figure 3.1. Mapping of a Potential Rap1 AD to Amino Acids 600-671. *A.* Schematic of the Rap1 protein. Shown are the well characterized Rap1 DNA Binding Domain (**DBD; aa's 339-600**), **N-terminus aa's 1-339**, and **C-terminus aa's 600-827.** The C-terminus is further divided into a Silencing Domain (**SD**) as well as the region suspected to contain the AD (**AD? aa's 600-671**). *B.* Growth analysis of yeast strains carrying the 3T4A version of the *HIS3* reporter (left column; *UAS$_{Rap1}$*-**red**; labeled **3T4A**) and various forms of Rap1 (labeled **Rap1**, second column) either Rap1^{AS} (**AS**, **red**), Rap1^{WT} (**WT**, **blue**), or the indicated Rap1^{AS} deletion mutants (**ΔN, ΔC, ΔNΔC, ΔAD?, ΔSD**; **red**). Serial dilutions of cells were plated and grown on non-selective (**+ His**), or reporter gene selective (**+ 3-AT**) media as in the growth assays performed in Chapter II. Images are representative of two independent replicates. *C.* Immunoblot analysis was of Rap1^{AS} variants performed as described in **Figure 2.8.** *D.* Schematic indicating the location of the potential Rap1 activation domain (**AD?; aa's 600-671**) mapped through the deletion mutagenesis experiments shown here.

growth. Negative control cells expressing only Rap1^{WT} (which is unable to bind 3T4A *UAS$_{Rap1}$* (see Chapter II) fail to exhibit 3-AT^R as expected (**Figure 3.1B**). Rap1^{AS}ΔNΔC phenocopies Rap1^{WT} in these growth analyses, indicating that the Rap1^{AS} DBD alone is insufficient for reporter expression. Meanwhile, Rap1^{AS}ΔN and Rap1^{AS}ΔSD show 3-AT^R, phenocopying Rap1^{AS} (which binds 3T4A *UAS$_{Rap1}$* (see Chapter II)) and demonstrating that the aa's deleted in these Rap1 variants are not required for 3T4A *UAS$_{Rap1}$-HIS3* expression. Finally, as might be expected, the Rap1^{AS}ΔC and Rap1^{AS}ΔAD? forms, which were expressed at levels comparable to that of Rap1^{AS} (**Figure 3.1C**) were unable to

confer 3-AT^R (**Figure 3.1B**). These growth data suggest that an activation domain indeed resides within Rap1 C-terminal aa's 600-671 (**Figure 3.1D**).

<u>Expression of a Glycolytic Reporter Depends on the Rap1 N-Terminus</u>

Rap1 activates both the TFIID-dependent RP genes and the SAGA-dependent GE genes (Chambers et al., 1989, 1995; Huisinga and Pugh, 2004; Knight et al., 2014; Lieb et al., 2001; Rudra and Warner, 2004). Because these two robustly transcribed genes depend on two different coregulators, I wondered if they also depended on the same or different Rap1 aa's. To provide a means to investigate the possibility that glycolytic and RP genes depend on distinct Rap1 sequences, I designed a series of glycolytic reporters ($UAS_{Rap1-Gcr1}$-$HIS3$) (**Figure 3.2A**). These reporters were similar to the UAS_{Rap1}-$HIS3$ reporter used in the analyses above and in Chapter II except that the two UAS_{Rap1} sites in UAS_{Rap1}-$HIS3$ derived from the RP gene $RPS8A$ were replaced with UAS_{Rap1} and UAS_{Gcr1} sites derived from the glycolytic gene $PGK1$.

To demonstrate that $UAS_{Rap1-Gcr1}$-$HIS3$ depends on both the UAS_{Rap1} and UAS_{Gcr1} and that a $UAS_{Rap13T4A-Gcr1}$-$HIS3$ reporter can be driven by Rap1^{AS}, four $UAS_{Rap1-Gcr1}$-$HIS3$ reporters were generated: (1) $UAS_{Rap1WT-Gcr1WT}$-$HIS3$ containing WT versions of UAS_{Rap1} and UAS_{Gcr1}, (2) $UAS_{Rap1WT-Gcr1mut}$-$HIS3$ containing WT UAS_{Rap1} and a mutant UAS_{Gcr1} that has been shown to drastically reduce expression of a glycolytic gene in a previous study (Scott and Baker, 1993), (3) $UAS_{Rap13T4A-Gcr1WT}$-$HIS3$ containing the Rap1^{AS} binding site and WT UAS_{Gcr1}, and (4) $UAS_{Rap13T4A-Gcr1mut}$-$HIS3$ containing $UAS_{Rap13T4A}$ and the mutant UAS_{Gcr1} (Scott and Baker, 1993) (**Figure 3.2A**). Growth assays were performed to assess the AT^R of yeast containing these reporters and either a second copy of Rap1^{WT} or Rap1^{AS}. These analyses showed that 3-AT^R depended on both the UAS_{Rap1} and UAS_{Gcr1} sites (**Figure 3.2A**). Additionally as expected, Rap1^{AS} conferred AT^R to yeast containing the $UAS_{Rap13T4A-Gcr1WT}$-$HIS3$ (**Figure 3.2A**).
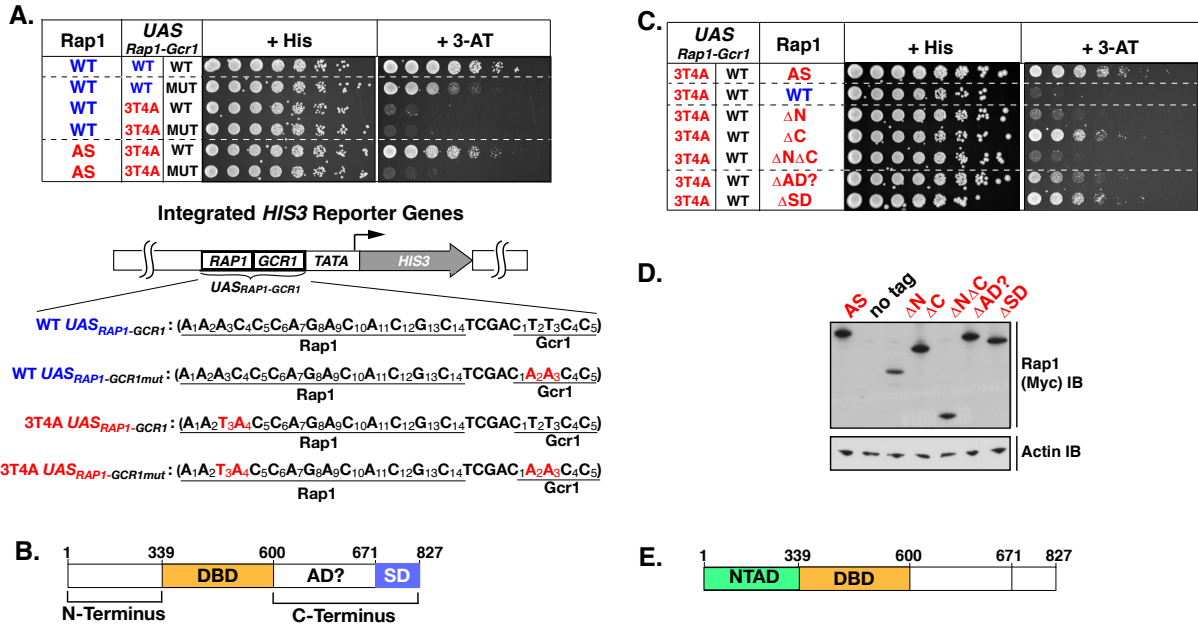
Figure 3.2. Activation of the *UAS_Rap1-Gcr1* Glycolytic Reporter Gene Depends on the Rap1 N-terminus. *A.* The *UAS_Rap1-Gcr1*-*HIS3* reporter depends on both the *UAS_Rap1* and the *UAS_Gcr1* and Rap1AS can drive expression of *UAS_Rap1AS-Gcr1*-*HIS3*. Upper: Test of the ability of WT and AS forms of Rap1 to bind different enhancers to confer ATR. Yeast strains carrying the indicated *UAS_Rap1-Gcr1*-*HIS3* reporter variant (**WT *UAS_Rap1-Gcr1*, WT *UAS_Rap1-Gcr1mut*, 3T4A *UAS_Rap1-Gcr1* or 3T4A *UAS_Rap1-Gcr1mut*,** as shown) and either a second copy of Rap1WT (**blue**) or Rap1AS (**red**) were grown on non-selective (**+ His**) or *HIS3*-reporter gene selection (**+ 3-AT**) media. Images shown are representative of one replicate. Lower: detailed structures of the *UAS_Rap1-Gcr1*-*HIS3* reporters used in these growth tests. *B.* Schematic of the Rap1 protein, highlighting the well-characterized Rap1 domains shown in **Figure 3.1**, including the **DBD**, **N-terminus**, and **C-terminus** (divided into **AD?** and **SD** regions). The aa coordinates of each domain are indicated in the figure and are the same as those shown in **Figure 3.1**. *C.* Growth analysis of yeast strains carrying the 3T4A *UAS_Rap1-Gcr1*-*HIS3* reporter (left column; *UAS_Rap1*-**red**; labeled **3T4A**) and various forms of Rap1 (labeled **Rap1**, second column) either Rap1AS (**AS**, **red**), Rap1WT (**WT**, **blue**), or the indicated Rap1AS deletion mutant (**ΔN, ΔC, ΔNΔC, ΔAD?, ΔSD**; **red**). Growth assay was performed as in "*A*". Image is of one biological replicate *D.* Immunoblot analysis of Rap1AS variants performed as described in **Figure 2.8** *E.* Schematic indicating the location of the Rap1 region required for glycolytic reporter expression (Rap1 N-terminal activation domain? (**NTAD**; **aa's 1-339**) mapped through the deletion mutagenesis experiments shown here.

To assess the contribution of Rap1 domains to glycolytic reporter expression, yeast carrying the integrated *UAS_Rap13T4A-Gcr1WT*-*HIS3* reporter were used to score the ability of Rap1WT, Rap1AS, and the Rap1AS deletion variants used above (**Figure 3.2B**) to promote ATR growth. Surprisingly, Rap1ASΔN was unable to support ATR in *UAS_Rap13T4A-Gcr1WT*-*HIS3* yeast (**Figure 3.2C**). Although Rap1ASΔN protein expression levels are somewhat reduced compared to Rap1AS (**Figure 3.2D**), the failure to support ATR can likely be attributed to

activity of the Rap1 N-terminus since Rap1^{AS}ΔN supported AT^R in the 3T4A *UAS$_{Rap1}$-HIS3*

reporter (*cf* **Figure 3.1**). Thus, in contrast to the 3T4A *UAS$_{Rap1}$-HIS3* reporter (*cf* **Figure**

3.1), expression of *UAS$_{Rap13T4A-Gcr1WT}$-HIS3* depends on aa in the Rap1 N-terminus (labeled

"Rap1 N-terminal AD (NTAD), **Figure 3.2D**).

<u>Systematic AD? Deletion Mutagenesis Further Defines the Potential Activation Domain</u>

I focused my continuing AD mapping studies on the Rap1 AD? because I am

interested in TFIID coactivator function, and unlike the Rap1 N-terminus, the Rap1 C-

terminus (which contains AD?) interacts with TFIID and is thus likely critical for activation

of the TFIID-dependent RP genes (Garbett et al., 2007). Yeast carrying the 3T4A *UAS$_{Rap1}$-*

HIS3 reporter were used to further define which of the aa's within AD? (aa's 600-671)

comprise the AD (**Figure 3.3A**). Rap1^{WT}, Rap1^{AS}, and Rap1$^{ASΔAD?}$ were used as controls in

these experiments. The aa interval that contains AD function was subjected to systematic

internal, N-terminal, and C-terminal deletion. Data for the series of seven internal 10 aa

deletions moving through Rap1 aa's 600-671 is shown in **Figures 3.3B-D**; labeled **Δ600-**

610, **Δ611-620**, **Δ621-630**, **Δ631-640**, **Δ641-650**, **Δ651-660**, **Δ660-671**). These Rap1^{AS}

variants were tested for 3T4A *UAS$_{Rap1}$-HIS3* expression by scoring growth on 3-AT-

containing plates and mRNA^{HIS3} levels by qRT-PCR. To ensure that all constructs were

stably expressed, steady-state protein levels were monitored in parallel using the same

cells tested for AT^R and mRNA^{HIS3} levels (**Figure 3.3D**). Deletion of the first 30 amino acids

of the 600-671 region (i.e. constructs **Δ600-610**; **Δ611-620**; **Δ621-630**; **Figure 3.3B,C**)

had no significant effect upon either growth in the presence of 3-AT, or *HIS3* reporter

mRNA transcript levels. By contrast, removal of aa's within the distal 40 aa's of Rap1 AD?
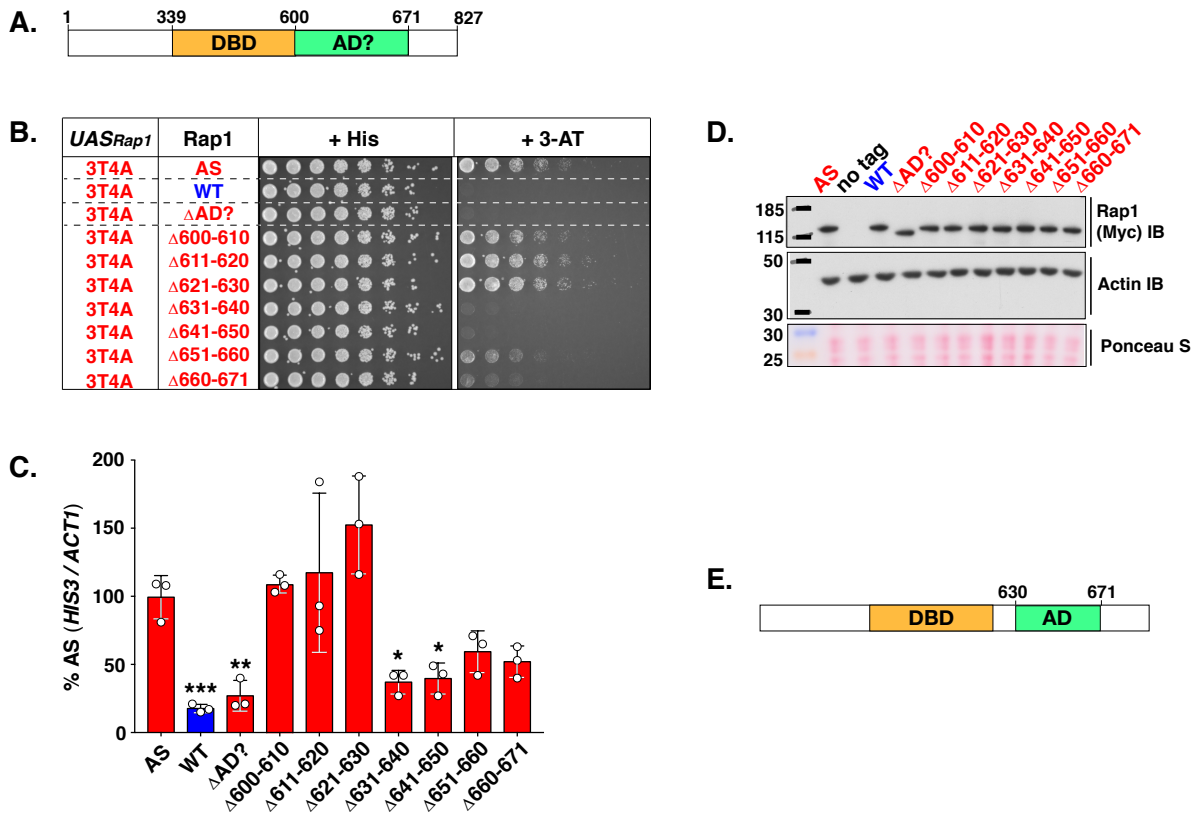
Figure 3.3. Mapping the Activation Domain of Rap1 to Amino Acids 630-671. *A.* Schematic of the Rap1 protein indicating the **AD?** region (**aa's 600-671***)* located C-terminal of the **DBD (aa's 339-600)** to be subjected to further deletion analysis. *B.* Growth analysis of yeast strains carrying the 3T4A version of the *HIS3* reporter (left column; *UAS*$_{Rap1}$-**red**; labeled **3T4A**) and various forms of Rap1 (labeled **Rap1**, second column) either Rap1^{AS} (**AS**, **red**), Rap1^{WT} (**WT**, **blue**), or the indicated Rap1^{AS} deletion mutant (**ΔAD?**, **Δ600-610**, **Δ611-620, Δ621-630**, **Δ631-640**, **Δ641-650**, **Δ651-660**, **Δ660-671**; **red**). Assay was performed as described in **Figure 3.1** and Chapter II. Images are representative of three independent replicates. *C.* qRT-PCR analysis to score reporter *HIS3* mRNA expression levels in the various yeast strains tested in **panel B**. Results of these analyses are plotted as in **Figure 2.8** in Chapter II, except that data are expressed as a percentage of the relative *HIS3* mRNA levels in yeast carrying Rap1^{AS} instead of Rap1^{WT}. Data represent three biological replicates (white circles) measured in duplicate. Mean ± SD is depicted. * = p < 0.05, ** = p < 0.01, *** = p < 0.005. *D.* Immunoblot analysis of Rap1^{AS}, Rap1^{WT}, and Rap1^{AS} deletion variant protein expression levels. This analysis was performed as detailed in **Figure 2.8**. Images are representative of three independent replicates. *E.* Schematic indicating the location of the Rap1 activation domain (**AD**; **aa's 630-671**) mapped through the deletion mutagenesis experiments shown here.

sequences (**Δ631-640**; **Δ641-650**; **Δ651-660**; **Δ660-671; Figure 5B,C**) dramatically

reduced *HIS3* reporter expression as scored by AT^{R} growth (**Figure 3.3B**) and mRNA^{HIS3}

levels (**Figure 3.3C**). All Rap1^{AS} deletion constructs were as stable as Rap1^{WT}, results

excluding any contribution of Rap1^{AS} protein abundance to reporter gene expression

A.

UAS_Rap1	Rap1	+ His	+ 3-AT
3T4A	AS		
3T4A	ΔAD?		
3T4A	Δ600-610		
3T4A	Δ600-620		
3T4A	Δ600-630		
3T4A	Δ600-640		
3T4A	Δ600-650		
3T4A	Δ600-660		
3T4A	Δ610-671		
3T4A	Δ620-671		
3T4A	Δ630-671		
3T4A	Δ640-671		
3T4A	Δ650-671		
3T4A	Δ660-671		

B.

AS, no tag, Δ600-610, Δ600-620, Δ600-630, Δ600-640, Δ600-650, Δ600-660, Δ610-671, Δ620-671, Δ630-671, Δ640-671, Δ650-671, Δ660-671

Rap1 (Myc) IB

Actin IB

C.

630   671

DBD   AD
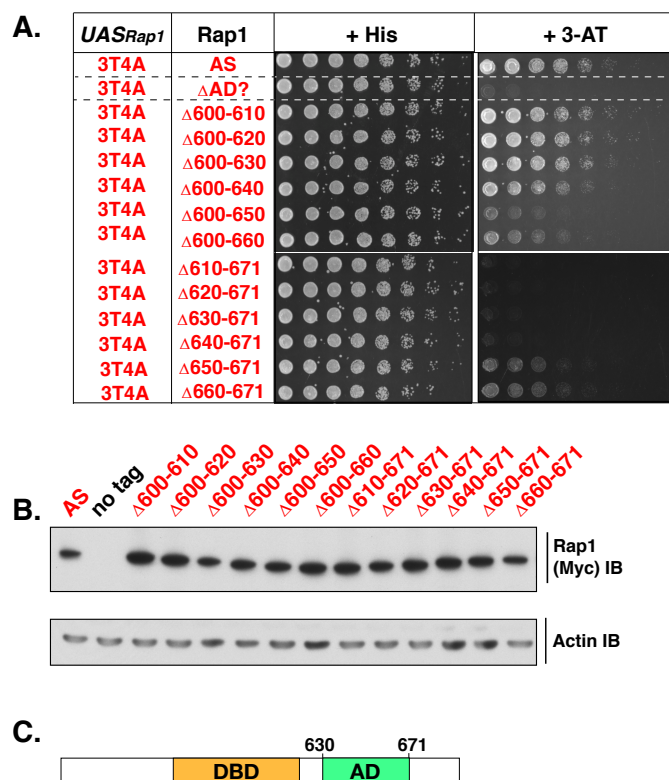
Figure 3.4. Rap1 N- and C-terminal Truncation Analysis of ΔAD? Maps the AD to Amino Acids 630-671. *A.* Growth analysis of yeast strains carrying the 3T4A version of the *HIS3* reporter (left column; *UAS_Rap1*-**red**; labeled **3T4A**) and various forms of Rap1 (labeled **Rap1**, second column) either Rap1[AS] (**AS**, **red**) or the indicated Rap1[AS] deletion mutant (**ΔAD?, Δ600-610, Δ600-620, Δ600-630, Δ600-640, Δ600-650, Δ600-660, Δ610-671, Δ620-671, Δ630-671, Δ640-671, Δ650-671, Δ660-671**; **red**). Assay was performed as described in **Figure 3.1**. Images are representative of two independent replicates. *B.* Immunoblot analysis of Rap1[AS] and Rap1[AS] deletion variant protein expression levels. This analysis was performed as detailed in **Figure 2.8**. Images are representative of two independent replicates. Note: Rap1ΔAD? is not shown in this blot, but multiple blots have demonstrated that its expression levels are comparable to those of Rap1[AS] (*cf* **Figures 3.1, 3.2,** and **3.3**)*C.* Schematic indicating the location of the Rap1 activation domain (**AD**; **aa's 630-671**) mapped through the deletion mutagenesis experiments shown here and **Figure 3.3.**

(**Figure 3.3D**). These data, which are consistent with the data obtained from the N- and C-terminal AD? deletion variants (**Figure 3.4A-C**), indicate that the Rap1 AD resides within aa's 630-671 (domain labeled **AD**; **Figure 3.3E**).

Identification of Key Rap1 AD Amino Acids

The deletion mutagenesis-defined AD of Rap1[AS] (i.e. aa's 630-671) was subjected to further site-directed mutagenesis in order to identify the specific aa residues that contribute essential AD function. Based on the idea that evolutionary sequence conservation implies conservation of function, Rap1 AD-like sequences from *Saccharomyces cerevisiae* and the distantly related *sensu lato* yeast strains *Saccharomyces castelli* and *Saccharomyces kluyveri*

were subjected to a multiple sequence alignment to identify aa's conserved in all three yeast species (labeled **S. cer**, **S. cas**, and **S. klu**, respectively, **Figure 3.5A**). Alignment shows that 24 of the 41 aa's within the Rap1 AD were identical among *S. cerevisiae* and *sensu lato* yeast (**Figure 3.5A**). Based on this sequence conservation, single point mutant variants were generated within the AD of Rap1^{AS} by changing each of the 24 identical aa's to Alanine (A) (except for A670, which was mutated to arginine (R)). These Rap1^{AS} point mutant variants were transformed into the 3T4A *UAS$_{Rap1}$-HIS3* reporter yeast strain and tested for the ability to confer AT^R. Growth assays performed with very high levels of 3-AT (300mM) revealed that eight aa's, seven of which were hydrophobic, were required for robust AT^R growth (**Figure 3.5B**; hydrophobic aa's **L639**, **F646**, **L650**, **L654**, **F663**, **Y665**, and **I669**, as well as **A670R**; all boxed). Steady state protein levels of all variant proteins were essentially identical to WT (data not shown). Parallel qRT-PCR analyses of mRNA^{HIS3} levels in these same strains showed some correlation with AT^R patterns (**Figure 3.5C**). Importantly, the L650A mutant that displayed the largest growth defect also showed a large significant reduction in mRNA^{HIS3} levels (**Figure 3.5C**). These data suggest that Rap1 AD activity depends on key hydrophobic aa's.

Because prior AD mutational analyses showed that mutation of at least two key hydrophobic aa's was required to significantly impact transcription (Deng et al., 2001; Drysdale et al., 1995; Lin et al., 1994; Mader, S et al., 1989; Regier et al., 1993), Rap1^{AS} AD variants were created in which key hydrophobic aa mutations were combined. Specifically, the best single point mutant (L650A) was combined with each of the other six key hydrophobic aa's (i.e. **L650A + L639A, L650A + F646A, L650A + L654A, L650A + F663A, L650A + Y665A**, and **L650A + I669A**). Growth analyses were performed in the 3T4A
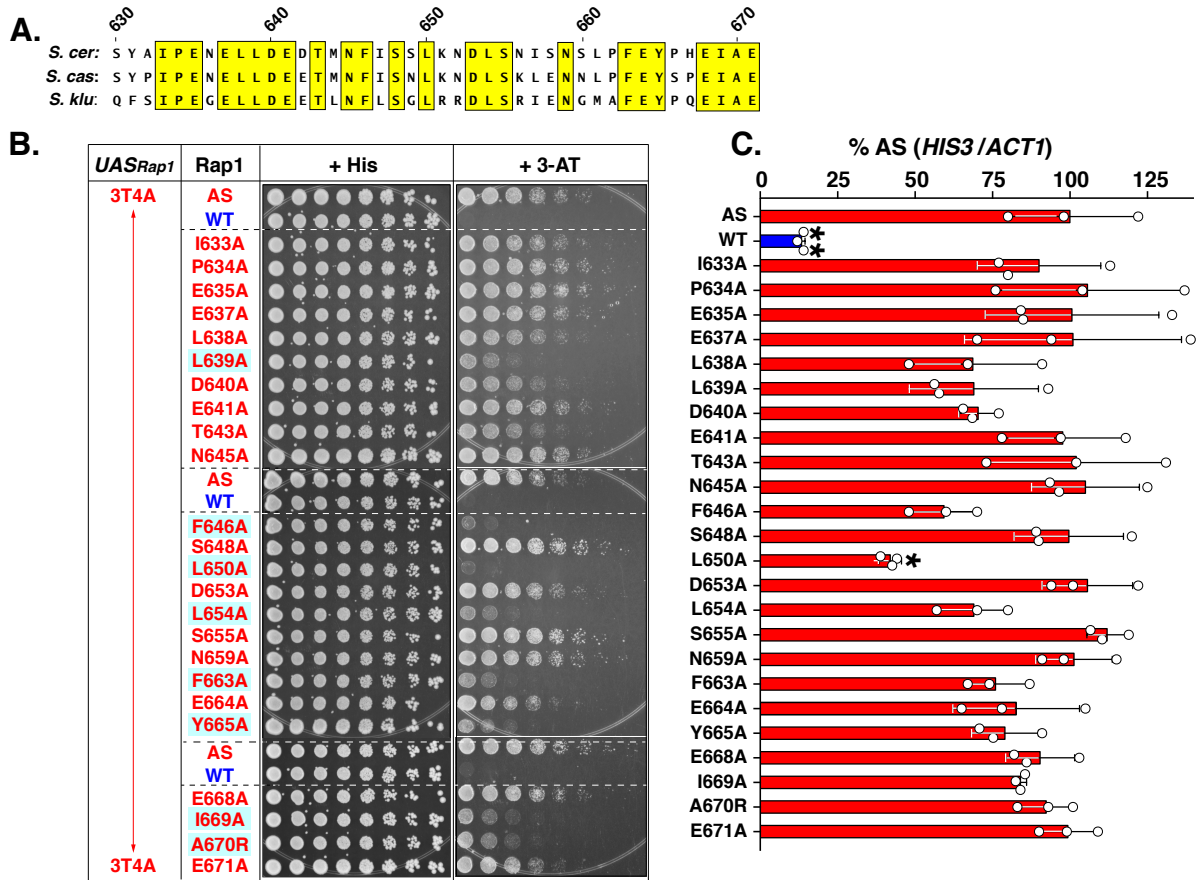
Figure 3.5. The activation function of the Rap1 AD depends upon evolutionarily conserved hydrophobic amino acids. *A.* Multiple sequence alignment of *S. cerevesiae* (*S. cer*) Rap1 activation domain amino acids 630-671 with the corresponding region of Rap1 proteins from the *sensu lato* yeast *Saccharomyces castelli* (*S. cas.*) and *Saccharomyces kluyveri* (*S. klu*). Amino acids that are identical in all three yeast species are boxed in yellow. These conserved amino acids were targeted for site-directed mutagenesis. *B.* Growth analysis of yeast strains carrying the 3T4A *UAS_Rap1*-*HIS3* reporter and either positive (AS, **Rap1^AS**) and negative (WT, **Rap1^WT**) control forms of Rap1 on the three sets of plates shown (i.e. **AS**, **WT** to **N645A**; **AS**, **WT** to **Y665A**; or **AS**, **WT** to **E671E**) or the indicated Rap1^AS mutant variant (shown, **I633A** to **E671A**). Growth tests were performed as in **Figures 3.1-3.4**, by plating serial dilutions of cells on either non-selective (**+ His**) or reporter gene-selective (**+ 3-AT**) media. Rap1^AS AD point mutants that display a large decrease in growth relative to Rap1^AS are blue-boxed. Images are representative of five independent replicates. *C.* qRT-PCR analysis performed on total RNA prepared from yeast carrying the 3T4A *UAS_Rap1*-*HIS3* reporter and either Rap1^AS (**AS**), Rap1^WT (**WT**), or the indicated Rap1^AS AD point mutant variant. Analyses were performed as detailed for **Figure 3.3C.** Data are representative of three biological replicates, each measured in duplicate. Mean ± SD is depicted. * = p < 0.005, ** = p = 0.0001.

UAS_Rap1-*HIS3* yeast reporter strain to test the hypothesis that combined mutation of key

hydrophobic aa's would result in decreases in AT^R, with combination of the two strongest

inactivating single point mutations (**L650A + F646A**) causing the strongest reduction in

AT^R. While all Rap1^AS AD combinations showed reduced AT^R compared to the **L650A**
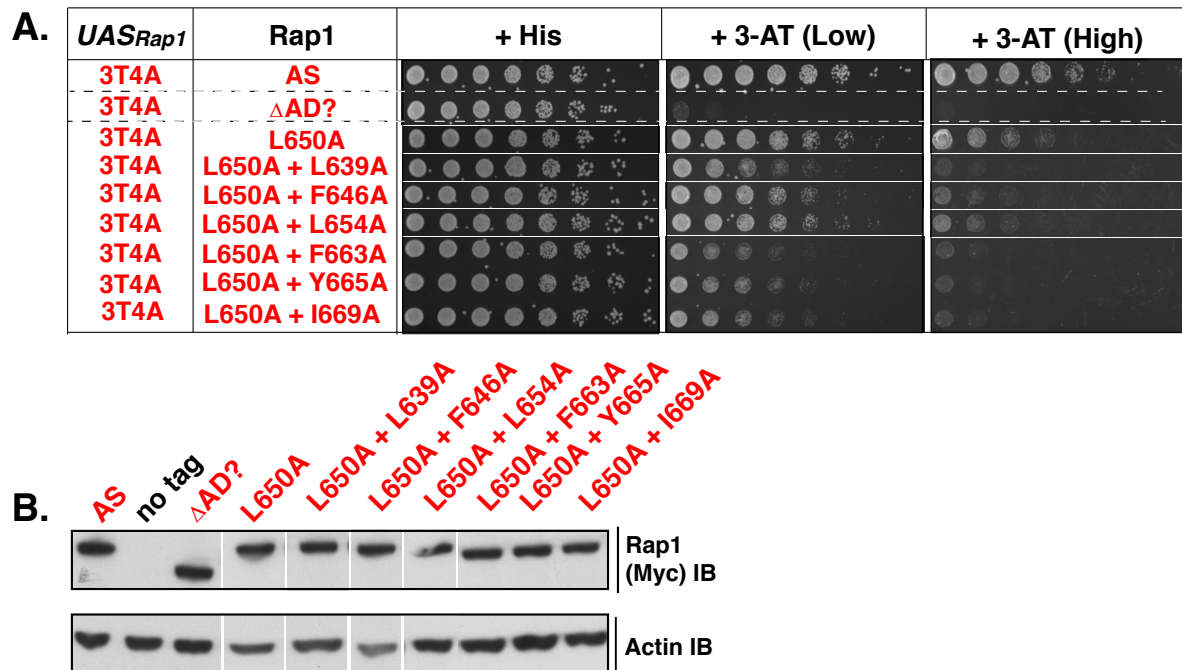
Figure 3.6. Rap1 AD Combination Mutant Analysis.. *A.* Growth analysis of yeast strains carrying the 3T4A version of the *HIS3* reporter (left column; *UAS_{Rap1}*-**red**; labeled **3T4A**) and various forms of Rap1 (labeled **Rap1**, second column), either Rap1^AS (**AS**, **red**) or the indicated Rap1^AS point mutant variants (**ΔAD?**, **L650A**, etc; **red**). Assay was performed as described in **Figure 3.1**. Two different 3-AT growth plates are shown; one contains a "low" concentration of 3-AT (10mM) while the other contains a "high" concentration of 3-AT (100mM). *B.* Immunoblot analysis of Rap1^AS and Rap1^AS deletion variant protein expression levels. This analysis was performed as detailed in **Figure 2.8**.

single mutant, surprisingly, **L650A + L639A**, **L650A + F663A**, **L650A + Y665A**, and **L650A + I669A** all showed weaker AT^R than **L650A + F646A** (**Figure 3.6A**). All proteins were equivalently expressed (**Figure 3.6B**); thus, these interesting results suggest that the key identified aa within the Rap1 AD likely make different contributions to AD activity.

Finally, to test the hypothesis that the majority, if not all, of the AD activity of Rap1 is conferred by the key hydrophobic amino acids within the AD (aa's 630-671), two more Rap1^AS AD variants were prepared. Each was predicted to ablate, or knock out (KO) AD activity. The first 'AD-KO' variant of Rap1^AS lacked the entire mapped Rap1 AD region (aa's 630-671 (**Figure 3.7A, top,** labeled **Δ630-671**.) The second Rap1^AS AD-KO variant was
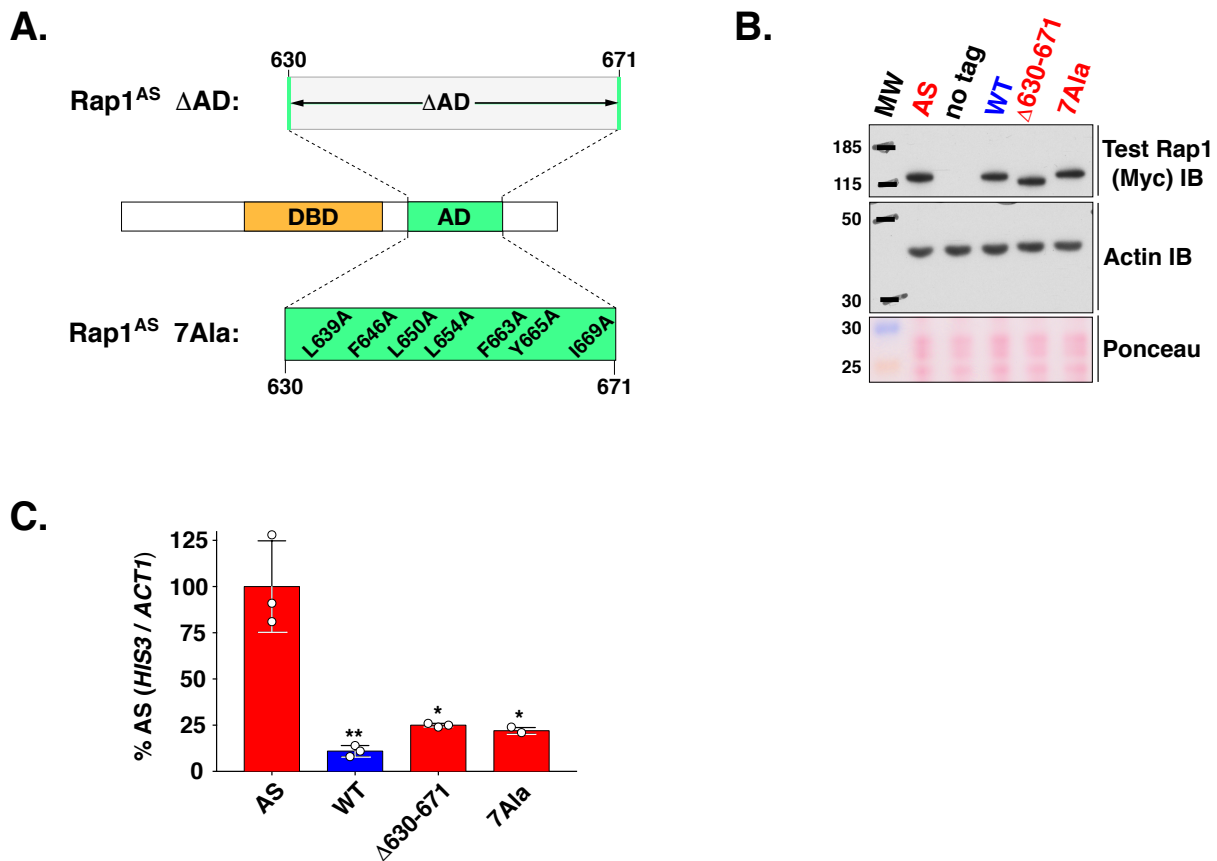
Figure 3.7. Seven hydrophobic Rap1 AD amino acids confer Rap1 activation function.
A. Schematic of Rap1 illustrating the structures of two AD Knock-out alleles. Middle, schematic of intact Rap1 illustrating the location of known functional domains (**DBD, AD, SD**). Top, Rap1 AD sequences 630 to 671 that were deleted from Rap1. Bottom, the location and sequence of the seven hydrophobic amino acids identified by site-directed mutagenesis and functional assays (**Figure 6** above) that were all mutated to Alanine (L639A, F646A, L650A, L654A, F663A, Y665A and I669A) to create the Rap1^{AS} 7Ala variant. *B.* Steady state protein levels of Rap1 variants tested in **panel A** (**AS, WT**, **D630-671**, **7Ala**; specificity control = **no tag**, as labeled; blots performed as detailed in **Figure 2.8**). Images are representative of two independent replicates. *C.* qRT-PCR analysis performed on total RNA prepared from yeast carrying the 3T4A *UAS$_{Rap1}$-HIS3* reporter and either Rap1^{AS} (**AS**), Rap1^{WT} (**WT**), or Rap1^{AS} AD knockout variants (**Δ630-671**) or (**7Ala**). Analyses were performed as detailed for **Figures 3.3C, 3.6B**. Data are representative of three biological replicates, each measured in triplicate. Mean ± SD is depicted. * = p = 0.0002, ** = p = 0.0001.

created by simultaneously mutating all seven of the key (*cf.* **Figure 3.5B**) hydrophobic

amino acids to Alanine (**Figure 3.7A**, labeled **7Ala, bottom**). Plasmid borne genes

encoding Rap1^{AS}, Rap1^{WT}, Rap1$^{AS\ \Delta630-671}$ and Rap1$^{AS\ 7Ala}$ were transformed into the 3T4A-

UAS$_{Rap1}$-HIS3 test strain, and protein and mRNA^{HIS3} levels were scored by immunoblot and

qRT-PCR (**Figure 3.7B, C**, respectively). All proteins were equivalently expressed. Notably

though, the two AD-KO strains both displayed drastically reduced *HIS3* mRNA levels

relative to the WT version of Rap1[AS]. Thus, 3T4A *UAS$_{Rap1}$-HIS3* reporter gene expression

depends predominantly on the mapped Rap1 AD, particularly the 7 key hydrophobic amino

acids implicated in AD function by alanine scanning mutagenesis.

The Rap1 AD is Specific for Activation

Based on previous analyses described above and in Chapter I, I expected that the

Rap1 AD would be distinct from the SD (Chen et al., 2011; Feeser and Wolberger, 2008;

Kyrion et al., 1992; Moretti et al., 1994b). Thus, I hypothesized that Rap1 AD mutation

would not impact the silencing activity of Rap1. To test this hypothesis, I used a

hmrΔA::TRP1 WT *UAS$_{Rap1}$-HIS3* yeast strain, which contained both a reporter for Rap1-

dependent transcription activation (my WT *UAS$_{Rap1}$-HIS3*) and a previously characterized

Rap1-dependent silencing reporter (Feeser and Wolberger, 2008; Sussel and Shore,

1991)(**Figure 3.8A**). Because both reporters contain the WT *UAS$_{Rap1}$* binding site, the 7Ala

and ΔSD (control for silencing) mutations were introduced into the context of Rap1[WT].

Analyses of the activity of *hmrΔA::TRP1* WT *UAS$_{Rap1}$-HIS3* yeast carrying only Rap1[WT],

Rap1ΔSD, or Rap1 7Ala as the sole copy of Rap1 present in the cell showed that, unlike the

Rap1ΔSD, Rap1 7Ala failed to relieve transcription repression in an *HMRA* silencing

reporter strain (Feeser and Wolberger, 2008; Sussel and Shore, 1991)(**Figure 3.8C**). Since

all proteins were expressed equally in the *hmrΔA::TRP1* WT *UAS$_{Rap1}$-HIS3* yeast strain

(**Figure 3.8B**), this result indicates that, as expected, the Rap1 AD plays no significant role

in transcriptional repression.

A.

Activation Reporter

RPS8A Enhancer

Silencing Reporter

HMRE Silencer

B.

Test Rap1 (Myc) IB

Actin IB

Ponceau S

C.

Rap1	+ His, Trp (Control)	+ 3-AT (Activation)	- Trp (Silencing)
WT			
ΔSD			
7 Ala			
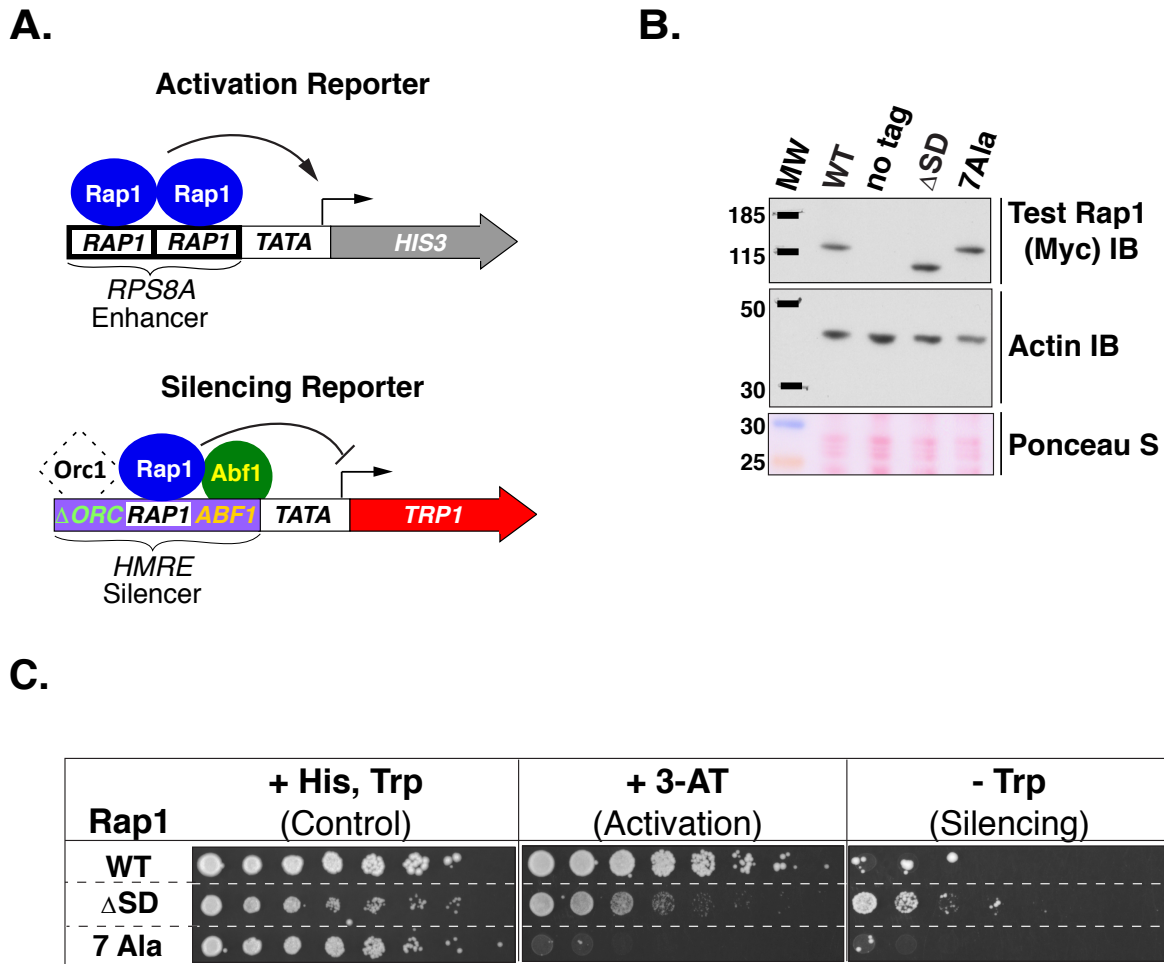
Figure 3.8. Mutation of the mapped Rap1 AD does not affect transcriptional silencing. *A.* Structures of yeast in vivo reporters. (Top) Structure of our yeast transcriptional activation *HIS3*-reporter gene. (Bottom) The prototypic yeast transcriptional silencing *TRP1*-reporter (Sussel and Shore (1991))]. Note that the *HMRE* silencer element integrated in the Shore strain is deleted for the Orc1 binding sites (i.e. ΔORC). The resulting absence of silencer-bound Orc1 protein is indicated by the dashed box labeled Orc1). Loss of Orc1 binding makes the resulting *HMRE* silencer-*TRP1* reporter more sensitive to Rap1 protein function. Yeast strain YLS34 (Sussel and Shore (1991) was engineered to contain our WT *UAS_{Rap1}-TATA-HIS3* reporter gene, which were integrated at the *HIS3* locus using *HIS3* selection since the *TRP1* marker located on the reporter integration construct had to be removed for this assay. This strain was then transformed with *ADE2*-marked *CEN-ARS* plasmids expressing Myc$_5$-NLS-WT, -7Ala or -ΔC (aa's 600-827 deleted) forms of Rap1. *B.* Equivalent expression of the various Rap1 forms. Rap1 protein levels were scored by immunoblotting as described previously *C.* In vivo tests of silencing and activation function via growth assays. Cells expressing the indicated forms of Rap1 (Rap1) were serially diluted and plated on Synthetic media containing histidine and tryptophan (+His, Trp/Control; left), 3-Aminotriazole (+3-AT) to score for Activation of the *UAS_{RAP1}*-regulated *HIS3*-reporter gene (center); or lacking Trp (-Trp) to score for Silencing of the *HMRE*-controlled *TRP1*. Data shown in panels *B*, *C* is representative of 2 and 4 biological replicates, respectively.

The Rap1 AD is Required for Normal Cell Growth and Transcription

We reasoned that if the Rap1 AD (and key AD aa's mapped therein using Rap1^AS)

truly represent the bona fide activation domain of Rap1, then introducing the 7Ala

mutation in the context of the Rap1^WT should cause a decrease in the transcription of

chromosomal Rap1-dependent genes and a concomitant decrease in growth rate.

Importantly, testing these mutations into the context of the WT version of the protein also

controls for potential synthetic genetic interactions between the altered DBD sequences of

Rap1^AS and the altered sequences that were introduced into the mapped AD. To probe the

question of the essentiality of the Rap1 AD for growth, the ability of the 7Ala mutation in

the otherwise Rap1^WT protein, carefully scored for complementation of a *rap1Δ* null mutant

strain using the plasmid shuffle method. Rap1^WT and empty plasmid vector respectively,

served as positive and negative controls for this test. While Rap1^WT efficiently and

specifically complements *rap1Δ*, the Rap1^7Ala variant only weakly complemented (compare

growth of **WT** vs. **7Ala** strains, row 1 vs. row 3; **Figure 3.9A**) despite the fact that the two

proteins were equally expressed (**Figure 3.9B**). The dramatic growth deficiency of the

Rap1^7Ala-expressing strain was quantified via growth curves. The WT strain doubling time

is 94 minutes while the Rap1^7Ala expressing strain requires nearly twice as long, 155

minutes, to double (**Figure 3.9C**). Thus, consistent with my expectations, the Rap1 AD is

required for normal rates of cell growth.

Assuming that the Rap1 activation domain mapped here actually functions

specifically in the activation of authentic chromosomal target genes, it is reasonable to

predict that Rap1 AD loss-of-function mutants would exhibit reduced expression of both

RP- and GE-encoding genes. Indeed, extensive cis-element mapping, use of conditional

A.

rap1*	Unshuffled (*RAP1*, *rap1Δ*, *rap1**)	Shuffled (— , *rap1Δ*, *rap1**)
WT		
-		
7Ala		

B.

Test Rap1 (Myc) IB

Actin IB

Ponceau

C.

D.
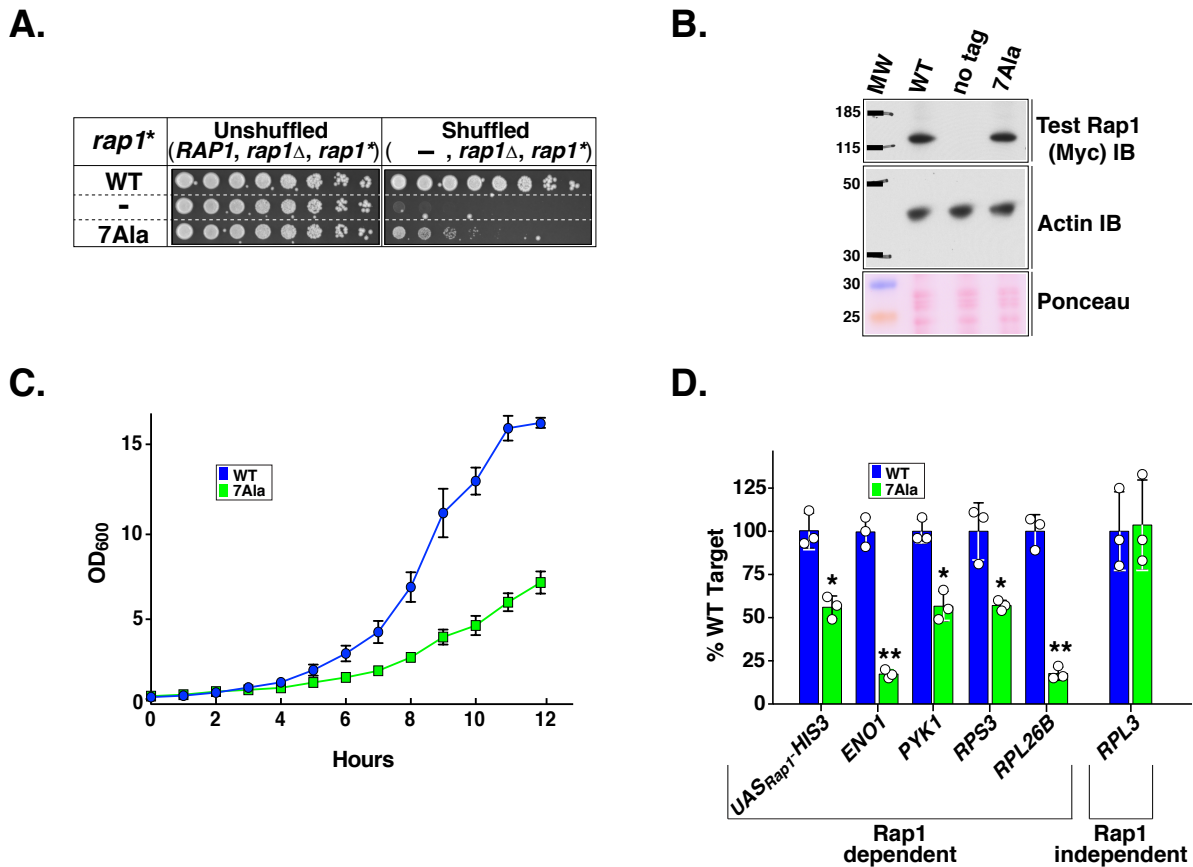
Figure 3.9. The Rap1 AD is required both for normal growth and transcription of authentic chromosomal Rap1-target genes. *A.* The ability of the Rap1[7Ala] variant to support cell viability was assessed by plasmid shuffle analyses. Yeast carrying a chromosomal null *RAP1* allele (*rap1Δ*) and a *URA3*-marked *RAP1* covering plasmid were transformed with a test variant of *RAP1*, labeled **rap1***: (*i*) a second plasmid-borne copy of *RAP1* (labeled **WT**); (*ii*) empty plasmid vector (labeled **-**); or (*iii*) the same plasmid vector expressing the Rap1[7Ala] variant (labeled **7Ala**). Yeast were serially diluted 1:4 (left to right) and growth was scored on media either lacking 5-FOA ("**Unshuffled**"; relevant genotype: ***RAP1, rap1Δ, rap1****), or containing 5-FOA ("**Shuffled**" relevant genotype: **-, *rap1Δ, rap1****) as detailed in "Chapter II" **Figure 2.7**. Images are representative of five independent replicates. *B.* Immunoblot analysis of the in vivo steady state levels of Rap1[WT] and Rap1[7Ala] proteins. Analysis was performed as described in above. Images are representative of four independent replicates. *C.* Growth curve analysis of three biological replicates of shuffled yeast strains expressing either only Rap1[WT] or Rap1[7Ala], performed and plotted as described in "Chapter II" **Figure 2.8**. *D.* Analysis of nascent RNA levels for several chromosomal yeast genes (integrated ***UAS_Rap1-HIS3* reporter**, ***ENO1***, ***PYK1***, ***RPS3***, ***RPL26B***, ***RPL3***) in cells solely expressing WT *RAP1* or the 7Ala variant of *RAP1*. Cellular RNAs were pulse-labeled with 4sU for 2.5 minutes, extracted, purified, RNA thiol groups chemically biotinylated, and affinity purified and analyzed via qRT-PCR to quantify the amount of nascent transcripts produced from each of the six genes noted above. qRT-PCR analyses were performed as described previously except that data were normalized to *Schizosaccharomyces pombe tubulin* mRNA present due to the spike-in of 4sU pulse-labeled *S. pombe* cells into each sample prior to RNA extraction. Data are representative of three biological replicates, each measured in triplicate. Mean ± SD is depicted. * = $p < 0.0025$, ** = $p < 0.0001$. See "Nascent RNA Labeling and Purification" section for details.

118

alleles, and ChIP-based *in vivo* occupancy studies all support the idea that Rap1 contributes importantly to the expression of these two gene classes (Knight et al., 2014; Kurtz and Shore, 1991; Lickwar et al., 2012b; Lieb et al., 2001; Reja et al., 2015; Yarragudi et al., 2006). However, two considerations preclude straightforward interpretation of the effects of mutations in Rap1 (or other transcription proteins) on cellular steady state mRNA levels. First, unlike the synthetic chimeric *UAS$_{Rap1}$-HIS3* reporter gene studied in the experiments in Chapter II and **Figures 3.1-3.7**, expression of both RP- and GE-encoding genes is modulated by multiple transactivator proteins in addition to Rap1 (Hall et al., 2006; Kasahara et al., 2007b; Knight et al., 2014; Marion et al., 2004; Mencía et al., 2002; Reid et al., 2000; Rudra et al., 2005; Schwalder et al., 2004; Scott and Baker, 1993; Wade et al., 2004b). As a consequence, mutations in the AD of Rap1 will likely not result in as large a decrement in authentic chromosomal target gene transcription as observed with the *HIS3* reporter gene (*cf.* **Figures 3.3, 3.5, 3.7**). Second, another, and perhaps more important factor complicating interpretation of such experiments that monitor steady state mRNA levels is the fact that transcription and mRNA degradation are linked. Both prokaryotic and eukaryotic cells can maintain steady state transcript levels despite loss of key proteins involved in either transcription/transcription activation, or mRNA degradation by modulating these dynamic processes (Bonnet et al., 2014; Chow and Dennis, 1994; Haimovich et al., 2013; Schulz et al., 2014; Sun et al., 2012, 2013).

To circumvent these caveats the 4-thiouracil (s4U) nascent RNA pulse labeling method of RNA analysis (Bonnet et al., 2014; Duffy et al., 2015; Schulz et al., 2014; Sun et al., 2012, 2013) was employed to monitor nascent transcript levels in cells expressing either WT Rap1 or the 7Ala AD Rap1 variant as the sole source of Rap1 (i.e. the shuffled

strains analyzed in **Figure 3.9A-C**). [Note that both strains carry the integrated WT *UAS_Rap1-HIS3* reporter gene]. Nascent RNA levels for five actively-transcribed chromosomal genes and the integrated *HIS3* reporter gene were scored by qRT-PCR (see "Nascent RNA Labeling and Purification" for details). Four of the actively transcribed chromosomal genes are Rap1-dependent (two glycolytic, *ENO1*, *PYK1*; two RP-encoding genes, *RPS3*, *RPL26B*), while one chromosomal Rap1-independent RP-encoding gene was scored (*RPL3*). Alteration of the Rap1 AD by the 7Ala mutation dramatically, and specifically, reduced transcription of the known Rap1-dependent genes (*UAS_Rap1-HIS3*, *ENO1*, *PYK1*, *RPS3* and *RPL26B*), but not the Rap1-independent *RPL3* gene (**Figure 3.9D**). The specific reductions in transcription of the known Rap1-dependent genes ranged from ~50% for the synthetic reporter gene (***UAS_Rap1-HIS3***; **Figure 3.9D**) to ~80% for two of the Rap1-dependent chromosomal genes (***ENO1***, ***RPL26B***; **Figure 3.9D**). Collectively, this data demonstrates that the Rap1 AD, mapped and characterized here through the use of the altered DNA-binding specificity variant of Rap1, is a *bona fide* activation domain.

Mutation of the Rap1 Activation Domain Reduces Binding to the Rap1 Binding Domain (RBD) of the TFIID Coactivator Subunit Taf5

We have previously shown that Rap1 binds specifically, and with high affinity, to distinct RBDs within the Taf4, Taf5 and Taf12 subunits of TFIID (Garbett et al., 2007; Layer et al., 2010). Rap1-Taf RBD binding is sensitive to RBD mutation, and we found that yeast expressing such mutations in either Taf4 or Taf5 display reduced RP mRNA gene expression (Layer and Weil, 2013; Layer et al., 2010). These data argue that TFIID serves as a coactivator for Rap1. However, we did not know which domain(s) within Rap1 was

120

responsible for Rap1-Taf RBD interactions. I theorized that if the Rap1 AD plays a key role in Rap1-TFIID Taf-RBD interaction, then mutation of the AD should reduce Rap1-Taf binding. Because we had previously documented synthetic lethal interactions between Taf5 RBD mutants and Rap1 deletion variants (Layer et al., 2010), we decided to perform GST-Rap1/Taf5 pull-down binding experiments as a first test of our Rap1 AD-Taf RBD direct interaction hypothesis. These studies used an N-terminal RBD-containing fragment of Taf5 (aa's 1-337) and either GST- alone (GST-), GST-fused to WT Rap1 (GST-Rap1 **WT**), GST-fused to the 7Ala variant of Rap1 (GST-Rap1 **7Ala**), and GST-fused to Rap1 ΔC (GST Rap1 **ΔC**). I observed that both the 7Ala- and the ΔC-Rap1 variants reproducibly displayed an ~50% reduction in binding to the Taf5 RBD (**Figure 3.10**). These results are consistent with the hypothesis that the Rap1 AD I have mapped is central to transcriptional activation.

<u>Discussion</u>

Transcription factor AD mapping represents a critical step in the path towards determining the mechanism by which a gene, or group of co-regulated genes, are activated. Our lab is particularly interested in the Rap1 AD because Rap1 in budding yeast drives the transcription of 128 of the 138 genes encoding ribosomal proteins as well as many of the genes encoding the enzymes of glycolysis (Chambers et al., 1995; Knight et al., 2014; Lieb et al., 2001; Rudra and Warner, 2004). These two classes of genes are among the most vigorously transcribed families of genes in most organisms. Understanding the mechanisms controlling expression of such highly transcribed classes of genes will provide

A.
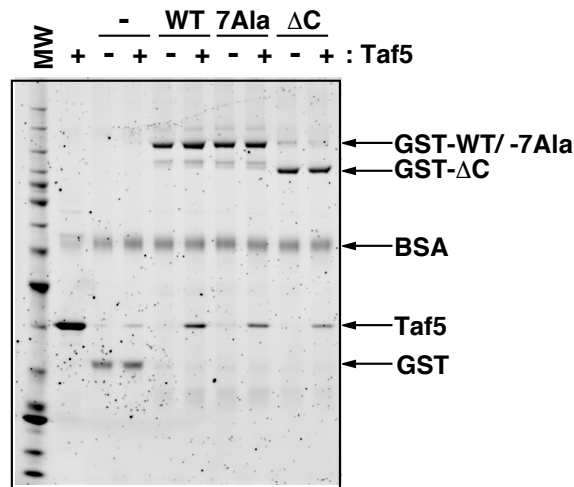
B.
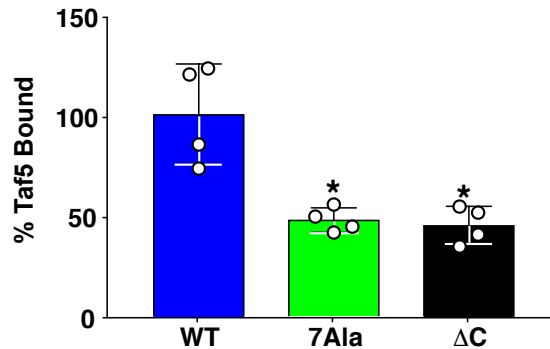
Figure 3.10. Mutation of the Rap1 AD Reduces Binding of Rap1 to the Rap1 Binding Domain (RBD) of the TFIID Coactivator Subunit Taf5. *A.* Sypro Stained NuPAGE gel of Taf5/GST-Rap1 pulldown protein-protein binding reactions. Pull-down experiments were conducted using negative control GST-, positive control GST-WT Rap1, test GST-7Ala Rap1, and test GST-ΔC Rap1-loaded GST-agarose beads and the N-terminal RBD-containing fragment of Taf5 (aa's 1-337). Glutathione sepharose beads loaded with either 12 pmol of GST or 6 pmol of GST-Rap1 variant (**GST-**, **GST-WT Rap1**, **GST-7Ala Rap1, GST-ΔC Rap1**; **labels, arrows**) were incubated with either 0 or 100 pmol of purified Taf5 fragment under the conditions detailed in "GST Pull-down Assays". All incubations contained Bovine Serum Albumin (**BSA**; **label, arrow**) to minimize non-specific protein binding to the beads. Bead-bound proteins were eluted with SDS-sample buffer, heat-denatured and fractionated on an SDS-PAGE gel in parallel with molecular weight standards (**MW**) and 25 pmol purified Taf5 (**Taf5**). Gels were stained with Sypro Ruby and images were obtained using a Pharos Fx. Image is representative of four independent replicates. *B.* Quantification of the data shown in 'A.' Quantity One software was used to score the intensity of GST-, GST-Rap1 variant, and Taf5 bands. The intensity of each Taf5 band was normalized to the intensity of each GST- or GST-Rap1 variant band and then Taf5 binding to GST-beads alone was subtracted from the Taf5 binding of all GST-Rap1 variants. Taf5 binding data obtained from four independent replicates are plotted using Graph Pad Prism 7 software as a percentage of the Taf5 binding to GST-Rap1 WT. Mean ± SD is depicted. * = p =0.002.

valuable and potentially generalizable mechanistic insights into how highly expressed eukaryotic genes are regulated.

In budding yeast, transcription of the genes encoding RPs is controlled through the action of multiple DNA binding transcription proteins. These include Rap1, Ifh1, Fhl1, Sfp1 and Hmo1 (Hall et al., 2006; Kasahara et al., 2007b; Marion et al., 2004; Reid et al., 2000; Rudra et al., 2005; Schwalder et al., 2004; Wade et al., 2004b). RP gene transcription is responsive to a variety of regulatory inputs, several of which respond to nutrient availability and/or cell size (Lempiäinen and Shore, 2009; Marion et al., 2004; Rudra and Warner, 2004; Rudra et al., 2005; Schwalder et al., 2004; Wade et al., 2004b). These two regulatory pathways appear to work through Ifh1/Fhl1 and Sfp1 (Marion et al., 2004; Rudra et al., 2005; Schwalder et al., 2004; Wade et al., 2004b), and thus appear distinct from Rap1 function(s). Meanwhile, Rap1 is the only activator that is absolutely required for transcription of the RP encoding genes, as deletion of the genes encoding these other factors (or their cognate DNA binding elements) reduces, but does not eliminate RP gene expression (Garbett et al., 2007; Mencía et al., 2002).

Our lab has had a long-standing interest in Rap1 and RP encoding genes because transcription of this gene family requires TFIID (Garbett et al., 2007; Holstege et al., 1998; Irvin and Pugh, 2006; Kuras et al., 2000; Layer and Weil, 2013; Layer et al., 2010; Li et al., 2000, 2002; Mencía et al., 2002; Ohtsuki et al., 2010; Papai et al., 2010; Shen and Green, 1997; Shen et al., 2003; Singh et al., 2004; Tsukihashi et al., 2001). The lab has previously shown that Rap1 directly interacts with the RP gene coactivator TFIID (Garbett et al., 2007), that this binding is specific, high affinity, and mediated through distinct Rap1 Binding Domains (RBDs) present in TFIID subunits Taf4, Taf5 and Taf12 (Garbett et al.,

2007; Layer et al., 2010). Deletion of the RBDs from either Taf4 or Taf5 is lethal, while the

aa's within these ca. 100-300 aa domains are mutable, and certain point mutations within

either RBD leads to temperature-conditional growth and reduced affinity of binding to

Rap1. Moreover, certain combinations of distinct, non-lethal *rap1* deletion mutants with

taf5^{ts} mutants induces synthetic lethality, while shifting strains carrying either *taf4^{ts}* or

taf5^{ts} mutant alleles to non-permissive temperatures induces a large and selective decrease

in expression of essentially the entire complement of RP encoding genes (Layer et al.,

2010).

The lab also previously documented and characterized important interactions

between Rap1 and TFIIA. Mutations that compromise these interactions decrease TFIIA-

TFIID and TFIIA-Taf4 interaction/binding, RP gene expression *in vivo*, and Rap1-driven

reporter gene transcription *in vitro* (Layer and Weil, 2013). Finally, the lab has previously

described unique Rap1-induced, TFIIA- and TFIID-dependent DNA looping and Rap1-

dependent protein structural transitions of TFIIA within a quaternary Rap1-TFIIA-TFIID-

UAS_{Rap1}-*TATA* DNA complex (the enhancer-promoter reporter DNA used in my work)

(Papai et al., 2010).   Collectively these data lead us to propose that Rap1 directly and

specifically binds subunits of both TFIID and TFIIA in order to activate transcription of the

RP encoding genes (Garbett et al., 2007; Layer and Weil, 2013; Layer et al., 2010; Papai et

al., 2010, 2011). As a prerequisite to advance these studies, and to more fully dissect the

molecular mechanisms utilized by Rap1 to activate transcription, it is essential to have a

collection of AD variants of Rap that are defective in RP gene transcription activation.

Unfortunately, though much is known regarding the TFIID coactivator subunit

targets of Rap1, prior to the work described in my dissertation, there was no unambiguous

data regarding whether Rap1 actually contains a functional AD. As a consequence, I decided to use the Rap1[AS] described in Chapter II as a novel tool to facilitate the identification and high-resolution characterization of an AD within Rap1. My unambiguous AD mapping data also show that the best of my altered DNA-binding specificity variants, Rap1[AS], represents a powerful tool to study Rap1 structure-function relationships. Activator proteins, such as Rap1, can contain one or more ADs, usually 30-100 aa's in size. ADs have been classified based on the kinds of aa's that dominate the activation domain: acidic, proline-rich, and glutamine-rich (Mitchell and Tjian, 1989; Titz, 2006).

Using Rap1[AS], I have found that both the Rap1 C-terminus and the Rap1 N-terminus can contribute to activation, depending on whether the assayed reporter gene was designed based on an RP or a glycolytic gene, respectively. I focused on the Rap1-C-terminal aa's involved in activation for because, unlike the N-terminus, the Rap1 C-terminus interacts with TFIID (Garbett et al., 2007) and is thus, likely critical for activation of the TFIID-dependent RP genes as well as the RP gene reporter. There is no evidence, to my knowledge, that the Rap1 N-terminus interacts directly with a coactivator (such as SAGA) at present, and thus does not fit the classical criteria for AD designation. Indeed, prior analyses have led to the proposition that the Rap1 N-terminus contributes to GE gene transcription through facilitating the binding of the Gcr1 and Gcr2 DNA-binding transcription activators to GE enhancer (*UAS*) sequences (López et al., 1998; Mizuno et al., 2004). Focusing on the Rap1 C-terminus, a single AD of the protein was successfully mapped to Rap1 aa's 630-671. This 41-aa region exhibits a predicted pI of 3.84 due to the fact that it contains nine glutamate and aspartate amino acids, 20% of the total AD residues. Thus, the Rap1 AD falls into the acidic class of ADs.

Although this acidic AD is located within the AD mapped using the Gal4 DBD-Rap1

fusion approach (aa's 630-692)(Hardy et al., 1992a), my analyses provide important

additional insights. Studies of acidic ADs have shown that typically they contain small

clusters of key hydrophobic aa's that actually confer AD activity (Deng et al., 2001;

Drysdale et al., 1995; Lin et al., 1994; Regier et al., 1993) rather than their acidic aa's

(Brzovic et al., 2011; Lin et al., 1994). Consistent with this principle, my mutational

analyses of individual Rap1 AD aa's showed, for the first time, that specific individual

hydrophobic aa's (i.e. L639, F646, L650, L654, F663, Y665, and I669) contribute critically

to Rap1 AD function. My Rap1 AD analysis, however, did reveal a few interesting

differences between the Rap1 AD and other well-studied activator ADs. First, in contrast to

other activators such as VP16, Zta, Gcn4, p53, and glucocorticoid receptor (GR), where at

least two AD mutations must be made to noticeably decrease transcriptional activity of an

intact AD in reporter assays (Deng et al., 2001; Drysdale et al., 1995; Iñiguez-Lluhí et al.,

1997; Lin et al., 1994; Regier et al., 1993), several single point Rap1 AD mutant variants (i.e.

L639A, F646A, L650A, L654A, F663A, Y665A, and I669A; **Figure 3.5B**) displayed defects in

activity as scored by growth. It is also surprising that it was the non-polar L650A mutant

that showed a significant decrease in mRNA^{HIS3} levels in qRT-PCR (**Figure 3.5C**), instead of

a bulky aromatic hydrophobic amino acid (i.e. F, Y, or P), which have been shown to be the

most critical contributors to AD function in other well-characterized ADs (Deng et al., 2001;

Drysdale et al., 1995; Iñiguez-Lluhí et al., 1997; Lin et al., 1994; Regier et al., 1993). Finally,

the Rap1 AD activity is spread over a large number of contiguous aa's (i.e. seven aa's; see

Figures 3.5-3.10) compared with other ADs whose activity is concentrated on only 2-3

aa's (Drysdale et al., 1995; Iñiguez-Lluhí et al., 1997; Lin et al., 1994; Regier et al., 1993;

Warfield et al., 2014). It is tempting to speculate that these seven key hydrophobic aa's

may represent separate/overlapping binding domains for the known, distinct coactivator

targets of Rap1 (Garbett et al., 2007; Layer and Weil, 2013; Layer et al., 2010; Tomar et al.,

2008). Alternatively, collectively, these seven critical AD aa's may enable Rap1 to bind with

unusually high affinity to its coactivator targets and thus drive the high levels of

transcription observed at the RP-encoding genes. Indeed, it was recently shown that the

addition of hydrophobic aa's to a small nine residue AD sub-motif of yeast Gcn4 could

increase coactivator binding affinity and transcription activity (Warfield et al., 2014). I

believe that the collection of Rap1 AD point mutants generated here will prove to be

powerful reagents for investigating these possibilities.

Importantly, my studies also demonstrate, for the first time, that transcription of

authentic chromosomal Rap1-dependent target genes and Rap1-TFIID Taf5 coactivator

target binding depend on a discrete AD within Rap1. The results of my Rap1^{WT} and

Rap1^{7Ala} variant pulse-labeling studies provide compelling evidence that the Rap1 AD

functions to specifically modulate transcription activation of chromosomal Rap1 target

genes (**Figure 3.8**). These results are all the more notable given the number of recent

studies that document the robust ability of yeast to maintain normal steady-state transcript

levels in the face of mutations in genes encoding key mRNA synthesis and mRNA

degradation proteins. It is highly likely that these findings would have been difficult to

observe without the use of the nascent RNA labeling technique. My pulse-labeling analyses

also revealed that the Rap1 AD played a role on both the RP and GE genes tested, in

contrast to my glycolytic reporter gene expression analyses which suggested that the Rap1

N-terminus contains the Rap1 aa's most important for glycolytic gene expression. A

possible explanation for this observation is that the Rap1 domains involved in activation may vary among the GE genes, each of which encodes an independently functioning enzyme.

Finally, my GST-Rap1/Taf5 pull-down binding experiments (**Figure 3.10**) show that the Rap1 AD binds coactivator targets as expected and provides an important starting point for dissecting the biochemical mechanism of transcription activation by the Rap1 AD. Admittedly, the 2-fold reduction in Taf5 binding observed in the Rap1[7Ala] mutant may seem weak compared to the magnitude of reduction in coactivator target binding expected from mutation of the key aa's of the sole Rap1 AD. It is very likely, however, that the Rap1 AD-Taf5 interaction is not the only AD-coactivator interaction driving Rap1-dependent gene transcription given that within the TFIID coactivator Rap1 additionally targets Tafs 4 and 12 and could possibly interact with TFIIA (Garbett et al., 2007; Layer et al., 2010; Papai et al., 2010). Indeed, mutation of the RBDs within these Tafs 4, 5, and 12 resulted in reductions in Rap1 binding of magnitude comparable to the reduction in Taf5 binding resulting from the Rap1 7Ala mutation (Layer et al., 2010). Alternatively, the affect of Rap1 AD mutation on Taf5 binding in the pull-down assay could be partially masked by Rap1-binding to Taf5 surfaces that are not available when Taf5 is in the context of the TFIID complex.

The Rap1 AD may also target other coactivators. Because Rap1 can bind nucleosomal UAS_{Rap1} sites (Koerber et al., 2009) and reposition nucleosomes (Yu and Morse, 1999), the Rap1 AD may target chromatin remodeling factors, in addition to TFIID and TFIIA subunits, in order to modulate target gene transcription. In fact, several recent studies have suggested that the high level of RP and GE gene transcription requires altered

nucleosome stabilities and/or positioning (Knight et al., 2014; Kubik et al., 2015; Reja et al., 2015). Consistent with these observations, the ATP-dependent nucleosome remodeling complex Swi/Snf has been shown to interact with Rap1 (Tomar et al., 2008). The Rap1 AD may also directly contact the chromatin remodeling RSC complex (Kubik et al., 2015) and/or the histone acetyltransferase NuA4 complex, both of which have been identified as important regulators of Rap1-dependent gene transcription (Reid et al., 2000; Rohde and Cardenas, 2003; Uprety et al., 2015). Future studies can address these important questions.

In conclusion, the Rap1 AD mapping and the Rap1 AD mutants generated through my studies represent an important advance in Rap1 biology. These advances were made possible by the generation of a true altered DNA-binding specificity Rap1[AS] and provide a case study demonstrating the power of the Rap1[AS] approach.   This information and the reagents generated will enable future important work aimed at molecularly dissecting the mechanisms responsible for regulating the robustly transcribed RP- and GE-encoding genes, including testing our lab's novel "Lock to Load" model of transcription activation.

CHAPTER IV

FUTURE DIRECTIONS

Summary

The work presented in this dissertation represents my efforts to determine the

domain(s) and molecular mechanism(s) Rap1 uses to activate protein-coding gene

transcription. This work achieved two important goals. The first of these goals was the

generation of Rap1^{AS}, presented in Chapter II of this dissertation. Rap1^{AS} represents both

an achievement for the field of protein engineering, where developing proteins with novel

DNA-binding specificity represents an important goal, and a tool to provide more precise

and straightforward dissections of the myriad functions of Rap1. The second goal was the

identification of the Rap1 AD and the determination of how it functions presented in

Chapter III of this dissertation. In addition to providing a thorough characterization of the

Rap1 AD and providing the critical demonstration that this AD functions on authentic

chromosomal Rap1 target genes, my efforts have resulted in the identification of the TFIID

Taf5 subunit as a target of the Rap1 AD. The identification of Taf5 as a target of the

physiologically relevant Rap1 AD represents a critical step towards systematic testing of

the "Lock to Load" model. Taken along with the lab's multiple demonstrations that Rap1-

TFIID and TFIID-TFIIA interactions are required for RP gene transcription (Layer and Weil,

2013; Layer et al., 2010), this result shows that the protein-protein interactions in the

"Lock to Load" model proposed based on EM structural analyses (Papai et al., 2010) are

important *in vivo*. It also links "Lock to Load" to an AD such that it is indeed possible that

the TFIIA conformational change identified in the Rap1-TFIID-TFIIA-complex is triggered

by direct Rap1 AD-coactivator interaction and therefore, represents a key step in transcription regulation.

These results lay the groundwork for future studies aimed at thoroughly testing the "Lock to Load" model of transcription activation. In my path to generating these results, I also made several observations that, while not pertaining directly to "Lock to Load," could provide interesting and important avenues for further experimentation. I explore these possible future directions in this final chapter of my dissertation.

How Do Rap1[AS] Screen Hits Achieve Expanded and Altered DNA-binding Specificities?

My successful generation of Rap1[AS] in Chapter II presents a research opportunity to advance knowledge of protein-DNA interactions and provide guidance for protein engineering efforts. My Rap1[AS] demonstrates true altered DNA-binding specificity *in vivo* and *in vitro*. How is this true altered DNA-binding specificity achieved?

To achieve true altered DNA-binding specificity, a DNA-binding protein must both gain the ability to bind a mutant *UAS* site while reducing/losing its ability to bind the WT *UAS*. The MEME-generated motif of Rap1[AS] sequences revealed that all Rap1[AS] screen hit sequences possessed an N401 mutation to either a non-polar aa (such as G, P, or A) or (in the case of Rap1 mutant **#2** a charged polar mutation (R). They also all possess an H405 mutation to either a bulky non-polar aa (W or F) or a small non-polar aa. The fact that the same kinds of changes in aa's N401 and H405 were found in the sequences of all Rap1[AS] screen hits suggests that these changes enable functional interaction with the 3T4A *UAS*. Meanwhile, as discussed in Chapter II, comparison of the Rap1[AS] hit sequences of those variants that showed true altered compared to those that showed expanded specificity

suggests that a bulky non-polar hydrophobic mutation at aa 405 and a mutation at aa 408 reduce Rap1 variant binding to the WT *UAS*. Finally, the variability in the kinds of mutations present at aa 409 shows that there is little selection on this aa, and it likely does not contribute to either expanded or altered DNA-binding specificity.

These hypotheses could be tested using a family of Rap1 variants generated by systematically introducing mutations found in the Rap1[AS] sequence (N401R, H405W, R408L, V409C) or the H405S mutation proposed to contribute to expanded rather than true altered DNA-binding specificity individually and in combination into *RAP1*. This family of Rap1 variants could then be tested for the ability to functionally interact with 3T4A *UAS_{Rap1}* using the AT[R] growth assay and qRT-PCR. Variants that functionally interacted with 3T4A *UAS_{Rap1}* could then be tested for expanded vs. true altered DNA-binding specificity via the plasmid shuffle and gel shift DNA-binding competition assays utilized in this dissertation.

Completion of the proposed analyses of the family of Rap1 variants described above would result in the identification of the aa's required for both expanded and true altered DNA-binding specificity. To gain insight into how these aa's structurally achieve altered DNA-binding specificity, a structure-prediction program such as ROSETTA (Leaver-Fay et al., 2011) could be used to model the structure of Rap1 DBD variants in complex with the WT and 3T4A *UAS_{Rap1}* sites. These models could be tested by crystallizing the Rap1 DBD variants in complex with the WT and/or 3T4A *UAS_{Rap1}* sites (depending on whether the variant demonstrated expanded or true-altered DNA-binding specificity) using the protocol outlined by previous studies of Rap1 DBD-DNA co-crystal structures (König et al., 1996; Matot et al., 2012; Taylor et al., 2000). Finally, the data obtained from these co-

crystallization studies could be fed back into protein-DNA structure prediction algorithims

to improve their predictive capabilities. These studies, especially when combined with the

data obtained from the genetic and biochemical experiments performed on the family of

Rap1 variants designed based on the Rap1[AS] sequence, would provide a thorough

understanding of how expanded and true altered specificity are achieved by Rap1[AS] screen

hits.

<u>What is the Role of the Rap1 N-Terminus In Glycolytic Enzyme Gene Expression?</u>

    In the Rap1 AD mapping studies described in Chapter II, I found that, in contrast to

the RP reporter gene, my glycolytic reporter gene depended primarily on the Rap1 N-

terminus for expression. Although my pulse labeling studies show that the Rap1 AD

contributes to the expression of the chromosomal genes tested, this finding raises the

possibility that Rap1 domains may make differential contributions to the activation of the

TFIID-dependent RP genes compared to the SAGA-dependent GE genes. The Rap1 N-

terminus has been previously implicated in budding yeast GE gene expression; analyses

conducted prior to my study showed that the Rap1 N-terminus interacts genetically with

the glycolytic transcription activators Gcr1 and Gcr2 (Mizuno et al., 2004) and contributes

to Gcr1 DNA-binding in gel shift analyses (López et al., 1998).   However, these genetic and

biochemical interactions with Gcr1 and Gcr2 have not been further characterized.

    My Rap1[AS] and Rap1[AS]-dependent glycolytic reporter gene could be used to

precisely define which of the Rap1 N-terminal aa where required for glycolytic reporter

gene expression. First though, the glycolytic reporter gene would need further

characterization. Prior to the studies I conducted for my dissertation, our lab and others

showed via ChIP that, like authentic RP genes, the RP reporter gene I used for my AD

mapping is occupied by both Rap1 and TFIID (Garbett et al., 2007; Mencía et al., 2002). To

determine whether or not my glycolytic reporter gene behaves like the chromosomal *PGK1*

gene it is based on, ChIP analyses should be performed to test the occupancy of Rap1, Gcr1,

and SAGA-specific subunits on the *UAS* and promoter on my reporter and on *PGK1*.

Assuming that the chromosomal *PGK1* gene and my reporter gene show similar

transcription factor occupancy patterns, growth and qRT-PCR analyses could be conducted

on yeast containing this reporter and Rap1^{AS} N-terminal deletion/point mutants to define

the N-terminal aa's required for expression. Mutations that reduced expression of the

Rap1^{AS}-dependent glycolytic reporter gene could be introduced into the context of Rap1^{WT};

nascent RNA pulse labeling coupled with qRT-PCR could be used to determine if the N-

terminal regions mutated were required for expression of authentic chromosomal

glycolytic genes.   These analyses would determine whether the Rap1 BRCT domain, which

shows weak transcription activation and chromatin remodeling activity when fused to a

heterologous DBD (Miyake et al., 2000), or some other Rap1 N-terminal aa contribute to

glycolytic gene expression.

To find out whether or not any Rap1 N-terminal aa's required for GE gene

expression function as hypothesized via a protein-protein interaction with Gcr1 and/or

Gcr2, GST-Rap1^{WT} and GST-Rap1 mutant variants could be tested for interaction with

purified Gcr1 and Gcr2 via pull-down assays similar to those presented in Chapter III.

Alternatively, protein samples prepared via coimmunoprecipitation of Rap1^{WT} and Rap1 N-

terminus mutants from yeast cells could be analyzed via mass-spectrometry as an unbiased

approach to determining Rap1-interacting factors that require the Rap1 N-terminal aa's

needed for glycolytic gene expression. The Rap1 7 Ala mutant could be included in these analyses to identify Rap1 AD interacting factors and to test the hypothesis that the Rap1 AD and N-terminus interact with distinct sets of protein factors. Our lab has used this approach previously to identify protein factors that interact with each of the TFIID subunits (Sanders et al., 2002b). Completion of these studies would provide a stronger characterization of the Rap1 N-terminal domains and protein-protein interactions used to drive GE expression as well as insight into how Rap1 may differentially regulate the yeast GE and RP gene classes.

<h2 style="text-align:center">How Does the Rap1 AD Interact with TFIID/TFIID subunits?</h2>

As part of my efforts to determine how the Rap1 AD biochemically affects transcription activation, I have identified the TFIID subunit Taf5 as a Rap1 AD target. This exciting and important result suggests that Rap1 activates transcription through AD-TFIID interaction, as expected based on our prior investigations of Rap1-TFIID interactions (Garbett et al., 2007; Layer et al., 2010).   This result also merits further investigation, and several experiments could be performed to further define the Rap1 AD interaction with TFIID, let alone other possible coactivator targets.

Previous analyses performed in the lab have shown that Rap1 interacts with TFIID via RBDs located within Tafs 4, 5, and 12 (Garbett et al., 2007; Layer et al., 2010). Does the Rap1 AD interact with Tafs 4 and 12 in addition to interacting with Taf5? Pull-down experiments similar to those performed in Chapter III could be used to test this possibility. Because Taf4 is reportedly unstable when expressed individually (Justin H. Layer, unpublished observations), I have performed preliminary pull-down experiments to test

A.

B.
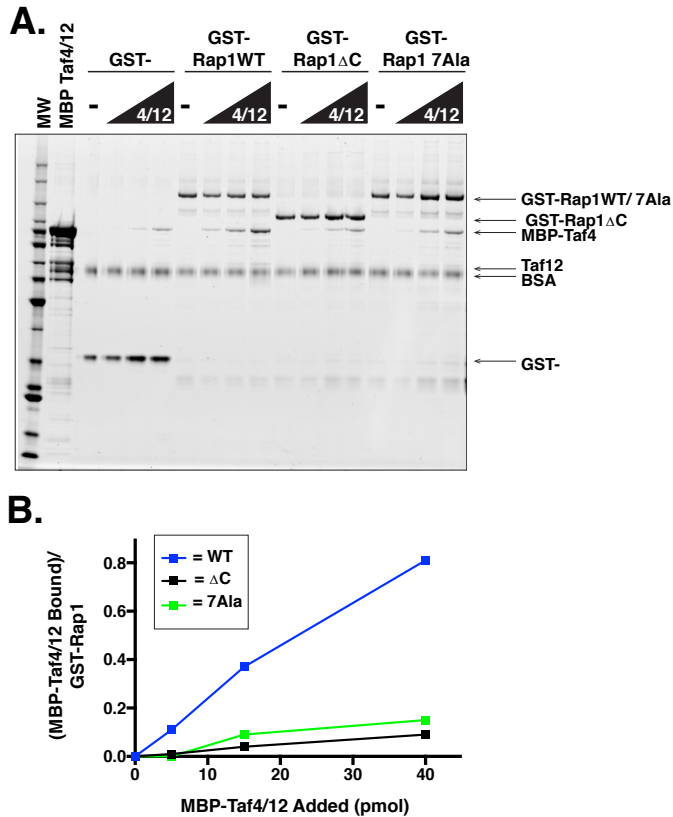
Figure 4.1. Rap1 ΔC and 7 Ala mutants show reduced Taf4/12 interaction. *A.* Sypro stained SDS-PAGE gel of GST- and GST-Rap1 variant pull-down reactions performed with increasing amounts of MBP-Taf4/12. *B.* Quantification of the data presented in "A" obtained by scoring the amount of MBP-Taf4 in each lane, normalizing for the amount of GST- or GST-Rap1 variant present in the reaction, and subtracting out the amount of MBP-Taf4 in the corresponding GST only reaction.

Rap1 AD interaction with Tafs 4 and 12 (**Figure 4.1A)** using MBP-Taf4/12 purified for a previous study (Layer and Weil, 2013). This MBP-Taf4/12 material is imperfect, as the intensity of the Taf4 and 12 bands suggests a much greater than 1:1 stoichiometry of Taf4 to Taf12 (see **Figure 4.1A** "Input"). Interestingly though, as in my Taf5 RBD pull-downs (*cf* **Figure 3.10**) my GST-Rap1 ΔC and GST-Rap1 7Ala bound less MBP-Taf4 than GST-Rap1 WT (**Figure 4.1A,B**). Additional pull-down assays using either Taf4/12 proven to be a heterodimer via gel filtration or Taf4 and Taf12 individually could be performed to validate this result,

which suggests that the Rap1 AD targets Taf4/12 as well as Taf5. The identification of multiple Rap1 AD interacting factors raises the possibility that the seven key hydrophobic amino acids identified in my Rap1 AD mapping actually make unique contacts with TFIID subunits. This possibility should be tested by performing GST pull-down assays with Rap1

AD single point (i.e. L650A) and combination (i.e. L650A + F663A) mutant variants, with the goal of identifying separation-of-function and graded-loss-of-function mutants.

Biophysical and cross-linking studies could also be used to further understand Rap1 AD TFIID-interaction. For example, nuclear magnetic resonance spectroscopy (NMR), which has been used to biophysically characterize the VP16, Gcn4, and p53 ADs (Brzovic et al., 2011; Jonker et al., 2005; Krois et al., 2016; Uesugi et al., 1997), could be used to define the Rap1 AD structure alone and in complex with the Taf5 as well as the Taf4 and Taf12 RBDs. These studies would test the hypothesis that the Rap1 AD amino acids identified as important for AD-Taf RBD interaction by the NMR structure would be the same as those required for the Rap1 transcription activation function. Additionally, the K_d of Rap1 AD interaction with the Taf 4, 5, and 12 RBDs could be determined and compared to each other and to the K_d's of other so characterized AD-coactivator binding interactions. Finally, site-specific cross-linking, which has been used to identify the *in vivo* targets of the Gal4 and Gcn4 ADs (Fishburn et al., 2005; Reeves and Hahn, 2005), could be used to determine whether or not the Rap1 AD interacts with Tafs 4, 5, and/or 12 *in vivo* as expected based on the complementary genetic and biochemical analyses performed in our lab (Garbett et al., 2007; Johnson and Weil, 2017; Layer et al., 2010). Taken together, the results of these studies would provide a thorough understanding of Rap1 AD-TFIID interaction.

What is the Mechanistic Consequence of Rap1 AD-TFIID Taf Interaction: Testing "Lock to "Load"

In addition to my identification of Taf5 as a Rap1 AD target and the experiments proposed above aimed at further defining the Rap1 AD-TFIID interaction, biochemical and

structural analyses could be performed to determine the mechanistic consequence of Rap1

AD-TFIID interaction. Since pull-down assays and biolayer interferometry have repeatedly

failed to detect a direct Rap1-TFIIA interaction (Amanda N. Meyer, Justin H. Layer, and

Scott G. Miller, unpublished observations), defining the biochemical consequences of Rap1

AD-TFIID interaction represents the most likely path to uncovering the mechanism of RP

gene transcription activation. These experiments would ultimately put our "Lock to Load"

model of transcription activation to the test. Immobilized template assays could be

performed to test the binding of TFIID and TFIIA to DNA along with Rap1[WT], Rap1[7Ala], and,

if identified in the proposed Rap1 AD-TFIID interaction experiments, a series of Rap1 AD

mutant graded loss-of-function variants. The "Lock to Load" model predicts that these

experiments will fail to show that the Rap1 AD is required for TFIID cooperative binding to

DNA. However, a variation of these assays could be performed to probe the stability of the

Rap1-TFIID-TFIIA-DNA complex, which may be enhanced by a Rap1 AD-TFIID interaction

triggered post-DNA recruitment TFIIA conformational change. Alternatively, Rap1-TFIID-

TFIIA-DNA complex formation and stability could be assessed via DNase I footprinting

and/or agarose gel shift analysis. The impact of the Rap1 AD on enhancer-promoter DNA

loop formation, which our "Lock to Load" model suggests is a consequence of TFIIA

conformational change could be assessed by DNA loop ligation assay. Although Rap1 itself

has been implicated in DNA-looping (Hofmann et al., 1989; Papai et al., 2010), it is not yet

clear whether or not this DNA-looping is influenced by the Rap1 AD via its interaction with

TFIID.

  Of course the most critical tests of the "Lock to Load" model would be performed via

EM. Specifically, EM analyses of the quaternary complexes formed by Rap1-TFIID-TFIIA-

DNA and Rap1^{7Ala}-TFIID-TFIIA-DNA could be used to test the requirement of the Rap1 AD

for TFIIA conformational change. Platinum shadowing could also be used to visualize DNA

loops formed in quarternary complexes containing Rap1^{WT} vs. Rap1 ^{7Ala}. These analyses

would ultimately determine if the Rap1 AD is required for TFIIA conformational change

and enhancer-promoter DNA loop formation; if so, these activities indeed likely represent

key components of our "Lock to Load" model of TFIID-dependent transcription activation.

 How Generalizable Is the TFIID Coactivator Activity Observed In Budding Yeast RP genes?

If indeed "Lock to Load" accurately represents the mechanism regulating

transcription activation of the RP genes, how generalizable is the "Lock to Load" model?

Does "Lock to Load" only operate on budding yeast RP genes? Is the transcription

activation of other robustly transcribed genes, including the RP genes of other organisms

regulated via "Lock to Load"?

Determining how RP genes are regulated in other organisms provides one means of

investigating the generalizability of the "Lock to Load" model. Surprisingly given the

intense selection pressure on RP genes based on their requirement for cell growth and

viability, the particular transcription activators that bind RP gene *UAS*/enhancer elements

varies drastically over the evolutionary tree. For example, while most budding yeast RP

genes depend on Rap1 (Knight et al., 2014; Reja et al., 2015), basal metazoan and human

RP gene enhancers contain binding sites for GABP, Sp1, and YY1 transcription factors

(Perina et al., 2011). Even the RP genes of other yeast contain *UAS* elements for factors

other than Rap1 (Hogues et al., 2008; Lavoie et al., 2009; Tanay et al., 2005; Tuch et al.,

2008).

As part of a collaborative project with Drs. Sandy Johnson and Trevor Sorrells at UCSF investigating the rewiring of RP genes, I have performed a few experiments to help define the molecular mechanism of RP gene regulation in the yeast *Kluyveromyces lactis* (*K. lactis*). Compared to *S. cerevisiae* RP genes, many *K. lactis* RP genes contain a binding site for Mcm1 located in proximity to a binding site for Rap1 (Tuch et al., 2008). In reporter assays performed using a *K. lactis* RP reporter gene consisting of the *GFP* ORF driven by a *TATA*, *UAS*$_{Rap1}$, and *UAS*$_{Mcm1}$ elements, Drs. Sorrells and Johnson have shown that *UAS*$_{Rap1}$ and *UAS*$_{Mcm1}$ drive reporter gene expression cooperatively, suggesting that Rap1 and Mcm1 cooperatively activate transcription. These investigators originally hypothesized that this cooperative activation was achieved via a protein-protein interaction between Rap1 and Mcm1 gained in *K. lactis* compared to *S. cerevisiae*. However, they found that the *UAS*$_{Rap1}$ and *UAS*$_{Mcm1}$ sites cooperatively activate expression of their RP reporter gene in *S. cerevisiae*, indicating that the ability of these factors to cooperatively activate transcription is likely ancestral. Further, gel shift DNA-binding assays performed using *K. lactis* and *S. cerevisiae* cell extract and purified proteins showed that Rap1 and Mcm1 bind DNA independently rather than cooperatively (manuscript in preparation). As a result, Drs. Johnson and Sorrells hypothesized that Rap1 and Mcm1 cooperatively activate gene expression through binding a shared transcription coregulator target.

Based on our lab's work on RP gene regulation in *S. cerevisiae* (Garbett et al., 2007; Layer and Weil, 2013; Layer et al., 2010), Drs. Johnson and Sorrells hypothesized that this shared transcription coregulator target was the TFIID coactivator. They solicited our lab's collaboration in testing this hypothesis. As part of this investigation, I set out to determine which Rap1 domains were required for expression of the *UAS*$_{Rap1-Mcm1}$ reporter in budding
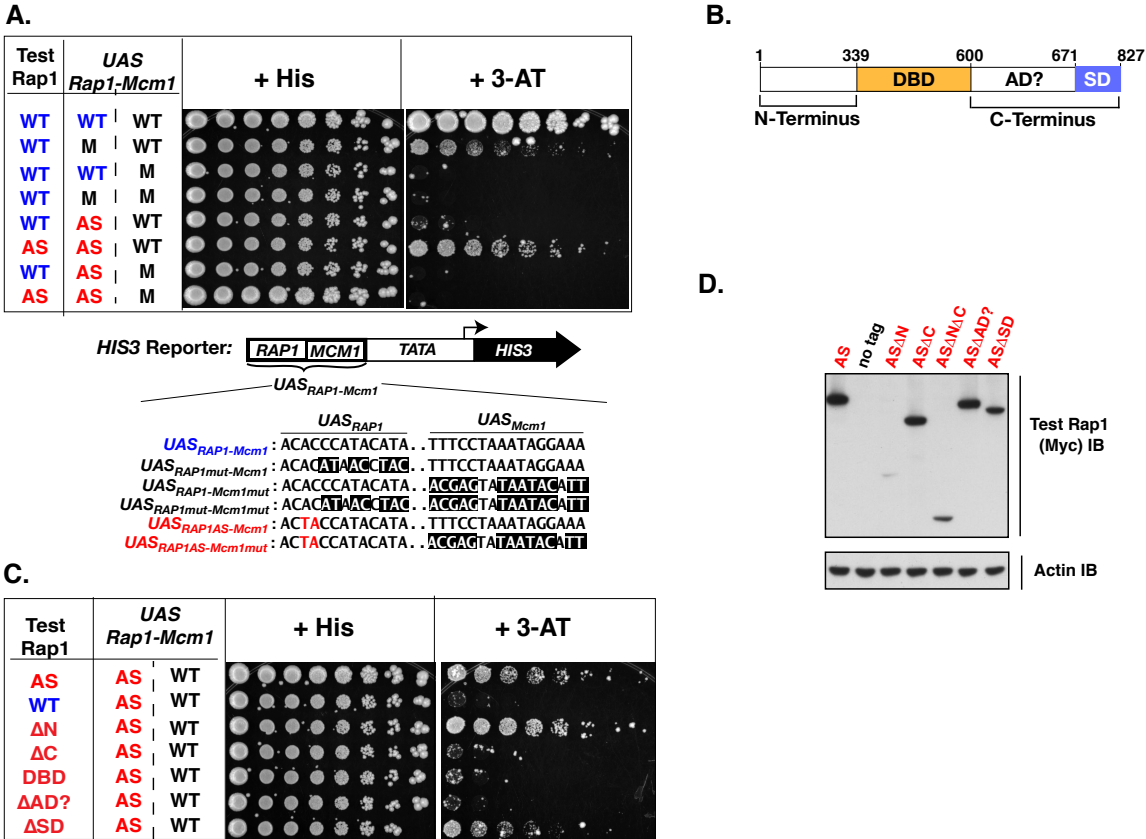
A.

Test Rap1	UAS Rap1-Mcm1		+ His	+ 3-AT
WT	WT	WT		
WT	M	WT		
WT	WT	M		
WT	M	M		
WT	AS	WT		
AS	AS	WT		
WT	AS	M		
AS	AS	M		

HIS3 Reporter: RAP1 MCM1 TATA HIS3

UAS$_{RAP1\text{-}Mcm1}$

UAS$_{RAP1}$　　　UAS$_{Mcm1}$

UAS$_{RAP1\text{-}Mcm1}$: ACACCCATACATA. .TTTCCTAAATAGGAAA
UAS$_{RAP1mut\text{-}Mcm1}$: ACAC**ATAACCTAC**. .TTTCCTAAATAGGAAA
UAS$_{RAP1\text{-}Mcm1mut}$: ACACCCATACATA. .**ACGAGTATAATAC**ATT
UAS$_{RAP1mut\text{-}Mcm1mut}$: ACAC**ATAACCTAC**. .**ACGAGTATAATAC**ATT
UAS$_{RAP1AS\text{-}Mcm1}$: AC**TA**CCATACATA. .TTTCCTAAATAGGAAA
UAS$_{RAP1AS\text{-}Mcm1mut}$: AC**TA**CCATACATA. .**ACGAGTATAATAC**ATT

B.

1　　339　　　600　　　671　827

DBD　AD?　SD

N-Terminus　　　C-Terminus

D.

AS / no tag / AS△N / AS△C / AS△N△C / AS△AD? / AS△SD

Test Rap1 (Myc) IB

Actin IB

C.

Test Rap1	UAS Rap1-Mcm1		+ His	+ 3-AT
AS	AS	WT		
WT	AS	WT		
ΔN	AS	WT		
ΔC	AS	WT		
DBD	AS	WT		
ΔAD?	AS	WT		
ΔSD	AS	WT		

Figure 4.2. The Rap1 ΔAD? is required for expression of the *UAS$_{Rap1\text{-}Mcm1}$ HIS3* reporter designed based on a *K. lactis* RP gene. *A.* Upper: AT[R] growth analyses performed as described in Chapters II and III on yeast containing either a second copy of Rap1[WT] or Rap1[AS] and the indicated *UAS$_{Rap1\text{-}Mcm1}$* reporter gene. Lower: structure of the *UAS$_{Rap1\text{-}Mcm1}$* reporter gene used in these assays. Mutations introduced into the *UAS$_{Rap1}$* and *UAS$_{Mcm1}$* sites by binding site nucleotide scrambling are highlighted in black. The 3T4A ("AS") mutations introduced into *UAS$_{Rap1}$* to generate the Rap1[AS] binding site are shown in red. *B.* Rap1 protein map indicating the location of the major Rap1 domains. *C.* AT[R] growth analyses performed in yeast carrying the *UAS$_{Rap1AS\text{-}Mcm1WT}$* reporter and either Rap1[WT], Rap1[AS], or the indicated Rap1[AS] mutant variant. *D.* Immunoblot analysis performed to assess steady-state Myc$_5$-tagged Rap1[AS] and Rap1[AS] variant protein expression levels using actin as a protein loading control.

yeast with the hypothesis that, if cooperative reporter activation depends on TFIID, then

reporter expression should depend on the Rap1 C-terminus, which interacts directly with

TFIID. To perform these experiments, I once again turned to the *HIS3* reporter and Rap1[AS].

AT[R] growth analyses of a series of WT and mutant *UAS$_{Rap1\text{-}Mcm1}$* reporters designed based on

the *GFP* reporters assayed by my collaborators (**Figure 4.2A**) showed that, like the *GFP*

reporters, expression of the *UAS$_{Rap1\text{-}Mcm1}$-HIS3* reporters depended on both *UAS$_{Rap1}$* and

UAS_{Mcm1} (**Figure 4.2A**). Additionally and importantly, Rap1[AS] conferred AT[R] to a $UAS_{Rap1AS-Mcm1}$-*HIS3* reporter; this AT[R] depended on UAS_{Mcm1} (**Figure 4.2A**). These results support the use of my Rap1[AS] and the $UAS_{Rap1AS-Mcm1}$-*HIS3* reporter gene for the dissection of the Rap1 domains (**Figure 4.2B**) involved in $UAS_{Rap1-Mcm1}$ reporter activation.

Analyses of AT[R] growth in $UAS_{Rap1AS-Mcm1}$-*HIS3* reporter budding yeast containing Rap1[AS] and Rap1[AS] deletion mutants revealed that expression of the $UAS_{Rap13T4A-Mcm1}$-*HIS3* reporter depends on the Rap1 C-terminus, particularly the AD? domain (**Figure 4.2C**). The Rap1[ASΔC] and Rap1[ASΔAD?] variants are stable and expressed at levels comparable to those of Rap1[AS] (**Figure 4.2D**). Thus, like my budding yeast RP reporter UAS_{Rap1}-*HIS3*, expression of the $UAS_{Rap1AS-Mcm1}$-*HIS3* reporter requires Rap1 domains known to interact with TFIID as hypothesized. To provide a better test of this hypothesis, I am currently repeating these analyses using my Rap1[AS7Ala] variant to determine if $UAS_{Rap1AS-Mcm1}$-*HIS3* reporter expression depends on the Rap1 AD that I have mapped and shown interacts with the TFIID subunit Taf5.

I have also performed Far Western protein-protein binding assays using purified holo-TFIID and TFIID Tafs to determine if Mcm1 directly interacts with TFIID subunits. Interestingly, I have found that Mcm1 interacts directly with Tafs 4, 5, and 12 in the Far Western assay (**Figure 4.3A,B**), the same TFIID subunits that bind Rap1. I am currently working on Far Western competition assays to test whether these interactions are specific. Assuming that the Mcm1-TFIID subunit interactions I have detected are specific, this result raises the possibility that Rap1 and Mcm1 cooperatively activate $UAS_{Rap1-Mcm1}$ reporter and *K. lactis* RP genes through the TFIID coactivator as originally postulated by Drs. Johnson and Sorrells. Additionally, this result suggests that transcription activator binding to TFIID
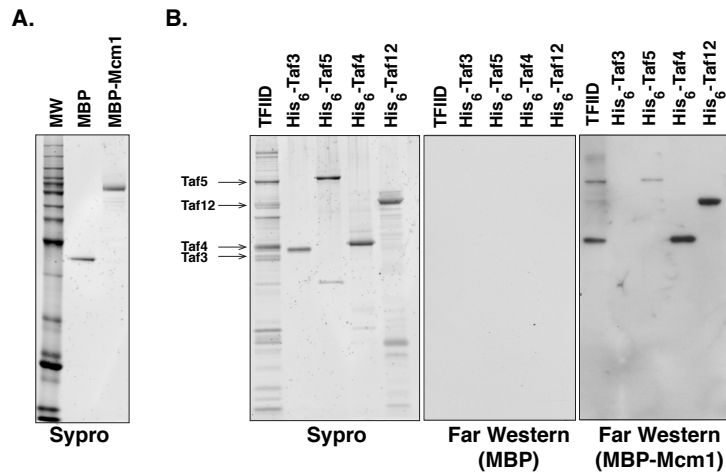
Figure 4.3. MBP-Mcm1 binds TFIID Tafs 4, 5, and 12 in the Far Western Assay. *A.* A Sypro-Ruby Stained SDS-PAGE gel containing MBP- and MBP-Mcm1 proteins tested for their ability to interact with TFIID subunits via Far Western. *B.* Far Western analysis of MBP- and MBP-Mcm1 binding to TFIID subunits. In this analysis, TFIID and His6-Tafs 4, 5, and 12 as well as Taf3 (included as a negative control) purified by Drs. Jordan T. Feigerle and Justin H. Layer were separated on an SDS-PAGE gel and either stained with Sypro Ruby (left panel) or transferred to a membrane for the Far Western assay (middle and right panels). These membranes were probed with either control MBP (middle panel) and MBP-Mcm1 (right panel). Binding of the probe protein to any of the proteins on the membrane was detected via immunoblot using an anti-MBP antibody.

is a conserved feature of RP gene transcription, at least across yeast species. Further testing will be required to determine whether Mcm1 and RP transcription activators in higher eukaryotes also directly interact with TFIID via their ADs and if this interaction results in the TFIIA conformational change and DNA loop locking that represent the key steps in the "Lock to Load" mechanism of transcription activation.

REFERENCES

Adelman, K., and Lis, J.T. (2012). Promoter-proximal pausing of RNA polymerase II: emerging roles in metazoans. Nat. Rev. Genet. *13*, 720–731.

Adkins, M.W., and Tyler, J.K. (2006). Transcriptional activators are dispensable for transcription in the absence of Spt6-mediated chromatin reassembly of promoter regions. Mol. Cell *21*, 405–416.

Albert, B., Knight, B., Merwin, J., Martin, V., Ottoz, D., Gloor, Y., Bruzzone, M.J., Rudner, A., and Shore, D. (2016). A Molecular Titration System Coordinates Ribosomal Protein Gene Transcription with Ribosomal RNA Synthesis. Mol. Cell *64*, 720–733.

Albright, S.R., and Tjian, R. (2000). TAFs revisited: more data reveal new twists and confirm old ideas. Gene *242*, 1–13.

Allard, S., Utley, R.T., Savard, J., Clarke, A., Grant, P., Brandl, C.J., Pillus, L., Workman, J.L., and Côté, J. (1999). NuA4, an essential transcription adaptor/histone H4 acetyltransferase complex containing Esa1p and the ATM-related cofactor Tra1p. EMBO J. *18*, 5108–5119.

Allison, L.A., Moyle, M., Shales, M., and Ingles, C.J. (1985). Extensive homology among the largest subunits of eukaryotic and prokaryotic RNA polymerases. Cell *42*, 599–610.

Allison, L.A., Wong, J.K., Fitzpatrick, V.D., Moyle, M., and Ingles, C.J. (1988). The C-terminal domain of the largest subunit of RNA polymerase II of Saccharomyces cerevisiae, Drosophila melanogaster, and mammals: a conserved structure with an essential function. Mol. Cell. Biol. *8*, 321–329.

Almer, A., and Hörz, W. (1986). Nuclease hypersensitive regions with adjacent positioned nucleosomes mark the gene boundaries of the PHO5/PHO3 locus in yeast. EMBO J. *5*, 2681–2687.

Almer, A., Rudolph, H., Hinnen, A., and Hörz, W. (1986). Removal of positioned nucleosomes from the yeast PHO5 promoter upon PHO5 induction releases additional upstream activating DNA elements. EMBO J. *5*, 2689–2696.

Almlöf, T., Gustafsson, J.-A., and Wright, A.P. (1997). Role of hydrophobic amino acid clusters in the transactivation activity of the human glucocorticoid receptor. Mol. Cell. Biol. *17*, 934–945.

An, Y., Ji, J., Wu, W., Lv, A., Huang, R., and Wei, Y. (2005). A rapid and efficient method for multiple-site mutagenesis with a modified overlap extension PCR. Appl. Microbiol. Biotechnol. *68*, 774–778.

Andrau, J.-C., van de Pasch, L., Lijnzaad, P., Bijma, T., Koerkamp, M.G., van de Peppel, J., Werner, M., and Holstege, F.C.P. (2006). Genome-Wide Location of the Coactivator

Mediator: Binding without Activation and Transient Cdk8 Interaction on DNA. Mol. Cell *22*, 179–192.

Andrews, F.H., Shinsky, S.A., Shanle, E.K., Bridgers, J.B., Gest, A., Tsun, I.K., Krajewski, K., Shi, X., Strahl, B.D., and Kutateladze, T.G. (2016). The Taf14 YEATS domain is a reader of histone crotonylation. Nat. Chem. Biol. *12*, 396–398.

Archer, T.K., Cordingley, M.G., Wolford, R.G., and Hager, G.L. (1991). Transcription factor access is mediated by accurately positioned nucleosomes on the mouse mammary tumor virus promoter. Mol. Cell. Biol. *11*, 688–698.

Attardi, L.D., and Tjian, R. (1993). Drosophila tissue-specific transcription factor NTF-1 contains a novel isoleucine-rich activation motif. Genes Dev. *7*, 1341–1353.

Awrey, D.E., Weilbaecher, R.G., Hemming, S.A., Orlicky, S.M., Kane, C.M., and Edwards, A.M. (1997). Transcription elongation through DNA arrest sites. A multistep process involving both RNA polymerase II subunit RPB9 and TFIIS. J. Biol. Chem. *272*, 14747–14754.

Bai, Y., Perez, G.M., Beechem, J.M., and Weil, P.A. (1997). Structure-function analysis of TAF130: identification and characterization of a high-affinity TATA-binding protein interaction domain in the N terminus of yeast TAF(II)130. Mol. Cell. Biol. *17*, 3081–3093.

Bannister, A.J., and Kouzarides, T. (2011). Regulation of chromatin by histone modifications. Cell Res. *21*, 381–395.

Barbaric, S., Münsterkötter, M., Goding, C., and Hörz, W. (1998). Cooperative Pho2-Pho4 interactions at the PHO5 promoter are critical for binding of Pho4 to UASp1 and for efficient transactivation by Pho4 at UASp2. Mol. Cell. Biol. *18*, 2629–2639.

Barbaric, S., Luckenbach, T., Schmid, A., Blaschke, D., Hörz, W., and Korber, P. (2007). Redundancy of chromatin remodeling pathways for the induction of the yeast PHO5 promoter in vivo. J. Biol. Chem. *282*, 27610–27621.

Barillà, D., Lee, B.A., and Proudfoot, N.J. (2001). Cleavage/polyadenylation factor IA associates with the carboxyl-terminal domain of RNA polymerase II in Saccharomyces cerevisiae. Proc. Natl. Acad. Sci. *98*, 445–450.

Basehoar, A.D., Zanton, S.J., and Pugh, B.F. (2004). Identification and distinct regulation of yeast TATA box-containing genes. Cell *116*, 699–709.

Bendjennat, M., and Weil, P.A. (2008). The Transcriptional Repressor Activator Protein Rap1p Is a Direct Regulator of TATA-binding Protein. J. Biol. Chem. *283*, 8699–8710.

Bergman, L.W., and Kramer, R.A. (1983). Modulation of chromatin structure associated with derepression of the acid phosphatase gene of Saccharomyces cerevisiae. J. Biol. Chem. *258*, 7223–7227.

Bergman, L.W., Stranathan, M.C., and Preis, L.H. (1986). Structure of the transcriptionally repressed phosphate-repressible acid phosphatase gene (PHO5) of Saccharomyces cerevisiae. Mol. Cell. Biol. *6*, 38–46.

Berlow, R.B., Dyson, H.J., and Wright, P.E. (2015). Functional advantages of dynamic protein disorder. FEBS Lett. *589*, 2433–2440.

Bhaumik, S.R., and Green, M.R. (2001). SAGA is an essential in vivo target of the yeast acidic activator Gal4p. Genes Dev. *15*, 1935–1945.

Bhaumik, S.R., and Green, M.R. (2003). Interaction of Gal4p with Components of Transcription Machinery In Vivo. B.-M. in Enzymology, ed. (Academic Press), pp. 445–454.

Bhaumik, S.R., Raha, T., Aiello, D.P., and Green, M.R. (2004). In vivo target of a transcriptional activator revealed by fluorescence resonance energy transfer. Genes Dev. *18*, 333–343.

Bieniossek, C., Papai, G., Schaffitzel, C., Garzoni, F., Chaillet, M., Scheer, E., Papadopoulos, P., Tora, L., Schultz, P., and Berger, I. (2013a). The architecture of human general transcription factor TFIID core complex. Nature *493*, 699–702.

Bieniossek, C., Papai, G., Schaffitzel, C., Garzoni, F., Chaillet, M., Scheer, E., Papadopoulos, P., Tora, L., Schultz, P., and Berger, I. (2013b). The architecture of human general transcription factor TFIID core complex. Nature *493*, 699–702.

Birck, C., Poch, O., Romier, C., Ruff, M., Mengus, G., Lavigne, A.C., Davidson, I., and Moras, D. (1998). Human TAF(II)28 and TAF(II)18 interact through a histone fold encoded by atypical evolutionary conserved motifs also found in the SPT3 family. Cell *94*, 239–249.

Blattner, F.R., Plunkett, G., Bloch, C.A., Perna, N.T., Burland, V., Riley, M., Collado-Vides, J., Glasner, J.D., Rode, C.K., Mayhew, G.F., et al. (1997). The complete genome sequence of Escherichia coli K-12. Science *277*, 1453–1462.

Boeke, J.D., Trueheart, J., Natsoulis, G., and Fink, G.R. (1987). 5-Fluoroorotic acid as a selective agent in yeast molecular genetics. Methods Enzymol. *154*, 164–175.

Bonnet, J., Wang, C.-Y., Baptista, T., Vincent, S.D., Hsiao, W.-C., Stierle, M., Kao, C.-F., Tora, L., and Devys, D. (2014). The SAGA coactivator complex acts on the whole transcribed genome and is required for RNA polymerase II transcription. Genes Dev. *28*, 1999–2012.

Brachmann, C.B., Davies, A., Cost, G.J., Caputo, E., Li, J., Hieter, P., and Boeke, J.D. (1998). Designer deletion strains derived from Saccharomyces cerevisiae S288C: a useful set of strains and plasmids for PCR-mediated gene disruption and other applications. YEAST-CHICHESTER- *14*, 115–132.

Brennan, M.B., and Struhl, K. (1980). Mechanisms of increasing expression of a yeast gene in Escherichia coli. J. Mol. Biol. *136*, 333–338.

Brownell, J.E., Zhou, J., Ranalli, T., Kobayashi, R., Edmondson, D.G., Roth, S.Y., and Allis, C.D. (1996). Tetrahymena histone acetyltransferase A: a homolog to yeast Gcn5p linking histone acetylation to gene activation. Cell *84*, 843–851.

Browning, D.F., and Busby, S.J.W. (2004). The regulation of bacterial transcription initiation. Nat. Rev. Microbiol. *2*, 57–65.

Brzovic, P.S., Heikaus, C.C., Kisselev, L., Vernon, R., Herbig, E., Pacheco, D., Warfield, L., Littlefield, P., Baker, D., Klevit, R.E., et al. (2011). The Acidic Transcription Activator Gcn4 Binds the Mediator Subunit Gal11/Med15 Using a Simple Protein Interface Forming a Fuzzy Complex. Mol. Cell *44*, 942–953.

Buratowski, S., and Zhou, H. (1993). Functional domains of the transcription factor TFIIB. PNAS *90*, 5633–5637.

Buratowski, S., Hahn, S., Guarente, L., and Sharp, P.A. (1989). Five intermediate complexes in transcription initiation by RNA polymerase II. Cell *56*, 549–561.

Buratowski, S., Sopta, M., Greenblatt, J., and Sharp, P.A. (1991). RNA polymerase II-associated proteins are required for a DNA conformation change in the transcription initiation complex. Proc. Natl. Acad. Sci. *88*, 7509–7513.

Burgess, R.R., Travers, A.A., Dunn, J.J., and Bautz, E.K.F. (1969). Factor Stimulating Transcription by RNA Polymerase. Nature *221*, 43–46.

Burke, T.W., and Kadonaga, J.T. (1997). The downstream core promoter element, DPE, is conserved fromDrosophila to humans and is recognized by TAFII60 of Drosophila. Genes Dev. *11*, 3020–3031.

Bushnell, D.A., Cramer, P., and Kornberg, R.D. (2002). Structural basis of transcription: alpha-Amanitin-RNA polymerase II cocrstyal at 2.8 A resolution. PNAS *99*, 1218–1222.

Cadwell, R.C., and Joyce, G.F. (1992). Randomization of genes by PCR mutagenesis. PCR Methods Appl. *2*, 28–33.

Cadwell, R.C., and Joyce, G.F. (1994). Mutagenic PCR. PCR Methods Appl. *3*, S136-140.

Callebaut, I., and Mornon, J.-P. (1997). From BRCA1 to RAP1: a widespread BRCT module closely associated with DNA repair. FEBS Lett. *400*, 25–30.

Carrozza, M.J., Li, B., Florens, L., Suganuma, T., Swanson, S.K., Lee, K.K., Shia, W.-J., Anderson, S., Yates, J., Washburn, M.P., et al. (2005). Histone H3 methylation by Set2 directs deacetylation of coding regions by Rpd3S to suppress spurious intragenic transcription. Cell *123*, 581–592.

Chalkley, G.E., and Verrijzer, C.P. (1999). DNA binding site selection by RNA polymerase II TAFs: a TAF(II)250-TAF(II)150 complex recognizes the initiator. EMBO J. *18*, 4835–4845.

Chambers, A., Tsang, J.S., Stanway, C., Kingsman, A.J., and Kingsman, S.M. (1989). Transcriptional control of the Saccharomyces cerevisiae PGK gene by RAP1. Mol. Cell. Biol. *9*, 5516–5524.

Chambers, A., Packham, E.A., and Graham, I.R. (1995). Control of glycolytic gene expression in the budding yeast (Saccharomyces cerevisiae). Curr. Genet. *29*, 1–9.

Chan, S.S.-K., and Kyba, M. (2013). What is a Master Regulator? J. Stem Cell Res. Ther. *3*.

Chandrasekharan, M.B., Huang, F., and Sun, Z.-W. (2009). Ubiquitination of histone H2B regulates chromatin dynamics by enhancing nucleosome stability. Proc. Natl. Acad. Sci. U. S. A. *106*, 16686–16691.

Chang, J., Kim, D.-H., Lee, S.W., Choi, K.Y., and Sung, Y.C. (1995). Transactivation ability of p53 transcriptional activation domain is directly related to the binding affinity to TATA-binding protein. J. Biol. Chem. *270*, 25014–25019.

Chatterjee, S., and Struhl, K. (1995). Connecting a promoter-bound protein to TBP bypasses the need for a transcriptional activation domain. Nature *374*, 820–822.

Chen, J.-L., Attardi, L., Verrijzer, C.P., Yokomori, K., and Tjian, R. (1994). Assembly of Recombinant TFIID Reveals Differential Coactivator Requirements for Distinct Transcriptional Activators. Cell *79*, 93–105.

Chen, W.-Y., Zhang, J., Geng, H., Du, Z., Nakadai, T., and Roeder, R.G. (2013). A TAF4 coactivator function for E proteins that involves enhanced TFIID binding. Genes Dev. *27*, 1596–1609.

Chen, Y., Rai, R., Zhou, Z.-R., Kanoh, J., Ribeyre, C., Yang, Y., Zheng, H., Damay, P., Wang, F., Tsujii, H., et al. (2011). A conserved motif within RAP1 has diversified roles in telomere protection and regulation in different organisms. Nat. Struct. Mol. Biol. *18*, 213–221.

Cheng, J.X., Floer, M., Ononaji, P., Bryant, G., and Ptashne, M. (2002). Responses of four yeast genes to changes in the transcriptional machinery are determined by their promoters. Curr. Biol. CB *12*, 1828–1832.

Chi, T., and Carey, M. (1996). Assembly of the isomerized TFIIA--TFIID--TATA ternary complex is necessary and sufficient for gene activation. Genes Dev. *10*, 2540–2550.

Chiang, Y.-C., Komarnitsky, P., Chase, D., and Denis, C.L. (1996). ADR1 Activation Domains Contact the Histone Acetyltransferase GCN5 and the Core Transcriptional Factor TFIIB. J. Biol. Chem. *271*, 32359–32365.

Cho, E.-J., Takagi, T., Moore, C.R., and Buratowski, S. (1997). mRNA capping enzyme is recruited to the transcription complex by phosphorylation of the RNA polymerase II carboxy-terminal domain. Genes Dev. *11*, 3319–3326.

Cho, E.J., Kobor, M.S., Kim, M., Greenblatt, J., and Buratowski, S. (2001). Opposing effects of Ctk1 kinase and Fcp1 phosphatase at Ser 2 of the RNA polymerase II C-terminal domain. Genes Dev. *15*, 3319–3329.

Choder, M., Bratosin, S., and Aloni, Y. (1984). A direct analysis of transcribed minichromosomes: all transcribed SV40 minichromosomes have a nuclease-hypersensitive region within a nucleosome-free domain. EMBO J. *3*, 2929–2936.

Chow, J., and Dennis, P.P. (1994). Coupling between mRNA synthesis and mRNA stability in Eschericia coli. Mol. Microbiol. *11*, 919–931.

Chu, S.W., Noyes, M.B., Christensen, R.G., Pierce, B.G., Zhu, L.J., Weng, Z., Stormo, G.D., and Wolfe, S.A. (2012). Exploring the DNA-recognition potential of homeodomains. Genome Res. *22*, 1889–1898.

Cianfrocco, M.A., Kassavetis, G.A., Grob, P., Fang, J., Juven-Gershon, T., Kadonaga, J.T., and Nogales, E. (2013). Human TFIID binds to core promoter DNA in a reorganized structural state. Cell *152*, 120–131.

Cirillo, L.A., McPherson, C.E., Bossard, P., Stevens, K., Cherian, S., Shim, E.Y., Clark, K.L., Burley, S.K., and Zaret, K.S. (1998). Binding of the winged-helix transcription factor HNF3 to a linker histone site on the nucleosome. EMBO J. *17*, 244–254.

Cirillo, L.A., Lin, F.R., Cuesta, I., Friedman, D., Jarnik, M., and Zaret, K.S. (2002). Opening of Compacted Chromatin by Early Developmental Transcription Factors HNF3 (FoxA) and GATA-4. Mol. Cell *9*, 279–289.

Coleman, R.A., Qiao, Z., Singh, S.K., Peng, C.S., Cianfrocco, M., Zhang, Z., Piasecka, A., Aldeborgh, H., Basishvili, G., and Liu, W.L. (2017). p53 dynamically directs TFIID assembly on target gene promoters. Mol. Cell. Biol. MCB.00085-17.

Conaway, J.W., Shilatifard, A., Dvir, A., and Conaway, R.C. (2000). Control of elongation by RNA polymerase II. Trends Biochem. Sci. *25*, 375–380.

Consortium, I.H.G.S., and others (2004). Finishing the euchromatic sequence of the human genome. Nature *431*, 931–945.

Corden, J.L., Cadena, D.L., Ahearn, J.M., and Dahmus, M.E. (1985). A unique structure at the carboxyl terminus of the largest subunit of eukaryotic RNA polymerase II. Proc. Natl. Acad. Sci. *82*, 7934–7938.

Cramer, P., Bushnell, D.A., and Kornberg, R.D. (2001). Structural Basis of Transcription: RNA Polymerase II at 2.8 Ångstrom Resolution. Science *292*, 1863–1876.

Cress, W.D., and Triezenberg, S.J. (1991). Critical Structural Elements of the VP16 Transcriptional Activation Domain. Science *251*, 87–90.

Crick, F. (1970). Central dogma of molecular biology. Nature *227*, 561–563.

Crowley, T.E., Hoey, T., Liu, J.-K., Jan, Y.N., Jan, L.Y., and Tjian, R. (1993). A new factor related to TATA-binding protein has highly restricted expression patterns in Drosophila. Nature *361*, 557–561.

Dabrowski, S., and Kur, J. (1998). Cloning and expression in Escherichia coli of the recombinant his-tagged DNA polymerases from Pyrococcus furiosus and Pyrococcus woesei. Protein Expr. Purif. *14*, 131–138.

D'Alessio, J.A., Wright, K.J., and Tjian, R. (2009). Shifting Players and Paradigms in Cell-Specific Transcription. Mol. Cell *36*, 924–931.

Daugherty, P.S., Chen, G., Iverson, B.L., and Georgiou, G. (2000). Quantitative analysis of the effect of the mutation frequency on the affinity maturation of single chain Fv antibodies. Proc. Natl. Acad. Sci. U. S. A. *97*, 2029–2034.

Davis, R.L., Weintraub, H., and Lassar, A.B. (1987). Expression of a single transfected cDNA converts fibroblasts to myoblasts. Cell *51*, 987–1000.

Deato, M.D.E., and Tjian, R. (2007). Switching of the core transcription machinery during myogenesis. Genes Amp Dev. *21*, 2137–2149.

Deato, M.D.E., Marr, M.T., Sottero, T., Inouye, C., Hu, P., and Tjian, R. (2008). MyoD Targets TAF3/TRF3 to Activate Myogenin Transcription. Mol. Cell *32*, 96–105.

Deng, Z., Chen, C.-J., Zerby, D., Delecluse, H.-J., and Lieberman, P.M. (2001). Identification of Acidic and Aromatic Residues in the Zta Activation Domain Essential for Epstein-Barr Virus Reactivation. J. Virol. *75*, 10334–10347.

Dikstein, R., Zhou, S., and Tjian, R. (1996). Human TAFII105 Is a Cell Type-Specific TFIID Subunit Related to hTAFII130. Cell *87*, 137–146.

Djebali, S., Davis, C.A., Merkel, A., Dobin, A., Lassmann, T., Mortazavi, A., Tanzer, A., Lagarde, J., Lin, W., Schlesinger, F., et al. (2012). Landscape of transcription in human cells. Nature *489*, 101–108.

Dove, S.L., and Hochschild, A. (1998). Conversion of the ω subunit of Escherichia coli RNA polymerase into a transcriptional activator or an activation target. Genes Dev. *12*, 745–754.

Dover, J., Schneider, J., Tawiah-Boateng, M.A., Wood, A., Dean, K., Johnston, M., and Shilatifard, A. (2002). Methylation of Histone H3 by COMPASS Requires Ubiquitination of Histone H2B by Rad6. J. Biol. Chem. *277*, 28368–28371.

Dower, W.J., Miller, J.F., and Ragsdale, C.W. (1988). High efficiency transformation of E. coli by high voltage electroporation. Nucleic Acids Res. *16*, 6127–6145.

Drysdale, C.M., Dueñas, E., Jackson, B.M., Reusser, U., Braus, G.H., and Hinnebusch, A.G. (1995). The transcriptional activator GCN4 contains multiple activation domains that are critically dependent on hydrophobic amino acids. Mol. Cell. Biol. *15*, 1220–1233.

Duffy, E.E., Rutenberg-Schoenberg, M., Stark, C.D., Kitchen, R.R., Gerstein, M.B., and Simon, M.D. (2015). Tracking Distinct RNA Populations Using Efficient and Reversible Covalent Chemistry. Mol. Cell *59*, 858–866.

Durso, R.J., Fisher, A.K., Albright-Frey, T.J., and Reese, J.C. (2001). Analysis of TAF90 mutants displaying allele-specific and broad defects in transcription. Mol. Cell. Biol. *21*, 7331–7344.

Dynlacht, B.D., Hoey, T., and Tjian, R. (1991). Isolation of coactivators associated with the TATA-binding protein that mediate transcriptional activation. Cell *66*, 563–576.

Ebmeier, C.C., and Taatjes, D.J. (2010). Activator-Mediator binding regulates Mediator-cofactor interactions. Proc. Natl. Acad. Sci. U. S. A. *107*, 11283–11288.

Edwards, A.M., Darst, S.A., Feaver, W.J., Thompson, N.E., Burgess, R.R., and Kornberg, R.D. (1990). Purification and lipid-layer crystallization of yeast RNA polymerase II. Proc. Natl. Acad. Sci. *87*, 2122–2126.

El Kaderi, B., Medler, S., Raghunayakula, S., and Ansari, A. (2009). Gene Looping Is Conferred by Activator-dependent Interaction of Transcription Initiation and Termination Machineries. J. Biol. Chem. *284*, 25015–25025.

Emami, K.H., Jain, A., and Smale, S.T. (1997). Mechanism of synergy between TATA and initiator: synergistic binding of TFIID following a putative TFIIA-induced isomerization. Genes Dev. *11*, 3007–3019.

ENCODE Project Consortium (2012). An integrated encyclopedia of DNA elements in the human genome. Nature *489*, 57–74.

Feaver, W.J., Henry, N.L., Bushnell, D.A., Sayre, M.H., Brickner, J.H., Gileadi, O., and Kornberg, R.D. (1994). Yeast TFIIE. Cloning, expression, and homology to vertebrate proteins. J. Biol. Chem. *269*, 27549–27553.

Feaver, W.J., Henry, N.L., Wang, Z., Wu, X., Svejstrup, J.Q., Bushnell, D.A., Friedberg, E.C., and Kornberg, R.D. (1997). Genes for Tfb2, Tfb3, and Tfb4 subunits of yeast transcription/repair factor IIH. Homology to human cyclin-dependent kinase activating kinase and IIH subunits. J. Biol. Chem. *272*, 19319–19327.

Feeser, E.A., and Wolberger, C. (2008). Structural and functional studies of the Rap1 C-terminus reveal novel separation-of-function mutants. J. Mol. Biol. *380*, 520–531.

Feigerle, J.T., and Weil, P.A. (2016). The C Terminus of the RNA Polymerase II Transcription Factor IID (TFIID) Subunit Taf2 Mediates Stable Association of Subunit Taf14 into the Yeast TFIID Complex. J. Biol. Chem. *291*, 22721–22740.

Fishburn, J., Mohibullah, N., and Hahn, S. (2005). Function of a eukaryotic transcription activator during the transcription cycle. Mol. Cell *18*, 369–378.

Flores, O., Maldonado, E., and Reinberg, D. (1989). Factors involved in specific transcription by mammalian RNA polymerase II. Factors IIE and IIF independently interact with RNA polymerase II. J. Biol. Chem. *264*, 8913–8921.

Flores, O., Lu, H., Killeen, M., Greenblatt, J., Burton, Z.F., and Reinberg, D. (1991). The small subunit of transcription factor IIF recruits RNA polymerase II into the preinitiation complex. Proc. Natl. Acad. Sci. U. S. A. *88*, 9999–10003.

Fong, Y.W., Cattoglio, C., Yamaguchi, T., and Tjian, R. (2012). Transcriptional Regulation by Coactivators in Embryonic Stem Cells. Trends Cell Biol. *22*, 292–298.

Fox, T.D., Losick, R., and Pero, J. (1976). Regulatory gene 28 of bacteriophage SPO1 codes for a phage-induced subunit of RNA polymerase. J. Mol. Biol. *101*, 427–433.

Fraenkel, E., Rould, M.A., Chambers, K.A., and Pabo, C.O. (1998). Engrailed homeodomain-DNA complex at 2.2 A resolution: a detailed view of the interface and comparison with other engrailed structures. J. Mol. Biol. *284*, 351–361.

Freeman, K., Gwadz, M., and Shore, D. (1995). Molecular and genetic analysis of the toxic effect of RAP1 overexpression in yeast. Genetics *141*, 1253–1262.

Ganapathi, M., Palumbo, M.J., Ansari, S.A., He, Q., Tsui, K., Nislow, C., and Morse, R.H. (2011). Extensive role of the general regulatory factors, Abf1 and Rap1, in determining genome-wide chromatin structure in budding yeast. Nucleic Acids Res. *39*, 2032–2044.

Gangloff, Y.G., Sanders, S.L., Romier, C., Kirschner, D., Weil, P.A., Tora, L., and Davidson, I. (2001). Histone folds mediate selective heterodimerization of yeast TAF(II)25 with TFIID components yTAF(II)47 and yTAF(II)65 and with SAGA component ySPT7. Mol. Cell. Biol. *21*, 1841–1853.

Garbett, K.A., Tripathi, M.K., Cencki, B., Layer, J.H., and Weil, P.A. (2007). Yeast TFIID Serves as a Coactivator for Rap1p by Direct Protein-Protein Interaction. Mol. Cell. Biol. *27*, 297–311.

Geiger, J.H., Hahn, S., Lee, S., and Sigler, P.B. (1996). Crystal Structure of the Yeast TFIIA/TBP/DNA Complex. Science *272*, 830–836.

Geles, K.G., Freiman, R.N., Liu, W.-L., Zheng, S., Voronina, E., and Tjian, R. (2006). Cell-type-selective induction of c-jun by TAF4b directs ovarian-specific transcription networks. Proc. Natl. Acad. Sci. U. S. A. *103*, 2594–2599.

Gentry, D.R., and Burgess, R.R. (1989). rpoZ, encoding the omega subunit of Escherichia coli RNA polymerase, is in the same operon as spoT. J. Bacteriol. *171*, 1271–1277.

Ghazy, M.A., Brodie, S.A., Ammerman, M.L., Ziegler, L.M., and Ponticelli, A.S. (2004). Amino acid substitutions in yeast TFIIF confer upstream shifts in transcription initiation and altered interaction with RNA polymerase II. Mol. Cell. Biol. *24*, 10975–10985.

Gietz, R.D., and Schiestl, R.H. (2007). High-efficiency yeast transformation using the LiAc/SS carrier DNA/PEG method. Nat. Protoc. *2*, 31–34.

Gileadi, O., Feaver, W.J., and Kornberg, R.D. (1992). Cloning of a subunit of yeast RNA polymerase II transcription factor b and CTD kinase. Science *257*, 1389–1392.

Gill, G., Pascal, E., Tseng, Z.H., and Tjian, R. (1994). A glutamine-rich hydrophobic patch in transcription factor Sp1 contacts the dTAFII110 component of the Drosophila TFIID complex and mediates transcriptional activation. Proc. Natl. Acad. Sci. *91*, 192–196.

Gilmour, D.S., and Lis, J.T. (1986). RNA polymerase II interacts with the promoter region of the noninduced hsp70 gene in Drosophila melanogaster cells. Mol. Cell. Biol. *6*, 3984–3989.

Goffeau, A., Barrell, B.G., Bussey, R., Davis, R.W., Dujon, H., Feldmann, H., Galibert, F., Hoheisel, J.D., Jacq, C., Johnston, M., et al. (1996). Life with 6000 genes. Science *274*, 563–567.

Golub, E.I. (1988). "One minute" transformation of competent E. coli by plasmid DNA. Nucleic Acids Res. *16*, 1641.

Gordân, R., Shen, N., Dror, I., Zhou, T., Horton, J., Rohs, R., and Bulyk, M.L. (2013). Genomic regions flanking E-box binding sites influence DNA binding specificity of bHLH transcription factors through DNA shape. Cell Rep. *3*, 1093–1104.

Graham, I.R., Haw, R.A., Spink, K.G., Halden, K.A., and Chambers, A. (1999). In vivo analysis of functional regions within yeast Rap1p. Mol. Cell. Biol. *19*, 7481–7490.

Grant, P.A., Duggan, L., Côté, J., Roberts, S.M., Brownell, J.E., Candau, R., Ohba, R., Owen-Hughes, T., Allis, C.D., Winston, F., et al. (1997). Yeast Gcn5 functions in two multisubunit complexes to acetylate nucleosomal histones: characterization of an Ada complex and the SAGA (Spt/Ada) complex. Genes Dev. *11*, 1640–1650.

Green, M.R. (2005). Eukaryotic Transcription Activation: Right on Target. Mol. Cell *18*, 399–402.

Gregory, B.D., Nickels, B.E., Darst, S.A., and Hochschild, A. (2005). An altered-specificity DNA-binding mutant of Escherichia coliσ70 facilitates the analysis of σ70 function in vivo: An altered-specificity mutant of σ70. Mol. Microbiol. *56*, 1208–1219.

Gregory, P.D., Schmid, A., Zavari, M., Münsterkötter, M., and Hörz, W. (1999). Chromatin remodelling at the PHO8 promoter requires SWI-SNF and SAGA at a step subsequent to activator binding. EMBO J. *18*, 6407–6414.

Gulyas, K.D., and Donahue, T.F. (1992). SSL2, a suppressor of a stem-loop mutation in the HIS4 leader encodes the yeast homolog of human ERCC-3. Cell *69*, 1031–1042.

Gupta, A., Christensen, R.G., Rayla, A.L., Lakshmanan, A., Stormo, G.D., and Wolfe, S.A. (2012). An optimized two-finger archive for ZFN-mediated gene targeting. Nat. Methods *9*, 588–590.

Guzder, S.N., Sung, P., Bailly, V., Prakash, L., and Prakash, S. (1994). RAD25 is a DMA helicase required for DNA repair and RNA polymerase II transcription. Nature *369*, 578–581.

Ha, I., Roberts, S., Maldonado, E., Sun, X., Kim, L.U., Green, M., and Reinberg, D. (1993). Multiple functional domains of human transcription factor IIB: distinct interactions with two general transcription factors and RNA polymerase II. Genes Dev. *7*, 1021–1032.

Haag, J.R., and Pikaard, C.S. (2011). Multisubunit RNA polymerases IV and V: purveyors of non-coding RNA for plant gene silencing. Nat. Rev. Mol. Cell Biol. *12*, 483–492.

Hahn, S. (2004). Structure and mechanism of the RNA polymerase II transcription machinery. Nat. Struct. Mol. Biol. *11*, 394.

Hahn, S., and Young, E.T. (2011). Transcriptional Regulation in Saccharomyces cerevisiae: Transcription Factor Regulation and Function, Mechanisms of Initiation, and Roles of Activators and Coactivators. Genetics *189*, 705–736.

Hahn, S., Buratowski, S., Sharp, P.A., and Guarente, L. (1989). Isolation of the gene encoding the yeast TATA binding protein TFIID: a gene identical to the SPT15 suppressor of Ty element insertions. Cell *58*, 1173–1181.

Haimovich, G., Medina, D.A., Causse, S.Z., Garber, M., Millán-Zambrano, G., Barkai, O., Chávez, S., Pérez-Ortín, J.E., Darzacq, X., and Choder, M. (2013). Gene Expression Is Circular: Factors for mRNA Degradation Also Foster mRNA Synthesis. Cell *153*, 1000–1011.

Haldenwang, W.G., Lang, N., and Losick, R. (1981). A sporulation-induced sigma-like regulatory protein from B. subtilis. Cell *23*, 615–624.

Hall, D.B., Wade, J.T., and Struhl, K. (2006). An HMG Protein, Hmo1, Associates with Promoters of Many Ribosomal Protein Genes and throughout the rRNA Gene Locus in Saccharomyces cerevisiae. Mol. Cell. Biol. *26*, 3672–3679.

Han, M., and Grunstein, M. (1988). Nucleosome loss activates yeast downstream promoters in vivo. Cell *55*, 1137–1145.

Hanahan, D. (1983). Studies on transformation of Escherichia coli with plasmids. J. Mol. Biol. *166*, 557–580.

Hardy, C.F., Balderes, D., and Shore, D. (1992a). Dissection of a carboxy-terminal region of the yeast regulatory protein RAP1 with effects on both transcriptional activation and silencing. Mol. Cell. Biol. *12*, 1209–1217.

Hardy, C.F., Sussel, L., and Shore, D. (1992b). A RAP1-interacting protein involved in transcriptional silencing and telomere length regulation. Genes Dev. *6*, 801–814.

Hastings, P.J., McGill, C., Shafer, B., and Strathern, J.N. (1993). Ends-in Vs. Ends-Out Recombination in Yeast. Genetics *135*, 973–980.

He, Y., Yan, C., Fang, J., Inouye, C., Tjian, R., Ivanov, I., and Nogales, E. (2016). Near-atomic resolution visualization of human transcription promoter opening. Nature *533*, 359–365.

Heckman, K.L., and Pease, L.R. (2007). Gene splicing and mutagenesis by PCR-driven overlap extension. Nat. Protoc. *2*, 924–932.

Hengartner, C.J., Myer, V.E., Liao, S.-M., Wilson, C.J., Koh, S.S., and Young, R.A. (1998). Temporal regulation of RNA polymerase II by Srb10 and Kin28 cyclin-dependent kinases. Mol. Cell *2*, 43–53.

Henry, N.L., Sayre, M.H., and Kornberg, R.D. (1992). Purification and characterization of yeast RNA polymerase II general initiation factor g. J. Biol. Chem. *267*, 23388–23392.

Henry, N.L., Campbell, A.M., Feaver, W.J., Poon, D., Weil, P.A., and Kornberg, R.D. (1994). TFIIF-TAF-RNA polymerase II connection. Genes Dev. *8*, 2868–2878.

Henry, Y.A.L., Chambers, A., Tsang, J.S.H., Kingsman, A.J., and Kingsman, S.M. (1990). Characterisation of the DNA binding domain of the yeast RAP1 protein. Nucleic Acids Res. *18*, 2617–2623.

Herbig, E., Warfield, L., Fish, L., Fishburn, J., Knutson, B.A., Moorefield, B., Pacheco, D., and Hahn, S. (2010). Mechanism of Mediator Recruitment by Tandem Gcn4 Activation Domains and Three Gal11 Activator-Binding Domains. Mol. Cell. Biol. *30*, 2376–2390.

Higgins, D.R., Prakash, S., Reynolds, P., Polakowska, R., Weber, S., and Prakash, L. (1983). Isolation and characterization of the RAD3 gene of Saccharomyces cerevisiae and inviability of rad3 deletion mutants. Proc. Natl. Acad. Sci. *80*, 5680–5684.

Hiller, M. (2004). Testis-specific TAF homologs collaborate to control a tissue-specific transcription program. Development *131*, 5297–5308.

Hisatake, K., Ohta, T., Takada, R., Guermah, M., Horikoshi, M., Nakatani, Y., and Roeder, R.G. (1995). Evolutionary conservation of human TATA-binding-polypeptide-associated factors

TAFII31 and TAFII80 and interactions of TAFII80 with other TAFs and with general transcription factors. Proc. Natl. Acad. Sci. U. S. A. *92*, 8195–8199.

Hofmann, J.F., Laroche, T., Brand, A.H., and Gasser, S.M. (1989). RAP-1 factor is necessary for DNA loop formation in vitro at the silent mating type locus HML. Cell *57*, 725–737.

Hogues, H., Lavoie, H., Sellam, A., Mangos, M., Roemer, T., Purisima, E., Nantel, A., and Whiteway, M. (2008). Transcription factor substitution during the evolution of fungal ribosome regulation. Mol. Cell *29*, 552–562.

Holstege, F.C., van der Vliet, P.C., and Timmers, H.T. (1996). Opening of an RNA polymerase II promoter occurs in two distinct steps and requires the basal transcription factors IIE and IIH. EMBO J. *15*, 1666–1677.

Holstege, F.C., Fiedler, U., and Timmers, H.T.M. (1997). Three transitions in the RNA polymerase II transcription complex during initiation. EMBO J. *16*, 7468–7480.

Holstege, F.C., Jennings, E.G., Wyrick, J.J., Lee, T.I., Hengartner, C.J., Green, M.R., Golub, T.R., Lander, E.S., and Young, R.A. (1998). Dissecting the regulatory circuitry of a eukaryotic genome. Cell *95*, 717–728.

Hsin, J.-P., and Manley, J.L. (2012). The RNA polymerase II CTD coordinates transcription and RNA processing. Genes Dev. *26*, 2119–2137.

Huet, J., Cottrelle, P., Cool, M., Vignais, M.L., Thiele, D., Marck, C., Buhler, J.M., Sentenac, A., and Fromageot, P. (1985). A general upstream binding factor for genes of the yeast translational apparatus. EMBO J. *4*, 3539.

Huisinga, K.L., and Pugh, B.F. (2004). A genome-wide housekeeping role for TFIID and a highly regulated stress-related role for SAGA in Saccharomyces cerevisiae. Mol. Cell *13*, 573–585.

Hwang, W.W., Venkatasubrahmanyam, S., Ianculescu, A.G., Tong, A., Boone, C., and Madhani, H.D. (2003). A conserved RING finger protein required for histone H2B monoubiquitination and cell size control. Mol. Cell *11*, 261–266.

Idrissi, F.-Z., Fernández-Larrea, J.B., and Piñ, B. (1998). Structural and functional heterogeneity of Rap1p complexes with telomeric and UASrpg-like DNA sequences. J. Mol. Biol. *284*, 925–935.

Idrissi, F.-Z., Garcia-Reyero, N., Fernandez-Larrea, J.B., and Pina, B. (2001). Alternative Mechanisms of Transcriptional Activation by Rap1p. J. Biol. Chem. *276*, 26090–26098.

Imbalzano, A.N., Zaret, K.S., and Kingston, R.E. (1994). Transcription Factor (TF) IIB and TFIIA Can Independently Increase the Affinity of the TATA-binding Protein for DNA. J. Biol. Chem. *269*, 8280–8286.

Iñiguez-Lluhí, J.A., Lou, D.Y., and Yamamoto, K.R. (1997). Three amino acid substitutions selectively disrupt the activation but not the repression function of the glucocorticoid receptor N terminus. J. Biol. Chem. *272*, 4149–4156.

Inostroza, J., Flores, O., and Reinberg, D. (1991). Factors involved in specific transcription by mammalian RNA polymerase II. Purification and functional analysis of general transcription factor IIE. J. Biol. Chem. *266*, 9304–9308.

Inoue, H., Nojima, H., and Okayama, H. (1990). High efficiency transformation of Escherichia coli with plasmids. Gene *96*, 23–28.

Irvin, J.D., and Pugh, B.F. (2006). Genome-wide Transcriptional Dependence on TAF1 Functional Domains. J. Biol. Chem. *281*, 6404–6412.

Jacob, F., and Monod, J. (1961). Genetic Regulatory Mechanisms in the Synthesis or Proteins. J. Mol. Biol. *3*, 318–356.

Jakobovits, E.B., Bratosin, S., and Aloni, Y. (1980). A nucleosome-free region in SV40 minichromosomes. Nature *285*, 263–265.

Jedidi, I., Zhang, F., Qiu, H., Stahl, S.J., Palmer, I., Kaufman, J.D., Nadaud, P.S., Mukherjee, S., Wingfield, P.T., Jaroniec, C.P., et al. (2010). Activator Gcn4 Employs Multiple Segments of Med15/Gal11, Including the KIX Domain, to Recruit Mediator to Target Genes in Vivo. J. Biol. Chem. *285*, 2438–2455.

Jiang, L., Althoff, E.A., Clemente, F.R., Doyle, L., Röthlisberger, D., Zanghellini, A., Gallaher, J.L., Betker, J.L., Tanaka, F., Barbas, C.F., et al. (2008). De novo computational design of retro-aldol enzymes. Science *319*, 1387–1391.

Johnson, A.N., and Weil, P.A. (2017). Identification of a transcriptional activation domain in yeast repressor activator protein 1 (Rap1) using an altered DNA-binding specificity variant. J. Biol. Chem. *292*, 5705–5723.

Jolma, A., Yan, J., Whitington, T., Toivonen, J., Nitta, K.R., Rastas, P., Morgunova, E., Enge, M., Taipale, M., Wei, G., et al. (2013). DNA-Binding Specificities of Human Transcription Factors. Cell *152*, 327–339.

Jonker, H.R.A., Wechselberger, R.W., Boelens, R., Folkers, G.E., and Kaptein, R. (2005). Structural properties of the promiscuous VP16 activation domain. Biochemistry (Mosc.) *44*, 827–839.

Kadonaga, J.T. (2012). Perspectives on the RNA polymerase II core promoter. Wiley Interdiscip. Rev. Dev. Biol. *1*, 40–51.

Kadosh, D., and Struhl, K. (1998). Histone deacetylase activity of Rpd3 is important for transcriptional repression in vivo. Genes Dev. *12*, 797–805.

Kalderon, D., Roberts, B.L., Richardson, W.D., and Smith, A.E. (1984). A short amino acid sequence able to specifiy nuclear location. Cell *39*, 499–509.

Kasahara, K., Ohtsuki, K., Ki, S., Aoyama, K., Takahashi, H., Kobayashi, T., Shirahige, K., and Kokubo, T. (2007a). Assembly of Regulatory Factors on rRNA and Ribosomal Protein Genes in Saccharomyces cerevisiae. Mol. Cell. Biol. *27*, 6686–6705.

Kasahara, K., Ki, S., Aoyama, K., Takahashi, H., and Kokubo, T. (2007b). Saccharomyces cerevisiae HMO1 interacts with TFIID and participates in start site selection by RNA polymerase II. Nucleic Acids Res. *36*, 1343–1357.

Keaveney, M., and Struhl, K. (1998). Activator-Mediated Recruitment of the RNA Polymerase II Machinery Is the Predominant Mechanism for Transcriptional Activation in Yeast. Mol. Cell *1*, 917–924.

Keegan, L., Gill, G., and Ptashne, M. (1986). Separation of DNA binding from the transcription-activating function of a eukaryotic regulatory protein. Science *231*, 699–704.

Keogh, M.-C., Podolny, V., and Buratowski, S. (2003). Bur1 kinase is required for efficient transcription elongation by RNA polymerase II. Mol. Cell. Biol. *23*, 7005–7018.

Keogh, M.-C., Kurdistani, S.K., Morris, S.A., Ahn, S.H., Podolny, V., Collins, S.R., Schuldiner, M., Chin, K., Punna, T., Thompson, N.J., et al. (2005). Cotranscriptional set2 methylation of histone H3 lysine 36 recruits a repressive Rpd3 complex. Cell *123*, 593–605.

Killeen, M., Coulombe, B., and Greenblatt, J. (1992). Recombinant TBP, Transcription Factor IIB and RAP30 Are Sufficient for Promoter Recognition by Mammalian RNA Polymerase II. J. Biol. Chem. *267*, 9463–9466.

Kim, J., Tzamarias, D., Ellenberger, T., Harrison, S.C., and Struhl, K. (1993). Adaptability at the protein-DNA interface is an important aspect of sequence recognition by bZIP proteins. Proc. Natl. Acad. Sci. *90*, 4513–4517.

Kizer, K.O., Phatnani, H.P., Shibata, Y., Hall, H., Greenleaf, A.L., and Strahl, B.D. (2005). A novel domain in Set2 mediates RNA polymerase II interaction and couples histone H3 K36 methylation with transcript elongation. Mol. Cell. Biol. *25*, 3305–3316.

Klages, N., and Strubin, M. (1995). Stimulation of RNA polymerase II transcription initiation by recruitment of TBP in vivo. Nature *374*, 822–823.

Klebanow, E.R., Poon, D., Zhou, S., and Weil, P.A. (1996). Isolation and characterization of TAF25, an essential yeast gene that encodes an RNA polymerase II-specific TATA-binding protein-associated factor. J. Biol. Chem. *271*, 13706–13715.

Klebanow, E.R., Poon, D., Zhou, S., and Weil, P.A. (1997). Cloning and characterization of an essential Saccharomyces cerevisiae gene, TAF40, which encodes yTAFII40, an RNA

polymerase II-specific TATA-binding protein-associated factor. J. Biol. Chem. *272*, 9436–9442.

Klein, C., and Struhl, K. (1994a). Increased recruitment of TATA-binding protein to the promoter by transcriptional activation domains in vivo. Science *266*, 280–282.

Klein, C., and Struhl, K. (1994b). Protein kinase A mediates growth-regulated expression of yeast ribosomal protein genes by modulating RAP1 transcriptional activity. Mol. Cell. Biol. *14*, 1920–1928.

Knight, B., Kubik, S., Ghosh, B., Bruzzone, M.J., Geertz, M., Martin, V., Dénervaud, N., Jacquet, P., Ozkan, B., Rougemont, J., et al. (2014). Two distinct promoter architectures centered on dynamic nucleosomes control ribosomal protein gene transcription. Genes Dev. *28*, 1695–1709.

Kobayashi, N., Boyer, T.G., and Berk, A.J. (1995). A class of activation domains interacts directly with TFIIA and stimulates TFIIA-TFIID-promoter complex assembly. Mol. Cell. Biol. *15*, 6465–6473.

Koerber, R.T., Rhee, H.S., Jiang, C., and Pugh, B.F. (2009). Interaction of Transcriptional Regulators with Specific Nucleosomes across the Saccharomyces Genome. Mol. Cell *35*, 889–902.

Köhrer, K., and Domdey, H. (1991). Preparation of high molecular weight RNA. Methods Enzymol. *194*, 398–405.

Kokubo, T., Swanson, M.J., Nishikawa, J., Hinnebusch, A.G., and Nakatani, Y. (1998). The yeast TAF145 inhibitory domain and TFIIA competitively bind to TATA-binding protein. Mol. Cell. Biol. *18*, 1003–1012.

Koleske, A.J., and Young, R.A. (1994). An RNA polymerase II holoenzyme responsive to activators. Nature *368*, 466–469.

Kolodziej, P.A., Woychik, N., Liao, S.M., and Young, R.A. (1990). RNA polymerase II subunit composition, stoichiometry, and phosphorylation. Mol. Cell. Biol. *10*, 1915–1920.

Komarnitsky, P., Cho, E.-J., and Buratowski, S. (2000). Different phosphorylated forms of RNA polymerase II and associated mRNA processing factors during transcription. Genes Dev. *14*, 2452–2460.

König, P., Giraldo, R., Chapman, L., and Rhodes, D. (1996). The Crystal Structure of the DNA-Binding Domain of Yeast RAP1 in Complex with Telomeric DNA. Cell *85*, 125–136.

Kornberg, R.D. (1974). Chromatin Structure: A Repeating Unit of Histones and DNA. Science *184*, 868–871.

Kotani, T., Miyake, T., Tsukihashi, Y., Hinnebusch, A.G., Nakatani, Y., Kawaichi, M., and Kokubo, T. (1998). Identification of highly conserved amino-terminal segments of dTAFII230 and yTAFII145 that are functionally interchangeable for inhibiting TBP-DNA interactions in vitro and in promoting yeast cell growth in vivo. J. Biol. Chem. *273*, 32254–32264.

Kries, H., Blomberg, R., and Hilvert, D. (2013). De novo enzymes by computational design. Curr. Opin. Chem. Biol. *17*, 221–228.

Krietenstein, N., Wal, M., Watanabe, S., Park, B., Peterson, C.L., Pugh, B.F., and Korber, P. (2016). Genomic Nucleosome Organization Reconstituted with Pure Proteins. Cell *167*, 709–721.e12.

Krishnamurthy, S., He, X., Reyes-Reyes, M., Moore, C., and Hampsey, M. (2004). Ssu72 Is an RNA polymerase II CTD phosphatase. Mol. Cell *14*, 387–394.

Krogan, N.J., Dover, J., Khorrami, S., Greenblatt, J.F., Schneider, J., Johnston, M., and Shilatifard, A. (2002). COMPASS, a histone H3 (Lysine 4) methyltransferase required for telomeric silencing of gene expression. J. Biol. Chem. *277*, 10753–10755.

Krogan, N.J., Kim, M., Tong, A., Golshani, A., Cagney, G., Canadien, V., Richards, D.P., Beattie, B.K., Emili, A., Boone, C., et al. (2003). Methylation of histone H3 by Set2 in Saccharomyces cerevisiae is linked to transcriptional elongation by RNA polymerase II. Mol. Cell. Biol. *23*, 4207–4218.

Krois, A.S., Ferreon, J.C., Martinez-Yamout, M.A., Dyson, H.J., and Wright, P.E. (2016). Recognition of the disordered p53 transactivation domain by the transcriptional adapter zinc finger domains of CREB-binding protein. Proc. Natl. Acad. Sci. *113*, E1853–E1862.

Kubik, S., Bruzzone, M.J., Jacquet, P., Falcone, J.-L., Rougemont, J., and Shore, D. (2015). Nucleosome Stability Distinguishes Two Different Promoter Types at All Protein-Coding Genes in Yeast. Mol. Cell *60*, 422–434.

Kunkel, G.R., and Martinson, H.G. (1981). Nucleosomes will not form on double-stranded RNa or over poly(dA).poly(dT) tracts in recombinant DNA. Nucleic Acids Res. *9*, 6869–6888.

Kuras, L., and Struhl, K. (1999). Binding of TBP to promoters in vivo is stimulated by activators and requires Pol II holoenzyme. Nature *399*, 609–613.

Kuras, L., Kosa, P., Mencia, M., and Struhl, K. (2000). TAF-Containing and TAF-Independent Forms of Transcriptionally Active TBP in Vivo. Science *288*, 1244–1248.

Kurtz, S., and Shore, D. (1991). RAP1 protein activates and silences transcription of mating-type genes in yeast. Genes Dev. *5*, 616–628.

Kushnirov, V.V. (2000). Rapid and reliable protein extraction from yeast. Yeast *16*, 857–860.

Kyrion, G., Boakye, K.A., and Lustig, A.J. (1992). C-terminal truncation of RAP1 results in the deregulation of telomere size, stability, and function in Saccharomyces cerevisiae. Mol. Cell. Biol. *12*, 5159–5173.

Lagrange, T., Kapanidis, A.N., Tang, H., Reinberg, D., and Ebright, R.H. (1998). New core promoter element in RNA polymerase II-dependent transcription: sequence-specific DNA binding by transcription factor IIB. Genes Dev. *12*, 34–44.

Längle-Rouault, F., and Jacobs, E. (1995). A method for performing precise alterations in the yeast genome using a recycable selectable marker. Nucleic Acids Res. *23*, 3079–3081.

Larschan, E., and Winston, F. (2001). The S. cerevisiae SAGA complex functions in vivo as a coactivator for transcriptional activation by Gal4. Genes Dev. *15*, 1946–1956.

Lascaris, R.F., Mager, W.H., and Planta, Rudi J. (1999). DNA-binding requirements of the yeast protein Rap1p as selected in silico from ribosomal protein gene promoter sequences. Bioinformations *15*, 267–277.

Lauberth, S.M., Nakayama, T., Wu, X., Ferris, A., Tang, Z., Hughes, S.H., and Roeder, R.G. (2013). H3K4me3 Interactions with TAF3 Regulate Preinitiation Complex Assembly and Selective Gene Activation. Cell *152*, 1021–1036.

Lavoie, H., Hogues, H., and Whiteway, M. (2009). Rearrangements of the transcriptional regulatory networks of metabolic pathways in fungi. Curr. Opin. Microbiol. *12*, 655–663.

Layer, J.H., and Weil, P.A. (2013). Direct TFIIA-TFIID Protein Contacts Drive Budding Yeast Ribosomal Protein Gene Transcription. J. Biol. Chem. *288*, 23273–23294.

Layer, J.H., Miller, S.G., and Weil, P.A. (2010). Direct Transactivator-Transcription Factor IID (TFIID) Contacts Drive Yeast Ribosomal Protein Gene Transcription. J. Biol. Chem. *285*, 15489–15499.

Leaver-Fay, A., Tyka, M., Lewis, S.M., Lange, O.F., Thompson, J., Jacak, R., Kaufman, K., Renfrew, P.D., Smith, C.A., Sheffler, W., et al. (2011). ROSETTA3: an object-oriented software suite for the simulation and design of macromolecules. Methods Enzymol. *487*, 545–574.

Lee, J.M., and Greenleaf, A.L. (1991). CTD kinase large subunit is encoded by CTK1, a gene required for normal growth of Saccharomyces cerevisiae. Gene Expr. *1*, 149–167.

Lempiäinen, H., and Shore, D. (2009). Growth control and ribosome biogenesis. Curr. Opin. Cell Biol. *21*, 855–863.

Leonard, D.A., Rajaram, N., and Kerppola, T.K. (1997). Structural basis of DNA bending and oriented heterodimer binding by the basic leucine zipper domains of Fos and Jun. Proc. Natl. Acad. Sci. *94*, 4913–4918.

Letovsky, J., and Dynan, W.S. (1989). Measurement of the binding of transcription factor Sp1 to a single GC box recognition sequence. Nucleic Acids Res. *17*, 2639–2653.

Leurent, C., Sanders, S., Ruhlmann, C., Mallouh, V., Weil, P.A., Kirschner, D.B., Tora, L., and Schultz, P. (2002). Mapping histone fold TAFs within yeast TFIID. EMBO J. *21*, 3424–3433.

Leurent, C., Sanders, S.L., Demény, M.A., Garbett, K.A., Ruhlmann, C., Weil, P.A., Tora, L., and Schultz, P. (2004). Mapping key functional sites within yeast TFIID. EMBO J. *23*, 719–727.

Leuther, K.K., Salmeron, J.M., and Johnston, S.A. (1993). Genetic evidence that an activation domain of GAL4 does not require acidity and may form a β sheet. Cell *72*, 575–585.

Levo, M., and Segal, E. (2014). In pursuit of design principles of regulatory sequences. Nat. Rev. Genet. *15*, 453–468.

Li, A.G., Piluso, L.G., Cai, X., Gadd, B.J., Ladurner, A.G., and Liu, X. (2007). An acetylation switch in p53 mediates holo-TFIID recruitment. Mol. Cell *28*, 408–421.

Li, W., Notani, D., and Rosenfeld, M.G. (2016). Enhancers as non-coding RNA transcription units: recent insights and future perspectives. Nat. Rev. Genet. *17*, 207–223.

Li, X.-Y., Bhaumik, S.R., and Green, M.R. (2000). Distinct classes of yeast promoters revealed by differential TAF recruitment. Science *288*, 1242–1244.

Li, X.-Y., Bhaumik, S.R., Zhu, X., Li, L., Shen, W.-C., Dixit, B.L., and Green, M.R. (2002). Selective recruitment of TAFs by yeast upstream activating sequences: implications for eukaryotic promoter structure. Curr. Biol. *12*, 1240–1244.

Li, Y., Flanagan, P., Tschochner, H., and Kornberg, R. (1994). RNA polymerase II initiation factor interactions and transcription start site selection. Science *263*, 805–807.

Lickwar, C.R., Mueller, F., Hanlon, S.E., McNally, J.G., and Lieb, J.D. (2012a). Genome-wide protein–DNA binding dynamics suggest a molecular clutch for transcription factor function. Nature *484*, 251–255.

Lickwar, C.R., Mueller, F., Hanlon, S.E., McNally, J.G., and Lieb, J.D. (2012b). Genome-wide protein–DNA binding dynamics suggest a molecular clutch for transcription factor function. Nature *484*, 251–255.

Lieb, J.D., Liu, X., Botstein, D., and Brown, P.O. (2001). Promoter-specific binding of Rap1 revealed by genome-wide maps of protein-DNA association. Nat. Genet. *28*, 327–334.

Lieberman, P. (1994). Identification of functional targets of the Zta transcriptional activator by formation of stable preinitiation complex intermediates. Mol. Cell. Biol. *14*, 8365–8375.

Lieberman, P.M., and Berk, A.J. (1994). A mechanism for TAFs in transcriptional activation: activation domain enhancement of TFIID-TFIIA–promoter DNA complex formation. Genes Dev. *8*, 995–1005.

Lieberman, P.M., Ozer, J., and Gürsel, D.B. (1997). Requirement for transcription factor IIA (TFIIA)-TFIID recruitment by an activator depends on promoter structure and template competition. Mol. Cell. Biol. *17*, 6624–6632.

Lim, C.Y., Santoso, B., Boulay, T., Dong, E., Ohler, U., and Kadonaga, J.T. (2004). The MTE, a new core promoter element for transcription by RNA polymerase II. Genes Dev. *18*, 1606–1617.

Lin, J., Chen, J., Elenbaas, B., and Levine, A.J. (1994). Several hydrophobic amino acids in the p53 amino-terminal domain are required for transcriptional activation, binding to mdm-2 and the adenovirus 5 E1B 55-kD protein. Genes Dev. *8*, 1235–1246.

Liu, F., and Posakony, J.W. (2012). Role of Architecture in the Function and Specificity of Two Notch-Regulated Transcriptional Enhancer Modules. PLoS Genet. *8*, e1002796.

Liu, W.-L., Coleman, R.A., Ma, E., Grob, P., Yang, J.L., Zhang, Y., Dailey, G., Nogales, E., and Tjian, R. (2009). Structures of three distinct activator-TFIID complexes. Genes Dev. *23*, 1510–1521.

López, M.C., Smerage, J.B., and Baker, H.V. (1998). Multiple domains of repressor activator protein 1 contribute to facilitated binding of glycolysis regulatory protein 1. Proc. Natl. Acad. Sci. U. S. A. *95*, 14112–14117.

Lorch, Y., and Kornberg, R.D. (2015). Chromatin-remodeling and the initiation of transcription. Q. Rev. Biophys. *48*, 465–470.

Lorch, Y., LaPointe, J.W., and Kornberg, R.D. (1987). Nucleosomes inhibit the initiation of transcription but allow chain elongation with the displacement of histones. Cell *49*, 203–210.

Louder, R.K., He, Y., López-Blanco, J.R., Fang, J., Chacón, P., and Nogales, E. (2016). Structure of promoter-bound TFIID and model of human pre-initiation complex assembly. Nature *531*, 604–609.

Lu, C., and Erickson, H.P. (1997). Expression in Escherichia coli of the thermostable DNA polymerase from Pyrococcus furiosus. Protein Expr. Purif. *11*, 179–184.

Lu, H., Zawel, L., Fisher, L., Egly, J.-M., and Reinberg, D. (1992). Human general transcription factor IIH phosphorylates the C-terminal domain of RNA polymerase II. Nature *358*, 641–645.

Luger, K., Mäder, A.W., Richmond, R.K., Sargent, D.F., and Richmond, T.J. (1997). Crystal structure of the nucleosome core particle at 2.8 Å resolution. Nature *389*, 251–260.

Ma, J., and Ptashne, M. (1987). Deletion analysis of GAL4 defines two transcriptional activating segments. Cell *48*, 847–853.

Mader, S, Kumar, V, de Verneuil, H, and Chambon, P (1989). Three amino acids of the oestrogen receptor are essential to its ability to distinguish an oestrogen from a glucocorticoid-responsive element. Nature *338*, 271–274.

Maldonado, E., Ha, I., Cortes, P., Weis, L., and Reinberg, D. (1990). Factors involved in specific transcription by mammalian RNA polymerase II: role of transcription factors IIA, IID, and IIB during formation of a transcription-competent complex. Mol. Cell. Biol. *10*, 6335–6347.

Malkowska, M., Kokoszynska, K., Rychlewski, L., and Wyrwicz, L. (2013). Structural bioinformatics of the general transcription factor TFIID. Biochimie *95*, 680–691.

Marion, R.M., Regev, A., Segal, E., Barash, Y., Koller, D., Friedman, N., and O'Shea, E.K. (2004). Sfp1 is a stress-and nutrient-sensitive regulator of ribosomal protein gene expression. Proc. Natl. Acad. Sci. U. S. A. *101*, 14315–14322.

Matangkasombut, O., Buratowski, R.M., Swilling, N.W., and Buratowski, S. (2000). Bromodomain factor 1 corresponds to a missing piece of yeast TFIID. Genes Dev. *14*, 951–962.

Matot, B., Le Bihan, Y.-V., Lescasse, R., Perez, J., Miron, S., David, G., Castaing, B., Weber, P., Raynal, B., Zinn-Justin, S., et al. (2012). The orientation of the C-terminal domain of the Saccharomyces cerevisiae Rap1 protein is determined by its binding to DNA. Nucleic Acids Res. *40*, 3197–3207.

Matsui, T., Segall, J., Weil, P.A., and Roeder, R.G. (1980). Multiple Factors Required for Accurate Initiation of Transcription by Purified RNA Polymerase II. J. Biol. Chem. *255*, 11992–11996.

Maxon, M.E., Goodrich, J.A., and Tjian, R. (1994). Transcription factor IIE binds preferentially to RNA polymerase IIa and recruits TFIIH: a model for promoter clearance. Genes Dev. *8*, 515–524.

McKenna, B., Guo, M., Reynolds, A., Hara, M., and Stein, R. (2015). Dynamic recruitment of functionally distinct Swi/Snf chromatin remodeling complexes modulates Pdx1 activity in islet β cells. Cell Rep. *10*, 2032–2042.

Mencía, M., Moqtaderi, Z., Geisberg, J.V., Kuras, L., and Struhl, K. (2002). Activator-specific recruitment of TFIID and regulation of ribosomal protein genes in yeast. Mol. Cell *9*, 823–833.

Meng, X., and Wolfe, S.A. (2006). Identifying DNA sequences recognized by a transcription factor using a bacterial one-hybrid system. Nat. Protoc. *1*, 30–45.

Meng, X., Brodsky, M.H., and Wolfe, S.A. (2005). A bacterial one-hybrid system for determining the DNA-binding specificity of transcription factors. Nat. Biotechnol. *23*, 988–994.

Meyer, K.D., Lin, S., Bernecky, C., Gao, Y., and Taatjes, D.J. (2010). p53 activates transcription by directing structural shifts in Mediator. Nat. Struct. Mol. Biol. *17*, 753–760.

Miller, T., Krogan, N.J., Dover, J., Erdjument-Bromage, H., Tempst, P., Johnston, M., Greenblatt, J.F., and Shilatifard, A. (2001). COMPASS: a complex of proteins associated with a trithorax-related SET domain protein. Proc. Natl. Acad. Sci. U. S. A. *98*, 12902–12907.

Minakhin, L., Bhagat, S., Brunning, A., Campbell, E.A., Darst, S.A., Ebright, R.H., and Severinov, K. (2001). Bacterial RNA polymerase subunit ω and eukaryotic RNA polymerase subunit RPB6 are sequence, structural, and functional homologs and promote RNA polymerase assembly. Proc. Natl. Acad. Sci. *98*, 892–897.

Mitchell, P.J., and Tjian, R. (1989). Transcriptional regulation in mammalian cells by sequence-specific DNA binding proteins. Science *244*, 371–378.

Mitchell, J.E., Zheng, D., Busby, S.J.W., and Minchin, S.D. (2003). Identification and analysis of 'extended –10' promoters in Escherichia coli. Nucleic Acids Res. *31*, 4689.

Miyake, T., Hu, Y.-F., David, S.Y., and Li, R. (2000). A functional comparison of BRCA1 C-terminal domains in transcription activation and chromatin remodeling. J. Biol. Chem. *275*, 40169–40173.

Mizuno, T., Kishimoto, T., Shinzato, T., Haw, R., Chambers, A., Wood, J., Sinclair, D., and Uemura, H. (2004). Role of the N-terminal region of Rap1p in the transcriptional activation of glycolytic genes inSaccharomyces cerevisiae. Yeast *21*, 851–866.

Moqtaderi, Z., Yale, J.D., Struhl, K., and Buratowski, S. (1996). Yeast homologues of higher eukaryotic TFIID subunits. Proc. Natl. Acad. Sci. *93*, 14654–14658.

Moretti, P., Freeman, K., Coodly, L., and Shore, D. (1994a). Evidence that a complex of SIR proteins interacts with the silencer and telomere-binding protein RAP1. Genes Dev. *8*, 2257–2269.

Moretti, P., Freeman, K., Coodly, L., and Shore, D. (1994b). Evidence that a complex of SIR proteins interacts with the silencer and telomere-binding protein RAP1. Genes Dev. *8*, 2257–2269.

Morse, R.H. (2000). RAP, RAP, open up! New wrinkles for RAP1 in yeast. Trends Genet. *16*, 51–53.

Morse, R.H. (2003). Getting into chromatin: how do transcription factors get past the histones? Biochem. Cell Biol. *81*, 101–112.

Mosley, A.L., Hunter, G.O., Sardiu, M.E., Smolle, M., Workman, J.L., Florens, L., and Washburn, M.P. (2013). Quantitative Proteomics Demonstrates That the RNA Polymerase II Subunits Rpb4 and Rpb7 Dissociate during Transcriptional Elongation. Mol. Cell. Proteomics *12*, 1530–1538.

Müller, T., Gilson, E., Schmidt, R., Giraldo, R., Sogo, J., Gross, H., and Gasser, S.M. (1994). Imaging the asymmetrical DNA bend induced by repressor activator protein 1 with scanning tunneling microscopy. J. Struct. Biol. *113*, 1–12.

Murakami, K. (2015). Structural Biology of Bacterial RNA Polymerase. Biomolecules *5*, 848–864.

Murakami, K., Gibbons, B.J., Davis, R.E., Nagai, S., Liu, X., Robinson, P.J., Wu, T., Kaplan, C.D., and Kornberg, R.D. (2012). Tfb6, a previously unidentified subunit of the general transcription factor TFIIH, facilitates dissociation of Ssl2 helicase after transcription initiation. Proc. Natl. Acad. Sci. *109*, 4816–4821.

Murthy, M.S.S., Rao, B.S., Reddy, N.M.S., Subrahmanyam, P., and Madhvanath, U. (1975). Non-equivalence of YEPD and synthetic complete media in yeast reversion studies. Mutat. Res. *27*, 219–223.

Muse, G.W., Gilchrist, D.A., Nechaev, S., Shah, R., Parker, J.S., Grissom, S.F., Zeitlinger, J., and Adelman, K. (2007). RNA polymerase is poised for activation across the genome. Nat. Genet. *39*, 1507–1511.

Myers, L.C., Leuther, K., Bushnell, D.A., Gustafsson, C.M., and Kornberg, R.D. (1997). Yeast RNA Polymerase II Transcription Reconstituted with Purified Proteins. Methods *12*, 212–216.

Nagalakshmi, U., Wang, Z., Waern, K., Shou, C., Raha, D., Gerstein, M., and Snyder, M. (2008). The Transcriptional Landscape of the Yeast Genome Defined by RNA Sequencing. Science *320*, 1344–1349.

Nagawa, F., and Fink, G.R. (1985). The relationship between the" TATA" sequence and transcription initiation sites at the HIS4 gene of Saccharomyces cerevisiae. Proc. Natl. Acad. Sci. *82*, 8557–8561.

Naumovski, L., and Friedberg, E.C. (1983). A DNA repair gene required for the incision of damaged DNA is essential for viability in Saccharomyces cerevisiae. Proc. Natl. Acad. Sci. U. S. A. *80*, 4818–4821.

Neugebauer, K.M., and Roth, M.B. (1997). Transcription units as RNA processing units. Genes Dev. *11*, 3279–3285.

Nguyen, D., Bail, M., Pesant, G., Dupont, V.N., Rouault, É., Deschênes, J., Rocha, W., Melançon, G., Steinberg, S.V., and Mader, S. (2007). Rational design of an estrogen receptor mutant with altered DNA-binding specificity. Nucleic Acids Res. *35*, 3465–3477.

Nieuwint, R.T.M., Mager, W.H., Maurer, K.C.T., and Planta, R.J. (1989). Mutational analysis of the upstream activation site of yeast ribosomal protein genes. Curr. Genet. *15*, 247–251.

Nilsson, M.T.I., and Widersten, M. (2004). Repertoire Selection of Variant Single-Chain Cro: Toward Directed DNA-Binding Specificity of Helix–Turn–Helix Proteins [†]. Biochemistry (Mosc.) *43*, 12038–12047.

Noyes, M.B., Meng, X., Wakabayashi, A., Sinha, S., Brodsky, M.H., and Wolfe, S.A. (2008). A systematic characterization of factors that regulate Drosophila segmentation via a bacterial one-hybrid system. Nucleic Acids Res. *36*, 2547–2560.

Obexer, R., Godina, A., Garrabou, X., Mittl, P.R.E., Baker, D., Griffiths, A.D., and Hilvert, D. (2017). Emergence of a catalytic tetrad during evolution of a highly active artificial aldolase. Nat. Chem. *9*, 50–56.

Ohkuma, Y., and Roeder, R.G. (1994). Regulation of TFIIH ATPase and kinase activities by TFIIE during active initiation complex formation. Nature *368*, 160–163.

Ohtsuki, K., Kasahara, K., Shirahige, K., and Kokubo, T. (2010). Genome-wide localization analysis of a complete set of Tafs reveals a specific effect of the taf1 mutation on Taf2 occupancy and provides indirect evidence for different TFIID conformations at different promoters. Nucleic Acids Res. *38*, 1805–1820.

O'Neill, E.M., Kaffman, A., Jolly, E.R., and O'Shea, E.K. (1996). Regulation of PHO4 Nuclear Localization by the PHO80-PHO85 Cyclin-CDK Complex. Science *271*, 209–212.

Ozer, J., Bolden, A.H., and Lieberman, P.M. (1996). Transcription factor IIA mutations show activator-specific defects and reveal a IIA function distinct from stimulation of TBP-DNA binding. J. Biol. Chem. *271*, 11182–11190.

Ozer, J., Mitsouras, K., Zerby, D., Carey, M., and Lieberman, P.M. (1998). Transcription factor IIA derepresses TATA-binding protein (TBP)-associated factor inhibition of TBP-DNA binding. J. Biol. Chem. *273*, 14293–14300.

Papai, G., Tripathi, M.K., Ruhlmann, C., Werten, S., Crucifix, C., Weil, P.A., and Schultz, P. (2009). Mapping the initiator binding Taf2 subunit in the structure of hydrated yeast TFIID. Struct. Lond. Engl. 1993 *17*, 363–373.

Papai, G., Tripathi, M.K., Ruhlmann, C., Layer, J.H., Weil, P.A., and Schultz, P. (2010). TFIIA and the transactivator Rap1 cooperate to commit TFIID for transcription initiation. Nature *465*, 956–960.

Papai, G., Weil, P.A., and Schultz, P. (2011). New insights into the function of transcription factor TFIID from recent structural studies. Curr. Opin. Genet. Dev. *21*, 219–224.

Pardee, T.S., Bangur, C.S., and Ponticelli, A.S. (1998). The N-terminal Region of Yeast TFIIB Contains Two Adjacent Functional Domains Involved in Stable RNA Polymerase II Binding and Transcription Start Site Selection. J. Biol. Chem. *273*, 17859–17864.

Park, E., Guzder, S.N., Koken, M.H., Jaspers-Dekker, I., Weeda, G., Hoeijmakers, J.H., Prakash, S., and Prakash, L. (1992). RAD25 (SSL2), the yeast homolog of the human xeroderma pigmentosum group B DNA repair gene, is essential for viability. Proc. Natl. Acad. Sci. U. S. A. *89*, 11416–11420.

Parry, T.J., Theisen, J.W.M., Hsu, J.-Y., Wang, Y.-L., Corcoran, D.L., Eustice, M., Ohler, U., and Kadonaga, J.T. (2010). The TCT motif, a key component of an RNA polymerase II transcription system for the translational machinery. Genes Dev. *24*, 2013–2018.

Perina, D., Korolija, M., Roller, M., Harcet, M., Jeličić, B., Mikoč, A., and Ćetković, H. (2011). Over-represented localized sequence motifs in ribosomal protein gene promoters of basal metazoans. Genomics *98*, 56–63.

Perlmann, T., and Wrange, O. (1988). Specific glucocorticoid receptor binding to DNA reconstituted in a nucleosome. EMBO J. *7*, 3073.

Pfau, J., Arvidson, D.N., Youderian, P., Pearson, L.L., and Sigman, D.S. (1994). A site-specific endonuclease derived from a mutant Trp repressor with altered DNA-binding specificity. Biochemistry (Mosc.) *33*, 11391–11403.

Pinto, I., Ware, D.E., and Hamsey, M. (1992). The yeast SUA7 gene encodes a homolog of human transcription factor TFIIB and is required for normal start site selection in vivo. Cell *68*, 977–988.

Pokholok, D.K., Harbison, C.T., Levine, S., Cole, M., Hannett, N.M., Lee, T.I., Bell, G.W., Walker, K., Rolfe, P.A., Herbolsheimer, E., et al. (2005). Genome-wide map of nucleosome acetylation and methylation in yeast. Cell *122*, 517–527.

Ponticelli, A.S., Pardee, T.S., and Struhl, K. (1995). The glutamine-rich activation domains of human Sp1 do not stimulate transcription in Saccharomyces cerevisiae. Mol. Cell. Biol. *15*, 983–988.

Poon, D., Bai, Y., Campbell, A.M., Bjorklund, S., Kim, Y.-J., Zhou, S., Kornberg, R.D., and Weil, P.A. (1995). Identification and characterization of a TFIID-like multiprotein complex from Saccharomyces cerevisiae. Proc. Natl. Acad. Sci. *92*, 8224–8228.

Pribnow, D. (1975). Nucleotide sequence of an RNA polymerase binding site at an early T7 promoter. Proc. Natl. Acad. Sci. U. S. A. *72*, 784–788.

Prunell, A. (1982). Nucleosome reconstitution on plasmid-inserted poly(dA) . poly(dT). EMBO J. *1*, 173–179.

Ptashne, M. (1988). How eukaryotic transcriptional activators work. Nature *335*, 683–689.

Ptashne, M., and Gann, A. (1997). Transcriptional activation by recruitment. Nature *386*, 569–577.

Ptashne, M., and Gann, A.A.F. (1990). Activators and targets. Nature *346*, 329–331.

Pugh, B.F., and Tjian, R. (1990). Mechanism of transcriptional activation by Sp1: evidence for coactivators. Cell *61*, 1187–1197.

Qiu, H., Hu, C., and Hinnebusch, A.G. (2009). Phosphorylation of the Pol II CTD by KIN28 enhances BUR1/BUR2 recruitment and Ser2 CTD phosphorylation near promoters. Mol. Cell *33*, 752–762.

Radhakrishnan, I., Pérez-Alvarado, G.C., Parker, D., Dyson, H.J., Montminy, M.R., and Wright, P.E. (1997). Solution structure of the KIX domain of CBP bound to the transactivation domain of CREB: a model for activator:coactivator interactions. Cell *91*, 741–752.

Raisner, R.M., Hartley, P.D., Meneghini, M.D., Bao, M.Z., Liu, C.L., Schreiber, S.L., Rando, O.J., and Madhani, H.D. (2005). Histone variant H2A.Z marks the 5' ends of both active and inactive genes in euchromatin. Cell *123*, 233–248.

Rani, P.G., Ranish, J.A., and Hahn, S. (2004). RNA polymerase II (Pol II)-TFIIF and Pol II-mediator complexes: the major stable Pol II complexes and their activity in transcription initiation and reinitiation. Mol. Cell. Biol. *24*, 1709–1720.

Ranish, J.A., and Hahn, S. (1991). The Yeast General Transcription Factor TFIIA Is Composed of Two Polypeptide Subunits. J. Biol. Chem. *266*, 19320–19327.

Ranish, J.A., Lane, W.S., and Hahn, S. (1992). Isolation of two yeast genes that encode subunits of the yeast transcription factor IIA. Science *255*, 1127–1129.

Ranish, J.A., Hahn, S., Lu, Y., Yi, E.C., Li, X., Eng, J., and Aebersold, R. (2004). Identification of TFB5, a new component of general transcription and DNA repair factor IIH. Nat. Genet. *36*, 707–713.

Rappaport, J., Reinberg, D., Zandomeni, R., and Weinmann, R. (1987). Purification and functional characterization of transcription factor SII from calf thymus. Role in RNA polymerase II elongation. J. Biol. Chem. *262*, 5227–5232.

Rastegar, S., Hess, I., Dickmeis, T., Nicod, J.C., Ertzer, R., Hadzhiev, Y., Thies, W.-G., Scherer, G., and Strähle, U. (2008). The words of the regulatory code are arranged in a variable manner in highly conserved enhancers. Dev. Biol. *318*, 366–377.

Ray, B.L., White, C.I., and Haber, J.E. (1991). The TSM1 gene of Saccharomyces cerevisiae overlaps the MAT locus. Curr. Genet. *20*, 25–31.

Reese, J.C., Apone, L., Walker, S.S., Griffin, L.A., and Green, M.R. (1994). Yeast TAF IIS in a multisubunit complex required for activated transcription. Nature *371*, 523–527.

Reeves, W.M., and Hahn, S. (2005). Targets of the Gal4 transcription activator in functional transcription complexes. Mol. Cell. Biol. *25*, 9092–9102.

Regier, J.L., Shen, F., and Triezenberg, S.J. (1993). Pattern of aromatic and hydrophobic amino acids critical for one of two subdomains of the VP16 transcriptional activator. Proc. Natl. Acad. Sci. *90*, 883–887.

Reid, J.L., Iyer, V.R., Brown, P.O., and Struhl, K. (2000). Coordinate regulation of yeast ribosomal protein genes is associated with targeted recruitment of Esa1 histone acetylase. Mol. Cell *6*, 1297–1307.

Reinberg, D., and Roeder, R.G. (1987). Factors involved in specific transcription by mammalian RNA polymerase II. Transcription factor IIS stimulates elongation of RNA chains. J. Biol. Chem. *262*, 3331–3337.

Reja, R., Vinayachandran, V., Ghosh, S., and Pugh, B.F. (2015). Molecular mechanisms of ribosomal protein gene coregulation. Genes Dev. *29*, 1942–1954.

Ren, X., Siegel, R., Kim, U., and Roeder, R.G. (2011). Direct Interactions of OCA-B and TFII-I Regulate Immunoglobulin Heavy-Chain Gene Transcription by Facilitating Enhancer-Promoter Communication. Mol. Cell *42*, 342–355.

Rhee, H.S., and Pugh, B.F. (2011). Comprehensive Genome-wide Protein-DNA Interactions Detected at Single-Nucleotide Resolution. Cell *147*, 1408–1419.

Rhee, H.S., and Pugh, B.F. (2012). Genome-wide structure and organization of eukaryotic pre-initiation complexes. Nature *483*, 295–301.

Risher, R., and Blumenthal, T. (1980). Analysis of RNA Polymerase by Trypsin Cleavage. J. Biol. Chem. *255*, 11056–11062.

Riva, M., Schäffner, A.R., Sentenac, A., Hartmann, G.R., Mustaev, A.A., Zaychikov, E.F., and Grachev, M.A. (1987). Active site labeling of the RNA polymerases A, B, and C from yeast. J. Biol. Chem. *262*, 14377–14380.

Roeder, R.G. (2005). Transcriptional regulation and the role of diverse coactivators in animal cells. FEBS Lett. *579*, 909–915.

Roeder, R.G., and Rutter, W.J. (1969). Multiple Forms of DNA-dependent RNA Polymerase in Eukaryotic Organisms. Nature *224*, 234–237.

Roguev, A., Schaft, D., Shevchenko, A., Pijnappel, W.W.M.P., Wilm, M., Aasland, R., and Stewart, A.F. (2001). The Saccharomyces cerevisiae Set1 complex includes an Ash2 homologue and methylates histone 3 lysine 4. EMBO J. *20*, 7137–7148.

Rohde, J.R., and Cardenas, M.E. (2003). The Tor Pathway Regulates Gene Expression by Linking Nutrient Sensing to Histone Acetylation. Mol. Cell. Biol. *23*, 629–635.

Rohs, R., Jin, X., West, S.M., Joshi, R., Honig, B., and Mann, R.S. (2010). Origins of Specificity in Protein-DNA Recognition. Annu. Rev. Biochem. *79*, 233–269.

Ross, W., Gosink, K.K., Salomon, J., Igarashi, K., Zou, C., Ishihama, A., Severinov, K., and Gourse, R.L. (1993). A third recognition element in bacterial promoters: DNA binding by the alpha subunit of RNA polymerase. Science *262*, 1407–1413.

Rossetti, L., Cacchione, S., De Menna, A., Chapman, L., Rhodes, D., and Savino, M. (2001). Specific interactions of the telomeric protein rap1p with nucleosomal binding sites. J. Mol. Biol. *306*, 903–913.

Rudra, D., and Warner, J.R. (2004). What better measure than ribosome synthesis? Genes Dev. *18*, 2431–2436.

Rudra, D., Zhao, Y., and Warner, J.R. (2005). Central role of Ifh1p–Fhl1p interaction in the synthesis of yeast ribosomal proteins. EMBO J. *24*, 533–542.

Sandelin, A. (2004). JASPAR: an open-access database for eukaryotic transcription factor binding profiles. Nucleic Acids Res. *32*, 91D–94.

Sanders, S.L., and Weil, P.A. (2000). Identification of Two Novel TAF Subunits of the YeastSaccharomyces cerevisiae TFIID Complex. J. Biol. Chem. *275*, 13895–13900.

Sanders, S.L., Garbett, K.A., and Weil, P.A. (2002a). Molecular Characterization of Saccharomyces cerevisiae TFIID. Mol. Cell. Biol. *22*, 6000–6013.

Sanders, S.L., Jennings, J., Canutescu, A., Link, A.J., and Weil, P.A. (2002b). Proteomics of the Eukaryotic Transcription Machinery: Identification of Proteins Associated with Components of Yeast TFIID by Multidimensional Mass Spectrometry. Mol. Cell. Biol. *22*, 4723–4738.

Santos-Rosa, H., Schneider, R., Bannister, A.J., Sherriff, J., Bernstein, B.E., Emre, N.C.T., Schreiber, S.L., Mellor, J., and Kouzarides, T. (2002). Active genes are tri-methylated at K4 of histone H3. Nature *419*, 407–411.

Saragosti, S., Moyne, G., and Yaniv, M. (1980). Absence of nucleosomes in a fraction of SV40 chromatin between the origin of replication and the region coding for the late leader RNA. Cell *20*, 65–73.

Sauer, F., Hansen, S.K., and Tjian, R. (1995a). DNA template and activator-coactivator requirements for transcriptional synergism by Drosophila bicoid. Science *270*, 1825–1828.

Sauer, F., Hansen, S.K., and Tjian, R. (1995b). Multiple TAFIIs Directing Synergistic Activation of Transcription. Science *270*, 1783–1788.

Sawadogo, M. (1988). Multiple forms of the human gene-specific transcription factor USF. II. DNA binding properties and transcriptional activity of the purified HeLa USF. J. Biol. Chem. *263*, 11994–12001.

Sayre, M.H., Tschochner, H., and Kornberg, R.D. (1992). Reconstitution of Transcription with Five Purified Initiation Factors and RNA Polymerease II from Saccharomyces cerevisiae. J. Biol. Chem. *267*, 23376–23382.

Schaller, H., Gray, C., and Herrmann, K. (1975). Nucleotide sequence of an RNA polymerase binding site from the DNA of bacteriophage fd. Proc. Natl. Acad. Sci. U. S. A. *72*, 737–741.

Scheer, E., Delbac, F., Tora, L., Moras, D., and Romier, C. (2012). TFIID TAF6-TAF9 complex formation involves the HEAT repeat-containing C-terminal domain of TAF6 and is modulated by TAF5 protein. J. Biol. Chem. *287*, 27580–27592.

Schultz, L.D., and Hall, B.D. (1976). Transcription in yeast: alpha-amanitin sensitivity and other properties which distinguish between RNA polymerases I and III. Proc. Natl. Acad. Sci. *73*, 1029–1033.

Schulz, D., Pirkl, N., Lehmann, E., and Cramer, P. (2014). Rpb4 Subunit Functions Mainly in mRNA Synthesis by RNA Polymerase II. J. Biol. Chem. *289*, 17446–17452.

Schwalder, S.B., Kabani, M., Howald, I., Choudhurry, U., Werner, M., and Shore, D. (2004). Growth-regulated recruitment of the essential yeast ribosomal protien gene activator Ifh1. Nature *432*, 1058–1061.

Scott, E.W., and Baker, H.V. (1993). Concerted action of the transcriptional activators REB1, RAP1, and GCR1 in the high-level expression of the glycolytic gene TPI. Mol. Cell. Biol. *13*, 543–550.

Seipel, K., Georgiev, O., and Schaffner, W. (1992). Different activation domains stimulate transcription from remote ('enhancer') and proximal ('promoter') positions. EMBO J. *11*, 4961–4968.

Sekimizu, K., Nakanishi, Y., Mizuno, D., and Natori, S. (1979). Purification and preparation of antibody to RNA polymerase II stimulatory factors from Ehrlich ascites tumor cells. Biochemistry (Mosc.) *18*, 1582–1588.

Selleck, W., Howley, R., Fang, Q., Podolny, V., Fried, M.G., Buratowski, S., and Tan, S. (2001). A histone fold TAF octamer within the yeast TFIID transcriptional coactivator. Nat. Struct. Biol. *8*, 695–700.

Sera, T., and Uranga, C. (2002). Rational design of artificial zinc-finger proteins using a nondegenerate recognition code table. Biochemistry (Mosc.) *41*, 7074–7081.

Sezonov, G., Joseleau-Petit, D., and D'Ari, R. (2007). Escherichia coli Physiology in Luria-Bertani Broth. J. Bacteriol. *189*, 8746–8749.

Shandilya, J., and Roberts, S.G.E. (2012). The transcription cycle in eukaryotes: From productive initiation to RNA polymerase II recycling. Biochim. Biophys. Acta BBA - Gene Regul. Mech. *1819*, 391–400.

Shanle, E.K., Andrews, F.H., Meriesh, H., McDaniel, S.L., Dronamraju, R., DiFiore, J.V., Jha, D., Wozniak, G.G., Bridgers, J.B., Kerschner, J.L., et al. (2015). Association of Taf14 with acetylated histone H3 directs gene transcription and the DNA damage response. Genes Dev. *29*, 1795–1800.

Shen, W.-C., and Green, M.R. (1997). Yeast TAF II 145 functions as a core promoter selectivity factor, not a general coactivator. Cell *90*, 615–624.

Shen, W.-C., Bhaumik, S.R., Causton, H.C., Simon, I., Zhu, X., Jennings, E.G., Wang, T.-H., Young, R.A., and Green, M.R. (2003). Systematic analysis of essential yeast TAFs in genome-wide transcription and preinitiation complex assembly. EMBO J. *22*, 3395–3402.

Shore, D. (1994). RAP1: a protean regulator in yeast. Trends Genet. *10*, 408–412.

Shore, D., and Nasmyth, K. (1987). Purification and cloning of a DNA binding protein from yeast that binds to both silencer and activator elements. Cell *51*, 721–732.

Simon, M., Seraphin, B., and Faye, G. (1986). KIN28, a yeast split gene coding for a putative protein kinase homologous to CDC28. EMBO J. *5*, 2697–2701.

Simpson, R.T. (1990). Nucleosome positioning can affect the function of a cis-acting DMA elementin vivo. Nature *343*, 387–389.

Singh, M.V., and Weil, P.A. (2002). A method for plasmid purification directly from yeast. Anal. Biochem. *307*, 13–17.

Singh, M.V., Bland, C.E., and Weil, P.A. (2004). Molecular and Genetic Characterization of a Taf1p Domain Essential for Yeast TFIID Assembly. Mol. Cell. Biol. *24*, 4929–4942.

Slattery, M., Riley, T., Liu, P., Abe, N., Gomez-Alcala, P., Dror, I., Zhou, T., Rohs, R., Honig, B., Bussemaker, H.J., et al. (2011). Cofactor binding evokes latent differences in DNA binding specificity between Hox proteins. Cell *147*, 1270–1282.

Smale, S.T., and Baltimore, D. (1989). The "initiator" as a transcription control element. Cell *57*, 103–113.

Smith, R.P., Taher, L., Patwardhan, R.P., Kim, M.J., Inoue, F., Shendure, J., Ovcharenko, I., and Ahituv, N. (2013). Massively parallel decoding of mammalian regulatory sequences supports a flexible organizational model. Nat. Genet. *45*, 1021–1028.

Strahl, B.D., Ohba, R., Cook, R.G., and Allis, C.D. (1999). Methylation of histone H3 at lysine 4 is highly conserved and correlates with transcriptionally active nuclei in Tetrahymena. Proc. Natl. Acad. Sci. U. S. A. *96*, 14967–14972.

Strahl, B.D., Grant, P.A., Briggs, S.D., Sun, Z.-W., Bone, J.R., Caldwell, J.A., Mollah, S., Cook, R.G., Shabanowitz, J., Hunt, D.F., et al. (2002). Set2 is a nucleosomal histone H3-selective methyltransferase that mediates transcriptional repression. Mol. Cell. Biol. *22*, 1298–1306.

Stringer, K.F., Ingles, C.J., and Greenblatt, J. (1990). Direct and selective binding of an acidic transcriptional activation domain to the TATA-box factor TFIID. Nature *345*, 783–786.

Strubin, Michel, and Struhl, Kevin (1992). Yeast and Human TFIID with Altered DNA-Binding Specificity for TATA Elements. Cell *68*, 721–730.

Struhl, K. (1995). Yeast transcriptional regulatory mechanisms. Annu. Rev. Genet. *29*, 651–674.

Struhl, K. (1999). Fundamentally Different Logic of Gene Regulation in Eukaryotes and Prokaryotes. Cell *98*, 1–4.

Sugiura, M., Okamoto, T., and Takanami, M. (1970). RNA polymerase sigma-factor and the selection of initiation site. Nature *225*, 598–600.

Suh, H., Ficarro, S.B., Kang, U.-B., Chun, Y., Marto, J.A., and Buratowski, S. (2016). Direct Analysis of Phosphorylation Sites on the Rpb1 C-Terminal Domain of RNA Polymerase II. Mol. Cell *61*, 297–304.

Sun, Z.-W., and Allis, C.D. (2002). Ubiquitination of histone H2B regulates H3 methylation and gene silencing in yeast. Nature *418*, 104–108.

Sun, M., Schwalb, B., Schulz, D., Pirkl, N., Etzold, S., Lariviere, L., Maier, K.C., Seizl, M., Tresch, A., and Cramer, P. (2012). Comparative dynamic transcriptome analysis (cDTA) reveals mutual feedback between mRNA synthesis and degradation. Genome Res. *22*, 1350–1359.

Sun, M., Schwalb, B., Pirkl, N., Maier, K.C., Schenk, A., Failmezger, H., Tresch, A., and Cramer, P. (2013). Global Analysis of Eukaryotic mRNA Degradation Reveals Xrn1-Dependent Buffering of Transcript Levels. Mol. Cell *52*, 52–62.

Sussel, L., and Shore, D. (1991). Separation of transcriptional activation and silencing functions of the RAP1-encoded repressor/activator protein 1: isolation of viable mutants affecting both silencing and telomere length. Proc. Natl. Acad. Sci. *88*, 7749–7753.

Svaren, J., Schmitz, J., and Hörz, W. (1994). The transactivation domain of Pho4 is required for nucleosome disruption at the PHO5 promoter. EMBO J. *13*, 4856–4862.

Svejstrup, J.Q., Feaver, W.J., LaPointe, J., and Kornberg, R.D. (1994). RNA Polymerase Transcription Factor IIH Holoenzyme from Yeast. J. Biol. Chem. *269*, 28044–28048.

Sweetser, D., Nonet, M., and Young, R.A. (1987). Prokaryotic and eukaryotic RNA polymerases have homologous core subunits. Proc. Natl. Acad. Sci. *84*, 1192–1196.

Taatjes, D.J., Näär, A.M., Andel, F., Nogales, E., and Tjian, R. (2002). Structure, function, and activator-induced conformations of the CRSP coactivator. Science *295*, 1058–1062.

Taatjes, D.J., Schneider-Poetsch, T., and Tjian, R. (2004). Distinct conformational states of nuclear receptor-bound CRSP-Med complexes. Nat. Struct. Mol. Biol. *11*, 664–671.

Tan, S., Hunziker, Y., Sargent, D.F., and Richmond, T.J. (1996). Crystal structure of a yeast TFIIA/TBP/DNA complex. Nature *381*, 127–151.

Tanay, A., Regev, A., and Shamir, R. (2005). Conservation and evolvability in regulatory networks: The evolution of ribosomal regulation in yeast. Proc. Natl. Acad. Sci. U. S. A. *102*, 7203–7208.

Tanese, N., Pugh, B.F., and Tjian, R. (1991). Coactivators for a proline-rich activator purified from the multisubunit human TFIID complex. Genes Dev. *5*, 2212–2224.

Tansey, W.P., and Herr, W. (1997). TAFs: guilt by association? Cell *88*, 729–732.

Tapscott, S.J., Davis, R.L., Thayer, M.J., Cheng, P.F., Weintraub, H., and Lassar, A.B. (1988). MyoD1: a nuclear phosphoprotein requiring a Myc homology region to convert fibroblasts to myoblasts. Science *242*, 405–411.

Taylor, H.O.., O'Reilly, M., Leslie, A.G.., and Rhodes, D. (2000). How the multifunctional yeast Rap1p discriminates between DNA target sites: a crystallographic analysis. J. Mol. Biol. *303*, 693–707.

Thanos, D., and Maniatis, T. (1995). Virus induction of human IFNβ gene expression requires the assembly of an enhanceosome. Cell *83*, 1091–1100.

Thomas, B.J., and Rothstein, R. (1989). Elevated recombination rates in transcriptionally active DNA. Cell *56*, 619–630.

Thomas, M.C., and Chiang, C.-M. (2006). The General Transcription Machinery and General Cofactors. Crit. Rev. Biochem. Mol. Biol. *41*, 105–178.

Thut, C.J., Chen, J.L., Klemm, R., and Tjian, R. (1995). p53 transcriptional activation mediated by coactivators TAFII40 and TAFII60. Science *267*, 100–104.

Thyme, S.B., Boissel, S.J.S., Arshiya Quadri, S., Nolan, T., Baker, D.A., Park, R.U., Kusak, L., Ashworth, J., and Baker, D. (2014). Reprogramming homing endonuclease specificity through computational design and directed evolution. Nucleic Acids Res. *42*, 2564–2576.

Titz, B. (2006). Transcriptional activators in yeast. Nucleic Acids Res. *34*, 955–967.

Todeschini, A.-L., Georges, A., and Veitia, R.A. (2014). Transcription factors: specific DNA binding and specific gene regulation. Trends Genet. *30*, 211–219.

Tomar, R.S., Zheng, S., Brunke-Reese, D., Wolcott, H.N., and Reese, J.C. (2008). Yeast Rap1 contributes to genomic integrity by activating DNA damage repair genes. EMBO J. *27*, 1575–1584.

Tora, L. (2002). A unified nomenclature for TATA box binding protein (TBP)-associated factors (TAFs) involved in RNA polymerase II transcription. Genes Dev. *16*, 673–675.

Treich, I., Carles, C., Riva, M., and Sentenac, A. (1992). RPC10 encodes a new mini subunit shared by yeast nuclear RNA polymerases. Gene Expr. *2*, 31–37.

Trowitzsch, S., Viola, C., Scheer, E., Conic, S., Chavant, V., Fournier, M., Papai, G., Ebong, I.-O., Schaffitzel, C., Zou, J., et al. (2015). Cytoplasmic TAF2-TAF8-TAF10 complex provides evidence for nuclear holo-TFIID assembly from preformed submodules. Nat. Commun. *6*, 6011.

Tsukihashi, Y., Kawaichi, M., and Kokubo, T. (2001). Requirement for Yeast TAF145 Function in Transcriptional Activation of the RPS5 Promoter That Depends on Both Core Promoter Structure and Upstream Activating Sequences. J. Biol. Chem. *276*, 25715–25726.

Tuch, B.B., Galgoczy, D.J., Hernday, A.D., Li, H., and Johnson, A.D. (2008). The evolution of combinatorial gene regulation in fungi. PLoS Biol. *6*, e38.

Uesugi, M., Nyanguile, O., Lu, H., Levine, A.J., and Verdine, G.L. (1997). Induced alpha helix in the VP16 activation domain upon binding to a human TAF. Science *277*, 1310–1313.

Uprety, B., Sen, R., and Bhaumik, S.R. (2015). Eaf1p Is Required for Recruitment of NuA4 in Targeting TFIID to the Promoters of the Ribosomal Protein Genes for Transcriptional Initiation *In Vivo*. Mol. Cell. Biol. *35*, 2947–2964.

Uprety, B., Kaja, A., Ferdoush, J., Sen, R., and Bhaumik, S.R. (2016). Regulation of Antisense Transcription by NuA4 Histone Acetyltransferase and Other Chromatin Regulatory Factors. Mol. Cell. Biol. *36*, 992–1006.

Valay, J.G., Simon, M., and Faye, G. (1993). The kin28 protein kinase is associated with a cyclin in Saccharomyces cerevisiae. J. Mol. Biol. *234*, 307–310.

Vannini, A., and Cramer, P. (2012). Conservation between the RNA Polymerase I, II, and III Transcription Initiation Machineries. Mol. Cell *45*, 439–446.

Vaquerizas, J.M., Kummerfeld, S.K., Teichmann, S.A., and Luscombe, N.M. (2009). A census of human transcription factors: function, expression and evolution. Nat. Rev. Genet. *10*, 252–263.

Venkatesh, S., and Workman, J.L. (2015). Histone exchange, chromatin structure and the regulation of transcription. Nat. Rev. Mol. Cell Biol. *16*, 178–189.

Venter, U., Svaren, J., Schmitz, J., Schmid, A., and Hörz, W. (1994). A nucleosome precludes binding of the transcription factor Pho4 in vivo to a critical target site in the PHO5 promoter. EMBO J. *13*, 4848–4855.

Venters, B.J., and Pugh, B.F. (2009). How eukaryotic genes are transcribed. Crit. Rev. Biochem. Mol. Biol. *44*, 117–141.

Vermeulen, M., Mulder, K.W., Denissov, S., Pijnappel, W.W.M.P., van Schaik, F.M.A., Varier, R.A., Baltissen, M.P.A., Stunnenberg, H.G., Mann, M., and Timmers, H.T.M. (2007). Selective anchoring of TFIID to nucleosomes by trimethylation of histone H3 lysine 4. Cell *131*, 58–69.

Verrijzer, C.P., Yokomori, K., Chen, J.L., and Tjian, R. (1994). Drosophila TAFII150: similarity to yeast gene TSM-1 and specific binding to core promoter DNA. Science *264*, 933–941.

Verrijzer, C.P., Chen, J.-L., Yokomori, K., and Tjian, R. (1995). Binding of TAFs to core elements directs promoter selectivity by RNA polymerase II. Cell *81*, 1115–1125.

Vignais, M.L., Woudt, L.P., Wassenaar, G.M., Mager, W.H., Sentenac, A., and Planta, R.J. (1987). Specific binding of TUF factor to upstream activation sites of yeast ribosomal protein genes. EMBO J. *6*, 1451.

Vignais, M.L., Huet, J., Buhler, J.M., and Sentenac, A. (1990). Contacts between the factor TUF and RPG sequences. J. Biol. Chem. *265*, 14669–14674.

Vojnic, E., Mourão, A., Seizl, M., Simon, B., Wenzeck, L., Larivière, L., Baumli, S., Baumgart, K., Meisterernst, M., Sattler, M., et al. (2011). Structure and VP16 binding of the Mediator Med25 activator interaction domain. Nat. Struct. Mol. Biol. *18*, 404–409.

Voss, T.C., Schiltz, R.L., Sung, M.-H., Yen, P.M., Stamatoyannopoulos, J.A., Biddie, S.C., Johnson, T.A., Miranda, T.B., John, S., and Hager, G.L. (2011). Dynamic Exchange at Regulatory Elements during Chromatin Remodeling Underlies Assisted Loading Mechanism. Cell *146*, 544–554.

Wach, A., Brachat, A., Pöhlmann, R., and Philippsen, P. (1994). New heterologous modules for classical or PCR-based gene disruptions in Saccharomyces cerevisiae. Yeast Chichester Engl. *10*, 1793–1808.

Wade, J.T., Hall, D.B., and Struhl, K. (2004a). The transcription factor Ifh1 is a key regulator of yeast ribosomal protein genes. Lett. Nat. *432*, 1054–1058.

Wade, J.T., Hall, D.B., and Struhl, K. (2004b). The transcription factor Ifh1 is a key regulator of yeast ribosomal protein genes. Nature *432*, 1054–1058.

Wallberg, A.E., Pedersen, K., Lendahl, U., and Roeder, R.G. (2002). p300 and PCAF Act Cooperatively To Mediate Transcriptional Activation from Chromatin Templates by Notch Intracellular Domains In Vitro. Mol. Cell. Biol. *22*, 7812–7819.

Warfield, L., Tuttle, L.M., Pacheco, D., Klevit, R.E., and Hahn, S. (2014). A sequence-specific transcription activator motif and powerful synthetic variants that bind Mediator using a fuzzy protein interface. Proc. Natl. Acad. Sci. *111*, E3506–E3513.

Warner, J.R. (1999). The economics of ribosome biosynthesis in yeast. Trends Biochem. Sci. *24*, 437–440.

Weake, V.M., and Workman, J.L. (2010). Inducible gene expression: diverse regulatory mechanisms. Nat. Rev. Genet. *11*, 426–437.

Weil, P.A., Luse, D.S., Segall, J., and Roeder, R.G. (1979). Selective and accurate initiation of transcription at the Ad2 major late promotor in a soluble system dependent on purified RNA polymerase II DNA. Cell *18*, 469–484.

Weinmann, R., and Roeder, R.G. (1974). Role of DNA-dependent RNA polymerase III in the transcription of the tRNA and 5S RNA genes. Proc. Natl. Acad. Sci. *71*, 1790–1794.

Werten, S., Mitschler, A., Romier, C., Gangloff, Y.-G., Thuault, S., Davidson, I., and Moras, D. (2002). Crystal structure of a subcomplex of human transcription factor TFIID formed by TATA binding protein-associated factors hTAF4 (hTAF(II)135) and hTAF12 (hTAF(II)20). J. Biol. Chem. *277*, 45502–45509.

Wigneshweraraj, S.R., Kuznedelov, K., Severinov, K., and Buck, M. (2003). Multiple Roles of the RNA Polymerase Subunit Flap Domain in 54-Dependent Transcription. J. Biol. Chem. *278*, 3455–3465.

Wolberger, C., Vershon, A.K., Liu, B., Johnson, A.D., and Pabo, C.O. (1991). Crystal structure of a MAT alpha 2 homeodomain-operator complex suggests a general model for homeodomain-DNA interactions. Cell *67*, 517–528.

Wood, A., Krogan, N.J., Dover, J., Schneider, J., Heidt, J., Boateng, M.A., Dean, K., Golshani, A., Zhang, Y., Greenblatt, J.F., et al. (2003). Bre1, an E3 ubiquitin ligase required for recruitment and substrate selection of Rad6 at a promoter. Mol. Cell *11*, 267–274.

Woodcock, C.L., and Ghosh, R.P. (2010). Chromatin Higher-order Structure and Dynamics. Cold Spring Harb. Perspect. Biol. *2*, a000596.

Woychik, N.A., and Young, R.A. (1989). RNA polymerase II subunit RPB4 is essential for high-and low-temperature yeast cell growth. Mol. Cell. Biol. *9*, 2854–2859.

Woychik, N.A., Lane, W.S., and Young, R.A. (1991). Yeast RNA Polymerase II Subunit RPB9 Is Essential for Growth at Temperature Extremes. J. Biol. Chem. *266*, 19053–19055.

Woychik, N.A., McKune, K., Lane, W.S., and Young, R.A. (1993). Yeast RNA polymerase II subunit RPB11 is related to a subunit shared by RNA polymerase I and III. Gene Expr. *3*, 77–82.

Wu, C., Wilson, S., Walker, B., Dawid, I., Paisley, T., Zimarino, V., and Ueda, H. (1987). Purification and properties of Drosophila heat shock activator protein. Science *238*, 1247–1253.

Xiao, H., Friesen, J.D., and Lis, J.T. (1995). Recruiting TATA-binding protein to a promoter: transcriptional activation without an upstream activator. Mol. Cell. Biol. *15*, 5757–5761.

Yarragudi, A., Parfrey, L.W., and Morse, R.H. (2006). Genome-wide analysis of transcriptional dependence and probable target sites for Abf1 and Rap1 in Saccharomyces cerevisiae. Nucleic Acids Res. *35*, 193–202.

Yokomori, K., Zeidler, M.P., Chen, J.-L., Verrijzer, C.P., Mlodzik, M., and Tjian, R. (1994). Drosophila TFIIA directs cooperative DNA binding with TBP and mediates transcriptional activation. Genes Dev. *8*, 2313–2323.

Yoon, H., Miller, S.P., Pabich, E.K., and Donahue, T.F. (1992). SSL1, a suppressor of a HIS4 5'-UTR stem-loop mutation, is essential for translation initiation and affects UV resistance in yeast. Genes Dev. *6*, 2463–2477.

Yu, L., and Morse, R.H. (1999). Chromatin opening and transactivator potentiation by RAP1 in Saccharomyces cerevisiae. Mol. Cell. Biol. *19*, 5279–5288.

Yu, L., Sabet, N., Chambers, A., and Morse, R.H. (2001). The N-terminal and C-terminal Domains of RAP1 Are Dispensable for Chromatin Opening and GCN4-mediated HIS4 Activation in Budding Yeast. J. Biol. Chem. *276*, 33257–33264.

Yuan, G.-C., Liu, Y.-J., Dion, M.F., Slack, M.D., Wu, L.F., Altschuler, S.J., and Rando, O.J. (2005). Genome-scale identification of nucleosome positions in S. cerevisiae. Science *309*, 626–630.

Yudkovsky, N., Ranish, J.A., and Hahn, S. (2000). A transcription reinitiation intermediate that is stabilized by activator. Nature *408*, 225–229.

Zaccolo, M., and Gherardi, E. (1999). The effect of high-frequency random mutagenesis on in vitro protein evolution: a study on TEM-1 beta-lactamase. J. Mol. Biol. *285*, 775–783.

Zaret, K.S., and Carroll, J.S. (2011). Pioneer transcription factors: establishing competence for gene expression. Genes Dev. *25*, 2227–2241.

Zehring, W.A., Lee, J.M., Weeks, J.R., Jokerst, R.S., and Greenleaf, A.L. (1988). The C-terminal repeat domain of RNA polymerase II largest subunit is essential in vivo but is not required for accurate transcription initiation in vitro. Proc. Natl. Acad. Sci. U. S. A. *85*, 3698–3702.

Zhang, G., and Darst, S.A. (1998). Structure of the Escherichia coli RNA polymerase alpha subunit amino-terminal domain. Science *281*, 262–266.

Zhang, W., Zhang, J., Zhang, X., Xu, C., and Tu, X. (2011). Solution structure of Rap1 BRCT domain from Saccharomyces cerevisiae reveals a novel fold. Biochem. Biophys. Res. Commun. *404*, 1055–1059.

Zhao, Y., McIntosh, K.B., Rudra, D., Schawalder, S., Shore, D., and Warner, J.R. (2006). Fine-Structure Analysis of Ribosomal Protein Gene Transcription. Mol. Cell. Biol. *26*, 4853–4862.

Zhu, C., Gupta, A., Hall, V.L., Rayla, A.L., Christensen, R.G., Dake, B., Lakshmanan, A., Kuperwasser, C., Stormo, G.D., and Wolfe, S.A. (2013). Using defined finger-finger interfaces as units of assembly for constructing zinc-finger nucleases. Nucleic Acids Res. *41*, 2455–2465.

Zylber, E.A., and Penman, S. (1971). Products of RNA polymerases in HeLa cell nuclei. Proc. Natl. Acad. Sci. *68*, 2861–2865.